Microparticles enhance natural product formation in native and metabolically engineered actinobacteria through accelerated morphological development

Dissertation

zur Erlangung des Grades

des Doktors der Ingenieurwissenschaften

der Naturwissenschaftlich-Technischen Fakultät

der Universität des Saarlandes

von

Martin Kuhl

Saarbrücken

2021

Tag des Kolloquiums:	03.12.2021
Dekan:	Prof. Dr. Jörn Walter
Berichterstatter:	Prof. Dr. Christoph Wittmann
	Prof. Dr. Andriy Luzhetskyy
Vorsitz:	Prof. Dr. Uli Kazmaier
Akad. Mitarbeiter:	Dr. Ruth Kiefer

Scientific contributions

Peer-reviewed articles

Kuhl M, Gläser L, Rebets Y, Rückert C, Sarkar N, Hartsch T, Kalinowski J, Luzhetskyy A, and Wittmann C (2020): Microparticles globally reprogram *Streptomyces albus* toward accelerated morphogenesis, streamlined carbon core metabolism and enhanced production of the antituberculosis polyketide pamamycin. *Biotechnol. Bioeng*. 117:3858-3875

Kuhl M, Rückert C, Gläser L, Beganovic S, Luzhetskyy A, Kalinowski J, and Wittmann C (2021): Microparticles enhance the formation of seven major classes of natural products in native and metabolically engineered actinobacteria through accelerated morphological development. *Biotechnol. Bioeng*. In press.

Gläser L, **Kuhl M**, Jovanovic S, Fritz M, Vögeli B, Erb T, Becker J, and Wittmann C (2020): A common approach for absolute quantification of short chain CoA thioesters in prokaryotic and eukaryotic microbes. *Microb. Cell Fact*. 19:160.

The following peer-reviewed articles were co-authored during this work, but are not part of the dissertation:

Gummerlich N, Manderscheid N, Rebets Y, Myronovskyi M, Gläser L, **Kuhl M**, Wittmann C, and Luzhetskyy A (2021): Modulating the production of pamamycins through engineering the precursor pool in the heterologous host *S. albus* J1074. *Met. Eng*. 67, 11-18.

Gläser L, **Kuhl M**, Stegmüller J, Rückert C, Myronovskyi M, Kalinowski J, Luzhetskyy A, and Wittmann C (2021): Superior production of heavy pamamycin derivatives using a *bkdR* deletion mutant of *Streptomyces albus* J1074/R2. *Microb. Cell Fact*. 20:111.

Conference contributions

Kuhl M, Gläser L, Rebets Y, Rückert C, Kalinowski J, Luzhetskyy A, and Wittmann C. Molecular reprogramming of *Streptomyces albus* for improved pamamycin production using microparticle enhanced cultivation, HIPS Helmholtz Institute for Pharmaceutical Research Saarland Symposium, 27th - 28th June 2019, Saarbrücken, Germany

Kuhl M, Gläser L, Rebets Y, Rückert C, Kalinowski J, Luzhetskyy A, and Wittmann C. Molecular reprogramming of *Streptomyces albus* for improved pamamycin production using microparticle enhanced cultivation, 14th International Symposium on the Genetics of Industrial Microorganisms, 8th - 11th September 2019, Pisa, Italy

Beganovic S, Becker J, **Kuhl M**, Gläser L, and Wittmann C. MISSION to Morphology - bioprocess engineering for natural product formation in *Streptomyces*, 13th Meeting of the Slovenian Biochemical Society, 24th - 27th September 2019, Dobrna, Slovenia

Danksagung

Mein größter Dank gilt Prof. Dr. Christoph Wittmann für all das, was er mir seit Beginn meines Forschungspraktikums am iSBio vor viereinhalb Jahren ermöglicht hat. Ich danke ihm zutiefst für all die Unterstützung auf und neben dem Platz, die wissenschaftlichen Ratschläge, das entgegengebrachte Vertrauen und die damit einhergehende Freiheit bei der Umsetzung der Forschungsarbeiten. Durch den vertrauensvollen Umgang, auch über die Forschungsarbeiten hinaus, konnte ich mich sowohl fachlich als auch persönlich sehr weiterentwickeln.

Bei Prof. Dr. Andriy Luzhetskyy möchte ich mich sehr für die Übernahme der Zweitkorrektur und die gelungene Zusammenarbeit im MyBio-Projekt bedanken.

Ein besonderer Dank gebührt meinem Freund und langjährigem Kollegen Lars Gläser, der mich auf meiner akademischen Laufbahn begleitet, seit ich 2015 nach Saarbrücken gekommen bin. Wir haben gleichzeitig unsere Masterarbeit begonnen und schließen nun auch gemeinsam unsere Promotion ab. Rock am Ring, Pisa und Braunwald sind nur einige der Dinge, die wir seither zusammen erlebt haben und auch wenn sich unsere beruflichen Wege fürs erste nun trennen, bin ich fest davon überzeugt, dass dies privat nicht der Fall sein wird.

Weiterhin möchte ich mich sehr bei meinen Freunden Demian Dietrich und Dr. Gideon Gießelmann bedanken. Für die Unterstützung im Labor, aber auch für die vielen unterhaltsamen Momente außerhalb.

Besonders möchte ich meinen Dank auch an Michel Fritz richten, der mir in allen Aspekten rund um das Thema Analytik stets zur Seite stand. Außerdem bedanke ich mich bei Christina Rohles, Sarah Hoffmann, meinen offiziellen Bürokollegen Peng Cao und Dennis Schulze, meinen inoffiziellen Bürokolleginnen Selma Beganovic und Sofija Jovanovic sowie allen aktuellen und ehemaligen Kollegen am iSBio, die entscheidend zu meinem Werdegang beigetragen haben. An dieser Stelle möchte ich mich außerdem auch bei Dr. Judith Becker bedanken, die sich zu Beginn meiner Forschungsarbeiten am iSBio um mich kümmerte und mir meinen Start leicht gemacht hat.

Abschließend möchte ich mich natürlich auch zutiefst bei meiner Familie sowie allen namentlich nicht genannten Freunden für die Unterstützung und die vielen schönen Momente abseits der Arbeit bedanken. Meinen Eltern Trude und Paul bin ich unendlich dankbar für die Sicherheit, die sie mir immer gegeben haben und auch jetzt noch geben, gleichwohl was ich mir vornehme. Meiner Freundin Karolin danke ich besonders für die moralische Stütze nach (zum Glück nicht so häufig vorkommenden) Rückschlägen. Auch wenn noch Unklarheit darüber besteht, wo genau unser Weg uns hinführen wird, bin ich froh ihn gemeinsam mit dir bestreiten zu dürfen.

Summary

Actinobacteria, especially the genus *Streptomyces*, provide a plethora of bioactive natural products. Over the last years, the ubiquitous use of antibiotics resulted in the increasing threat of resistant bacteria, explaining the intense research efforts nowadays to identify new bioactive substances and to improve production. Here, we studied the use of inorganic talc microparticles to enhance natural product formation in actinobacteria. Addition of talc to *S. albus* J1074/R2 tripled pamamycin production up to 50 mg L^{-1}, yielded a specific production spectrum of the derivatives, and strongly reduced pellet size. Systems biology analyses demonstrated the underlying mechanism of the production shift and revealed a globally reprogrammed gene expression. Supplied to *S. lividans* TK24 DG2-Km-P41hyg+, talc led to increased production of 109 mg L^{-1} of combined bottromycin A2, a promising antibiotic for drug development. Talc presence resulted in an increased production efficiency by rebalancing the cluster expression and caused an accelerated morphogenesis. Finally, we miniaturized the setup and examined the production of twelve natural products from different actinobacterial genera. In 75% of the studied cases, talc enhanced natural product formation and was even crucial for teicoplanin production. Due to the effectiveness and simplicity, morphology engineering of actinobacteria using talc microparticles appears as a promising approach for future applications.

Zusammenfassung

Actinobacteria, insbesondere die Gattung *Streptomyces*, liefern eine Vielzahl an bioaktiven Naturstoffen. In den letzten Jahren führte der verstärkte Einsatz von Antibiotika zu einer zunehmenden Bedrohung durch resistente Bakterien, was die heutige intensive Forschung nach neuen bioaktiven Substanzen und deren Produktionsoptimierung begründet. Hier untersuchten wir die Verwendung von anorganischen Talk-Mikropartikeln, um die Naturstoffbildung in Actinobacteria zu steigern. Die Zugabe der Mikropartikel zu *S. albus* J1074/R2 verdreifachte die Pamamycin-Produktion auf bis zu 50 mg L^{-1}, ergab ein spezifisches Spektrum der Derivate und reduzierte deutlich die Pelletgröße. Systembiologische Analysen offenbarten die Ursache der Produktverschiebung sowie eine global umprogrammierte Genexpression. Addition von Talk zu *S. lividans* TK24 DG2-Km-P41hyg+, führte zu einer beschleunigten Morphogenese und zu einer gesteigerten Produktion von 109 mg L^{-1} Bottromycin A2, indem es die Clusterexpression neu ausbalancierte. Abschließend miniaturisierten wir das Setup und untersuchten die Produktion von zwölf Naturstoffen aus verschiedenen Actinobacteria-Gattungen. In 75% der untersuchten Fälle förderte die Zufuhr von Talk die Bildung des Naturprodukts und war sogar entscheidend für die Produktion von Teicoplanin. Aufgrund seiner Effektivität und Einfachheit erscheint Morphologie-Engineering von Actinobacteria mittels Talk-Mikropartikeln als vielversprechender Ansatz für zukünftige Anwendungen.

Table of content

1 Introduction

1.1 General introduction

Actinobacteria are the most important source of natural products, chemically diverse molecules with an extremely high industrial interest (Harvey, 2000; Barka et al., 2016). This interest has been steadily increasing, since Alexander Fleming discovered the first industrially used antibiotic penicillin in 1928 (Fleming, 2001). Most compounds with antibacterial activities were discovered between the 1950s and the 1970s, also known as 'the Golden Era' of microbial natural product discovery (Brown & Wright, 2016). The time period after the Golden Era was marked by a severe decline in natural product identification, due to frequent rediscovery of known compounds and the opinion that one strain is unable to produce more than 3-4 molecular entities (Horbal et al., 2018). This theory was refuted with the discovery from genome sequencing that microbes with large genomes are able to produce about ten times as many secondary metabolites as previously recognized and that the most gifted Actinomycetes have even the capacity to produce around 30-50 secondary metabolites (Katz & Baltz, 2016). Again, a new era in natural product discovery has begun (Katz & Baltz, 2016). Many natural products have potent biological activities that function nowadays as antibiotics (Fleming, 2001), anti-cancer drugs (Arcamone et al., 1969), immunosuppressants (Vézina et al., 1975), -infectants (Campbell et al., 1983), herbicides (Bayer et al., 1972), insecticides (Butterworth & Morgan, 1968), and fungicides (Takeuchi et al., 1958; Kuhl et al. 2021). Thus, the discovery and commercial use of natural products and their derivatives helped to double human life expectations during the last century (Demain, 2006). As wide-ranged as their commercial application, is also their chemical diversity, relying on complex biosynthetic pathways and distinct backbones, as e.g. polyketides, β-lactams, peptides, and pyrroles, amongst many others (Challis & Hopwood, 2003; Berdy, 2005; van Wezel & McDowall, 2011).

Every year, around 700,000 people die due to an infection with a multi-drug resistant superbug (Plackett, 2020). It is estimated that, if no action is taken, this number could rise to 10 million people by 2050, which would be more than the number of people who currently die from cancer worldwide every year (Plackett, 2020). Therefore, the development of natural products into new commercially applied drugs is of great importance. Two interesting natural product candidates for this next step are the polyketide pamamycin, with high antimicrobial activity against Gram-positive bacteria, fungi and mycobacteria, and the ribosomally synthesized and post-translationally modified peptide (RiPP) bottromycin, effective against methicillin-resistant

Staphylococcus aureus (MRSA) and vancomycin-resistant *Enterococci* (VRE), among other Gram-positive bacteria and mycoplasma (Lefèvre et al., 2004; Kobayashi et al., 2010). Researchers today still have a high interest in their examination, despite the fact that both substances were already isolated from *Streptomyces* cultures for the first time in the Golden Era (Waisvisz et al., 1957; McCann & Pogell, 1979). The genus *Streptomyces*, belonging to the phylum of actinobacteria, provides today more than two-third of all known antibiotics of microbial origin (Bibb, 2013) and more than half of the FDA-approved antibacterial natural products (Patridge et al., 2015). Unfortunately, cultivation of a microbe out of its natural habitat is not always feasible and actinobacteria often produce natural products in insufficient amounts or do not form them at all under laboratory conditions (Ren et al., 2017). Therefore, it does not seem too surprising that immense efforts are being made to investigate and manipulate their unique morphological life cycle, as the link between morphological development and natural product formation is well known for a long period of time (Chater, 1984; Angert, 2005; Van Wezel et al., 2006; van Dissel et al., 2014; Barka et al., 2016). A promising method in this regard could be microparticle-enhanced cultivation (MPEC). Recent reports showed that MPEC could be beneficial to enhance product formation in filamentous prokaryotes (Ren et al., 2015; Holtmann et al., 2017; Walisko et al., 2017; Liu et al., 2019). The approach was introduced in 2008 to enhance enzyme production in eukaryotic filamentous fungi and pioneering studies demonstrated that with the supply of inorganic microparticles it is possible to streamline the morphology of these organisms (Kaup et al., 2008; Driouch et al., 2010c; Driouch et al., 2010b; Driouch et al., 2012). Since then, several studies reported great success stories of MPEC with fungi, as they were able to enhance the formation of further enzymes, alcohols, polyketides, and drugs (Walisko et al., 2012; Coban et al., 2015; Etschmann et al., 2015; Antecka et al., 2016b; Gonciarz et al., 2016; Yatmaz et al., 2016).

1.2 Main objectives

The aim of this work was to establish a new production platform for natural products in actinobacteria based on the concept of microparticle-enhanced cultivation. In a first step, the exploration of pamamycin production in recombinant *Streptomyces albus* J1074/R2 and bottromycin production in recombinant *Streptomyces lividans* TK24 DG2-Km-P41hyg+ should give insights on how particles affected the physiology of the hosts. Careful analysis of submerged pellet morphology, substrate consumption, precursor supply, and global gene expression should reveal similarities and differences between the two setups. The data should give a systems-level portrait on how microparticles affect morphogenesis.

Then, in a second step, the approach should be tested on a broader scale to investigate its potential in generally overproducing natural compounds of commercial interest from different structural classes in native and metabolically engineered actinobacteria, including Streptomycetes but also other genera, i.e. *Amycolatopsis, Actinoplanes,* and *Kitasatospora.* Thereby, potential application of microparticle-enhanced cultivation of actinobacteria in industrial processes should be evaluated.

2 Theoretical Background

2.1 The biology of actinobacteria

Actinobacteria form one of the greatest bacterial phyla and can be found equally in terrestrial and aquatic ecosystems (Barka et al., 2016). They not only play an important role as symbionts and pathogens in plant-associated microbial communities, but they are also of great industrial importance for biotechnology, medicine, and agriculture, as they hold a treasure for bioactive secondary metabolites and produce the majority of naturally occurring antibiotics (Barka et al., 2016). The first antibiotics of actinobacteria were already discovered in the early 1940s: actinomycin from a culture of *Streptomyces antibioticus* in 1940, streptothricin from a culture of *Streptomyces lavendulae* in 1942, and streptomycin from a culture of *Streptomyces griseus* in 1944 (Waksman & Woodruff, 1940; Waksman & Woodruff, 1942; Schatz & Waksman, 1944). Besides *Streptomyces,* genera such as *Mycobacterium, Micromonospora, Amycolatopsis,* or *Kitasatospora* are famous for their production of secondary metabolites (Barka et al., 2016). Actinobacteria are Gram-positive bacteria with a high guanine-plus-cytosine (G+C) DNA content in their genomes, which results in a higher stability of the genome, but also can hinder the genetic accessibility (Sinden, 1994). With some exceptions, actinobacteria are aerobic. Most of them are chemoheterotrophic and are able to use a wide variety of nutrients, including numerous complex polysaccharides (Lechevalier & Lechevalier, 1965; Zimmermann, 1990; Barka et al., 2016). The majority of actinobacteria is mesophilic and favors a neutral pH. They grow optimally at a temperature between 25 and 30 °C and a pH value between 6 and 9, with maximum growth around neutrality (Edwards, 1993). Actinobacteria exhibit a wide variety of morphologies with many of them, especially Actinomycetes, possessing a mycelial life-cycle with complex morphological differentiation such as eukaryotic fungi (Barka et al., 2016). The morphology mainly differs with regard to the presence or absence of a substrate mycelium or aerial mycelium, the color of the mycelium, the production of diffusible melanoid pigments, and the structure and appearance of spores (Figure 1) (Barka et al., 2016). Mycelial fragmentation is regarded as a special form of vegetative reproduction, albeit actinobacteria with primarily mycelial lifestyles usually reproduce by forming asexual spores (Barka et al., 2016). These spores dominate the life-cycles of most actinobacteria, as they live for the majority of their life-span under nutritional limitation, waiting for the occurrence of nutrients and ensuring the survival of the progenies (Mayfield et

al., 1972). Populations isolated from soil are dominated by the genus *Streptomyces,* which accounts for 95% of the isolated strains (Williams & Vickers, 1988).

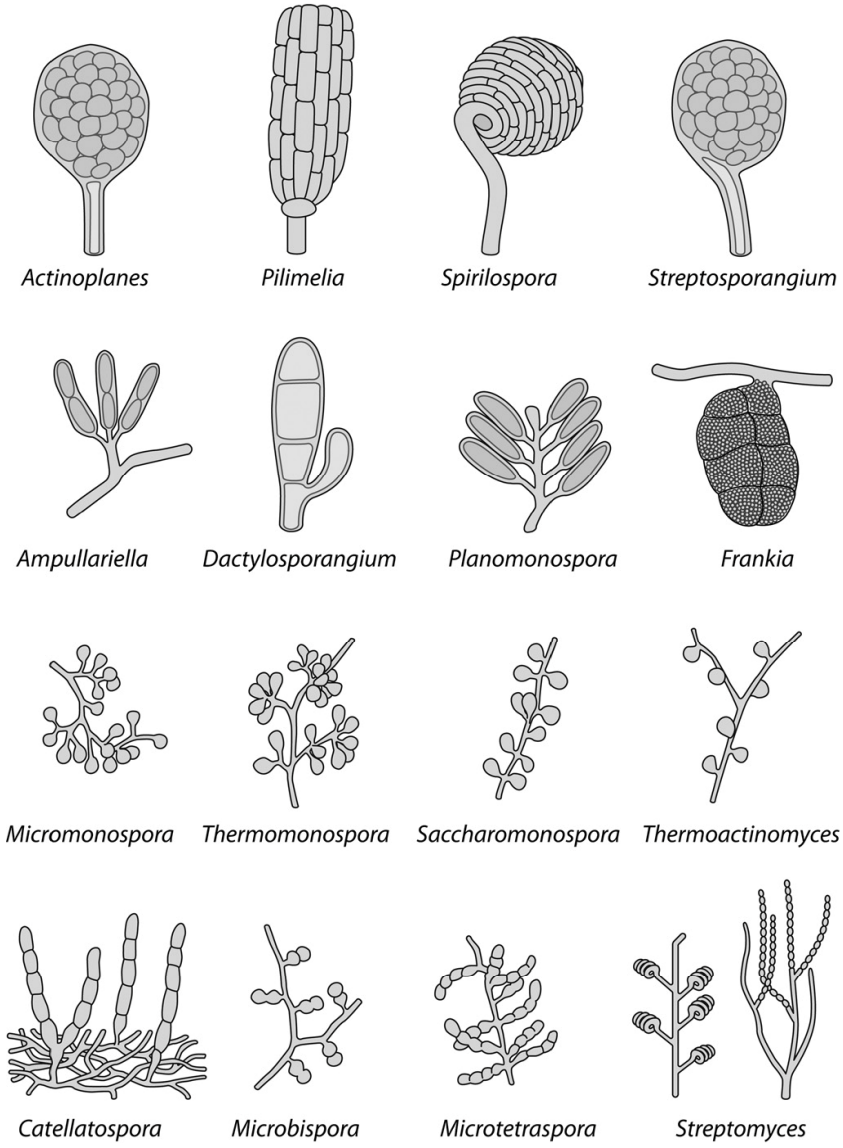

Figure 1: Schematic drawings of spore chains produced by different genera of Actinomycetes. Besides the presence or absence of a substrate or aerial mycelium, the color of the mycelia, and the production of diffusible melanoid pigments, the morphology of actinobacteria differs in the structure and appearance of their spores. From (Barka et al., 2016). Reprinted with permission of AMS.

2.2 The genus *Streptomyces* and its role in antibiotic production

Antimicrobial Resistance (AMR) occurs when bacteria, viruses, fungi and parasites adopt over time and no longer respond to medicines making infections harder to treat and increasing the risk of disease spread, severe illness and death (WHO, 2020). Resistance is strongly increasing

today, largely driven by ubiquitous use of antibiotics (Figure 2), often with little or no therapeutic benefit, e.g. to treat viral respiratory ailments and the non-therapeutically use in agriculture to promote livestock growth (Van Boeckel et al., 2017; Pouwels et al., 2018; Roope et al., 2019). Additionally, widespread use of broad-spectrum antibiotics, which are effective against a variety of bacteria, has greater potential for selecting for extensive antibiotic resistance than drugs that target specific bacteria. Antibiotic resistance undermines much of modern health care, which relies on access to effective antibiotics to prevent and treat infections associated with routine medical procedures (Roope et al., 2019). Streptomycetes produce approximately two-thirds of all known antibiotics of microbial origin (Bibb, 2013). Therefore, the microbes play a crucial role in the development of new drugs and in the fight against multi-resistant superbugs (Hopwood et al., 1995; Ilic et al., 2007).

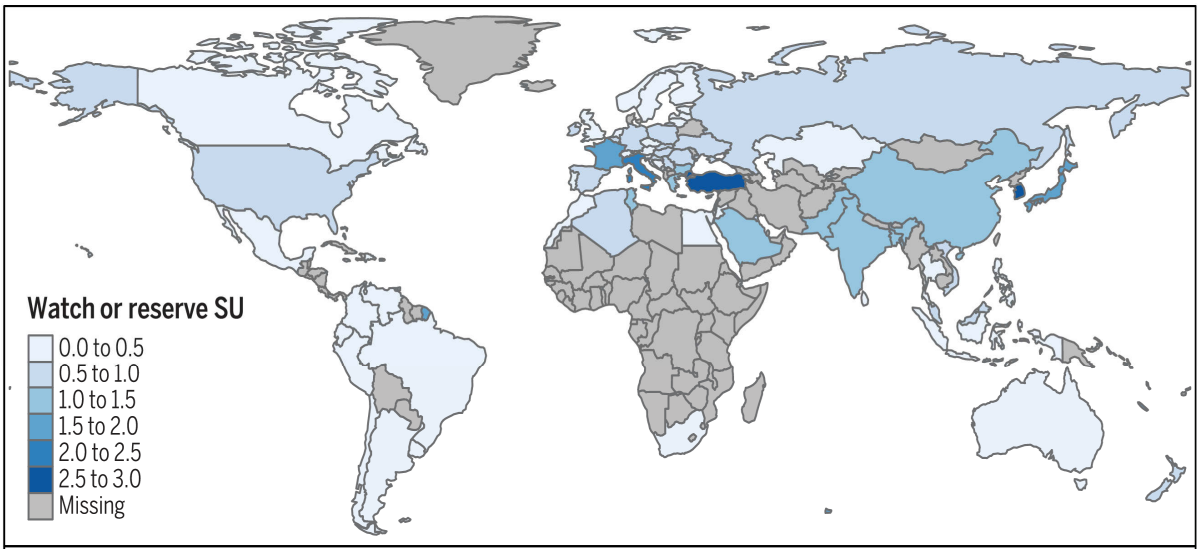

Figure 2: Excess antibiotic use versus access-related mortality in young children. The map demonstrates use of so-called "watch" and "reserve" antibiotics in standard units (SU) per 100,000 children under the age of 6. The World Health Organization's watch group includes antibiotics that are recommended as first- or second-choice treatments for only a small number of infections. The reserve group includes antibiotics that should be considered last-resort options and used only in the most severe circumstances, when all other alternatives have failed. From (Roope et al., 2019). Reprinted with permission from AAAS.

Scientists have known for many years that single *Streptomyces* strains are able to produce a rich spectrum of bioactive secondary metabolites and famous compounds like actinorhodin (Act), undecylprodigiosin (Red) or the calcium dependent antibiotic (CDA) were isolated very early (Rudd & Hopwood, 1979; Hopwood & Wright, 1983; Feitelson et al., 1985). However, with the ability to sequence numerous complete genomes at low costs, scientists discovered that the

potential of the microbes was underestimated for a long time and that single strains with large genomes have the capacity to produce more than ten times as many antibiotics as previously recognized (Katz & Baltz, 2016). As for the example of *S. coelicolor,* a well-studied member, its genome holds more than 20 different (cryptic) biosynthetic gene clusters (Barka et al., 2016). Therefore, the importance of Streptomycetes for production of novel drugs is even higher than previously assumed and scientists aim for new genetic approaches to activate these cryptic, silent, or sleeping antibiotics (Gross, 2009; Zerikly & Challis, 2009; Medema et al., 2011). In addition, activation of silent clusters can be achieved by manipulating cultivation parameters, such as nutrient content, temperature, pH value, the addition of enzyme inhibitors, and rate of aeration. The use of cultivation based approaches is commonly known under the name OSMAC (one strain many compounds) and underlines how a single strain can produce different molecules when grown under different environmental conditions (Romano et al., 2018). In a recent study, the marine-derived *Streptomyces sp.* YB104 was grown in different media and screened for bioactive natural products. The analysis of metabolic profiles from different conditions resulted in the discovery of new compounds that were only present, when the strain was cultured in ACM medium, which indicates how dependent the production of secondary metabolites is on cultivation parameters (Wu et al., 2018; Ahmed, 2019). The model organism for control of antibiotic production in *Streptomyces* is *S. coelicolor* (Barka et al., 2016). Secondary metabolite production in *Streptomyces* correlates to the onset of morphological development (Bibb, 2005). This correlation is highly conserved and presumably evolved as strains need to compete with other microbes, when undergoing programmed cell death (PCD) under nutrient limiting conditions (van Wezel & McDowall, 2011).

2.2.1 The morphology of *Streptomyces*

Streptomycetes play key roles in soil ecology because of their ability to hydrolyze a wide range of polysaccharides (cellulose, chitin, xylan, and agar) and other natural macromolecules (Chater et al., 2010). The life-cycle of multicellular Streptomycetes starts with the germination of a single spore after sensing local nutrients (Figure 3) (Chater, 1972). The spores develop into hyphal filaments, which, in contrast to unicellular bacteria, grow linear by tip extension (Flärdh, 2003). Exponential growth is characterized by a combination of tip extension and a branching of these vegetative hyphae, which is defined as cell division. Thereby, a dense substrate mycelium is formed, which is present in submerged and solid-grown cultures (Angert, 2005; van Dissel et al., 2014). Unfavored conditions, such as environmental stress or local nutrient

depletion, trigger a complex signaling cascade, which causes the production of a surfactant that coats emerging filaments to form sporogenic structures, called aerial hyphae (Barka et al., 2016). The unbranched cells at the end of the aerial filaments differentiate and form synchronously uninucleoid cells that further develop into spores, where the whole cycle repeats (Angert, 2005). In competitive soil habitants, the timing of development is crucial. Under conditions with sufficient nutrient supply, *Streptomyces* strive for maximum vegetative growth, while during starvation, sporulation and subsequent spore dispersal are essential for the survival of the colony (Barka et al., 2016). To provide building blocks for these aerial mycelia in times of nutrient depletion, *Streptomyces* degrades the substrate mycelium in a way similar to programmed cell death (PCD) mechanisms (Méndez et al., 1985; Miguélez et al., 1999; Manteca et al., 2006). This allows cells to gather precursors for the next round of biomass formation, such as amino acids, lipids, carbohydrates, and nucleotides (Kim et al., 1995; Manteca et al., 2006; Rigali et al., 2006). It is understandable that this time point coincides with the period of highest antibiotic formation, as the increased building block availability, in a usually nutrient depleted area, attracts competing motile microbes (Barka et al., 2016; Tenconi et al., 2018). DNA binding of the nutrient sensory regulator DasR is mediated by binding *N*-acetylglucosamine-related metabolites as ligands, giving an example for the metabolic control of antibiotic production and morphogenesis (Rigali et al., 2006).

Prominent categories of developmental genes required for the formation of aerial hyphae and spores include the *bld* genes (bald, “hairless”, aerial hyphae of mutants lack fluffy characteristic), the *whi* genes (white, mutants fail to produce the gray spore pigment), the *ram* genes (for rapid aerial mycelium), and the *ssgA*-like genes (for sporulation of *Streptomyces griseus*) (Figure 4) (Hopwood et al., 1970; Merrick, 1976; Ma & Kendall, 1994; Traag & van Wezel, 2008; Barka et al. 2016). Over the years, extensive research has unraveled the regulation of aerial mycelium and spore formation. The majority of *bld* and *whi* genes, known today, has regulatory function, with many of them encoding transcription factors (Barka et al., 2016). Among the most studied genes are the highly pleiotropic transcription factor *bldD*, the RNA polymerase σ-factors *bldN, sigN* and *whiG*, and *whiH* (Mendez & Chater, 1987; Den Hengst et al., 2010; Bibb et al., 2012; Persson et al., 2013; Barka et al. 2016; Rebets et al., 2018).

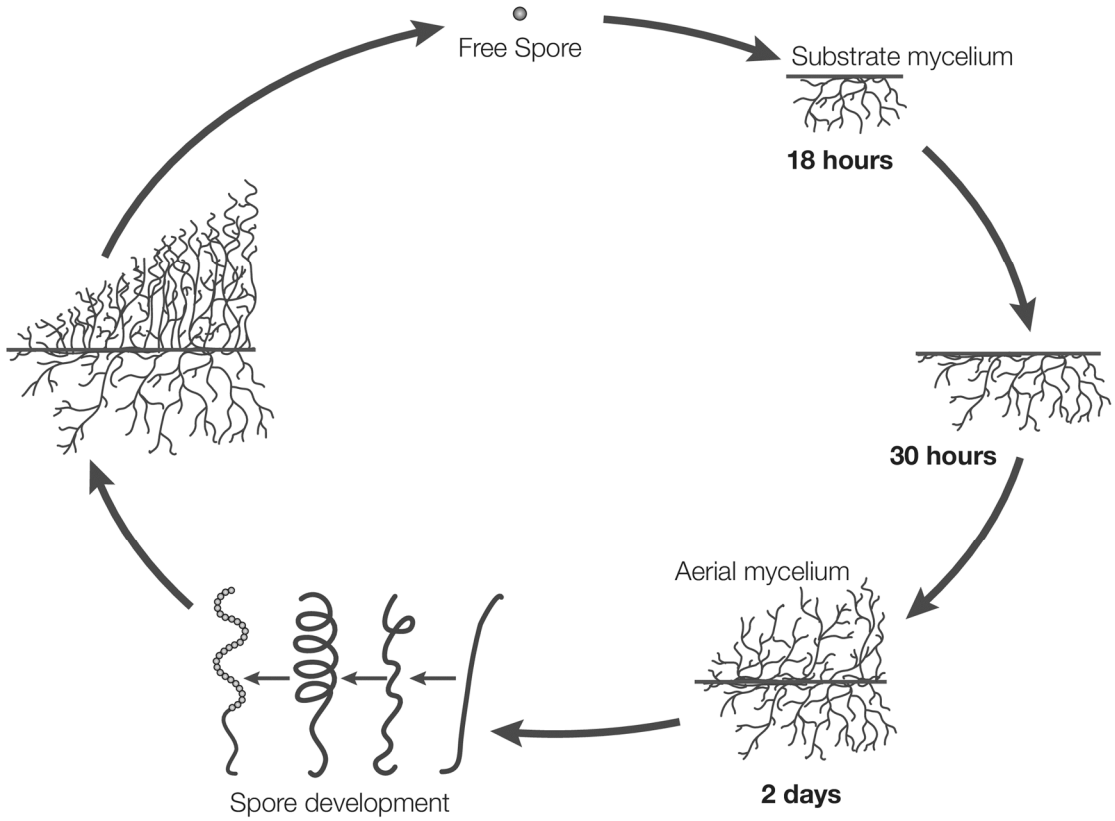

Figure 3: Schematic drawings of the morphological development of Streptomycetes. The life-cycle starts with the germination of singles spores, from which a hyphal filament emerges and grows by tip extension. Cell division is defined by a branching of these hyphae and leads to a dense network, called substrate mycelium. Environmental stress, such as nutrient depletion, causes a complex signaling cascade, which triggers the production of a surfactant that coats emerging filaments. These aerial hyphae possess different characteristics from those of the substrate mycelium. At the end of these aerial filaments, the unbranched cells synchronously divide and form uninucleoid cells, which maturate again into spores. From (Angert, 2005). Reprinted with permission from Springer Nature.

Aerial hyphae are responsible for the fluffy characteristic of *Streptomyces* colonies (Flärdh & Buttner, 2009). The characteristics of aerial hyphae vary significantly from the vegetative ones of the substrate mycelium, as they do not branch as extensively, as they are nearly twice as wide as the vegetative hyphae, and as they are surrounded by a hydrophobic layer (Wildermuth et al., 1971; Claessen et al., 2003). This layer, the so-called rodlet layer, is formed by a number of hydrophobic chaplin and rodlin proteins (Claessen et al., 2004). The *chp* and *rdl* genes, encoding for these proteins, give just two examples for the numerous genes regulated by the σ-factor *bldN* (Bibb et al., 2012). Chaplin proteins form the main building blocks of the rodlet layer (van Dissel et al., 2014). Eight chaplins are present in *S. coelicolor*, three large (ChpABC) and five smaller ones (ChpDEFGH). ChpC, ChpE, and ChpH are essential for sporulation (Claessen et al., 2003; Di Berardo et al., 2008). Although the rodlin proteins are required for

the alignment of the rodlet structures, they are not essential for sporulation (Claessen et al., 2002).

Ultimately, the *Streptomyces* life-cycle requires the cessation of aerial hyphae growth and the onset of sporulation-specific cell division (Figure 4) (Barka et al., 2016). Mutations of *whiA, whiB,* and *ssgB*, involved in this signal transmission resulted in cultures with proportionally large aerial mycelia (Chater, 1972; Kormanec et al., 1998; Keijser et al., 2003). In contrast to cell division in vegetative mycelia, sporulation-specific cell division in aerial hyphae occurs simultaneously by forming many septa that divide the hyphae into spore compartments. Cell fission then results in chains of individual spores, each with a single copy of the chromosome (Jakimowicz & van Wezel, 2012). The SsgA-like proteins (SALPs) play a key role in septum localization, with both *ssgA* and *ssgB* required for sporulation (Barka et al., 2016). While the sporulation and cell division protein SsgA activates sporulation-specific cell division, SsgB directly recruits and stimulates polymerization of FtsZ (Van Wezel et al., 2006; van Dissel et al., 2014). Thereby, SsgB is responsible for the symmetrical spacing of the Z-rings (Willemse et al., 2011). FtsZ is highly conserved among prokaryotes and also crucial for binary fission, the mode how most bacteria divide (Angert, 2005). The large impact of SsgA on morphogenesis was demonstrated by microarray analysis, which showed that deletion of *ssgA* affects expression of an unprecedented large number of genes, with many hundreds of genes up- or downregulated by at least twofold, including most developmental genes (e.g. *bld*, *whi* and *ssg* genes), as well as many genes involved in DNA segregation and topology (Noens et al., 2005; Traag & van Wezel, 2008). On the other hand, a *ssgA*-overexpressing mutant of *S. coelicolor* led to an increased septum formation, a high production of spore-like compartments, and significantly wider hyphae that contained irregular and often extremely thick septa (van Wezel et al., 2000). Furthermore, s*sgA* has a strong influence on antibiotic production, as an overexpressing mutant of *S. coelicolor* indicated a strongly enhanced undecylprodigiosin (Red) production (van Wezel et al., 2000). Simultaneously, the strain was no longer capable of actinorhodin production, possibly due to an arrest in development at a time where actinorhodin production has not been initiated (van Wezel et al., 2000). In contrast, Red production occurs during vegetative growth and (perhaps as a consequence) benefits from fast and fragmented growth of the *ssgA* mutant (van Dissel et al., 2014). Additionally, a *ssgA*-overexpressing strain of *S. lividans* revealed a twofold increased yield of enzyme production (Van Wezel et al., 2006)

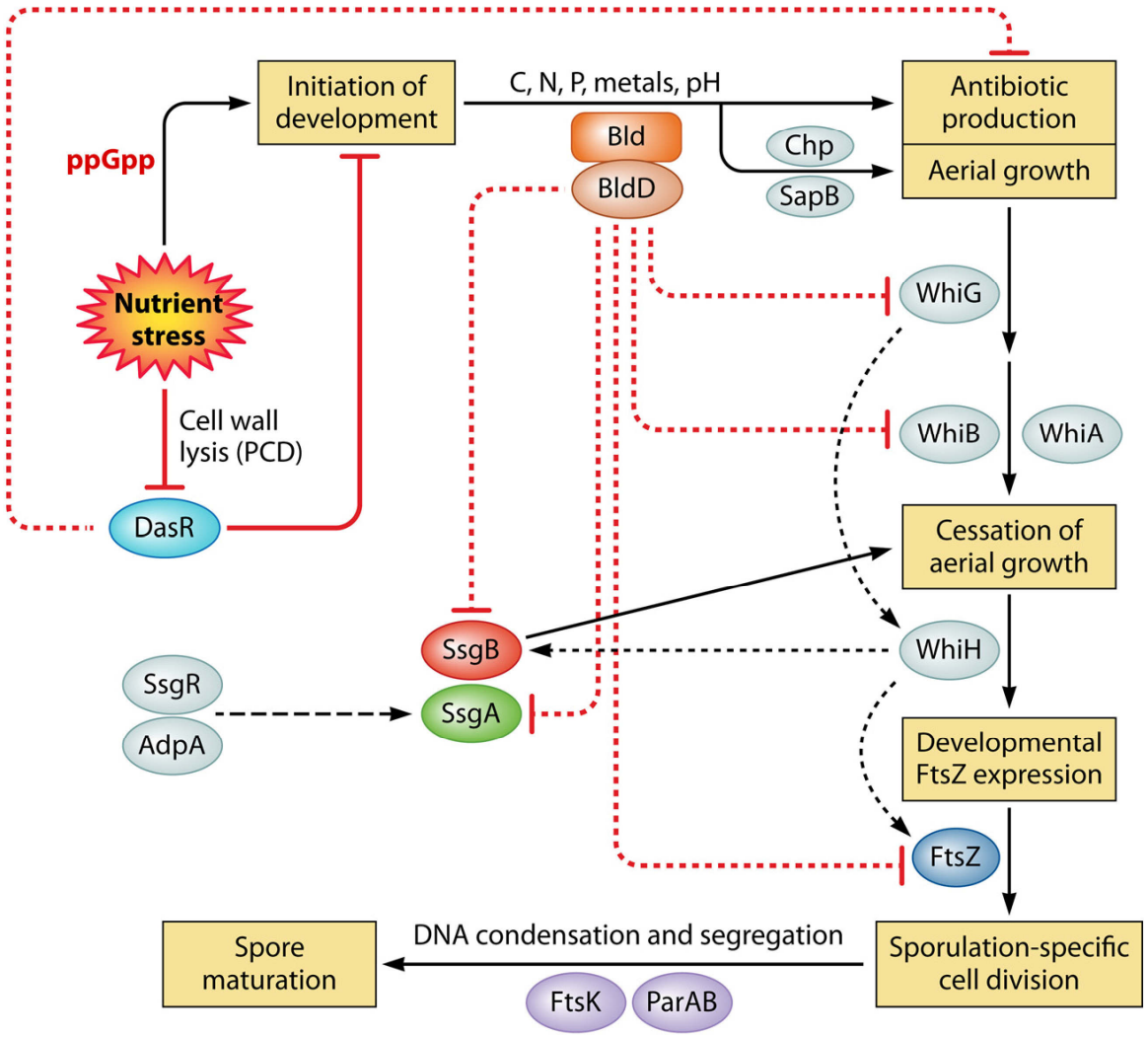

Figure 4: *Streptomyces* morphogenesis. Nutrient limitation and environmental stress are major triggers of development, leading to the accumulation of ppGpp. This results in cessation of early growth and repression of the nutrient sensory DasR protein by PCD of the substrate mycelium. Bld proteins and environmental signals control the procession toward aerial growth and antibiotic production. The developmental master regulator BldD only represses the transcription of genes for many key developmental regulatory proteins when bound to tetrameric cyclic-di-GMP. These genes include *whiB*, *whiG*, *ssgAB*, and *ftsZ*. FtsZ accumulates, localizes to septum sites in an SsgAB-dependent manner and ladders of FtsZ subsequently define spore compartments, followed by spore maturation. The production of antibiotics is typically linked to the morphological differentiation from vegetative to aerial growth. Solid black arrows represent major transitions in development, while dotted lines indicate transcriptional control. From (Barka et al., 2016). Reprinted with permission of AMS.

Growth and morphology of mycelial mass is in part strain-dependent, especially in submerged cultures (van Dissel et al., 2014). In general, morphologies in liquid cultures can be categorized in three types: freely dispersed mycelia that behave like single cells with high mass transfer properties (e.g. *S. venezuelae*), open mycelial networks that generally have good mass transfer characteristics, but increase the viscosity of the media (e.g. *S. albus*), and pellets that do not increase the viscosity significantly, but often contain a nutrient-deprived center (e.g. *S. lividans*)

(Paul & Thomas, 1998; van Dissel et al., 2014). The great number of parameters that influence how the mycelia grow, branch, aggregate, and fragment, also leads to a large heterogeneity of phenotypes that coexist inside the bioreactor (van Dissel et al., 2014). It also has to be noted that not all Streptomycetes form spores in liquid cultures and that some strains only sporulate in nutrient-limiting media (Kendrick & Ensign, 1983). For instance, *S. lividans*, in contrast to *S. albus,* does not sporulate in liquid culture (Daza et al., 1989; Rebets et al., 2018). However, a big advantage of sporulation studies in submerged cultures over studies in solid-grown cultures is that they enable global expression profiling by systems biology approaches like transcriptome, proteome, or metabolome analysis (Zhou et al., 2011). We are only beginning to unravel the mechanisms that control morphogenesis of Streptomycetes, and this is particularly true for mycelial growth in submerged cultures. At the same time, understanding the correlation between morphogenesis and productivity is of critical importance for the exploitation of Streptomycetes in the industrial domain (van Dissel et al., 2014).

2.3 Natural Products of actinobacteria

Due to the extensive research for the past decades, more than ten thousand natural compounds have been derivatized from different microbial sources (Nair & Abraham, 2020). Because of their wide application possibilities in the biotechnological, pharmaceutical, and agricultural industries, products have been used extensively as antibiotics, anti-tumor agents, immunosuppressants, insecticides, herbicides, and antifungal agents (Nair & Abraham, 2020). Examples of major antibiotic groups are tetracyclines, cephalosporines, aminoglycosides, glycopeptides, polyketides, and RiPPs (ribosomally synthesized and post-translationally modified peptides), highly diverse in their molecular structures (Figure 5) (van Wezel & McDowall, 2011). As previously mentioned, the great majority of bioactive substances is derived from the genus *Streptomyces,* but also other secondary metabolite producers, such as *Amycolatopsis, Actinoplanes, Micromonospora* and Myxobacteria are of great importance (Bibb, 2013; Barka et al., 2016). Certain compounds produced by *Streptomyces spp*. have such a high toxicity that they are even lethal for human consumption, regardless of the kind of application (Nair & Abraham, 2020). Some natural products occur at a much higher frequency than others. For example, streptothricin (10%), streptomycin (1%), and actinomycin (0.1%) are present in a higher proportion among random *Streptomyces* isolates than e.g. erythromycin (0.001%), vancomycin (0.001%), and daptomycin (0.00001%) (Baltz, 2007; Barka et al., 2016).

Therefore, it is no surprise that actinomycin, streptomycin, and streptothricin were the first antibiotics isolated from actinobacteria (Barka et al., 2016). Albeit the natural function of many secondary metabolites is considered to be as antibiotics that thwart the growth of competing microorganisms, there are clear examples of roles in cell communication and signaling (van Wezel & McDowall, 2011). In the following, the polyketide pamamycin and the RiPP bottromycin, the main products that were investigated in this work and the used strains, will be highlighted in more detail.

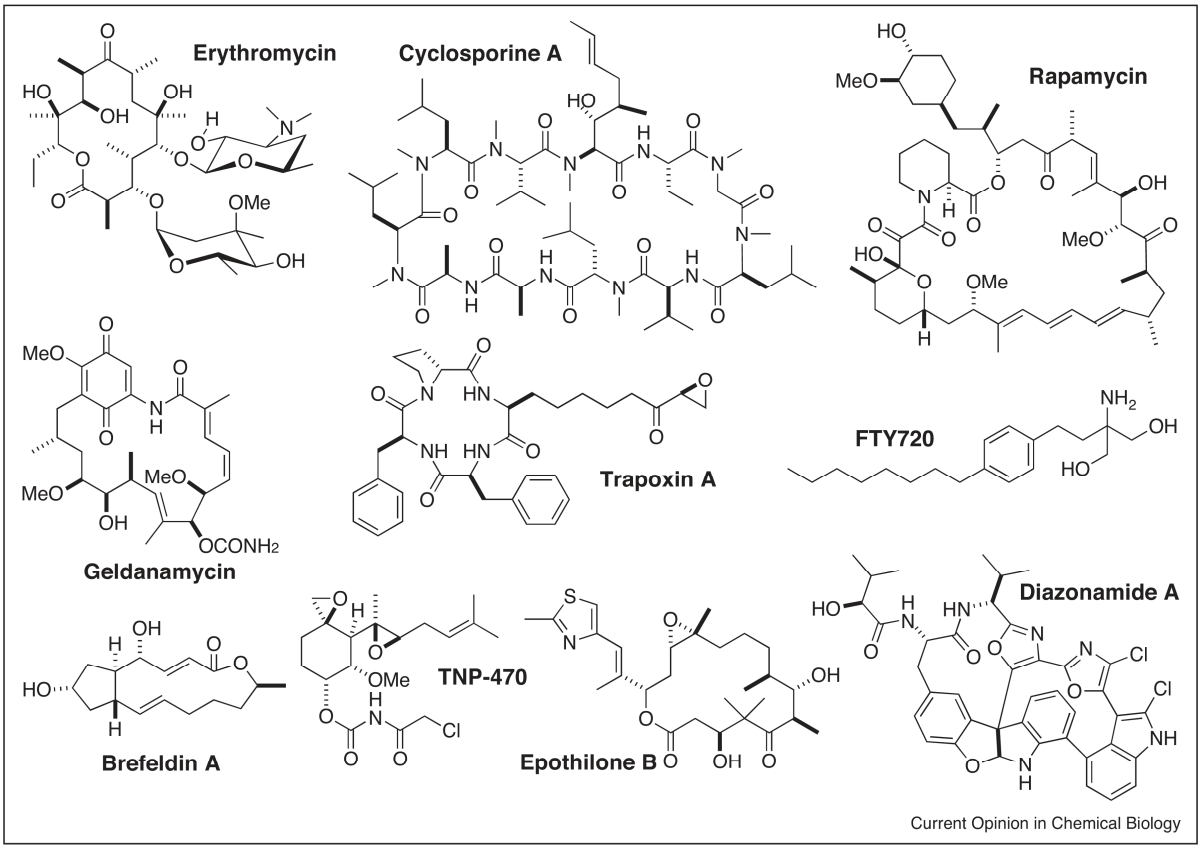

Figure 5: Examples of natural products used in chemical biology and drug discovery. The given compounds highlight the large diversity in natural product structures. From (Hong, 2011). Reprinted with permission of Elsevier.

2.3.1 The heterologous host *Streptomyces albus* J1074

The strain *S. albus* J1074 is a widely used chassis strain for the heterologous production of bioactive natural products. Its genetic accessibility, as it is defective in the *Sal* I (*Sal* GI) restriction-modification system, allows genetic modification in a straightforward fashion, and its minimized genome allows fast growth (Zaburannyi et al., 2014; Kallifidas et al., 2018). With a size of only 6.8 Mbp, its genome is the smallest within the genus of *Streptomyces* (Zaburannyi

et al., 2014). Furthermore, organic extracts from routine laboratory *S. albus* fermentation broths lack endogenous secondary metabolites (Kallifidas et al., 2018). The strain is capable to produce a wide selection of heterologous secondary metabolites, ranging from marine *Micromonospora* secondary metabolites to potent anticancer agents (Lombó et al., 2006; Baltz, 2010). For example, it was used to express biosynthetic gene clusters for steffimycin, fredericamycin, isomigrastatin, napyradiomycin, cyclooctatin, thiocoraline, and moenomycin production (Wendt-Pienkowski et al., 2005; Gullón et al., 2006; Lombó et al., 2006; Winter et al., 2007; Feng et al., 2009; Kim et al., 2009; Makitrynskyy et al., 2010; Zaburannyi et al., 2014). Recently, the generation of *S. albus* Del14, a cluster-free *S. albus* chassis strains, further improved the capability for heterologous expression of secondary metabolite clusters. The strain obtained 15 deletions of clusters encoding secondary metabolite biosynthetic pathways in its chromosome, resulting in a maximized production capacity and a substantially improved compound detection limit (Myronovskyi et al., 2018).

2.3.2 The polyketide pamamycin

Natural products whose biosynthesis can be traced to an intermediate that contains repeating ketide units are known as polyketides. Polyketides are synthesized by bacteria and fungi and have significant roles in drug discovery and nature (Ridley & Khosla, 2009). Although only a limited number of these antibiotics have been isolated by conventional screening methods, new genomic technologies have provided compelling evidence that the biosynthetic potential for structurally diverse polyketides in nature is truly immense (Ridley & Khosla, 2009). They are a large family of natural products, which are formed through the condensation of acylthioester units such as malonyl-CoA and methylmalonyl-CoA by polyketide synthases to yield metabolites with diverse structures and biological activities (Ridley et al., 2008). Thereby, the biosynthesis of polyketides is similar to that of fatty acid anabolism, where decarboxylative condensation of the acyl thioester unit, malonyl-coenzyme A (CoA), leads to the extension of the fatty acid. However, PKSs are also able to use other substrates besides malonyl-CoA, such as propionyl-CoA, methylmalonyl- CoA, ethylmalonyl-CoA, and methoxymalonyl-CoA (Ridley & Khosla, 2009). In general, there are three types of polyketide synthases (PKSs) in bacteria that are able to synthesize these complex substances: Type I (multimodular) PKSs, type II (iterative) PKSs, and type III PKSs (Ridley et al., 2008). Type I PKSs consist of one or more multifunctional proteins containing multiple modules of catalysts, of which each is responsible for one round of chain elongation and associated reduction reactions. Depending on the catalytic

domains present, multimodular PKSs can generate polyketides of remarkable structural diversity (Ridley & Khosla, 2009) Type II PKSs consist of a disconnected set of proteins, each with one or two active sites. The catalysts repetitively construct a polyketide chain of defined length (Ridley & Khosla, 2009). The enzymatic structure of type III PKSs is the simplest, as no acyl carrier proteins are involved and the CoA-thioesters are directly condensed to form small aromatic compounds (Ridley & Khosla, 2009). A common feature of all three pathways is that frequently additional enzymes, such as oxidoreductases, cyclases, or functional group transferases modify the polyketide to generate the immense structural diversity of these natural products (Ridley et al., 2008; Ridley & Khosla, 2009).

A promising polyketide is pamamycin. The pamamycin family consists of 16 macrodiolide homologues, which are produced by several *Streptomyces spp* (Rebets et al., 2015). They were first isolated in 1979 by a group researchers that identified their ability to induce aerial mycelium formation in *S. alboniger* DSMZ 40043 (McCann & Pogell, 1979). In addition to autoregulatory, anioniphoric and antifungal activities, pamamycins are active against multi-resistant *Mycobacterium tuberculosis* (Lefèvre et al., 2004; Rebets et al., 2015). Thereby, they are regarded as promising lead molecules for the development of novel antituberculosis drugs (Metz, 2005). The polyketide origin of pamamycins was verified by feeding experiments with ^{13}C-labeled acetate, propionate, and succinate (Hashimoto et al., 2005). This is especially interesting since succinate cannot directly participate in a Claisen condensation (Rebets et al., 2015). By a combination of genetic and biochemical data, researchers were able to identify the pamamycin biosynthetic gene cluster in *S. alboniger* and to decipher its biosynthetic pathway (Figure 6). The cluster consists of 20 genes, which are grouped into two cores of KS genes, the right and left core (Rebets et al., 2015). Pamamycin production starts with the condensation of succinyl-CoA and (methyl)malonyl-CoA, catalyzed by PamA. Incorporation of different extender units, i.e. malonyl-CoA, methylmalonyl-CoA, and ethylmalonyl-CoA, finally determines the molecular structure, mass, and biological activity (Rebets et al., 2015). In a final step, the production of these complex molecules relies on the assembly of two asymmetrical parts, called small and large hydroxy acids (Rebets et al., 2015). Interestingly, the different pamamycin derivatives vary in their biological activity (Lefèvre et al., 2004; Natsume, 2016). Therefore, it is crucial to understand the molecular basis of pamamycin biosynthesis and it appears interesting to manipulate the production process towards more favorable derivatives.

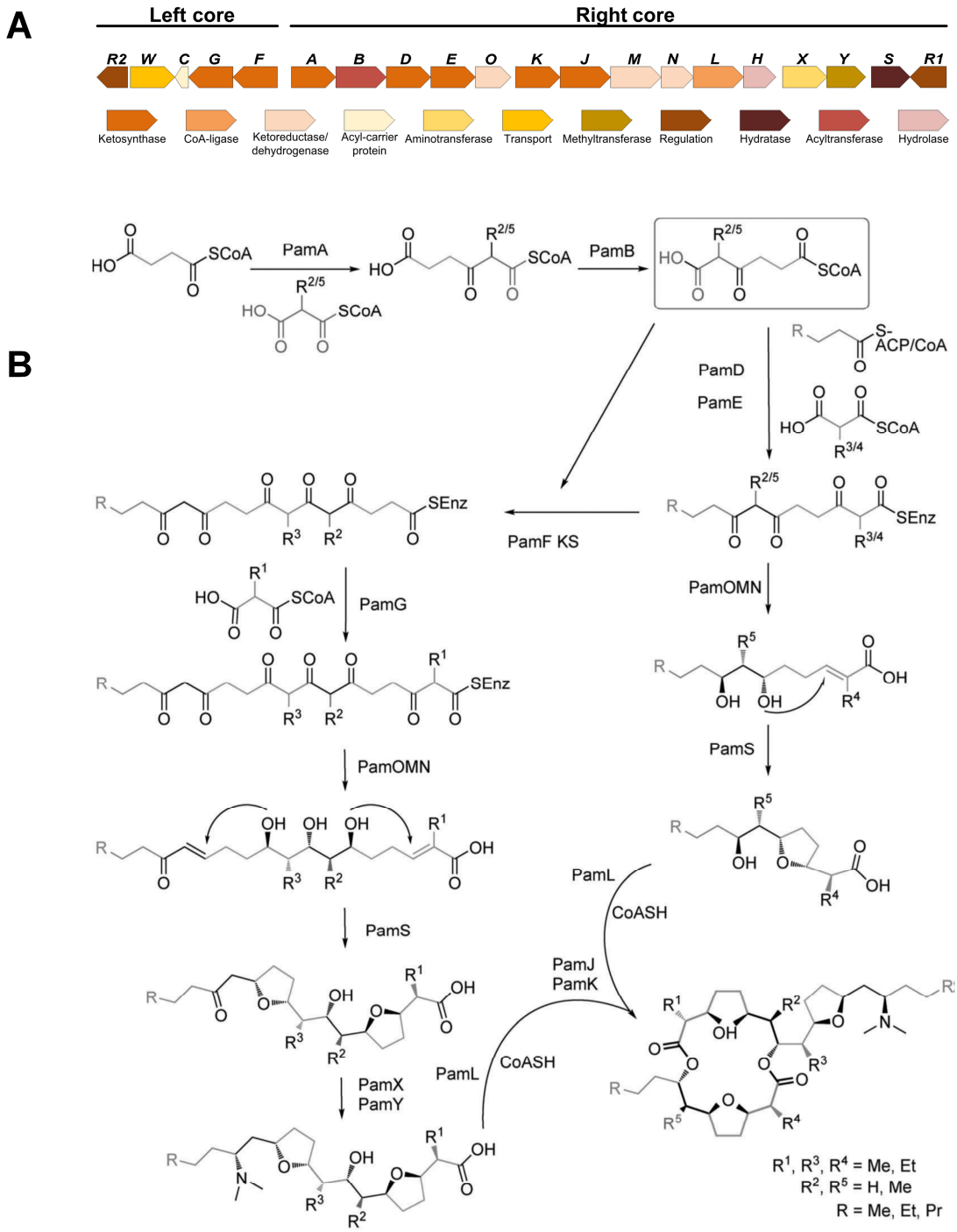

Figure 6: Pamamycin biosynthesis. A: Pamamycin biosynthetic gene cluster from *S. alboniger* DSMZ 40043. B: Pamamycin biosynthetic pathway. PamA (KS) catalyzes the condensation of succinyl-CoA with malonyl- or methylmalonyl-CoA, followed by a rotation by PamB. The resulting 4-oxoadipyl-CoA and 5-methyl-4-oxoadipyl-CoA are key intermediates, which are used as extenders for a Claisen condensation facilitating the succinate incorporation. Starter units are most likely supplied as ACP-esters. Eventually, the pathway divides into two branches. Activity of the ketoreductases PamO, PamM, and PamN coupled with the closure of the tetrahydrofuran ring by PamS, results in formation of the small hydroxy acids. In the other branch, PamF adds the second molecule of adipate followed by the final extension with malonate catalyzed by PamG. Ketoreduction, closure of the tetrahydrofuran rings, and amination, catalyzed by PamO, PamM, PamN, PamS, PamX, and PamY, result in the formation of the large hydroxy acids. Reactivation of the hydroxy acids by the acyl-Coa ligase PamL and unusual C-O condensations, facilitated by the KSs PamJ and PamK, result in the final pamamycin. Adapted from (Rebets et al., 2015). Reprinted with permission of Wiley.

2.3.3 *Streptomyces lividans* – A host for heterologous peptide and protein production

S. lividans is well known to produce extracellular peptides and proteins in large amounts (Anné & Van Mellaert, 1993). It is the standard host for heterologous expression of proteins and antibiotic-synthesizing enzymes and as such, is often used as microbial cell factory to produce industrial enzymes and antibiotics (Rückert et al., 2015). Many examples have shown the feasibility to use *S. lividans* for the production of proteins of prokaryotic and eukaryotic origin (Anné & Van Mellaert, 1993). Additionally, there are examples that *S. lividans* can glycosylate proteins, which is of importance to produce eukaryotic proteins (Hu et al., 1993). *S. coelicolor* A3(2), an important strain for genetics research in *Streptomyces,* has a strong restriction towards incoming foreign DNA. This characteristic, appears to be widespread among *Streptomyces spp*. (Anné & Van Mellaert, 1993). In contrast, *S. lividans*, does not cleave exogenous methylated DNA, allowing transformation with DNA isolated from *E. coli* or with bifunctional plasmids (Kieser & Hopwood, 1991; Anné & Van Mellaert, 1993). This results in a high efficiency of conjugative transfer, particularly important for experiments that require a high-throughput transfer of arrayed library clones for screening genomic or metagenomic libraries (Wang et al., 2000; Peng et al., 2018). Recently, a set of clean *S. lividans* chassis strains (*S. lividans* ΔYA11, originating from *S. lividans* TK24) was constructed by deleting eleven endogenous gene clusters. The strain obtained a simplified metabolic background, as well as superior growth and production characteristics for heterologous secondary metabolites than its parental strain, which further facilitates heterologous expression of biosynthetic gene clusters (Ahmed et al., 2020).

2.3.4 The ribosomally synthesized and post-translationally modified peptide bottromycin

Another promising class of natural products to fight the rising threat of multi-resistant bacteria, with more than 20 sub-classes, are ribosomally synthesized and post-translationally modified peptides (RiPPs). RiPPs are produced by prokaryotes, eukaryotes, and archaea, and possess a wide range of biological properties (Arnison et al., 2013). Although many RiPPs display potent antibiotic activity and modes of action, distinct from currently used drugs, issues with poor solubility and bioavailability so far hindered a broader clinical use. Therefore, it was not possible to realize their full potential yet (Hudson & Mitchell, 2018). However, the extraordinary biosynthetic flexibility is what sets RiPPs apart from polyketides and non-ribosomal peptides, as RiPP biosynthetic enzymes typically display high levels of substrate tolerance (Arnison et al., 2013). This promiscuity is the result of a short recognition sequence

in the beginning of the precursor peptide, which is removed during maturation. This unique feature provides RiPPs with remarkable engineering potential and gives belief to overcome the abovementioned problems in the future (Weissman, 2016; Winn et al., 2016; Hudson & Mitchell, 2018). The biosynthesis begins with ribosomal synthesis of the precursor peptide, consisting of a N-terminal leader peptide, the core peptide, which develops into the final RiPP after post-translational maturation, and a C-terminal recognition sequence (Figure 7) (Arnison et al., 2013). Through the physical separation of the sites responsible for substrate binding and residue modification, it seems possible to utilize the RiPP biosynthetic enzymes to generate novel compounds to address the rise of antibiotic resistance (Hudson & Mitchell, 2018).

Bottromycins, antibacterial RiPPs, were already isolated in 1957 from cultures of *S. bottropensis* (Waisvisz et al., 1957). They represent a promising class of antibiotics, as mode of action studies revealed that they target the aminoacyl-*t*RNA binding site (A site) on the 50S ribosome, which ultimately leads to the inhibition of protein synthesis in the pathogen (Otaka & Kaji, 1976; Otaka & Kaji, 1981). Thereby, they are regarded as promising leads for new anti-infectives, as this target site is currently not addressed by clinically used antibiotics (Huo et al., 2012). By inhibiting translation, they are even active against clinically important pathogens, such as methicillin-resistant *Staphylococcus aureus* (MRSA) and vancomycin-resistant *Enterococci* (VRE) (Kobayashi et al., 2010). Structurally, bottromycins are strongly modified peptides exhibiting various biosynthetic features, including a unique "macrocyclodehydration" leading to amidine ring formation and a thiazole ring formation, besides various methylations and proteolytic digestion (Huo et al., 2012). The biosynthetic gene cluster of *S. sp.* BC16019, producing bottromycins A2, B2, and C2, was identified in 2012 (Huo et al., 2012). From then on, studies on the bottromycin biosynthesis steadily increased. This not only led to the production of numerous derivatives, but also to the finding that the bottromycin pathway in *S. scabies* stalls at several steps and produces inefficient side-products (Crone et al., 2016; Horbal et al., 2018; Vior et al., 2020). It was shown that constitutive high expression of the *btm* cluster is not the key to high titers of mature bottromycin, but instead leads to high yields of shunt metabolites. In contrast, controlled expression resulted in higher efficiency and thereby, mature bottromycin to shunt metabolite ratios (Horbal et al., 2018; Vior et al., 2020). Promoter choice is a key factor for optimizing the production of RiPPs, which also can depend on the timing of gene expression (Vior et al., 2020).

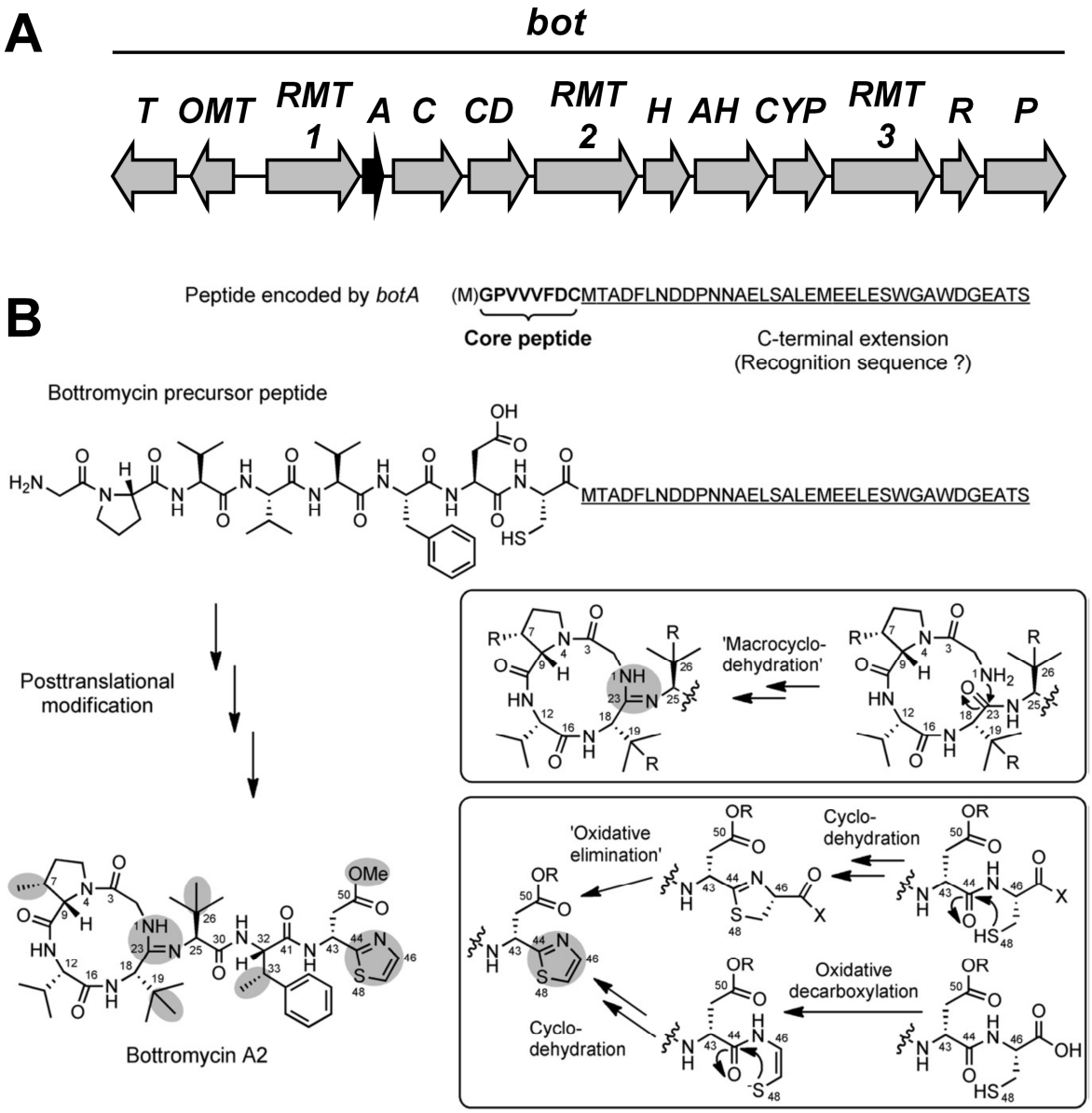

Figure 7: Bottromycin A2 biosynthesis. A: Bottromycin biosynthetic gene cluster from *S. sp.* BC16019. *botT*: multidrug transporter, *botOMT*: *O*-methyl transferase, *botRMT123*: radical *S*-adenosylmethionine methyltransferase, *botA*: bottromycin precursor peptide, *botC*: YcaO domain protein, *botCD*: YcaO domain protein, *botH*: hydrolase, *botAH*: aminohydrolase, *botCYP*: cytochrome P450 enzyme, *botR*: transcriptional regulator, *botP*: leucyl-aminopeptidase. B: Maturation of the bottromycin precursor peptide, consisting of a core peptide and a C-terminal extension as recognition sequence (underlined). The maturation requires various posttranslational modifications (gray), including proteolytic cleavage, methylations, "macrocyclodehydration", and thiazole ring formation (mechanisms for the latter two are boxed). Adapted from (Huo et al., 2012). Reprinted with permission of Elsevier.

2.4 Microparticle-enhanced cultivation

Microparticle-enhanced cultivation (MPEC) was introduced in 2008 to improve biomass and product formation during cultivation of filamentous microorganisms (Kaup et al., 2008). In a pioneering study, chloroperoxidase (CPO) formation of *Caldariomyces fumago* was analyzed

in the presence and absence of different microparticle concentrations of different size (Kaup et al., 2008). Particles with a diameter ≤ 42 µm led to dispersion of the *C. fumago* mycelia up to the level of single hyphae, an about fivefold increase in maximum specific productivity of CPO formation, and in a tenfold increase of CPO activity. In general, microparticles of a diameter comparable to the size of spores or spore agglomerates are most efficient (Antecka et al., 2016a). Furthermore, not all kinds of microparticles result in a similar response, a finding which was verified in several studies (Kaup et al., 2008; Driouch et al., 2010b; Driouch et al., 2012). The most commonly used microparticles today are made of talc (hydrous magnesium silicate), aluminum oxide, and titanate (titanium silicate oxide). Interestingly, use of titanate microparticles resulted in particle aggregation in the center of the pellets, leading to so-called core-shell pellets of *A. niger* (Driouch et al., 2012). A fluorescence-based analysis of GFP expression revealed that biomass of these core-shell pellets was completely active, due to their structure and reduced thickness, whereby large pellets of the control were only active in a 200 µm surface layer. This surface layer matched the critical penetration depth for nutrients and oxygen typically observed for fungal pellets (Driouch et al., 2012).

To investigate if the observed effects were caused by leaching minerals from the particles, *A. niger* and *Trichoderma atroviride* were cultivated in leached particle media, which were incubated with talc and iron oxide microparticles overnight and subsequently sterile-filtered (Etschmann et al., 2015). The majority of the particle-induced effects derived from the physicochemical properties, but the effects in *A. niger,* to small extent, could be contributed to leachable components of talc as well (Etschmann et al., 2015). Presently, it is still unclear how microparticles exactly change the morphology of fungi and, as a consequence, increase the productivity of the strains (Antecka et al., 2016a). The most probable explanation is that microparticles disturb the initial phase of spore aggregation (Driouch et al., 2010b). It was revealed that under talc microparticle supply, the typical spore agglomerates in *A. niger* control cultures disappeared so that only individual spores were present during germination. Interestingly, the time point of supplying the microparticles to the culture was crucial, as the morphology of *A. niger* was not affected when the microparticles were added during later phases of the cultivation. This indicated that the microparticles disturbed the initial phase of spore aggregation. (Driouch et al., 2010b; Antecka et al., 2016a).

3 Scientific articles

The results of this work have been published before.

3.1 Microparticles globally reprogram *Streptomyces albus* toward accelerated morphogenesis, streamlined carbon core metabolism, and enhanced production of the antituberculosis polyketide pamamycin

Martin Kuhl, Lars Gläser, Yuriy Rebets, Christian Rückert, Namrata Sarkar, Thomas Hartsch, Jörn Kalinowski, Andriy Luzhetskyy, and Christoph Wittmann

Biotechnology and Bioengineering. 2020; 117: 3858-3875.

https://doi.org/10.1002/bit.27537

C. W. designed the project. M. K. conducted the cultures. M. K. and Y. R. performed pamamycin analysis. M. K. and L. G. performed CoA ester analysis. C. R. and J. K. performed RNA sequencing. C. R., J. K., N. S., and T. H. processed and evaluated the RNA sequencing data. M. K. and C. W. analyzed the data, drew the figures, and wrote the first draft of the manuscript. All authors commented, extended, and improved the manuscript. All authors read and approved the final version of the manuscript.

 The supplementary information to this article is available in the appendix.

Received: 19 May 2020 | Revised: 13 August 2020 | Accepted: 14 August 2020

DOI: 10.1002/bit.27537

ARTICLE

BIOTECHNOLOGY & BIOENGINEERING WILEY

Microparticles globally reprogram *Streptomyces albus* toward accelerated morphogenesis, streamlined carbon core metabolism, and enhanced production of the antituberculosis polyketide pamamycin

Martin Kuhl[1] | Lars Gläser[1] | Yuriy Rebets[2] | Christian Rückert[3] | Namrata Sarkar[4] | Thomas Hartsch[4] | Jörn Kalinowski[3] | Andriy Luzhetskyy[2] | Christoph Wittmann[1]

[1]Institute of Systems Biotechnology, Saarland University, Saarbrücken, Germany

[2]Department of Pharmacy, Pharmaceutical Biotechnology, Saarland University, Saarbrücken, Germany

[3]Center for Biotechnology, Bielefeld University, Bielefeld, Germany

[4]Genedata GmbH, Munich, Germany

Correspondence
Christoph Wittmann, Institute of Systems Biotechnology, Saarland University, 66123 Saarbrücken, Germany.
Email: christoph.wittmann@uni-saarland.de

Funding information
Deutsche Forschungsgemeinschaft, Grant/Award Number: INST 256/418-1; Bundesministerium für Bildung und Forschung, Grant/Award Number: 031B0344

Abstract

Streptomyces spp. are a rich source for natural products with recognized industrial value, explaining the high interest to improve and streamline the performance of in these microbes. Here, we studied the production of pamamycins, macrodiolide homologs with a high activity against multiresistant pathogenic microbes, using recombinant *Streptomyces albus* J1074/R2. Talc particles (hydrous magnesium silicate, $3MgO{\cdot}4SiO_2{\cdot}H_2O$) of micrometer size, added to submerged cultures of the recombinant strain, tripled pamamycin production up to 50 mg/L. Furthermore, they strongly affected morphology, reduced the size of cell pellets formed by the filamentous microbe during the process up to sixfold, and shifted the pamamycin spectrum to larger derivatives. Integrated analysis of transcriptome and precursor (CoA thioester) supply of particle-enhanced and control cultures provided detailed insights into the underlying molecular changes. The microparticles affected the expression of 3,341 genes (56% of all genes), revealing a global and fundamental impact on metabolism. Morphology-associated genes, encoding major regulators such as SsgA, RelA, EshA, Factor C, as well as chaplins and rodlins, were found massively upregulated, indicating that the particles caused a substantially accelerated morphogenesis. In line, the pamamycin cluster was strongly upregulated (up to 1,024-fold). Furthermore, the microparticles perturbed genes encoding for CoA-ester metabolism, which were mainly activated. The altered expression resulted in changes in the availability of intracellular CoA-esters, the building blocks of pamamycin. Notably, the ratio between methylmalonyl CoA and malonyl-CoA was increased fourfold. Both metabolites compete for incorporation into pamamycin so that the altered availability explained the pronounced preference for larger derivatives in the microparticle-enhanced process. The novel insights into the behavior

of *S. albus* in response to talc appears of general relevance to further explore and upgrade the concept of microparticle enhanced cultivation, widely used for filamentous microbes.

KEYWORDS

filamentous microbe, microparticle, morphogenesis, polyketide, *Streptomyces*, transcriptome

1 | INTRODUCTION

Streptomycetes are an important source of natural products for pharmaceutical, medical, agricultural, and nutraceutical application, including more than two-third of all known antibiotics of microbial origin (Bibb, 2013). Over the past, they have provided a range of industrialized blockbuster drugs, including streptomycin (Ehrlich, Bartz, Smith, Joslyn, & Burkholder, 1947), chloramphenicol (Ehrlich et al., 1947), candicidin (Lechevalier, Acker, Corke, Haenseler, & Waksman, 1953), doxorubicin (Arcamone et al., 1969), ivermectin (Campbell, Fisher, Stapley, Albers-Schönberg, & Jacob, 1983; Juarez, Schcolnik-Cabrera, & Dueñas-Gonzalez, 2018), bialaphos (Bayer et al., 1972), and rapamycin (Sehgal, Baker, & Vézina, 1975; Vézina, Kudelski, & Sehgal, 1975), amongst others (Kieser, Bibb, Buttner, Chater, & Hopwood, 2000). It is easy to understand that strategies to activate and enhance the synthesis of natural products in Streptomycetes have been of a broad interest from early on and still display a topic of major relevance (Ahmed et al., 2020; Horbal, Marques, Nadmid, Mendes, & Luzhetskyy, 2018; Kallifidas, Jiang, Ding, & Luesch, 2018; Lopatniuk et al., 2019; Zhang et al., 2020).

Members of the genus are well known for a complex morphology linked to their multicellular life cycle, which starts with the germination of a single spore that grows into a vegetative mycelium by linear tip extension and hyphae branching (Chater & Losick, 1997; van Dissel, Claessen, & van Wezel, 2014), then forms an aerial mycelium, and finally differentiates into uninucleoid cells that further develop again into spores (Angert, 2005). In submerged culture, more relevant for industrial production, morphogenesis comprises primary and secondary mycelial networks, pellets, and sporulation (van Dissel et al., 2014).

Notably, morphological development and natural product formation are closely linked, and various efforts have been made to increase production through an altered morphology (Chater, 1984). Genetic perturbation, as an example, provided remarkable progress (van Dissel et al., 2014; Koebsch, Overbeck, Piepmeyer, Meschke, & Schrempf, 2009; van Wezel et al., 2006; Xu, Chater, Deng, & Tao, 2008). Other studies aimed to influence morphology on the process level, including the modification of agitation speed (Belmar-Beiny & Thomas, 1991; Xia, Lin, Xia, Cong, & Zhong, 2014), medium viscosity (O'Cleirigh, Casey, Walsh, & O'Shea, 2005), pH value (Glazebrook, Vining, & White, 1992), the addition of specific nutrients (Jonsbu, McIntyre, & Nielsen, 2002), and even subinhibitory antibiotic concentrations (Wang, Zhao, & Ding, 2017). These studies, however, have revealed a mixed outcome and largely remained on a trial and error level.

Strikingly, a breakthrough in tailored control of morphology was achieved with the introduction of inorganic microparticles, added to the cultures (R. Walisko, Krull, Schrader, & Wittmann, 2012). Pioneering studies successfully used such materials to streamline the morphology of eukaryotic filamentous fungi and enhance the formation of enzymes (Driouch, Hänsch, Wucherpfennig, Krull, & Wittmann, 2012; Driouch, Roth, Dersch, & Wittmann, 2010; Kaup, Ehrich, Pescheck, & Schrader, 2008), polyketides, and alcohols (Etschmann et al., 2015). More recently, several studies suggested that microparticles are also beneficial to enhance product formation in filamentous prokaryotes (Holtmann et al., 2017; Liu, Tang, Wang, & Liu, 2019; Ren et al., 2015; J. Walisko et al., 2017).

Here, we studied the use of talc microparticles for the production of pamamycins (Figure 1), a family of 16 macrodiolide homologs that are highly active against multiresistant pathogenic microbes, using recombinant *Streptomyces albus* J1074/R2 (Rebets et al., 2015). Carefully conducted cultures with analysis of growth, product formation and cellular morphology enabled us to specifically study the impact of the microparticle addition on production performance. In addition, transcriptome and intracellular CoA thioester analyses provided insights into the cellular response of *S. albus* and provided a systems-level picture on how the particles reprogrammed morphogenesis and streamlined metabolism for enhanced production and a notable shift toward heavier pamamycin homologs.

2 | MATERIALS AND METHODS

2.1 | Strain

S. albus J1074/R2 expressing the heterologous pamamycin gene cluster was obtained from previous work (Rebets et al., 2015). For strain maintenance, spores collected from agar plate cultures after 5-day incubation were resuspended in 20% glycerol and kept at −80°C.

2.2 | Media

Mannitol-soy flour agar contained per liter: 20 g mannitol (Sigma-Aldrich, Taufkirchen, Germany), 20 g soy flour (Schoenenberger

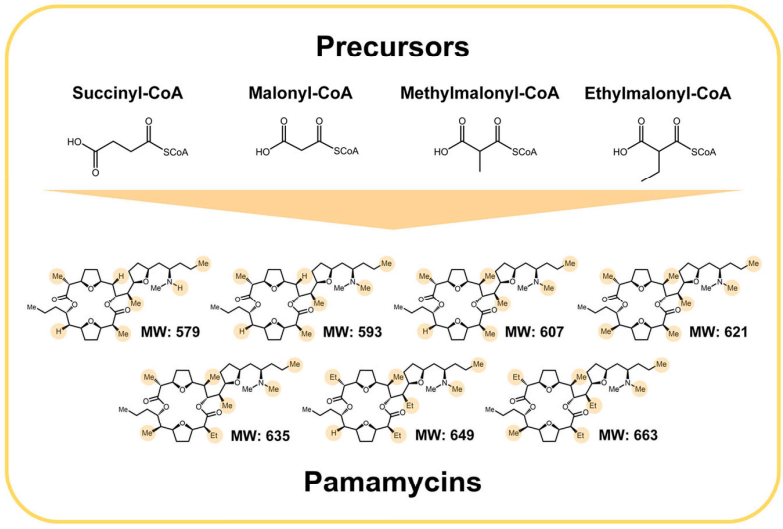

FIGURE 1 Chemical structure of the polyketide pamamycin family and the building blocks of its different derivatives succinyl-CoA, malonyl-CoA, methylmalonyl-CoA, and ethylmalonyl-CoA. The individual combination of different CoA-esters results in a different decoration of the product (-H, -CH_3, -C_2H_5) at specific positions and determines the molecular weight (MW). Except for Pam 607, several isomers exist for each pamamycin, differing by the exact position of the side chains (Hanquet, Salom-Roig, & Lanners, 2016). For every pamamycin mass derivative, one exemplary structure is shown [Color figure can be viewed at wileyonlinelibrary.com]

Hensel, Magstadt, Germany), and 20 g agar (Becton & Dickinson, Heidelberg, Germany). Liquid SGG medium was used for pre- and main cultures for pamamycin production and contained per liter: 10 g soluble starch (Sigma-Aldrich), 10 g glycerol, 2.5 g corn steep powder (Sigma-Aldrich), 5 g bacto peptone (Becton & Dickinson), 2 g yeast extract (Becton & Dickinson), 1 g sodium chloride, and 21 g MOPS. The pH of the medium was adjusted to 7.2, using 6 M NaOH. Talc microparticles (hydrous magnesium silicate, $3MgO{\bullet}4SiO_2{\bullet}H_2O$, 10 µm; Sigma-Aldrich) were resuspended in 50 mM Na-acetate buffer (pH 6.5), autoclaved at 121°C for 20 min, and added to the sterile medium before inoculation of selected experiments (Driouch, Sommer, & Wittmann, 2010).

2.3 | Cultivation

One loop of spores was scratched from a 5-day old plate culture and used to inoculate a liquid preculture, which was then grown overnight in a 500-ml baffled shake flask with 50 ml medium and 30 g soda-lime glass beads (5 mm; Sigma-Aldrich). When the preculture reached the late exponential phase, an appropriate amount of cells was collected (8,500*g*, room temperature, 5 min), resuspended in 10 ml fresh medium, and used to inoculate the main-culture (50 ml medium in 500-ml baffled shake flasks). Main cultures (with and without talc) were inoculated from the same preculture to enable identical starting conditions. All cultivation experiments were conducted in triplicate on a rotary shaker (28°C, 230 rpm, 75% relative humidity, 5-cm shaking diameter, Multitron, Infors AG, Bottmingen, Switzerland).

2.4 | Quantification of cell concentration

The cell dry weight (CDW) of *S. albus* was measured as follows. Cells were collected (10,000*g*, 4°C, 10 min), washed twice with 15 ml deionized water and freeze-dried. Subsequently, the CDW was gravimetrically determined (Gläser et al., 2020). In microparticle cultivations, the measurements were corrected for the added talc (Driouch, Sommer, et al., 2010). The optical density (OD_{600}) of a culture was measured at 600 nm (UV-1600PC spectrophotometer; VWR, Hannover, Germany). Individual correlations allowed to infer the CDW from optical density measurement for different talc concentrations: CDW (g/L) = 0.64 × OD_{600} (control), CDW (g/L) = 0.70 × OD_{600} (2.5 g/L talc), CDW (g/L) = 0.76 × OD_{600} (10 g/L talc; Figure S8), as described before (Becker, Klopprogge, Schröder, & Wittmann, 2009). All measurements were performed in triplicate.

2.5 | Quantification of substrates

Before analysis, starch was hydrolyzed to glucose monomers for 3 hr using 3 M HCl at 100°C. Glucose and glycerol were quantified by high-performance liquid chromatography (HPLC; 1260 Infinity Series; Agilent, Waldbronn, Germany) using an Aminex HPX-87H column (300 × 7.8 mm; Bio-Rad, München, Germany) and 7 mM H_2SO_4 as mobile phase (55°C, 0.7 ml/min). Refraction index measurement was used for detection and external standards were used for quantification. Phosphate was analyzed by HPIC (Dionex Integrion; Thermo Fisher Scientific, Karlsruhe, Germany) using a Dionex IonPac AS9-HC column (2 × 250 mm; Thermo Fisher Scientific) and 9 mM Na_2CO_3 as

mobile phase (35°C, 0.25 ml/min). Conductivity measurement was used for detection and an external standard was used for quantification. All measurements were performed in triplicate.

2.6 | Morphology analysis

Five microliter culture broth was transferred onto a glass for bright-field microscopy (Olympus IX70 microscope, Hamburg, Germany). The software ImageJ 1.52 (Schneider, Rasband, & Eliceiri, 2012) was used to automatically determine the size of pellets formed during growth (Krull et al., 2013). The diameter of a pellet was assumed as the smallest circle into which the complete aggregate fitted (Martin & Bushell, 1996). At least 150 aggregates were analyzed per sample.

2.7 | Natural compound extraction and quantification

Pamamycin was extracted from culture broth using a two-step process. First, 200 µl broth was mixed with 200 µl acetone and incubated for 15 min (1,000 rpm, room temperature, Thermomixer F1.5; Eppendorf, Wesseling, Germany). Subsequently, 200 µl ethyl acetate was added, and the mixture was incubated for further 15 min under the same conditions. Afterward, the organic phase was collected (20,000*g*, room temperature, 5 min). The solvents were evaporated under a laminar nitrogen stream. The extract was redissolved in 2 ml methanol, clarified from debris (20,000*g*, 4°C, 10 min) and analyzed, using HPLC-ESI-MS (Agilent Infinity 1290, Waldbronn, Germany; AB Sciex QTrap 6500, Darmstadt, Germany). The different pamamycin derivatives (Figure 1) were separated on a C18 column (Vision HT C18 HighLoad, 100 × 2 mm, 1.5 µm, Dr. Maisch, Ammerbuch-Entringen, Germany) at a flow rate of 300 µl/min (8 mM ammonium formate in 92% acetonitrile) and 45°C. Detection was carried out in positive selected ion monitoring mode, using the corresponding $[M + H]^+$ ion for each derivative (Figure 1). All measurements were performed in triplicate.

2.8 | Extraction and quantification of intracellular CoA-esters

The analysis of CoA-esters was conducted as recently described (Gläser et al., 2020). In short, a broth sample (8 mg CDW) was transferred into a precooled tube, which contained quenching and extraction solution (95% acetonitrile, 25 mM formic acid, −20°C) at a volume ratio of 1:4 followed by repetitive mixing and cooling on ice for 10 min, clarification from cell debris (15,000*g*, 4°C, 10 min) and the addition of 10 ml supercooled deionized water. The cell pellet was washed twice with 8 ml supercooled deionized water. All supernatants were combined, followed by freezing in liquid nitrogen and lyophilization. Before analysis, the obtained dry extract was dissolved in 500 µl precold buffer (25 mM ammonium formate, 2% methanol, pH 3.0, 4°C) and filtered (Ultrafree-MC 0.22 µm; Merck, Millipore, Germany). Analysis of the CoA-esters was performed on a triple quadrupole MS (QTRAP 6500+; AB Sciex, Darmstadt, Germany) coupled to an HPLC system (Agilent Infinity 1290 System). Separation of the analytes of interest was conducted at 40°C on a reversed phase column (Gemini 100 × 4.6 mm, 3 µm, 110 Å, Phenomenex, Aschaffenburg, Germany) using a gradient of formic acid (50 mM, adjusted to pH 8.1 with 25% ammonium hydroxide, eluent A) and methanol (eluent B) at a flow rate of 600 µl/min. The fraction of eluent B was as follows: 0–12 min, 0–15%; 12–16 min, 15–100%; 16–18 min, 100%; 18–20 min, 100–0%; 20–25 min, 0%. The first 3 min of the analysis were discharged to minimize the entry of salts into the mass spectrometer. CoA-esters of interest were analyzed in positive ionization mode, using multiple reaction monitoring. Analyte specific instrument settings such as declustering potential, collision energy, and collision cell exit potential were individually optimized for each CoA-ester, using synthetic standards. All measurements were done in triplicate.

2.9 | Transcriptome analysis

Cells (1 ml broth) were collected by centrifugation (20,000*g*, 4°C, 1 min) and immediately frozen in liquid nitrogen. RNA was extracted with the Qiagen RNA Mini Kit (Qiagen, Hilden, Germany) according to the manufacturer's instructions. Residual DNA was removed by digestion with 10 U RNase-free DNase I (Thermo Fisher Scientific) for 1 hr in the presence of RiboLock RNase inhibitor (Thermo Fisher Scientific). After DNA digestion, the RNA was again purified with the same kit. RNA quality was checked by Trinean Xpose (Gentbrugge, Belgium) and the Agilent RNA 6000 Nano Kit on an Agilent 2100 Bioanalyzer (Agilent Technologies, Böblingen, Germany). Ribosomal RNA molecules were removed from total RNA with the Ribo-Zero rRNA Removal Kit (Illumina, San Diego, CA) and removal of rRNA was checked with the Agilent RNA 6000 Pico Kit on an Agilent 2100 Bioanalyzer. Libraries of complementary DNA (cDNA) were prepared with the TruSeq Stranded mRNA Library Prep Kit (Illumina), and the resulting cDNA was sequenced paired end on an Illumina HiSeq 1500 system using 2 × 75 bp read length. Reads were mapped to the *S. albus* J1074/R2 genome sequence (CP059254.1) with Bowtie2 using standard settings (Langmead & Salzberg, 2012) except for increasing the maximal allowed distance for paired reads to 600 bases. For visualization of read alignments and raw read count calculation, ReadXplorer 2.2.3 was used (Hilker et al., 2014). Due to a high unspecific background over both strands, the raw read count for each CDS was corrected by subtracting the length-adjusted median read count calculated over all CDS from the respective noncoding strand. Using the resulting data, DESeq2 (Love, Huber, & Anders, 2014) was used to QC the datasets via, among others, calculation of the sample to sample distances (Figure S9) and PCA (Figure S10). In addition, DESeq2 was used to calculate DGE datasets. Raw datasets (sequenced reads) as well as processed datasets (input matrix and normalized read counts from DESeq2) are available from GEO (GSE155008). For statistical analysis, Student's *t* test was carried out

and the data were filtered for genes with a $\log_2$-fold change ≥ 1 ($p \leq 0.05$). Hierarchical clustering was conducted, using the software package gplots (R Core Team, 2014; Warnes, Bolker, Bonebakker, & Gentleman, 2016). For visualization, Voronoi tree maps were created, using the Voronto tool (Santamaría & Pierre, 2012) for Java (version 8, update 231, Build 1.8.0_231-b11). RNA extraction and sequencing were conducted as biological triplicates, except for one of the controls, where one replicate was lost during processing. Given the excellent reproducibility of all analyzed samples (Figures S10 and S11), the available dataset was regarded acceptable to enable a robust and reliable evaluation of gene expression.

3 | RESULTS

3.1 | Pamamycin production in *S. albus* J1074/R2

In a first set of experiments, the pamamycin production performance of *S. albus* J1074/R2 was assessed in liquid SGG medium, which contained starch and glycerol as carbon source (Figure 2a). After inoculation, cells immediately started to grow into mycelial networks, which then aggregated into pellets as typically observed for actinomycetes. Growth lasted for about 12 hr. The production of pamamycins started after ~9 hr at the end of the growth phase (when phosphate became limiting, Figure S11) and continued during the later stationary phase. The recombinant strain produced a rich spectrum of different pamamycins, which were attributed to derivatives with different side chains according to their molecular mass, that is, Pam 579, Pam 593, Pam 607, Pam 621, Pam 635, Pam 649, and Pam 663. Smaller pamamycins (Pam 579, Pam 593, and Pam 607) were most prominent. The total pamamycin titer was 18 mg/L. Interestingly, starch was the major carbon source until ~24 hr (Figure S11). Glycerol remained practically untouched during the initial process, but was consumed later when starch reached a lower level (although it was still present). During the cultivation, the pH value varied between 6.5 and 7.5. It decreased during the growth phase and increased again in later phases.

3.2 | The addition of talc to the culture of *S. albus* J1074/R2 increases the production of pamamycin up to threefold

S. albus J1074/R2, cultivated in SGG medium with microparticles (2.5 g/L talc), revealed an increased pamamycin titer of 22 mg/L

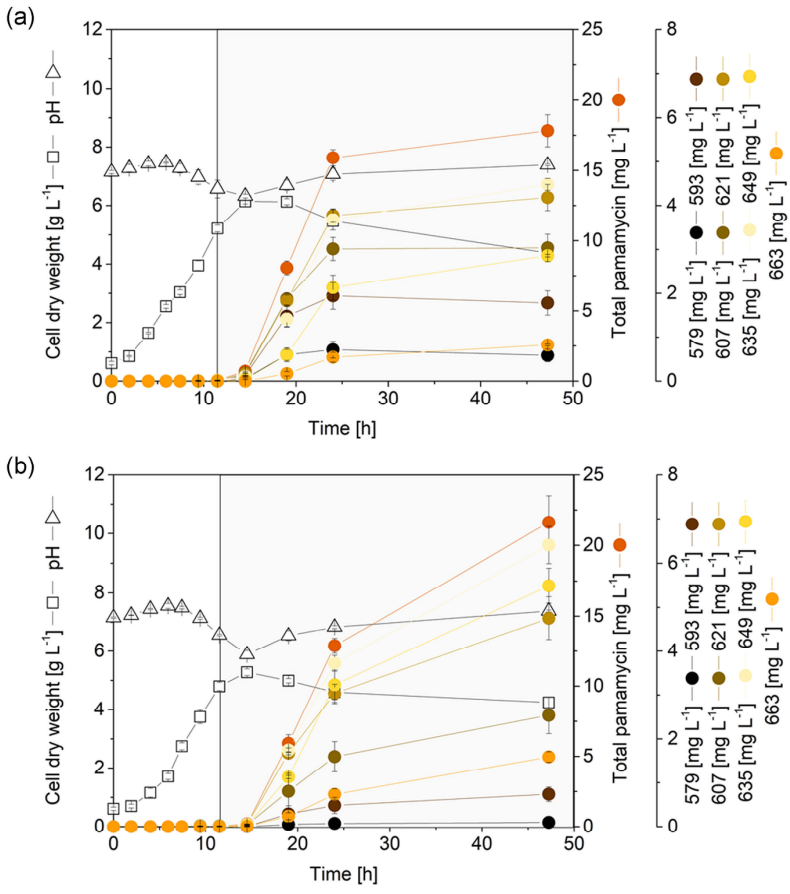

FIGURE 2 Impact of talc microparticles on growth and pamamycin production in *Streptomyces albus* J1074/R2 using complex SGG medium with starch and glycerol as main carbon source. (a) Control culture without microparticles. (b) Microparticle-enhanced culture with 2.5 g/L talc. Growth phase (white) and major pamamycin production phase (gray) are indicated by color [Color figure can be viewed at wileyonlinelibrary.com]

(Figure 2b). Interestingly, talc did not generally enhance production, but specifically affected the pamamycin spectrum. The titer of low molecular weight derivatives (Pam 579, Pam 593, Pam 607) was found reduced, whereas higher molecular weight pamamycins were increased (Pam 635, Pam 649, Pam 663). This effect was most prominent for the two heaviest pamamycins (Pam 649, Pam 663). These two derivatives were increased almost twofold. The presence of the talc particles resulted in a slightly faster use of phosphate (Figure S11). The mode of substrate utilization was the same as for the control, mainly starch consumption during the initial phase and activation of glycerol utilization after ~20 hr. Generally, glycerol uptake was more pronounced than in the control. It's uptake was faster, and a significantly lower amount of it was left at the end of the process (Figure S11). The pH profile was like the control.

Further studies revealed a strong impact of the amount of talc on the product level (Figure 3a). An optimum performance was observed for talc levels of 10 and 15 g/L. These concentrations provided 50 mg/L of total pamamycin. An even higher concentration of talc (20 g/L) resulted in a reduced titer (37 mg/L), slightly below the optimum. Notably, the stimulating effect of the microparticles on the formation of larger pamamycins was maintained even at the highest talc level: 20 g/L of talc specifically enhanced production of pamamycins Pam 649 and Pam 663. Altogether, a concentration of 10 g/L talc appeared optimal and was chosen for further studies.

3.3 | Talc microparticles reduce the pellet size of *S. albus* J1074/R2 more than sixfold

The addition of talc caused substantial changes in cellular morphology (Figure 3b). In control cultures without talc, the formed pellets exhibited an average diameter of ~435 µm. Already low levels of talc (2.5 g/L) led to a drastic decrease to 150 µm. With an increasing microparticle concentration, this effect was even more pronounced. The smallest pellet diameter (70 µm) was reached at 10 g/L talc. Further increase of the talc concentration did not result in a further reduction of the pellet size.

Taken together, smaller pellets were obviously beneficial for pamamycin production (Figure 3a). Microscopic analysis of the cultures revealed that the microparticles attached to the cells, which obviously loosened the inner structure of the aggregates (Figure 4c,d). The pellets of talc enhanced cultures appeared of a similar loose structure during growth and production phase. In contrast, the central core of pellets of the control culture showed signs of decomposition during production phase (Figure 4b).

3.4 | Microparticles globally reprogram the metabolism of *S. albus* J1074/R2

To assess the response of the actinomycete to the added microparticles in more detail, global gene expression analysis was conducted. We compared the transcriptome during the growth phase (5 hr) and the production phase (21 hr) between a talc (10 g/L) supplied culture and a control culture without talc using RNA sequencing. Generally, the transition of *S. albus* J1074/R2 from the nonproducing growth phase to the production phase was linked to a wide readjustment of gene expression. The expression of 1,468 genes, representing 24% of the genomic repertoire, was significantly altered in the control culture, when cells shifted from growth to production mode ($\log_2$-fold change ≥ 1, $p \leq .05$; Figures S1 and S7). On top of this general shift, talc supply induced a global change in the transcriptome. These talc-specific effects were observed for the growth as well as the production phase (Figures 5, S1, and S6). Altogether, 3,341 genes (56% of all genes) were specifically affected by the presence of talc, revealing a fundamental impact of the microparticles on the physiology of *S. albus*. During growth, the microparticles changed the expression of 2,133 genes (36%). This number

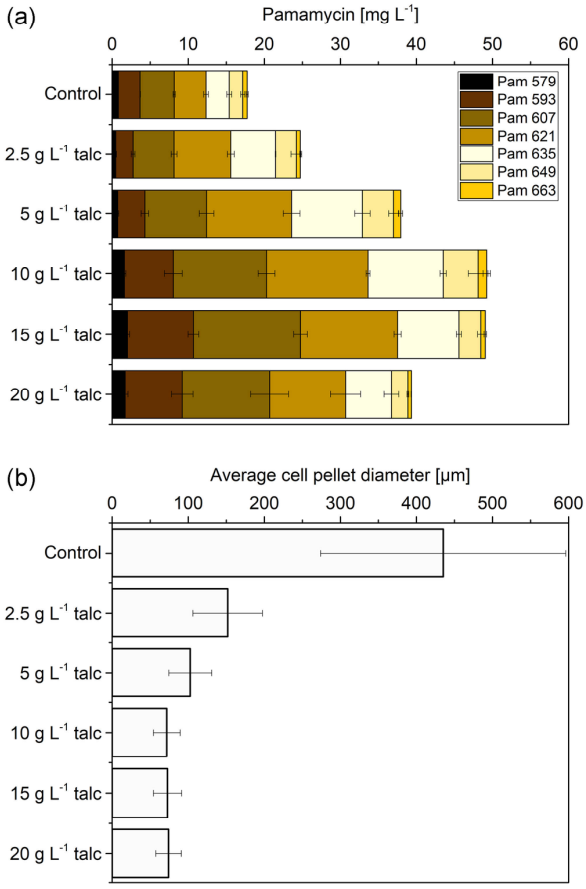

FIGURE 3 Streamlined pamamycin production using different concentrations of talc added to cultures of recombinant *Streptomyces albus* J1074/R2. (a) Total pamamycin titer and spectrum of different pamamycin derivatives assessed as final value after 48 hr of cultivation. (b) Average pellet diameter during the major production phase (20 hr), as assessed from optical analysis of at least 150 aggregates per condition [Color figure can be viewed at wileyonlinelibrary.com]

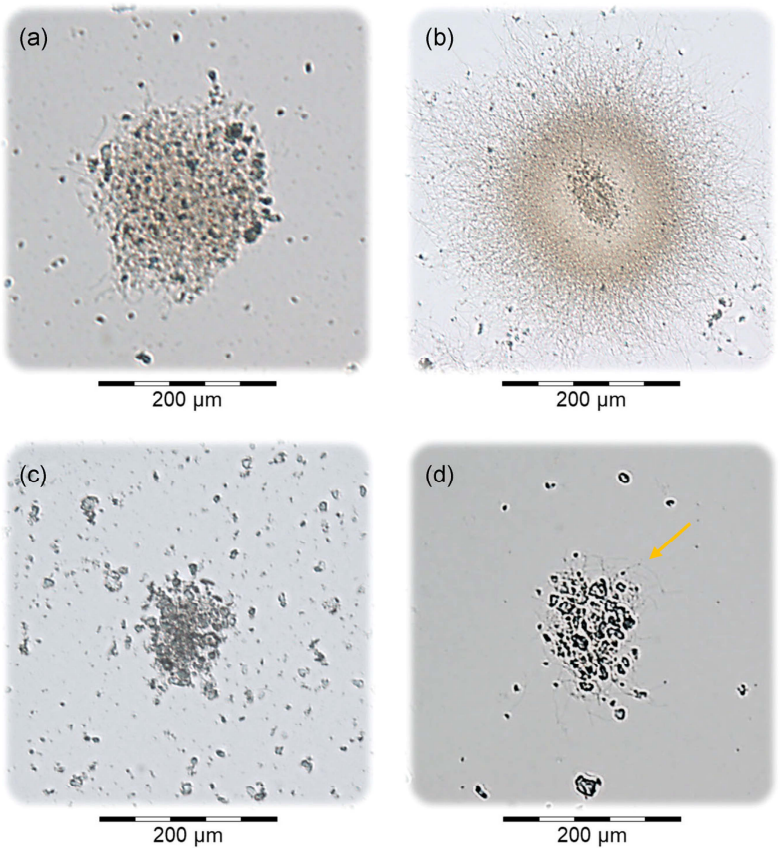

FIGURE 4 Impact of talc microparticles on the cellular morphology of *Streptomyces albus* J1074/R2. Control culture without microparticles during growth (5 hr) (a) and production (20 hr) (b). Microparticle-enhanced culture with 10 g/L talc during growth (5 hr) (c) and production (20 hr) (d). The arrow indicates the physical attachment of the mycelium to the microparticles [Color figure can be viewed at wileyonlinelibrary.com]

increased even further to 2,449 genes (41%), when talc supplemented cultures were in the production phase. The talc-induced changes covered almost all functional gene classes (Figure 5), which were found downregulated (shown in blue) or upregulated (yellow). As example, talc caused an upregulation of the biosynthetic pathways for branched chain amino acids, polyketide metabolism, and the biosynthesis of other secondary metabolites during the growth phase (Figure 5a). Talc specific gene expression changes during the production phase included an upregulation of starch and sucrose metabolism, valine, leucine and isoleucine degradation, butanoate metabolism, propanoate metabolism, fatty acid degradation, and secondary metabolite biosynthesis (Figure 5b). In addition, genes related to stress and cell death differed in transcription depending on culture conditions (Table S2).

3.5 | Talc microparticles affect the expression of morphology regulators

Since the microparticles obviously affected the morphology of *S. albus* (Figures 3b and 4), we searched within the transcriptome data for genes involved in morphology and secondary metabolism. Based on their similarity to known morphogenetic genes identified in other *Streptomyces*, we could identify 55 genes which were affected by the particles (Figures S2 and S3). As prominent example, the addition of microparticles resulted in an upregulation (log_2-fold change = 2.0) of the sporulation and cell division protein SsgA, encoded by *XNRR2_5315*, already during growth (Table 1). The upregulation was even higher during production (log_2-fold change = 3.0). A similar picture was observed for other prominent morphology genes, that is, the signaling protein Factor C (*XNRR2_2306*), the chaplin (*chp*) and rodlin (*rdl*) hydrophobic sheath proteins and a neutral zinc metalloprotease (*XNRR2_1391*), a homolog to *sgmA* in *S. griseus*, and a well-known morphology regulator (Table 1). In all cases, the microparticles caused an overexpression, which was most pronounced during the pamamycin production phase but partly started already during growth.

3.6 | Microparticles drive the expression of the pamamycin biosynthetic cluster

Causally linked to the enhanced production, *S. albus* J1074/R2 responded to the microparticles by a strong overexpression of the pamamycin cluster (log_2-fold change up to 10, Figure 6). The activation was most pronounced for the production phase, where 19 out

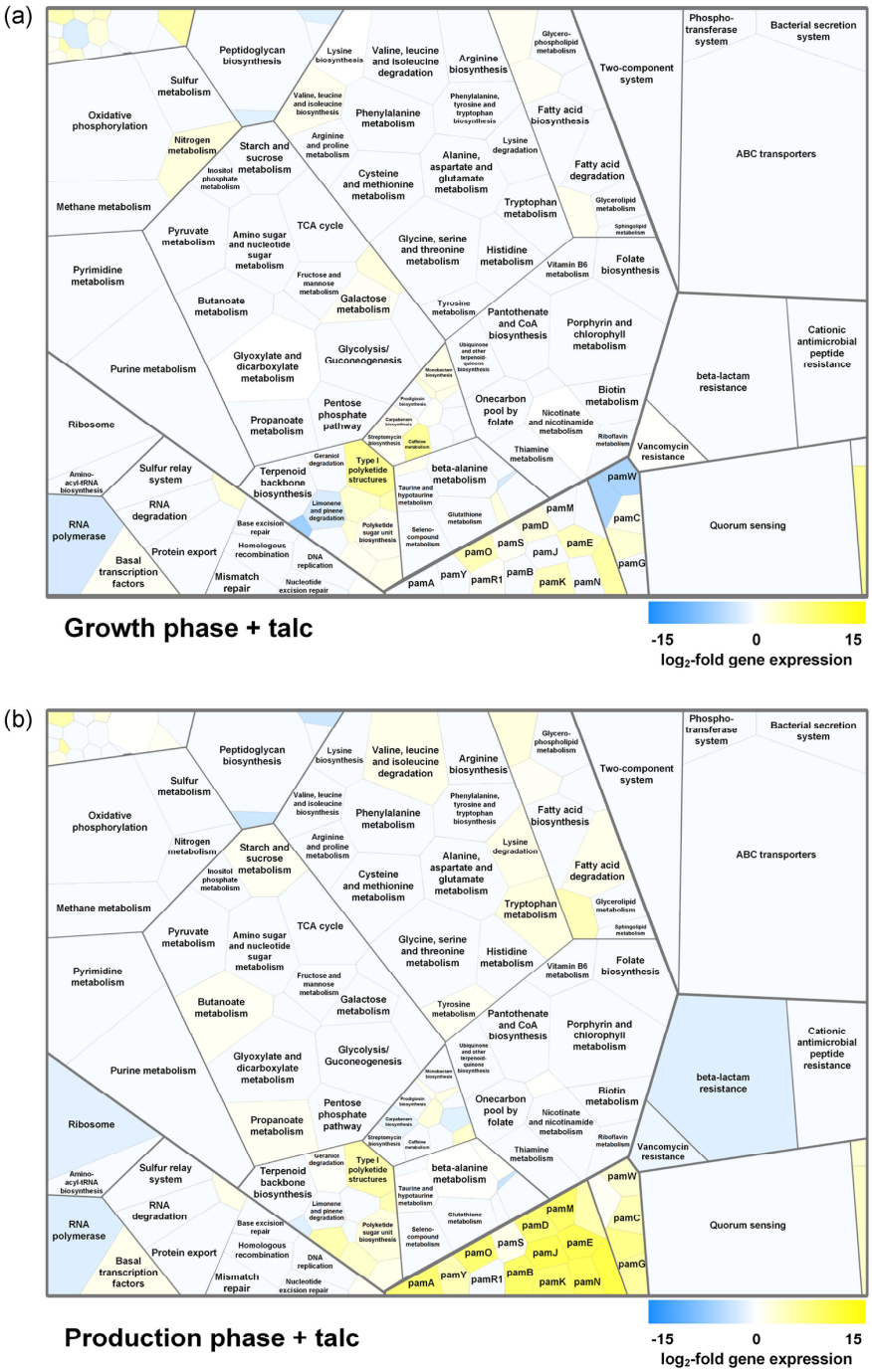

FIGURE 5 Global gene expression pattern for pamamycin producing *Streptomyces albus* J1074/R2 at different stages of the cultivation and under the impact of talc microparticles (10 g/L). Kyoto Encyclopedia of Genes and Genomes (KEGG)-orthology tree maps for the average gene expression of different functional classes of growing (a) and producing (b) *S. albus* J1074/R2 as compared to the control culture during as a reference. Each cell represents a functional class of the orthology: Carbohydrate metabolism, amino acid metabolism, lipid metabolism, nucleotide metabolism, energy metabolism, glycan biosynthesis and metabolism, xenobiotics biodegradation and metabolism, metabolism of cofactors and vitamins, metabolism of terpenoids and polyketides, biosynthesis of other secondary metabolites, metabolism of other amino acids, signal transduction, membrane transport, replication and repair, transcription, translation, folding, sorting and degradation, cellular community, and cell motility with their subclasses. The annotation was taken from the genome (entry T02545 in KEGG) of *S. albus* (Zaburannyi et al., 2014). In addition, the right and left core of the pamamycin gene cluster are shown [Color figure can be viewed at wileyonlinelibrary.com]

TABLE 1 Impact of talc microparticles on the expression of morphology associated genes in pamamycin producing *Streptomyces albus* J1074/R2

Gene	Annotation	Homolog and identity [%]	Growth (Talc)	Prod. (Talc)	Prod. (Control)	Reference
XNRR2_1044	Sporulation factor	*whiH*, SCO, 79.8	2.1	5.2	3.0	Flärdh, Kindlay, and Chater (1999)
XNRR2_1071	ppGpp synthetase	*relA*, SCO, 45.3	0.0	2.9	0.0	Hesketh et al. (2007)
XNRR2_5340	ppGpp synthetase I	*relA*, SCO, 85.6	0.0	0.0	0.0	Hesketh et al. (2007)
XNRR2_1554	Nucl. binding protein	*eshA*, SCO, 65.9	8.9	10.0	8.2	Saito et al. (2006)
XNRR2_1132	BldB	*bldB*, SALB	−1.0	−1.4	0.0	Flärdh et al. (1999)
XNRR2_1391	Metalloprotease	*sgmA*, SGR, 67.6	5.6	10.1	0.0	Kato, Suzuki, Yamazaki, Ohnishi, and Horinouchi (2002)
XNRR2_2151	Membrane protein	*chpD*, SALB	3.9	7.6	0.0	Zaburannyi et al. (2014)
XNRR2_2152	Secreted protein	*chpA*, SALB	0.0	7.0	0.0	Zaburannyi et al. (2014)
XNRR2_5022	Hypothetical protein	*chpE*, SALB	1.1	2.1	0.0	Zaburannyi et al. (2014)
XNRR2_5152	Membrane protein	*chpH*, SALB	3.3	8.1	4.3	Zaburannyi et al. (2014)
XNRR2_5153	Secreted protein	*chpC*, SALB	0.0	7.4	0.0	Zaburannyi et al. (2014)
XNRR2_2166	RdlB	*rdlB*, SALB	4.0	8.3	3.9	Claessen et al. (2004)
XNRR2_2167	RdlA	*rdlA*, SALB	5.2	10.5	4.1	Claessen et al. (2004)
XNRR2_2306	Factor C	*facC*, SALB	3.5	4.0	0.0	Birkó et al. (2007)
XNRR2_3527	BldN subunit	σ^{BldN}, SVE, 84.9	1.9	4.9	0.0	Bibb, Domonkos, Chandra, and Buttner (2012)
XNRR2_5117	TetR-type regulator	*wblA*, SCO, 67.8	4.2	4.5	4.2	van Wezel and McDowall (2011)
XNRR2_5315	SsgA	*ssgA*, SALB	2.0	3.0	1.8	van Wezel et al. (2000a)

Note: Samples were taken from a control and a talc supplied culture (10 g/L) in SGG medium during growth (5 hr) and production (21 hr). The values correspond to $\log_2$-fold expression changes, considering the control culture during growth (5 hr) as reference. The listed genes represent previously discovered morphology-associated genes in *S. albus* (SALB) and genes, identified by BLAST search as homologs to morphology-associated genes in *S. coelicolor* (SCO), *S. griseus* (SGR), and *S. venezuelae* (SVE), indicated by the percentage of homology The identification of homologs was supported by the fact that Streptomycetes share many genetic elements of morphology control (van Dissel et al., 2014), including SsgA like proteins (Traag & van Wezel, 2008) and Factor C (Birkó et al., 1999). In addition to genes identified in *S. albus* before (Zaburannyi, Rabyk, Ostash, Fedorenko, & Luzhetskyy, 2014), further candidates could be inferred from previous studies on morphological development in other *Streptomyces spp*., including *S. coelicolor* (Chakraburtty & Bibb, 1997; Hesketh et al., 2007; van Wezel & McDowall, 2011), *S. griseus* (Saito et al., 2006; van Wezel & McDowall, 2011), and *S. lividans* (van Wezel et al., 2006), among others.

of the 20 cluster genes were overexpressed as compared to the control. As exception, only the regulator gene *pamR1* remained relatively unaffected. It was interesting to note that the cluster activation was not fully balanced among the "two cores" of the gene cluster. In fact, genes of the "right core" were induced stronger than genes of the "left core." Most of the "right core" genes, that is, 11 out of 15, were upregulated with a $\log_2$-fold change of more than 8 by talc. A few genes of the pamamycin cluster (*pamC*, *pamD*, *pamE*, *pamF*, *pamH*, *pamK*, *pamO*, *pamS*, and *pamX*) were activated by the microparticles already during the growth phase. In contrast, the pamamycin transporter gene (*pamW*) and the regulator inside the "left core" (*pamR2*) were downregulated. In addition to the pamamycin cluster, also other genes of secondary metabolism were found significantly upregulated (Figure 5). The expression changes covered different gene functions: Type I polyketide structures (candicidin biosynthesis), polyketide sugar unit biosynthesis, siderophores (2,3-dihydroxybenzoate synthesis), sesquiterpenoid and triterpernoid biosynthesis (germacradienol/geosmin synthase), terpenoid backbone synthesis, and phenazine biosynthesis (Table S3).

3.7 | Microparticles modulate supporting pathways in central carbon metabolism

As shown, cells preferably produced higher mass pamamycin derivatives in the presence of microparticles. Generally, different derivatives originate from the incorporation of different precursor metabolites, that is, CoA-esters of different type (Figure 1). We, therefore, hypothesized that the microparticles could have impacted genes encoding enzymes for CoA-ester synthesis and interconversion. Indeed, talc supply affected the expression of CoA-ester related genes (Table 2; Figures S4 and S5). As example, talc led to a strong downregulation ($\log_2$-fold change = 6) of the α-subunit of the acetyl/propionyl-CoA carboxylase (*XNRR2_4211*), responsible for the formation of methylmalonyl-CoA

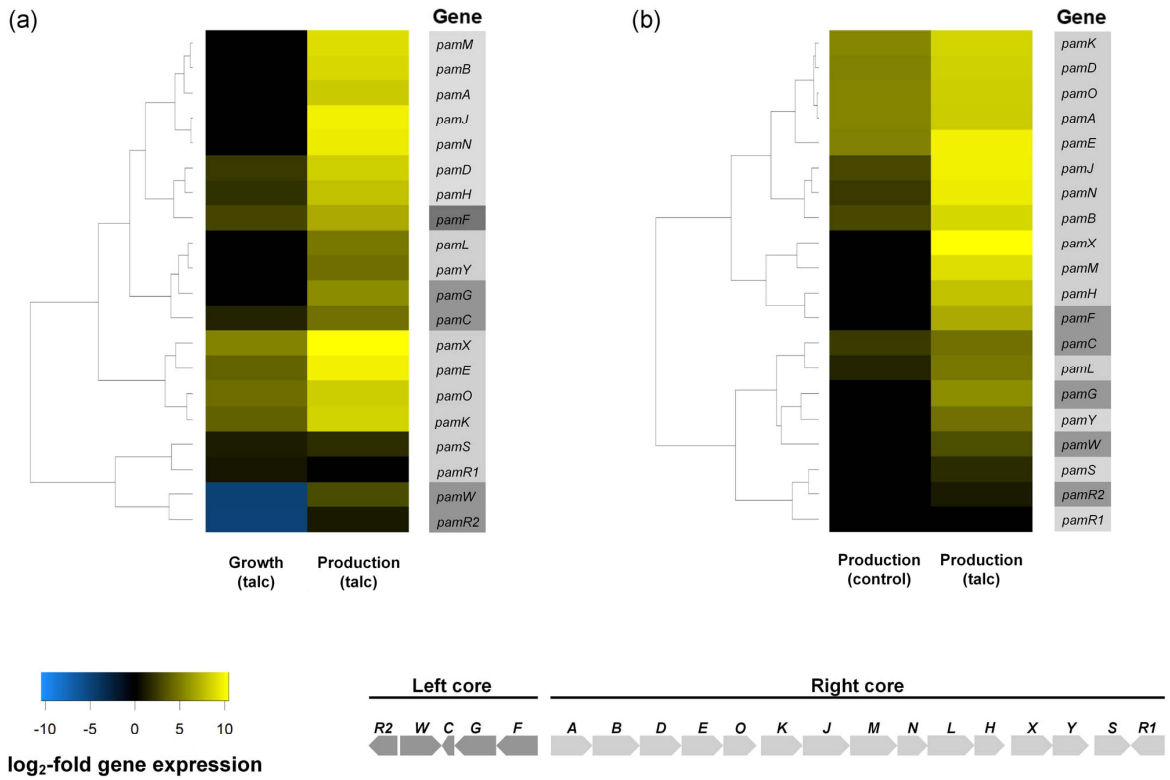

FIGURE 6 Hierarchical cluster analysis of the expression of the pamamycin biosynthetic pathway genes in *Streptomyces albus* J1074/R2. Samples were taken from a control and a talc supplied culture (10 g/L) in SGG medium during exponential growth (5 hr) and production phase (21 hr). The expression level of the control culture during growth (5 hr) was used as a reference. The cluster comprises the genes *pamA*, 3-oxoacyl-synthase 2; *pamB*, 3-oxoadipate CoA-transferase subunit A; *pamC*, acyl carrier protein; *pamD*, 3-oxoacyl-synthase 3 protein 1; *pamE*, 3-oxoacyl-synthase 3; *pamF*, 3-oxoacyl-synthase 2; *pamG*, 3-oxoacyl-synthase 3; *pamH*, aminohydrolase; *pamJ*, 3-oxoacyl-synthase 2; *pamK*, 3-oxoacyl-synthase 3; *pamL*, putative sulfoacetate-CoA ligase; *pamM*, 3-oxoacyl-reductase FabG; *pamN*, putative oxidoreductase; *pamO*, 3-oxoacyl-reductase FabG; *pamR1*, response regulator protein VraR; *pamR2*, tetracycline repressor protein class E; *pamS*, carnityl-CoA dehydratase; *pamW*, antiseptic resistance protein; *pamX*, L-lysine-8-amino-7-oxononanoate aminotransferase; *pamY*, cypemycin methyltransferase (Rebets et al., 2015) [Color figure can be viewed at wileyonlinelibrary.com]

from propionyl-CoA and the conversion of acetyl-CoA into malonyl-CoA. Moreover, talc supply resulted in the downregulation of methylmalonyl-CoA carboxyltransferase (*XNRR2_1278*). In contrast, elevated expression of acetyl-CoA acetyltransferase (*XNRR2_0301*, *XNRR2_1438*, *XNRR2_1987*), acetoacetyl-CoA synthetase (*XNRR2_5448*) crotonyl-CoA carboxylase/reductase (*XNRR2_0456*, *XNRR2_5889*), methylmalonyl-CoA mutase (*XNRR2_4665*, *XNRR2_4666*), and methylmalonyl-CoA epimerase (*XNRR2_1439*) was observed (Table 2).

3.8 | Microparticles affect intracellular CoA-ester pools during pamamycin production in *S. albus* J1074/R2

Due to the significant transcriptomic changes around the pamamycin cluster and the genes of its precursor metabolism, it appeared interesting to assess the availability of the product precursors during the production process. We focused our analysis on 11 CoA-esters that are either directly incorporated into pamamycins, that is, succinyl-CoA, malonyl-CoA, methylmalonyl-CoA, and ethylmalonyl-CoA (Figure 1), or are connected to these building blocks. For this purpose, we acquired CoA-ester levels in a talc supplied (10 g/L) and a control culture during the major phase of production (20 hr). Interestingly, the microparticles strongly affected the CoA-ester pools (Figure 7). The level of malonyl-CoA (−48%), methylsuccinyl-CoA (−46%), crotonyl-CoA (−32%), and acetyl-CoA (−19%) was strongly decreased. In contrast, the pool of methylmalonyl-CoA was increased by more than 100%. Furthermore, the microparticles increased the level of acetoacetyl-CoA (+250%) and the pool of the isomers butyryl-/isobutyryl-CoA (+169%). The abundance of succinyl-CoA, propionyl-CoA, and ethylmalonyl-CoA remained unchanged.

TABLE 2 Impact of talc microparticles on the expression of genes associated to CoA-thioester metabolism in pamamycin producing *Streptomyces albus* J1074/R2

Gene	Annotation	Growth (Talc)	Prod. (Talc)	Prod. (Control)
XNRR2_0221	Enoyl-CoA hydratase	0.0	5.0	0.0
XNRR2_0301	Acetyl-CoA acetyltransferase	0.0	4.3	0.0
XNRR2_0454	3-Hydroxybutyryl-CoA dehydrogenase	3.2	−1.0	0.0
XNRR2_0456	Crotonyl-CoA carboxylase/reductase	11.3	3.8	0.0
XNRR2_0457	Ethylmalonyl-CoA mutase	8.5	0.0	0.0
XNRR2_1278	Methylmalonyl-CoA decarboxylase	−3.2	−2.3	0.0
XNRR2_1304	Branched-chain amino acid aminotransferase	2.0	1.5	0.0
XNRR2_1417	Isobutyryl-CoA mutase	−1.0	1.3	0.0
XNRR2_1438	Acetyl-CoA acetyltransferase	2.9	4.3	0.0
XNRR2_1439	Methylmalonyl-CoA epimerase; ethylmalonyl-CoA epimerase	3.3	2.3	0.0
XNRR2_1452	3-Hydroxybutyryl-CoA dehydrogenase	1.0	1.3	0.0
XNRR2_1987	Acetyl-CoA acetyltransferase	3.3	3.7	0.0
XNRR2_2839	Valine dehydrogenase	1.1	2.2	0.0
XNRR2_3056	Branched-chain alpha-keto acid dehydrogenase E2	−1.7	0.0	0.0
XNRR2_3069	Branched-chain alpha-keto acid dehydrogenase E2	1.4	0.0	0.0
XNRR2_3858	Isobutyryl CoA mutase, small subunit	1.9	1.8	0.0
XNRR2_4024	Propionyl-CoA carboxylase, beta subunit	2.2	1.2	1.0
XNRR2_4211	Acetyl-/propionyl-CoA carboxylase α-subunit	−6.0	1.7	0.0
XNRR2_4665	Methylmalonyl-CoA mutase large subunit	1.6	2.2	0.0
XNRR2_4666	Methylmalonyl-CoA small subunit	2.2	2.3	0.0
XNRR2_5448	Acetoacetyl-CoA synthetase	8.0	5.9	0.0
XNRR2_5889	Crotonyl-CoA reductase	9.0	8.2	8.6

Note: Samples were taken from a control and a talc supplied culture (10 g/L) in SGG medium during growth (5 hr) and production (21 hr). The values correspond to $\log_2$-fold expression changes, considering the control during growth (5 hr) as reference. The annotation was taken from the genome (entry T02545 in KEGG) of *S. albus* (Zaburannyi et al., 2014).

4 | DISCUSSION

4.1 | Microparticle-enhanced production supports future exploration of pamamycins as lead molecules for novel antituberculosis drugs

As shown in this study, talc microparticles increased the production of pamamycins in recombinant *S. albus* J1074/R2 almost threefold to 50 mg/L, the highest titer observed so far for these polyketides (Figure 3). In this regard, the strongly improved pamamycin production by addition of talc is supposed to facilitate future exploration of this important polyketide. As shown, only small amounts of talc were required to achieve the stimulating effect (Figures 2 and 3), so that a use of this cheap material for pamamycin production appears feasible also from a cost perspective. Remarkably, the addition of talc selectively triggered the formation of larger variants (Figure 3a), that is, Pam 635, Pam 649, and Pam 663. Due to the fact that the different derivatives apparently differ in biological activity (Lefèvre et al., 2004; Natsume, 2016), a microparticle-based process might help to selectively enrich heavier pamamycin variants in the total product spectrum with potentially other activities.

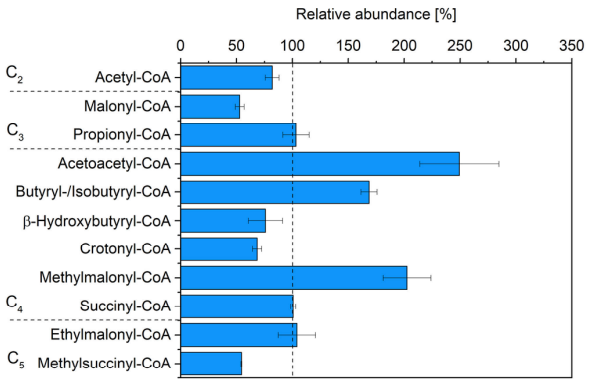

FIGURE 7 Relative changes of intracellular CoA-ester pools in pamamycin producing *Streptomyces albus* J1074/R2 by the addition of talc microparticles (10 g/L) to the culture during the major production phase (21 hr). The intracellular availability of 11 CoA-esters, directly and indirectly linked to pamamycin assembly was assessed during the production phase (21 hr) of a talc supplied and a control culture (set to 100%, shown as dashed line) [Color figure can be viewed at wileyonlinelibrary.com]

4.2 | Pamamycin production in *S. albus* is linked to morphological development

The obtained RNA sequencing data provided a detailed insight into the dynamics of morphology development along the production process (Figures 5, 6, and S1–S7; Tables 1 and 2). As shown for the control, genes encoding morphology regulators and morphogenetic proteins were strongly activated during the shift from growth to production (Figure 8). These comprised prominent players of morphology control in Streptomycetes: (a) *XNRR2_1071* (RelA) providing ppGpp, known to control morphogenetic proteins (Hesketh, Chen, Ryding, Chang, & Bibb, 2007), (b) *XNRR2_1554* (EshA) supporting ppGpp accumulation and essential for morphology development in *S. griseus* (Saito et al., 2006; van Wezel & McDowall, 2011); (c) *XNRR2_5315* (SsgA), limiting hyphae growth and branching, supporting septation, and formation of spore-like compartments (van Wezel, van der Meulen, Taal, Koerten, & Kraal, 2000b); (d) *XNRR2_2306* (Factor C protein), stimulating sporulation in submerged culture (Birkó et al., 1999; van Wezel & McDowall, 2011); (e) hydrophobic coat proteins such as chaplins and rodlins, which form the surface rodlet layer on spores (Claessen et al., 2004); and (f) *XNRR2_3527* (sigma factor BldN) controlling their expression in *S. venezuelae* (Bibb et al., 2012) and likely in *S. coelicolor* (McCormick & Flärdh, 2012; Figure 8; Table 1). There seems no doubt that this morphological development during the culture triggered the pamamycin formation (van Wezel & McDowall, 2011). It was interesting to note that the addition of talc influenced the utilization of nutrients, including phosphate and glycerol (Figure S8) and furthermore affected the amount of biomass formed (Figure 2). We cannot provide a clear conclusion on the underlying effects at this point but would like to notice that the understanding of these effects remains an important question.

4.3 | Microparticles accelerate the morphogenesis of *S. albus* toward sporulation-oriented mycelial development and cell division

Notably, the morphogenesis program was massively upregulated in the presence of the talc particles (Figure 8; Table 1). The activation was already visible during the initial growth phase and was even stronger during the later production phase. It was observed for practically all genes, which were identified as part of the morphology control cascade. We therefore conclude that the microparticles significantly speeded up the aging of the *S. albus* culture and accelerated the shift to second mycelium formation and submerged sporulation response. It appears highly likely that the enhanced pamamycin formation, including a strong overexpression of the *pam* cluster itself, was a consequence of the accelerated morphogenesis program, induced by the microparticles. It is well known that natural product formation is linked to morphological differentiation in Streptomycetes (Chater, 1984), so that its perturbation can be efficiently exploited to influence antibiotic production in *S. coelicolor*, *S. lividans*, and other species (Chakraburtty & Bibb, 1997; Hesketh et al., 2007; van Wezel & McDowall, 2011). Admittedly, the data did not allow to identify the specific link between morphology development, pamamycin cluster expression, and altered expression of its two regulators (Figure 6). More work will be needed in the future to resolve this in greater detail. *S. albus* possesses a range of different (mainly uncharacterized) ECF sigma factors and regulators, of which the majority was found affected by talc and gives a flavor of the complexity to be explored (Table S1).

4.4 | Talc microparticles orchestrate the regulatory and metabolic network of *S. albus* to a highly efficient program for pamamycin production

We now mapped the obtained transcriptomic and metabolomic data on the carbon core network of *S. albus* to obtain a systems-view on pamamycin production and supporting pathways (Figure 9). First, specific adjustments were observed in central carbon metabolism. Genes, related to conversion of glycerol were generally upregulated during the major production phase, linked to the on-set of glycerol consumption at this point (Figure S8). This substrate shift could also explain the increased expression of the EMP pathway genes alongside the downregulation of the oxidative PP pathway at the level of 6-phosphogluconate dehydrogenase. The effects were slightly more pronounced in the presence of talc. Second, most genes encoding for enzymes of CoA-ester metabolism were upregulated by the microparticles as

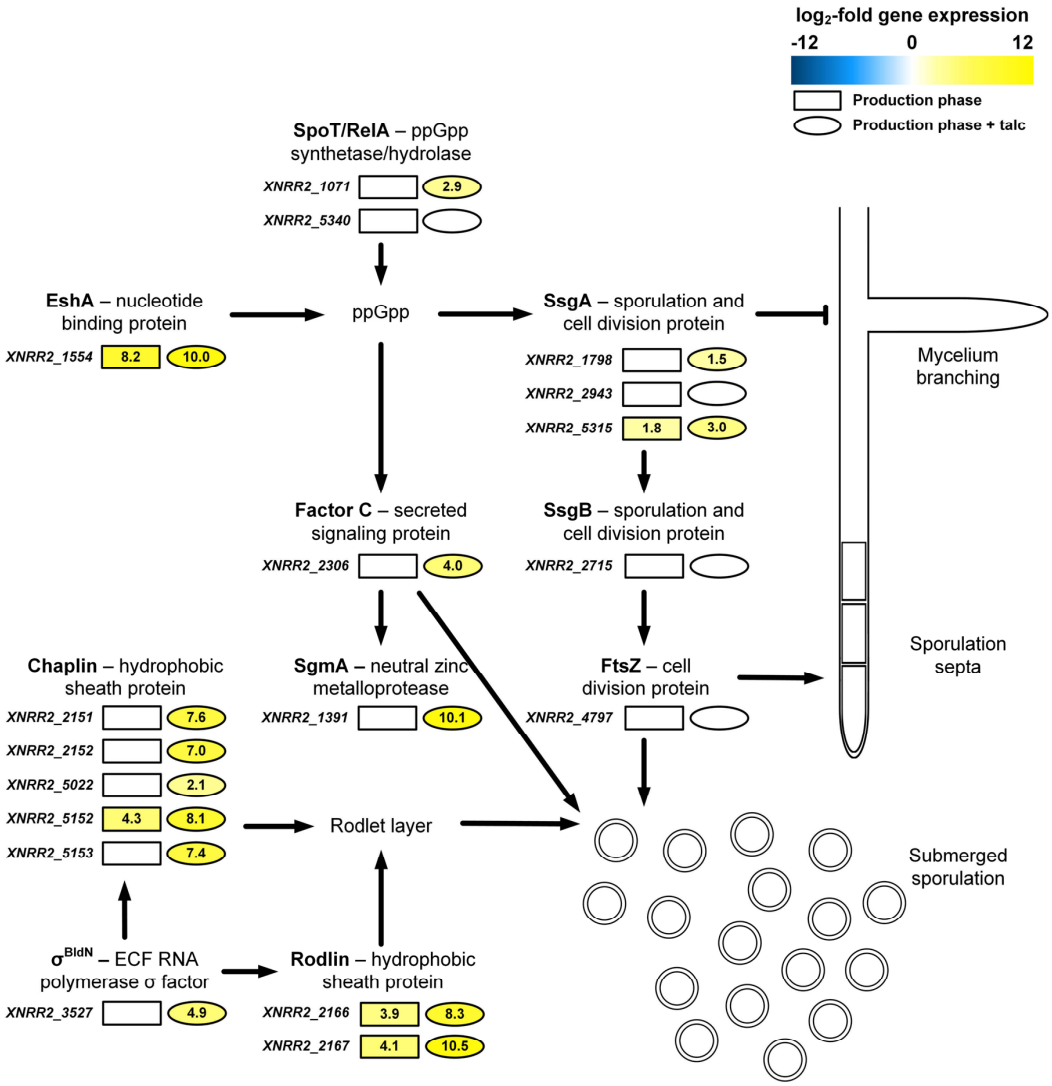

FIGURE 8 Impact of talc microparticles on the morphogenesis of pamamycin producing *Streptomyces albus* J1074/R2 in submerged culture. The data reflect differential gene expression of morphology-associated genes during the pamamycin production phase (21) in the presence of 10 g/L talc (ellipse) and the control process without particles (rectangle). The gene expression during the growth phase (5 hr) of the control is used as a reference. The numbers denote $\log_2$-fold expression change. Further details on the displayed components of the morphology cascade are given in Table 2 [Color figure can be viewed at wileyonlinelibrary.com]

well and resulted in a modulation of CoA-ester availability. Third, the changes in the CoA-ester metabolism had direct impact on the spectrum of pamamycins formed. It was interesting to note that the particles perturbed the ratio between malonyl-CoA, methylmalonyl-CoA, and ethylmalonyl-CoA (Figure 7). The three building blocks compete for incorporation into pamamycin. The polyketide assembly line equally accepts them as substrates, which leads to 16 pamamycin derivatives that differ in their side chains at six positions (Rebets et al., 2015). As shown, microparticle-affected cells produced more than twofold less small pamamycins (Pam 579 and Pam 593), whereas heavier derivatives were enriched (Pam 607, Pam 621, Pam 635, Pam 649, and Pam 663).

We conclude that this was the consequence of an increased availability of the larger building block methylmalonyl-CoA, together with a reduction in the malonyl-CoA pool.

It would be interesting to further explore this link in other natural producers, which obviously differ in the spectrum of pamamycin homologues (Natsume, Yasui, Kondo, & Marumo, 1991; Natsume et al., 1995; Kozone, Chikamoto, Abe, & Natsume, 1999). Metabolic engineering of CoA-ester supply appears promising to streamline pamamycin production towards selective derivatives (Lu, Zhang, Jiang, & Bai, 2016).

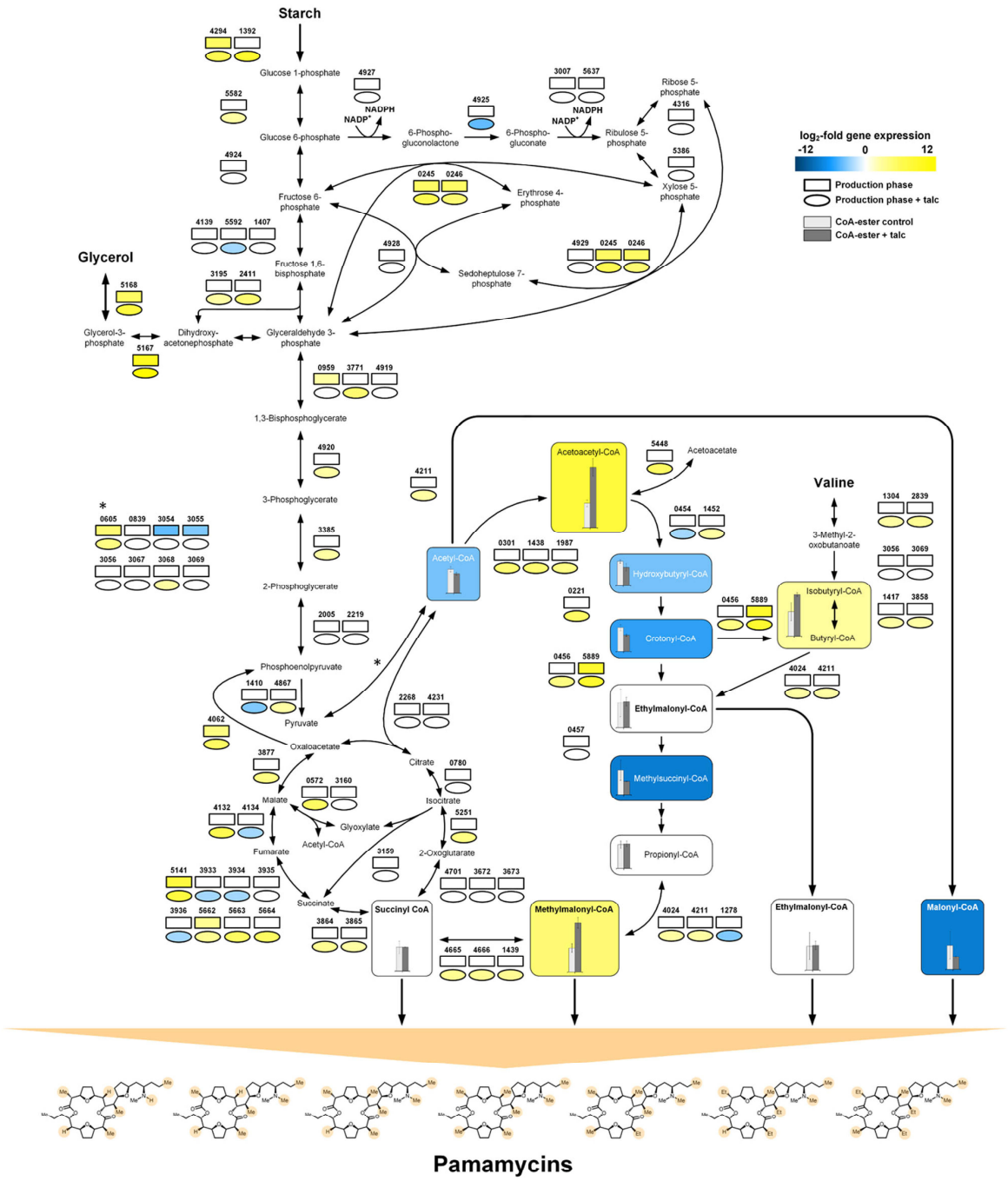
Starch
Glucose 1-phosphate
Glucose 6-phosphate
6-Phospho-gluconolactone
6-Phospho-gluconate
Ribulose 5-phosphate
Ribose 5-phosphate
Xylose 5-phosphate
Fructose 6-phosphate
Erythrose 4-phosphate
Sedoheptulose 7-phosphate
Fructose 1,6-bisphosphate
Glycerol
Glycerol-3-phosphate
Dihydroxy-acetonephosphate
Glyceraldehyde 3-phosphate
1,3-Bisphosphoglycerate
3-Phosphoglycerate
2-Phosphoglycerate
Phosphoenolpyruvate
Pyruvate
Oxaloacetate
Citrate
Isocitrate
Malate
Fumarate
Glyoxylate
Acetyl-CoA
2-Oxoglutarate
Succinate
Succinyl CoA
Acetoacetyl-CoA
Acetoacetate
Hydroxybutyryl-CoA
Crotonyl-CoA
Isobutyryl-CoA
Butyryl-CoA
Ethylmalonyl-CoA
Methylsuccinyl-CoA
Propionyl-CoA
Methylmalonyl-CoA
Valine
3-Methyl-2-oxobutanoate
Malonyl-CoA
log2-fold gene expression
-12 0 12
Production phase
Production phase + talc
CoA-ester control
CoA-ester + talc
Pamamycins

5 | CONCLUSIONS

We could show that talc microparticles globally reprogrammed the metabolism of *S. albus*, forced an accelerated morphological development, and triggered expression of the pamamycin cluster and supporting pathways. Despite the long tradition and the great success microparticles as process agents for filamentous microbes, it has remained largely unclear how the particles actually mediate the observed effects on the molecular level (Antecka, Bizukojc, & Ledakowicz, 2016). In this regard, our insights appear of general value for further exploration and industrialization of microparticle-enhanced processes. The use of microparticles, furthermore promises to support strain engineering by suggesting novel genetic targets, given the rich response on the genomic level observed in this study. Altogether, it appears fair to state that microparticle-enhanced production is advancing into a broadly applicable strategy to tailor *Streptomyces*, *Amycolatopsis*, and other related filamentous Actinomycetes for natural product formation (e.g. rifamycin, ivermectin, etc.) and should be further explored to support their discovery, development, and industrialization (Barton et al., 2018). During the work, the streamlined *S. albus* "clean" chassis turned out to grow fast and exhibit high and stable pamamycin biosynthesis, suggesting further use (Myronovskyi et al., 2018). "Cluster-free" chassis strains appear particularly promising for selective production in the future, given the activation of native clusters observed here (Figure 5).

ACKNOWLEDGMENTS

The work of Martin Kuhl, Lars Gläser, and Christoph Wittmann was supported by the German Ministry of Education and Research (BMBF) under Grant MyBio (FKZ 031B0344A) and the German Research Foundation (FKZ INST 256/418-1). The work of Yuri Rebets and Andriy Luzhetskyy was supported by the BMBF under Grant MyBio (FKZ 031B0344B). The work of Christian Rückert and Jörn Kalinowski acknowledge funding by the BMBF through the grant MyBio (FKZ 031B0344C). Thomas Hartsch and Namrata Sarkar was supported by the BMBF under Grant MyBio (FKZ 031B0344D). The funding bodies did not contribute to study design, data collection, analysis, and interpretation, or writing of the manuscript. Open access funding enabled and organized by Projekt DEAL.

CONFLICT OF INTERESTS

Yuriy Rebets and Andriy Luzhetskyy have submitted a patent application to produce pamamycin in *S. albus*. The other authors declare that there are no conflict of interests.

AUTHOR CONTRIBUTIONS

C. W. designed the project. M. K. conducted the cultures. M. K. and Y. R. performed pamamycin analysis. M. K. and L. G. performed CoA ester analysis. C. R. and J. K. performed RNA sequencing. C. R., J. K., N. S., and T. H. processed and evaluated the RNA sequencing data. M. K. and C. W. analyzed the data, drew the figures, and wrote the first draft of the manuscript. All authors commented, extended, and improved the manuscript. All authors read and approved the final version of the manuscript.

DATA AVAILABILITY STATEMENT

The raw and processed RNA sequencing data of this article are available as MIAME-compliant datasets in Gene Expression Omnibus under the accession number GSE155008. The authors declare that all other data supporting the findings of this study are available within the article and its supplementary information file.

ORCID

Jörn Kalinowski https://orcid.org/0000-0002-9052-1998
Andriy Luzhetskyy https://orcid.org/0000-0001-6497-0047
Christoph Wittmann http://orcid.org/0000-0002-7952-985X

REFERENCES

Ahmed, Y., Rebets, Y., Estevez, M. R., Zapp, J., Myronovskyi, M., & Luzhetskyy, A. (2020). Engineering of *Streptomyces lividans* for heterologous expression of secondary metabolite gene clusters. *Microbial Cell Factories*, *19*(1), 5. https://doi.org/10.1186/s12934-020-1277-8

Angert, E. R. (2005). Alternatives to binary fission in bacteria. *Nature Reviews Microbiology*, *3*(3), 214–224. https://doi.org/10.1038/nrmicro1096

Antecka, A., Bizukojc, M., & Ledakowicz, S. (2016). Modern morphological engineering techniques for improving productivity of filamentous fungi in submerged cultures. *World Journal of Microbiology & Biotechnology*, *32*(12), 193. https://doi.org/10.1007/s11274-016-2148-7

FIGURE 9 Multiomics view on the effect of talc microparticles on pathways supporting pamamycin biosynthesis in *Streptomyces albus* J1074/R2 during the production phase. The boxes indicate differential gene expression of the control (rectangle) and the talc supplied process (10 g/L talc, ellipse) during the major production phase, as compared to the reference (control in growth phase, boxes indicate XNRR2 numbers). The bar charts display relative CoA-ester availability. Although CCR (*XNRR2_0456* and *XNRR2_5889*) and PCC (*XNRR2_4024* and *XNRR2_4211*) might be able to convert crotonyl-CoA to butyryl-CoA and butyryl-CoA to ethylmalonyl-CoA, respectively, their main activity catalyzes the formation of ethylmalonyl-CoA and propionyl-CoA, respectively (Chan, Podevels, Kevany, & Thomas, 2009). The observed changes in CoA ester metabolism were complex. Direct correlations between one particular thioester and one enzyme appeared infeasible, due to this complexity and the known promiscuity of several of the CoA-ester converting enzymes (Chan et al., 2009). However, a few conclusions could be drawn. The genes, encoding for reactions upstream of increased CoA-ester pools, that is, acetoacetyl-CoA, (iso)butyryl-CoA, and methylmalonyl-CoA were found upregulated, which suggests that the accumulation was related to an enhanced biosynthesis. In addition, the entry steps into the CoA metabolism were found massively altered. The flux from acetyl-CoA was largely redirected to form acetoacetyl-CoA, instead of malonyl-CoA. The data further suggested that the increased amount of methylmalonyl CoA was mainly derived from succinyl-CoA. The alternative ethylmalonyl CoA route appeared attenuated because major intermediates involved, that is, hydroxybutyryl-CoA, crotonyl-CoA, methylsuccinyl-CoA, were found reduced [Color figure can be viewed at wileyonlinelibrary.com]

Arcamone, F., Cassinelli, G., Fantini, G., Grein, A., Orezzi, P., Pol, C., & Spalla, C. (1969). Adriamycin, 14-hydroxydaimomycin, a new antitumor antibiotic from *S. Peucetius var. caesius*. *Biotechnology and Bioengineering*, *11*(6), 1101–1110. https://doi.org/10.1002/bit.260110607

Barton, N., Horbal, L., Starck, S., Kohlstedt, M., Luzhetskyy, A., & Wittmann, C. (2018). Enabling the valorization of guaiacol-based lignin: Integrated chemical and biochemical production of cis, cis-muconic acid using metabolically engineered *Amycolatopsis* sp ATCC 39116. *Metabolic Engineering*, *45*, 200–210. https://doi.org/10.1016/j.ymben.2017.12.001

Bayer, E., Gugel, K., Hägele, K., Hagenmaier, H., Jessipow, S., König, W., & Zähner, H. (1972). Stoffwechselprodukte von Mikroorganismen. 98. Mitteilung. Phosphinothricin und Phosphinothricyl-Alanyl-Alanin. *Helvetica Chimica Acta*, *55*(1), 224–239. https://doi.org/10.1002/hlca.19720550126

Becker, J., Klopprogge, C., Schröder, H., & Wittmann, C. (2009). Metabolic engineering of the tricarboxylic acid cycle for improved lysine production by *Corynebacterium glutamicum*. *Applied and Environmental Microbiology*, *75*(24), 7866–7869. https://doi.org/10.1128/AEM.01942-09

Belmar-Beiny, M., & Thomas, C. (1991). Morphology and clavulanic acid production of *Streptomyces clavuligerus*: Effect of stirrer speed in batch fermentations. *Biotechnology and Bioengineering*, *37*(5), 456–462. https://doi.org/10.1002/bit.260370507

Bibb, M. J. (2013). Understanding and manipulating antibiotic production in Actinomycetes. *Biochemical Society Transactions*, *41*(6), 1355–1364. https://doi.org/10.1042/BST20130214

Bibb, M. J., Domonkos, Á., Chandra, G., & Buttner, M. J. (2012). Expression of the chaplin and rodlin hydrophobic sheath proteins in *Streptomyces venezuelae* is controlled by σBldN and a cognate anti-sigma factor, RsbN. *Molecular Microbiology*, *84*(6), 1033–1049. https://doi.org/10.1111/j.1365-2958.2012.08070.x

Birkó, Z., Bialek, S., Buzás, K., Szajli, E., Traag, B. A., Medzihradszky, K. F., … Biró, S. (2007). The secreted signaling protein factor C triggers the A-factor response regulon in *Streptomyces griseus*: Overlapping signaling routes. *Molecular & Cellular Proteomics*, *6*(7), 1248–1256. https://doi.org/10.1074/mcp.M600367-MCP200

Birkó, Z., Sümegi, A., Vinnai, A., Van Wezel, G., Szeszák, F., Vitális, S., … Biró, S. (1999). Characterization of the gene for factor C, an extracellular signal protein involved in morphological differentiation of *Streptomyces griseus*. *Microbiology*, *145*(9), 2245–2253. https://doi.org/10.1099/00221287-145-9-2245

Campbell, W. C., Fisher, M. H., Stapley, E. O., Albers-Schönberg, G., & Jacob, T. A. (1983). Ivermectin: A potent new antiparasitic agent. *Science*, *221*(4613), 823–828. https://doi.org/10.1126/science.6308762

Chakraburtty, R., & Bibb, M. (1997). The ppGpp synthetase gene (relA) of *Streptomyces coelicolor* A3 (2) plays a conditional role in antibiotic production and morphological differentiation. *Journal of Bacteriology*, *179*(18), 5854–5861. https://doi.org/10.1128/jb.179.18.5854-5861.1997

Chan, Y. A., Podevels, A. M., Kevany, B. M., & Thomas, M. G. (2009). Biosynthesis of polyketide synthase extender units. *Natural Product Reports*, *26*(1), 90–114. https://doi.org/10.1039/b801658p

Chater, K. F. (1984). Morphological and physiological differentiation in Streptomyces. *Microbial Development*, *16*, 89–115. https://doi.org/10.1101/0.89-115

Chater, K. F., & Losick, R. (1997). Mycelial life style of *Streptomyces coelicolor* A3 (2) and its relatives, *Multicellular and interactive behavior of bacteria: In nature, industry and the laboratory* (pp. 149–182). Oxford, UK: Oxford University Press.

Claessen, D., Stokroos, I., Deelstra, H. J., Penninga, N. A., Bormann, C., Salas, J. A., … Wösten, H. A. (2004). The formation of the rodlet layer of Streptomycetes is the result of the interplay between rodlins and chaplins. *Molecular Microbiology*, *53*(2), 433–443. https://doi.org/10.1111/j.1365-2958.2004.04143.x

van Dissel, D., Claessen, D., & van Wezel, G. P. (2014). Morphogenesis of *Streptomyces* in submerged cultures, *Advances in Applied Microbiology* (89, pp. 1–45). Amsterdam, The Netherlands: Elsevier.

Driouch, H., Hänsch, R., Wucherpfennig, T., Krull, R., & Wittmann, C. (2012). Improved enzyme production by bio-pellets of *Aspergillus niger*: Targeted morphology engineering using titanate microparticles. *Biotechnology and Bioengineering*, *109*(2), 462–471. https://doi.org/10.1002/bit.23313

Driouch, H., Roth, A., Dersch, P., & Wittmann, C. (2010). Filamentous fungi in good shape: Microparticles for tailor-made fungal morphology and enhanced enzyme production. *Bioengineered Bugs*, *2*(2), 100–104. https://doi.org/10.4161/bbug.2.2.13757

Driouch, H., Sommer, B., & Wittmann, C. (2010). Morphology engineering of *Aspergillus niger* for improved enzyme production. *Biotechnology and Bioengineering*, *105*(6), 1058–1068. https://doi.org/10.1002/bit.22614

Ehrlich, J., Bartz, Q. R., Smith, R. M., Joslyn, D. A., & Burkholder, P. R. (1947). Chloromycetin, a new antibiotic from a soil actinomycete. *Science*, *106*(2757), 417. https://doi.org/10.1126/science.106.2757.417

Etschmann, M. M., Huth, I., Walisko, R., Schuster, J., Krull, R., Holtmann, D., … Schrader, J. (2015). Improving 2-phenylethanol and 6-pentyl-α-pyrone production with fungi by microparticle-enhanced cultivation (MPEC). *Yeast*, *32*(1), 145–157. https://doi.org/10.1002/yea.3022

Flärdh, K., Kindlay, K. C., & Chater, K. F. (1999). Association of early sporulation genes with suggested developmental decision points in *Streptomyces coelicolor* A3(2). *Microbiology*, *145*(9), 2229–2243.

Glazebrook, M. A., Vining, L. C., & White, R. L. (1992). Growth morphology of *Streptomyces akiyoshiensis* in submerged culture: Influence of pH, inoculum, and nutrients. *Canadian Journal of Microbiology*, *38*(2), 98–103. https://doi.org/10.1139/m92-016

Gläser, L., Kuhl, M., Jovanovic, S., Fritz, M., Vögeli, B., Erb, T., … Wittmann, C. (2020). A common approach for absolute quantification of short chain CoA thioesters in industrially relevant gram-positive and gram-negative prokaryotic and eukaryotic microbes. *Microbial Cell Factories*, *19*, 160.

Hanquet, G., Salom-Roig, X., & Lanners, S. (2016). New insights into the synthesis and biological activity of the pamamycin macrodiolides. *Chimia*, *70*(1-2), 20–28. https://doi.org/10.2533/chimia.2016.20

Hesketh, A., Chen, W. J., Ryding, J., Chang, S., & Bibb, M. (2007). The global role of ppGpp synthesis in morphological differentiation and antibiotic production in *Streptomyces coelicolor* A3 (2). *Genome Biology*, *8*(8), R161. https://doi.org/10.1186/gb-2007-8-8-r161

Hilker, R., Stadermann, K. B., Doppmeier, D., Kalinowski, J., Stoye, J., Straube, J., … Goesmann, A. (2014). ReadXplorer—visualization and analysis of mapped sequences. *Bioinformatics*, *30*(16), 2247–2254. https://doi.org/10.1093/bioinformatics/btu205

Holtmann, D., Vernen, F., Müller, J., Kaden, D., Risse, J. M., Friehs, K., … Schrader, J. (2017). Effects of particle addition to *Streptomyces* cultivations to optimize the production of actinorhodin and streptavidin. *Sustainable Chemistry and Pharmacy*, *5*, 67–71. https://doi.org/10.1016/j.scp.2016.09.001

Horbal, L., Marques, F., Nadmid, S., Mendes, M. V., & Luzhetskyy, A. (2018). Secondary metabolites overproduction through transcriptional gene cluster refactoring. *Metabolic Engineering*, *49*, 299–315. https://doi.org/10.1016/j.ymben.2018.09.010

Jonsbu, E., McIntyre, M., & Nielsen, J. (2002). The influence of carbon sources and morphology on nystatin production by *Streptomyces noursei*. *Journal of Biotechnology*, *95*(2), 133–144. https://doi.org/10.1016/s0168-1656(02)00003-2

Juarez, M., Schcolnik-Cabrera, A., & Dueñas-Gonzalez, A. (2018). The multitargeted drug ivermectin: From an antiparasitic agent to a repositioned cancer drug. *American Journal of Cancer Research*, *8*(2), 317–331.

Kallifidas, D., Jiang, G., Ding, Y., & Luesch, H. (2018). Rational engineering of *Streptomyces albus* J1074 for the overexpression of secondary metabolite gene clusters. *Microbial Cell Factories*, *17*(1), 25. https://doi.org/10.1186/s12934-018-0874-2

Kato, J.-y, Suzuki, A., Yamazaki, H., Ohnishi, Y., & Horinouchi, S. (2002). Control by A-factor of a metalloendopeptidase gene involved in aerial mycelium formation in *Streptomyces griseus*.

Journal of Bacteriology, *184*(21), 6016–6025. https://doi.org/10.1128/JB.184.21.6016-6025.2002

Kaup, B. A., Ehrich, K., Pescheck, M., & Schrader, J. (2008). Microparticle-enhanced cultivation of filamentous microorganisms: Increased chloroperoxidase formation by *Caldariomyces fumago* as an example. *Biotechnology and Bioengineering*, *99*(3), 491–498. https://doi.org/10.1002/bit.21713

Kieser, T., Bibb, M. J., Buttner, M. J., Chater, K. F., & Hopwood, D. A. (2000). An introduction to *Streptomyces*, *Practical Streptomyces genetics* (p. 291). Norwich, UK: John Innes Foundation.

Koebsch, I., Overbeck, J., Piepmeyer, S., Meschke, H., & Schrempf, H. (2009). A molecular key for building hyphae aggregates: The role of the newly identified *Streptomyces* protein HyaS. *Microbial Biotechnology*, *2*(3), 343–360. https://doi.org/10.1111/j.1751-7915.2009.00093.x

Kozone, I., Chikamoto, N., Abe, H., & Natsume, M. (1999). De-N-methylpamamycin-593A and B, new pamamycin derivatives isolated from *Streptomyces alboniger*. *Journal of Antibiotics*, *52*(3), 329–331. https://doi.org/10.7164/antibiotics.52.329

Krull, R., Wucherpfennig, T., Esfandabadi, M. E., Walisko, R., Melzer, G., Hempel, D. C., … Wittmann, C. (2013). Characterization and control of fungal morphology for improved production performance in biotechnology. *Journal of Biotechnology*, *163*(2), 112–123. https://doi.org/10.1016/j.jbiotec.2012.06.024

Langmead, B., & Salzberg, S. L. (2012). Fast gapped-read alignment with Bowtie 2. *Nature Methods*, *9*(4), 357–359. https://doi.org/10.1038/nmeth.1923

Lechevalier, H., Acker, R. F., Corke, C. T., Haenseler, C. M., & Waksman, S. A. (1953). Candicidin, a new antifungal antibiotic. *Mycologia*, *45*(2), 155–171. https://doi.org/10.1080/00275514.1953.12024259

Lefèvre, P., Peirs, P., Braibant, M., Fauville-Dufaux, M., Vanhoof, R., Huygen, K., … Content, J. (2004). Antimycobacterial activity of synthetic pamamycins. *Journal of Antimicrobial Chemotherapy*, *54*(4), 824–827. https://doi.org/10.1093/jac/dkh402

Liu, X., Tang, J., Wang, L., & Liu, R. (2019). Mechanism of CuO nanoparticles on stimulating production of actinorhodin in Streptomyces coelicolor by transcriptional analysis. *Scientific Reports*, *9*(1), 11253. https://doi.org/10.1038/s41598-019-46833-1

Lopatniuk, M., Myronovskyi, M., Nottebrock, A., Busche, T., Kalinowski, J., Ostash, B., … Luzhetskyy, A. (2019). Effect of "ribosome engineering" on the transcription level and production of *S. albus* indigenous secondary metabolites. *Applied Microbiology and Biotechnology*, *103*, 7097–7110. https://doi.org/10.1007/s00253-019-10005-y

Love, M. I., Huber, W., & Anders, S. (2014). Moderated estimation of fold change and dispersion for RNA-seq data with DESeq2. *Genome Biology*, *15*(12), 550. https://doi.org/10.1186/s13059-014-0550-8

Lu, C., Zhang, X., Jiang, M., & Bai, L. (2016). Enhanced salinomycin production by adjusting the supply of polyketide extender units in *Streptomyces albus*. *Metabolic Engineering*, *35*, 129–137. https://doi.org/10.1016/j.ymben.2016.02.012

Martin, S. M., & Bushell, M. E. (1996). Effect of hyphal micromorphology on bioreactor performance of antibiotic-producing *Saccharopolyspora erythraea* cultures. *Microbiology*, *142*(7), 1783–1788. https://doi.org/10.1099/13500872-142-7-1783

McCormick, J. R., & Flärdh, K. (2012). Signals and regulators that govern *Streptomyces* development. *FEMS Microbiology Reviews*, *36*(1), 206–231. https://doi.org/10.1111/j.1574-6976.2011.00317.x

Myronovskyi, M., Rosenkranzer, B., Nadmid, S., Pujic, P., Normand, P., & Luzhetskyy, A. (2018). Generation of a cluster-free *Streptomyces albus* chassis strains for improved heterologous expression of secondary metabolite clusters. *Metabolic Engineering*, *49*, 316–324. https://doi.org/10.1016/j.ymben.2018.09.004

Natsume, M. (2016). Studies on bioactive natural products involved in the growth and morphological differentiation of microorganisms. *Journal of Pesticide Science*, *41*(3), 96–101. https://doi.org/10.1584/jpestics.J16-03

Natsume, M., Tazawa, J., Yagi, K., Abe, H., Kondo, S., & Marumo, S. (1995). Structure-activity relationship of pamamycins: Effects of alkyl substituents. *The Journal of Antibiotics*, *48*(10), 1159–1164. https://doi.org/10.1038/ja.2008.118

Natsume, M., Yasui, K., Kondo, S., & Marumo, S. (1991). The structures of four new pamamycin homologues isolated from *Streptomyces alboniger*. *Tetrahedron Letters*, *32*(26), 3087–3090. https://doi.org/10.1016/0040-4039(91)80696-4

O'Cleirigh, C., Casey, J. T., Walsh, P. K., & O'Shea, D. G. (2005). Morphological engineering of *Streptomyces hygroscopicus var. geldanus*: Regulation of pellet morphology through manipulation of broth viscosity. *Applied Microbiology and Biotechnology*, *68*(3), 305–310. https://doi.org/10.1007/s00253-004-1883-0

R Core Team (2014). *R: A language and environment for statistical computing*. Vienna, Austria: R Foundation for Statistical Computing.

Rebets, Y., Brötz, E., Manderscheid, N., Tokovenko, B., Myronovskyi, M., Metz, P., … Luzhetskyy, A. (2015). Insigths into the pamamycin biosynthesis. *Angewandte Chemie-International Edition*, *127*(7), 2309–2313. https://doi.org/10.1002/anie.201408901

Ren, X.-D., Xu, Y.-J., Zeng, X., Chen, X.-S., Tang, L., & Mao, Z.-G. (2015). Microparticle-enhanced production of ε-poly-L-lysine in fed-batch fermentation. *RSC Advances*, *5*(100), 82138–82143. https://doi.org/10.1039/C5RA14319E

Saito, N., Xu, J., Hosaka, T., Okamoto, S., Aoki, H., Bibb, M. J., & Ochi, K. (2006). EshA accentuates ppGpp accumulation and is conditionally required for antibiotic production in *Streptomyces coelicolor* A3(2). *Journal of Bacteriology*, *188*(13), 4952–4961. https://doi.org/10.1128/JB.00343-06

Santamaría, R., & Pierre, P. (2012). Voronto: Mapper for expression data to ontologies. *Bioinformatics*, *28*(17), 2281–2282. https://doi.org/10.1093/bioinformatics/bts428

Schneider, C. A., Rasband, W. S., & Eliceiri, K. W. (2012). NIH Image to ImageJ: 25 years of image analysis. *Nature Methods*, *9*(7), 671–675. https://doi.org/10.1038/nmeth.2089

Sehgal, S. N., Baker, H., & Vézina, C. (1975). Rapamycin (AY-22, 989), a new antifungal antibiotic. II. Fermentation, isolation and characterization. *The Journal of Antibiotics*, *28*(10), 727–732. https://doi.org/10.7164/antibiotics.28.727

Traag, B. A., & van Wezel, G. P. (2008). The SsgA-like proteins in actinomycetes: Small proteins up to a big task. *Antonie Van Leeuwenhoek*, *94*(1), 85–97. https://doi.org/10.1007/s10482-008-9225-3

Vézina, C., Kudelski, A., & Sehgal, S. (1975). Rapamycin (AY-22, 989), a new antifungal antibiotic. I. Taxonomy of the producing streptomycete and isolation of the active principle. *The Journal of antibiotics*, *28*(10), 721–726. https://doi.org/10.7164/antibiotics.28.721

Walisko, R., Krull, R., Schrader, J., & Wittmann, C. (2012). Microparticle based morphology engineering of filamentous microorganisms for industrial bio-production. *Biotechnology Letters*, *34*(11), 1975–1982. https://doi.org/10.1007/s10529-012-0997-1

Walisko, J., Vernen, F., Pommerehne, K., Richter, G., Terfehr, J., Kaden, D., … Krull, R. (2017). Particle-based production of antibiotic rebeccamycin with *Lechevalieria aerocolonigenes*. *Process Biochemistry*, *53*, 1–9. https://doi.org/10.1016/j.procbio.2016.11.017

Wang, H., Zhao, G., & Ding, X. (2017). Morphology engineering of *Streptomyces coelicolor* M145 by sub-inhibitory concentrations of antibiotics. *Scientific Reports*, *7*(1), 13226. https://doi.org/10.1038/s41598-017-13493-y

Warnes, M. G. R., Bolker, B., Bonebakker, L., & Gentleman, R. (2016). *Package 'gplots'*. Various R programming tools for plotting data.

van Wezel, G. P., Krabben, P., Traag, B. A., Keijser, B. J., Kerste, R., Vijgenboom, E., … Kraal, B. (2006). Unlocking *Streptomyces* spp. for use as sustainable industrial production platforms by morphological engineering. *Applied and Environmental Microbiology*, *72*(8), 5283–5288. https://doi.org/10.1128/AEM.00808-06

van Wezel, G. P., & McDowall, K. J. (2011). The regulation of the secondary metabolism of *Streptomyces:* New links and experimental

advances. *Natural Product Reports*, *28*(7), 1311–1333. https://doi.org/10.1039/c1np00003a

van Wezel, G. P., van der Meulen, J., Kawamoto, S., Luiten, R. G., Koerten, H. K., & Kraal, B. (2000a). ssgA is essential for sporulation of *Streptomyces coelicolor* A3 (2) and affects hyphal development by stimulating septum formation. *Journal of Bacteriology*, *182*(20), 5653–5662.

van Wezel, G. P., van der Meulen, J., Taal, E., Koerten, H., & Kraal, B. (2000b). Effects of increased and deregulated expression of cell division genes on the morphology and on antibiotic production of Streptomycetes. *Antonie Van Leeuwenhoek*, *78*(3-4), 269–276. https://doi.org/10.1023/a:1010267708249

Xia, X., Lin, S., Xia, X.-X., Cong, F.-S., & Zhong, J.-J. (2014). Significance of agitation-induced shear stress on mycelium morphology and lavendamycin production by engineered *Streptomyces flocculus*. *Applied Microbiology and Biotechnology*, *98*(10), 4399–4407. https://doi.org/10.1007/s00253-014-5555-4

Xu, H., Chater, K. F., Deng, Z., & Tao, M. (2008). A cellulose synthase-like protein involved in hyphal tip growth and morphological differentiation in *Streptomyces*. *Journal of Bacteriology*, *190*(14), 4971–4978. https://doi.org/10.1128/JB.01849-07

Zaburannyi, N., Rabyk, M., Ostash, B., Fedorenko, V., & Luzhetskyy, A. (2014). Insights into naturally minimised *Streptomyces albus* J1074 genome. *BMC Genomics*, *15*(1), 97.

Zhang, Y., Wang, M., Tian, J., Liu, J., Guo, Z., Tang, W., & Chen, Y. (2020). Activation of paulomycin production by exogenous γ-butyrolactone signaling molecules in *Streptomyces albidoflavus*. *Applied Microbiology and Biotechnology*, *104*(1), J1074–J1705. https://doi.org/10.1007/s00253-019-10329-9

SUPPORTING INFORMATION

Additional supporting information may be found online in the Supporting Information section.

How to cite this article: Kuhl M, Gläser L, Rebets Y, et al. Microparticles globally reprogram *Streptomyces albus* toward accelerated morphogenesis, streamlined carbon core metabolism, and enhanced production of the antituberculosis polyketide pamamycin. *Biotechnology and Bioengineering*. 2020;1–18. https://doi.org/10.1002/bit.27537

3.2 Microparticles enhance the formation of seven major classes of natural products in native and metabolically engineered actinobacteria through accelerated morphological development

Martin Kuhl, Christian Rückert, Lars Gläser, Selma Beganovic, Andriy Luzhetskyy, Jörn Kalinowski, and Christoph Wittmann

Biotechnology and Bioengineering. 2021; in press

https://doi.org/10.1002/bit.27818

C. W. designed and supervised the project. M. K. conducted the cultures and performed substrate and natural product analysis. C. R. and J. K. performed genomics and transcriptomics of *S. lividans*. M. K. and L. G. performed metabolomics of *S. lividans*. M. K. and C. W. analyzed the data, drew the figures, and wrote the first draft of the manuscript. All authors commented, extended, and improved the manuscript. All authors read and approved the final version of the manuscript.

 The supplementary information to this article is available in the appendix.

Received: 4 March 2021 | Revised: 17 April 2021 | Accepted: 30 April 2021

DOI: 10.1002/bit.27818

ARTICLE

BIOTECHNOLOGY BIOENGINEERING WILEY

Microparticles enhance the formation of seven major classes of natural products in native and metabolically engineered actinobacteria through accelerated morphological development

Martin Kuhl[1] | Christian Rückert[3] | Lars Gläser[1] | Selma Beganovic[1] | Andriy Luzhetskyy[2] | Jörn Kalinowski[3] | Christoph Wittmann[1]

[1]Institute of Systems Biotechnology, Saarland University, Saarbrücken, Germany

[2]Department of Pharmaceutical Biotechnology, Saarland University, Saarbrücken, Germany

[3]Center for Biotechnology, Bielefeld University, Bielefeld, Germany

Correspondence
Christoph Wittmann, Institute of Systems Biotechnology, Saarland University, Saarbrücken, Germany.
Email: christoph.wittmann@uni-saarland.de

Funding information
Deutsche Forschungsgemeinschaft, Grant/Award Number: INST 256/418-1; Bundesministerium für Bildung und Forschung, Grant/Award Numbers: 031B0344, 031B0611, 031B0868

Abstract

Actinobacteria provide a rich spectrum of bioactive natural products and therefore display an invaluable source towards commercially valuable pharmaceuticals and agrochemicals. Here, we studied the use of inorganic talc microparticles (hydrous magnesium silicate, $3MgO{\cdot}4SiO_2{\cdot}H_2O$, 10 µm) as a general supplement to enhance natural product formation in this important class of bacteria. Added to cultures of recombinant *Streptomyces lividans*, talc enhanced production of the macrocyclic peptide antibiotic bottromycin A2 and its methylated derivative Met-bottromycin A2 up to 109 mg L^{-1}, the highest titer reported so far. Hereby, the microparticles fundamentally affected metabolism. With 10 g L^{-1} talc, *S. lividans* grew to 40% smaller pellets and, using RNA sequencing, revealed accelerated morphogenesis and aging, indicated by early upregulation of developmental regulator genes such as *ssgA*, ssgB, wblA, *sigN*, and *bldN*. Furthermore, the microparticles re-balanced the expression of individual bottromycin cluster genes, resulting in a higher macrocyclization efficiency at the level of BotAH and correspondingly lower levels of non-cyclized shunt by-products, driving the production of mature bottromycin. Testing a variety of *Streptomyces* species, talc addition resulted in up to 13-fold higher titers for the RiPPs bottromycin and cinnamycin, the alkaloid undecylprodigiosin, the polyketide pamamycin, the tetracycline-type oxytetracycline, and the anthramycin-analogs usabamycins. Moreover, talc addition boosted production in other actinobacteria, outside of the genus of *Streptomyces*: vancomycin (*Amycolatopsis japonicum* DSM 44213), teicoplanin (*Actinoplanes teichomyceticus* ATCC 31121), and the angucyclinone-type antibiotic simocyclinone (*Kitasatospora* sp.). For teicoplanin, the microparticles were even crucial to activate production. Taken together, the use of talc was beneficial in 75% of all tested cases and optimized natural and heterologous hosts forming the substance of interest with clusters under native and

synthetic control. Given its simplicity and broad benefits, microparticle-supplementation appears as an enabling technology in natural product research of these most important microbes.

KEYWORDS
Actinoplanes, *Amycolatopsis*, bottromycin, *Kitasatospora*, morphology, *Streptomyces*

1 | INTRODUCTION

Natural products are chemically diverse molecules that are synthetized by living organisms (Harvey, 2000). Many of them have potent pharmacological activities, which has enabled the development of antibiotics (Fleming, 2001), anticancer drugs (Arcamone et al., 1969), immunosuppressants (Vézina et al., 1975), infectants (Campbell et al., 1983), and various agrochemicals, including herbicides (Bayer et al., 1972), insecticides (Butterworth & Morgan, 1968), and fungicides (Takeuchi et al., 1958). During the last century, natural products and their derivatives have greatly helped to double human life expectation (Demain, 2006) and display more than 50% of today's approved drugs (Cragg & Newman, 2013). However, drug development from natural products is declining, partly caused by unreliable access and supply, leading inter alia to cost and profit concerns among pharmaceutical companies (Li & Vederas, 2009).

Actinobacteria display the most important microbial source of natural products and therefore offer an immense treasure (Barka et al., 2016). The genus *Streptomyces* provides more than two-third of all known antibiotics of microbial origin (Bibb, 2013) and more than half of the FDA-approved antibacterial natural products (Patridge et al., 2015) but also related actinobacteria such as *Micromonospora*, *Actinoplanes*, and *Amycolatopsis* (Barka et al., 2016) have emerged as producers of potent bioactive molecules. Unfortunately, actinobacteria produce natural products often in minute amounts, making even structural identification almost impossible, or do not form them at all under laboratory conditions (Ren et al., 2017). Moreover, natural products exhibit complex, highly diverse biosynthetic pathways and structures (Figure 1), which complicates efforts to streamline and enhance production (Hanson, 2003). Towards optimized supply, general strategies that allow to enhance natural product formation in actinobacteria are highly desired.

At this point, a promising line of research seems to exploit the link between natural product formation and the unique morphological life cycle of actinobacteria (Chater, 1984), which differentiates them from most other bacteria (Barka et al., 2016). In liquid culture, their morphological development starts from germinated spores that grow into a vegetative mycelium by linear tip extension and hyphae branching (Chater & Losick, 1997; van Dissel et al., 2014), followed by the formation of an aerial mycelium, which finally differentiates into uninucleoid cells that develop again into spores (Angert, 2005).

Recently, we discovered that supplementation with inorganic talc microparticles (hydrous magnesium silicate, $3MgO{\cdot}4SiO_2{\cdot}H_2O$) reprogrammed recombinant *Streptomyces albus* J1074/R2 to live a life of accelerated morphogenesis, which enabled a three-fold enhanced production of the antituberculosis polyketide pamamycin (Kuhl et al., 2020).

Here, we took this approach further. Exemplified for recombinant *Streptomyces lividans* TK24 DG2-Km-P41hyg + (Horbal et al., 2018), the effects of talc were elucidated using transcriptomics and metabolomics together with detailed analysis of strain physiology and morphology. The recombinant producer, representing one of the most prestigious *Streptomyces* species used industrially (Sevillano et al., 2016), formed the ribosomally and posttranslationally modified peptide (RiPP) bottromycin under control of synthetic promoters, supposed to uncouple production from the morphological cell cycle. It displayed the leading cell factory to produce bottromycin (Vior et al., 2020). The cyclopeptide was first isolated from cultures of *Streptomyces bottropensis* (Waisvisz et al., 1957) and is active against methicillin-resistant *Staphylococcus aureus* and vancomycin-resistant *Enterococci* (Kobayashi et al., 2010). Its complex biosynthesis involves a unique posttranslational macrocyclization step (Huo et al., 2012) and has posed enormous challenges on bottromycin research and development over the past decades (Kazmaier, 2020).

Finally, the microparticle approach was scaled down to the microtiter plate scale to investigate its potential in overproducing twelve natural compounds of commercial interest from ten major structural classes in native and metabolically engineered actinobacteria, including various *Streptomyces* but also other genera and families (Figure 1).

2 | MATERIALS AND METHODS

2.1 | Strains

All strains used in this study are listed in Table 1. For strain maintenance, spores were collected from agar plate cultures after five-day incubation at 30°C, resuspended in 20% glycerol, and kept at −80°C.

2.2 | Media

Mannitol-soy flour agar was used for plate cultures of all strains. It contained per liter: 20 g mannitol (Sigma-Aldrich), 20 g soy flour

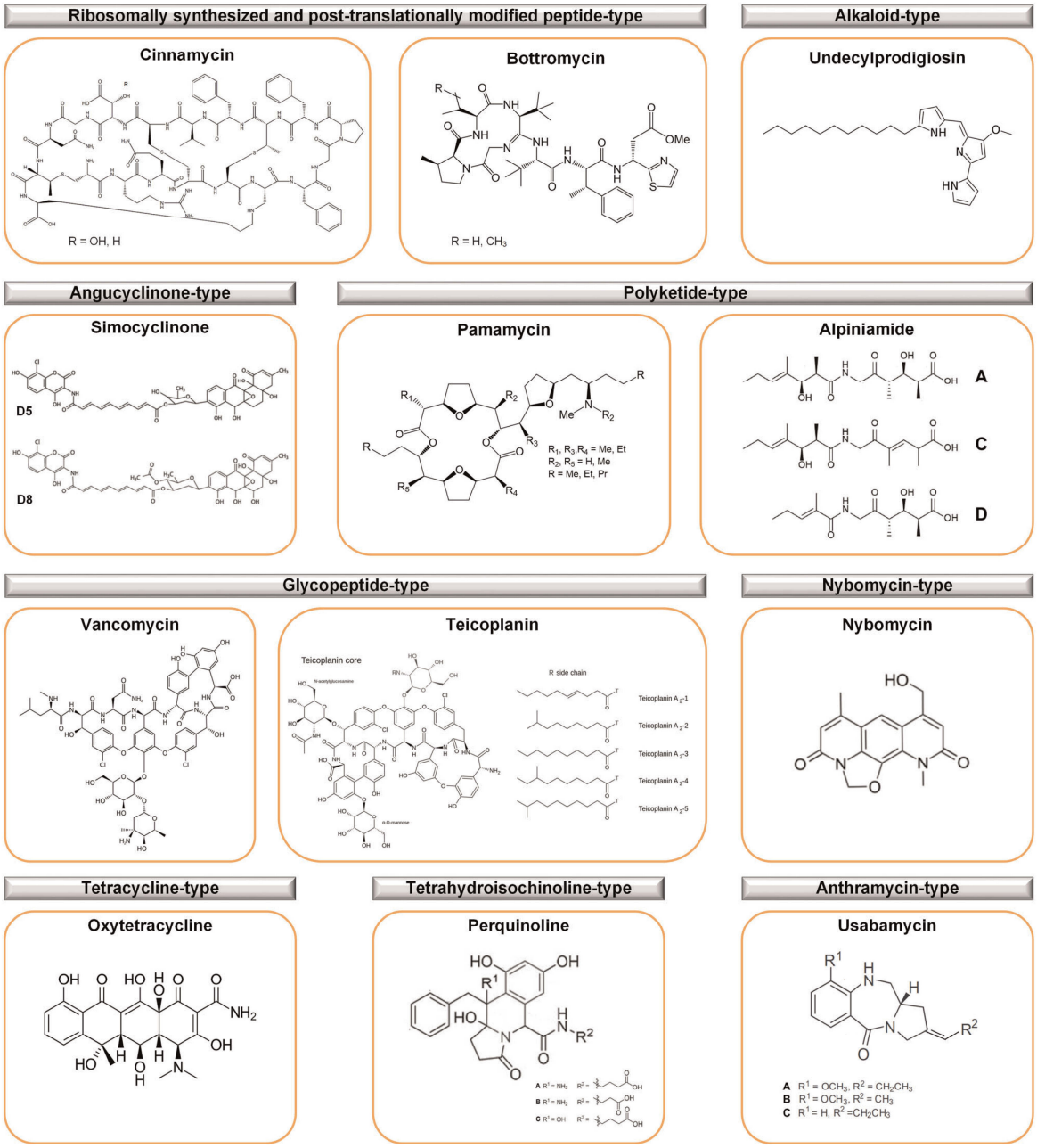

FIGURE 1 Natural products and their derivatives investigated in this study. The compounds comprise nine different chemical classes and have been previously described in different actinobacteria: *Streptomyces albus* pCinCatInt (cinnamycins) (Lopatniuk et al., 2017), *Streptomyces lividans* TK24 DG2-Km-P41hyg + (bottromycins) (Horbal et al., 2018), *Streptomyces lividans* TK24 (undecylprodigiosin) (Horinouchi & Beppu, 1984), *Kitasatospora* sp. (simocyclinones) (Bilyk et al., 2016) *Streptomyces albus* J1074/R2 (Rebets et al., 2015), *Streptomyces* sp. IB2014/011-12 (alpiniamides) (Paulus et al., 2018), *Amycolatopsis orientalis* (vancomycin) (Zmijewski & Briggs, 1989), *Actinoplanes teichomyceticus* ATCC 31121 (teicoplanin) (Horbal et al., 2012), *Streptomyces albus* subsp. *chlorinus* NRRL B-24108 (nybomycin) (Rodriguez Estevez et al., 2018), *Streptomyces rimosus* ATCC 10970 (oxytetracycline) (Pethick et al., 2013), *Streptomyces* sp. IB2014/016-6 (perquinolines) (Rebets et al., 2019), *Streptomyces lividans* ΔYA9 (usabamycins) (Ahmed et al., 2020)[Color figure can be viewed at wileyonlinelibrary.com]

TABLE 1 Strains and natural products investigated in this study and corresponding culture conditions

Strain	Natural product	Medium	Reference
Streptomyces albus J1074/R2	Pamamycins	SGG	Rebets et al. (2015)
Streptomyces lividans TK24 DG2-Km-P41hyg+	Bottromycins Undecylprodigiosin	SG	Horbal et al. (2018)
Streptomyces rimosus ATCC 10970	Oxytetracycline	GOTC	ATCC
Streptomyces albus pCinCatInt	Cinnamycins	TSB	Lopatniuk et al. (2017)
Streptomyces albus subsp. *chlorinus* NRRL B-24108	Nybomycin Usabamycins	DNPM	Myronovskyi et al. (2020)
Streptomyces sp. IB2014/011-12	Alpiniamides	TSB	Paulus et al. (2018)
Streptomyces sp. IB2014/016-6	Perquinolines	TSB	Rebets et al. (2019)
Amycolatopsis japonicum DSM 44213	Vancomycin	TSB	DSMZ
Actinoplanes teichomyceticus ATCC 31121	Teicoplanin	TSB	ATCC
Kitasatospora sp. DSM 102431	Simocyclinones	TSB	DSMZ

Abbreviations: ATCC, American Type Culture Collection; DSMZ, Deutsche Stammsammlung für Mikroorganismen und Zellkulturen (German Collection of Microorganisms and Cell Cultures).

(Schoenenberger Hensel), and 20 g agar (Becton & Dickinson). For liquid pre-cultures and main cultures, different growth media were used to meet the specific physiological demand of the investigated cells, as summarized in Table 1. Liquid TSB medium (Sigma Aldrich, pH 7.2) contained per liter: 17 g casein peptone (pancreatic), 2.5 g dipotassium hydrogen phosphate, 2.5 g glucose, 5 g NaCl, and 3 g soya peptone (papain digest.). Liquid SG medium (pH 7.2) contained per liter: 20 g glucose, 10 g soytone (Becton & Dickinson), 5 g yeast extract (Becton & Dickinson), and 2 g $CaCO_3$. Liquid SGG medium (pH 7.2) contained per liter: 10 g soluble starch (Sigma-Aldrich), 10 g glycerol, 2.5 g corn steep powder (Sigma-Aldrich), 5 g bacto peptone (Becton & Dickinson), 2 g yeast extract (Becton & Dickinson), 1 g NaCl, and 21 g MOPS. Liquid DNPM medium (pH 6.8) contained per liter: 40 g dextrin, 7.5 g soytone (Becton & Dickinson), 5 g yeast extract (Becton & Dickinson), and 21 g MOPS. Liquid GOTC medium (pH 7.0) contained per liter: 28 g corn starch (Sigma-Aldrich), 42 g soybean flour (Sigma-Aldrich), 6 g $(NH_4)_3PO_4$, 2 g $MgCl_2$, 1.5 g NaCl, 7.3 g $CaCO_3$, 10 ml 1% $ZnSO_4$, and 3.75 ml 1% $MnSO_4$. Talc (hydrous magnesium silicate, $3MgO \cdot 4SiO_2 \cdot H_2O$, 10 µm, Sigma-Aldrich) was resuspended in 50 mM Na-acetate buffer (pH 6.5), autoclaved at 121°C for 20 min, and added to the sterile medium before inoculation of selected microparticle experiments as given below (Kuhl et al., 2020).

2.3 | Cultivation

One loop of spores was scratched from a 5-day-old plate culture (incubated at 30°C) and used to inoculate a liquid pre-culture, which was grown overnight in a 500 ml baffled shake flask, filled with 50 ml medium and 30 g soda-lime glass beads (5 mm, Sigma-Aldrich). When the pre-culture had reached the late exponential phase, cells were collected (8500×*g*, room temperature, 5 min), resuspended in 10 ml fresh medium, and used to inoculate the main cultures, either containing talc or not. Main cultures were grown in shake flasks and in deep-well flower plates, respectively. Shake flask cultures were incubated in 500 ml baffled shake flasks (50 ml medium) on a rotary shaker (28°C, 230 rpm, 75% relative humidity, 5 cm shaking diameter, Multitron, Infors AG). For miniaturized screening, cells were grown in 48-well flower plates (1 ml medium) using a benchtop incubator (28°C, 1300 rpm, 75% relative humidity, BioLector m2p labs). All experiments were conducted as biological triplicate.

2.4 | Quantification of cell concentration

The cell dry weight (CDW) of *S. lividans* was measured as follows. Cells were collected (10,000×*g*, 4°C, 10 min), washed twice with 15 ml deionized water, and freeze-dried (Kuhl et al., 2020). Subsequently, the dry biomass was gravimetrically determined (Gläser et al., 2020). In microparticle cultivations of *S. lividans*, biomass data were corrected for the amount of talc added (Kuhl et al., 2020)

2.5 | Quantification of glucose

Glucose was quantified by HPLC (1260 Infinity Series, Agilent), using an Aminex HPX-87H column (300 × 7.8 mm; Bio-Rad) as stationary phase and 7 mM H_2SO_4 as mobile phase (55°C, 0.7 ml min^{-1}). Refraction index measurement was used for detection, and external standards were used for quantification (Kuhl et al., 2020).

2.6 | Microscopy

The 5 µl culture broth was transferred onto a glass for bright-field microscopy (Olympus IX70 microscope). The software ImageJ 1.52 (Schneider et al., 2012) was used to automatically determine the size

of pellets formed during growth (Kuhl et al., 2020). At least 150 aggregates were analyzed per sample.

2.7 | Natural compound extraction and quantification

The different natural products investigated in this study (Table 1) were extracted from culture broth using a two-step process (Kuhl et al., 2020). In short, 500 µl broth was mixed with 500 µl acetone and incubated for 15 min (1000 rpm, room temperature, Thermomixer F1.5, Eppendorf). Subsequently, ethyl acetate (500 µl) was added to extract bottromycin, undecylprodigiosin, pamamycins, vancomycin, teicoplanin, alpiniamides, perquinolines, simocyclinones usabamycins, and nybomycin, respectively, whereas 1-butanol (500 µl) was added to extract cinnamycins and thioholgamide A. Each mixture was incubated for 15 min under the same conditions. Afterward, the organic phase was collected (20,000×*g*, room temperature, 5 min), and the solvent was evaporated under a laminar nitrogen stream. Extracts were re-dissolved in methanol and clarified from debris (20,000×*g*, 4°C, 10 min). Subsequently, the analytes of interest were quantified, using HPLC-ESI-MS (C18 column, Vision HT C18 HighLoad, 100 × 2 mm, 1.5 µm, Dr. Maisch, Ammerbuch-Entringen, Agilent Infinity 1290, AB Sciex QTrap 6500). The individual chromatographic and mass spectrometric settings for each investigated compound are summarized in Table S1. To extract oxytetracycline, 250 µl culture broth was adjusted to pH 1.5 with 37% HCl and centrifuged twice (21,000×*g*, 15 min, 4°C). The resulting supernatant was analyzed by HPLC (Agilent 1260 Infinity Series, Agilent Technologies) on a C18 column (Nucleodur C18 Isis, 100 × 3 mm, 3 µm, Macherey-Nagel). Oxytetracycline was detected by a diode array detector (275 nm), and external standards were used for quantification.

2.8 | Extraction and quantification of intracellular amino acids

Intracellular amino acid sampling was done using fast vacuum filtration with nitrocellulose filters (0.2 µm pore size, Sartorius) (Wittmann et al., 2002). After vacuum filtration of 1 ml culture broth through a nitrocellulose filter (0.2 µm pore size, Sartorius), the cell-containing filter was washed twice with 15 ml 1.5% NaCl, transferred into a plastic cup containing 2 ml 200 µM α-aminobutyrate as internal standard for later quantification, and incubated 15 min at 100°C for amino acid extraction. Subsequently, the obtained extract was cooled on ice, and clarified from debris (20,000×*g*, 4°C, 5 min). The amino acids were quantified by HPLC using α-aminobutyrate as internal standard and pre-column derivatization with *o*-phthaldialdehyde (Schwechheimer et al., 2018).

2.9 | Transcriptome analysis

Total RNA was isolated using the Quick-RNA Miniprep Plus kit (Zymo Research). After DNase treatment, the obtained RNA was purified (RNA Clean & Concentrator-5 kit, Zymo Research) and quantified (DropSense 16, Trinean NV). The quality of the RNA was validated (RIN > 9) (RNA 6000 Nano kit, Agilent 2100 Bioanalyzer, Agilent Technologies). To construct whole transcriptome complementary DNA (cDNA) libraries, 2.5 µg of total RNA each was depleted of ribosomal RNA (rRNA) (Ribo-Zero rRNA Removal Kit (Bacteria), Illumina). Successful rRNA removal was validated (Agilent RNA Pico 6000 kit, Agilent 2100 Bioanalyzer, Agilent Technologies). The obtained messenger RNA (mRNA) was converted into a cDNA library according to the TruSeq Stranded mRNA Sample Preparation guide (Illumina). Appropriate cDNA quality and quantity was validated (Agilent High Sensitivity DNA kit, Agilent 2100 Bioanalyzer, Agilent Technologies). Sequencing was performed on an Illumina HiSeq. 1500 instrument using 70 bases read length (Illumina).

The obtained reads were mapped to the *S. lividans* D/G2 genome sequence (CP071123), which is based on the re-annotated *S. lividans* TK24 genome (Droste et al., 2021), using BOWTIE2 under standard settings (Langmead & Salzberg, 2012), except for increasing the maximally allowed distance for paired reads to 600 bases. To visualize read alignments, the software READXPLORER 2.2.3 (Hilker et al., 2016) was used. To count reads mapping to gene features, FEATURECOUNTS v.2.0.0 (Liao et al., 2014) was applied using the parameters -M -O, and -s 1. Quality control of the processed data sets was performed using DESEQ. 2 (Love et al., 2014), including calculation of sample-to-sample distances and principal component analysis. In addition, DESEQ. 2 was used to calculate DGE data sets. Raw data sets (sequenced reads) as well as processed data sets (input matrix and normalized read counts from DESEQ. 2) are available from GEO (GSE168044). For statistical analysis, Student's *t*-test was carried out and the data were filtered for genes with a $\log_2$-fold change ≥ 1 ($p \leq 0.05$) (Kuhl et al., 2020). RNA extraction and sequencing were conducted as biological triplicates for each strain.

3 | RESULTS

3.1 | Microparticles enhance the production of bottromycin A2, methyl-bottromycin A2, and undecylprodigiosin in recombinant *S. lividans*

To investigate the effect of the microparticles in detail, a bottromycin-producing mutant of *S. lividans* was studied in liquid culture with 10 g L^{-1} talc (Figure 2), an amount recently found optimal for the related strain *S. albus* J1074/R2 (Kuhl et al., 2020). A culture without talc served as control. The recombinant strain *S. lividans* TK24 DG2-Km-P41hyg+ expressed a refactored version of the *bot* cluster from *S. sp.* BC16019 (Huo et al., 2012) under control of two back-to-back synthetic promoters (Horbal et al., 2018). In the control culture, the strain grew from early on and reached a maximum biomass concentration of 7.4 (g CDW) L^{-1} after 48 h (Figure 2a). Then, growth stopped. However, the cells continued to consume glucose which was depleted after 120 h. The mature bottromycins, that is, bottromycin A2 and methyl-bottromycin A2,

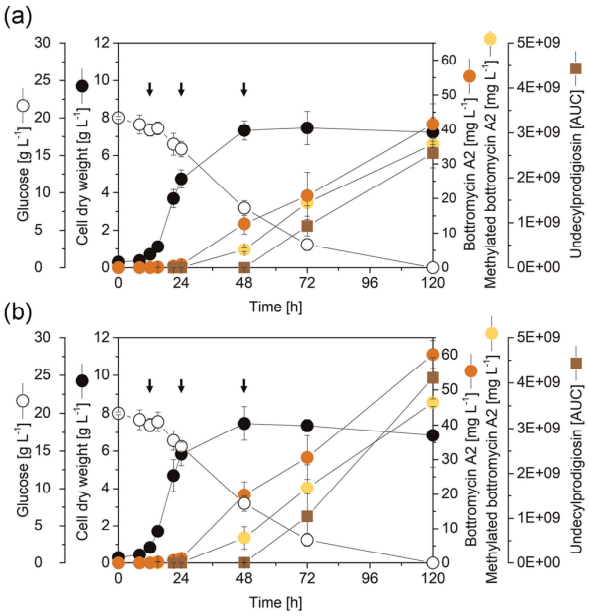

FIGURE 2 Impact of talc microparticles on growth and natural product formation in *Streptomyces lividans* TK24 DG2-Km-P41hyg+. The data show growth and production dynamics of a control culture without microparticles (a) and a microparticle-supplemented culture (10 g L^{-1} talc) (b). The arrows indicate the sampling time points for metabolome analysis (pre-bottromycins, bottromycin shunt products, intracellular amino acids), transcriptome analysis (RNA sequencing), and/or morphology analyzes. $n = 3$ [Color figure can be viewed at wileyonlinelibrary.com]

started to accumulate after approximately 20 h. The two products reached final titers of 42 mg L^{-1} and 35 mg L^{-1}, respectively. In contrast, bottromycin B and D were not observed. Alongside bottromycin, *S. lividans* formed undecylprodigiosin, a native alkaloid (van Wezel et al., 2000). The production of the latter started after 48 h and continued until the end of the process.

In comparison, the microparticle supplemented culture achieved significantly increased product titers. The final level of bottromycin A2 (60 mg L^{-1}) was 43% higher than that in the control, while the methyl-bottromycin A2 titer (46 mg L^{-1}) was increased by 31%. Increased product levels already occurred after 48 h. In addition, undecylprodigiosin production was increased by the particle supplementation (particularly during later stages of the cultivation) and resulted in a 64% increased final titer. The enhanced accumulation of the red pigment was even visible by the eye (Figure 3). Talc-supplemented cells appeared red, while cells from the control culture were less-intensively colored.

Interestingly, biomass formation and glucose consumption remained rather unchanged between the talc-supplemented culture and the control. However, talc had a major impact on cellular morphology. Grown without talc, the recombinant producer formed larger pellets with an average diameter of 390 ± 118 µm (Figure 3), while cellular aggregates in the talc supplied culture were significantly smaller and exhibited a 40% reduced pellet diameter of 279 ± 49 µm. In later stages of the cultivation, the morphology differed also in inner structure (Figure S1). The cell aggregates in the control reached up to 1 mm in diameter and pellets appeared decomposed inside. Pellets of the talc culture were less than half in size and exhibited an intact and denser structure. Further tests revealed a production optimum for total bottromycins (109 ± 24 mg L^{-1}) at 15 g L^{-1} talc (Figure S2). Higher talc levels were found detrimental.

3.2 | Microparticles do not affect bottromycin precursor availability during initial ribosomal translation but significantly change the abundance of intermediates of the posttranslational modification pathway

We hypothesized that the increased bottromycin titers could result from a higher precursor availability, as recently shown for other natural products (Gläser et al., 2020; Kuhl et al., 2020; Ser et al., 2016; Tang et al., 1994; Thykaer et al., 2010). Therefore, we analyzed the level of intracellular amino acids during growth (12 h, Figure 4b) and production (48 h, Figure 4c), including the building blocks of mature bottromycin A2: glycine, L-proline, L-valine, L-phenylalanine, L-aspartate, and L-cysteine (highlighted in blue in Figure 4b,c). Talc microparticles had virtually no effect: all intracellular amino acid pools remained unchanged. Generally, L-glutamate was most abundant, followed by L-alanine. Taken together, talc-enhanced bottromycin production was obviously not triggered by increased amino acid availability at the level of the initial ribosomal formation of the peptide backbone.

However, the talc particles affected the accumulation of biosynthetic intermediates from the posttranslational part of the biosynthetic pathway, including pre-forms of bottromycin and so-called shunt (degradation) products which appeared in addition to the mature bottromycins (carrying all major posttranslational modifications) (Figure 4a). Talc significantly increased the abundance of the pre-forms, that is, nonmethylated pre-bottromycin (*m/z* 855.4) and methylated pre-bottromycin (*m/z* 869.4). In contrast, the level of incomplete precursor peptides (*m/z* 452.2) was substantially reduced by talc addition, and non-cyclized shunt products exhibited a similar trend, although less significant.

3.3 | Microparticles rebalance the expression of individual bottromycin cluster genes

It was now interesting to see how bottromycin synthesis was affected on the transcriptional level. For this purpose, global transcription profiling of bottromycin-producing *S. lividans* was performed using RNA sequencing (Figure S3). The transcriptome of a talc supplied culture (10 g L^{-1}) was compared to that of a control at different stages of the cultivation: exponential growth (12 h), early production (24 h), and main production (48 h). Sample-level quality

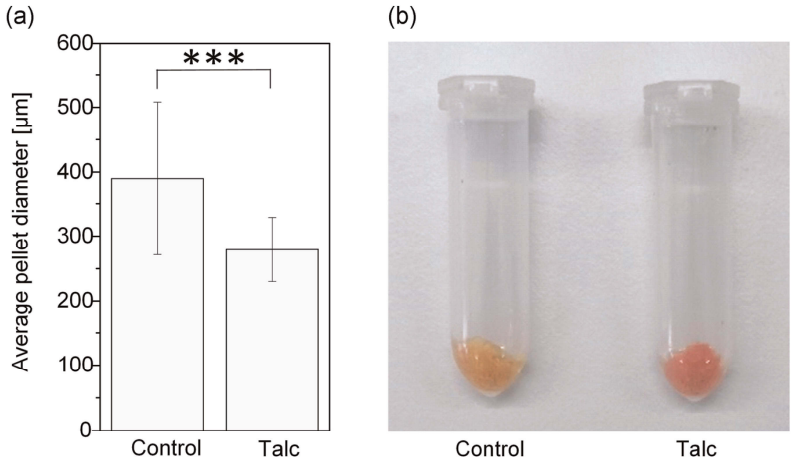

FIGURE 3 Impact of talc microparticles on the cellular morphology of *Streptomyces lividans* TK24 DG2-Km-P41hyg + in liquid culture. The data show the average pellet diameter of a microparticle-supplemented culture (10 g L^{-1} talc) and a control culture without microparticles at production start (24 h) (a, ***$p < 0.001$, $n = 150$). In addition, the pellet color of control culture and talc supplied culture after 5 days of incubation is shown, reflecting enhanced production of the red pigment undecylprodigiosin in the presence of talc (b) [Color figure can be viewed at wileyonlinelibrary.com]

control revealed excellent reproducibility (Figures 5 and S4). The individual replicates of all samples closely clustered together so that the observed expression differences could be fully attributed to the different experimental conditions. During early production, the expression of all bottromycin cluster genes remained unchanged in the control, whereas *botP*, was upregulated in the talc culture (2.0-fold) (Figure 6). During the main production phase, most bottromycin cluster genes were changed in expression. Obviously, the microparticles re-balanced the expression of the cluster in the microbe: *botAH* was specifically increased in the talc culture (2.4-fold) and *botC* and *botA* remained constant, while the latter two genes were found upregulated in the control (2.1-fold and 2.3-fold, respectively). Other genes equally behaved under both conditions: *botRMT1* was downregulated (0.4-fold), whereas *botCD*, *botH*, *botT*, *botRMT2*, and *botRMT3* remained unaffected over the entire process. It was interesting to note that the expression of the cluster was only weakly driven by the synthetic promoters (Figure S5a), but largely relied on the promoter of the hygromycin marker gene *hygR* (P_{hygR}), inserted in between them (Figure S5b). In addition, a so far unknown but apparently even stronger promoter downstream of *hygR*, designated P_{AS}, transcribed the cluster in the opposite (antisense) direction (Figure S5c).

3.4 | Microparticles accelerate morphological development and aging of *S. lividans*

On a global level, talc-supplied and non-supplied cells massively changed their gene expression during the process (Figure S3). In the control culture, 5% of all 7751 genes (414) were modulated in expression during the shift from growth to early production. The number of altered genes was increased to 2790 (36%) during the main production phase indicating a major shift of the cellular program at this stage. The expression changes, observed after 48 h, included prominent regulators of morphology and secondary metabolism, such as *ssgAB*, *chpABCDEFGH*, *rdlAB*, *rarABCDE*, *eshA*, and corresponding sigma factors (Tables 2 and 3), indicating ongoing morphological development and aging of the liquid-culture, a typical behavior of Streptomycetes, also observed in other species (van Dissel et al., 2014).

For the talc-amended culture, the transcription profile changed faster, and the dynamics involved more genes (Figure S3). The observed changes were related to the cultivation stage (Figure 5). Notably, the microparticles accelerated the shift in expression, leading to specific differences already during early production which indicated an accelerated morphological development. The number of genes, altered in expression after 24 h in the microparticle culture (1094 genes, 14%), was almost three times higher than that in the control. Key morphology genes and regulators, including *ssgA* (*SLIV_18635*, 3.3-fold), *ssgB* (*SLIV_30050*, 2.0-fold), *wblA* (*SLIV_20395*, 2.8-fold), *sigN* (*SLIV_18240*, 2.5-fold), and *bldN* (*SLIV_21180*, 3.2-fold, among others, were exclusively activated after 24 h in the presence of talc (Tables 2 and 3). In addition, various native biosynthetic genes for secondary metabolites were upregulated by talc at this early stage (Figure S6). During the main production after 48 h, the expression level of genes associated to morphology and secondary metabolism appeared rather similar with and without talc, although slight differences remained and totally more genes (38%, 2979) were modulated in the talc process. Interestingly, not even one single gene showed a significantly altered expression with talc supply during the growth phase (Figure S4).

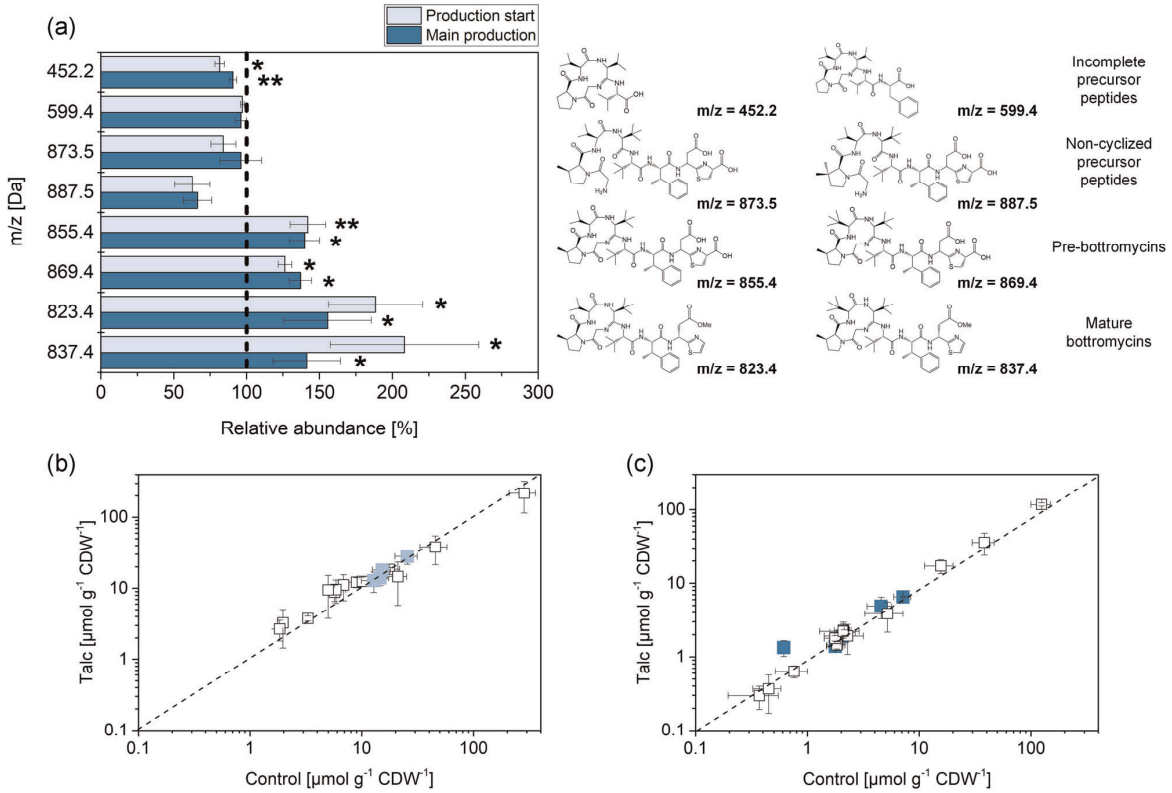

FIGURE 4 Metabolomic impact of talc microparticles on bottromycin-producing *Streptomyces lividans* TK24 DG2-Km-P41hyg+. The data show relative changes in the level of bottromycin pathway intermediates (a) and intracellular amino acids (b), (c), upon addition of talc microparticles to the medium (10 g L^{-1}). (a) The data show pre-bottromycin (m/z = 855.4), methylated pre-bottromycin (m/z = 869.4), four shunt products (m/z = 452.2, m/z = 599.4, m/z = 873.5, and m/z = 887.5), final mature bottromycin A2 (m/z = 823.4), and methylated-bottromycin A2 (m/z = 837.4), previously described (Crone et al., 2016; Vior et al., 2020). The data reflect the production start (24 h) and the major production phase (48 h), and the control culture (without talc), set to 100%, is shown as dashed line (*$p \leq 0.05$, **$p \leq 0.01$). The intracellular amino acid pools reflect the growth phase (12 h, b) and the major production phase (48 h, c). The amino acids that are incorporated into mature bottromycins (L -glycine, L-proline, L-valine, L-phenylalanine, L-aspartate, and L-cysteine) are highlighted in blue. The intracellular amino acid pools during early production were not found significantly changed (data not shown) [Color figure can be viewed at wileyonlinelibrary.com]

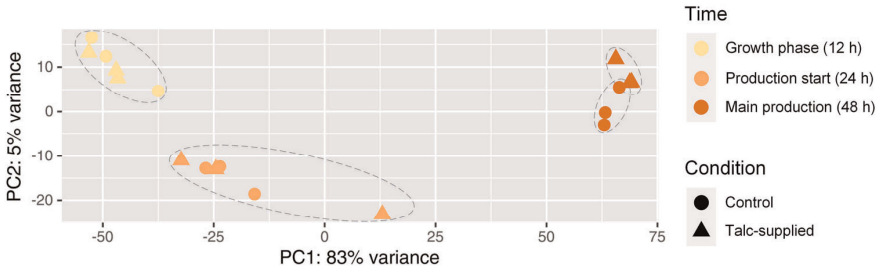

FIGURE 5 Statistical evaluation of gene expression profiles of *Streptomyces lividans* TK24 DG2-Km-P41hyg + using PCA. Global transcription profiling of the cultures was conducted using RNA sequencing during growth (12 h) and bottromycin production (24 h, 48 h) in the presence of talc (10 g L^{-1}) and without talc (control). For calculation of normalized read counts, the raw read count data were processed by DESeq. 2 (Love et al., 2014), including regularized log transformation (with blind dispersion estimation enabled). Subsequently, PCA was performed and visualized using ggplot2 (Wickham et al., 2016). $n = 3$ [Color figure can be viewed at wileyonlinelibrary.com]

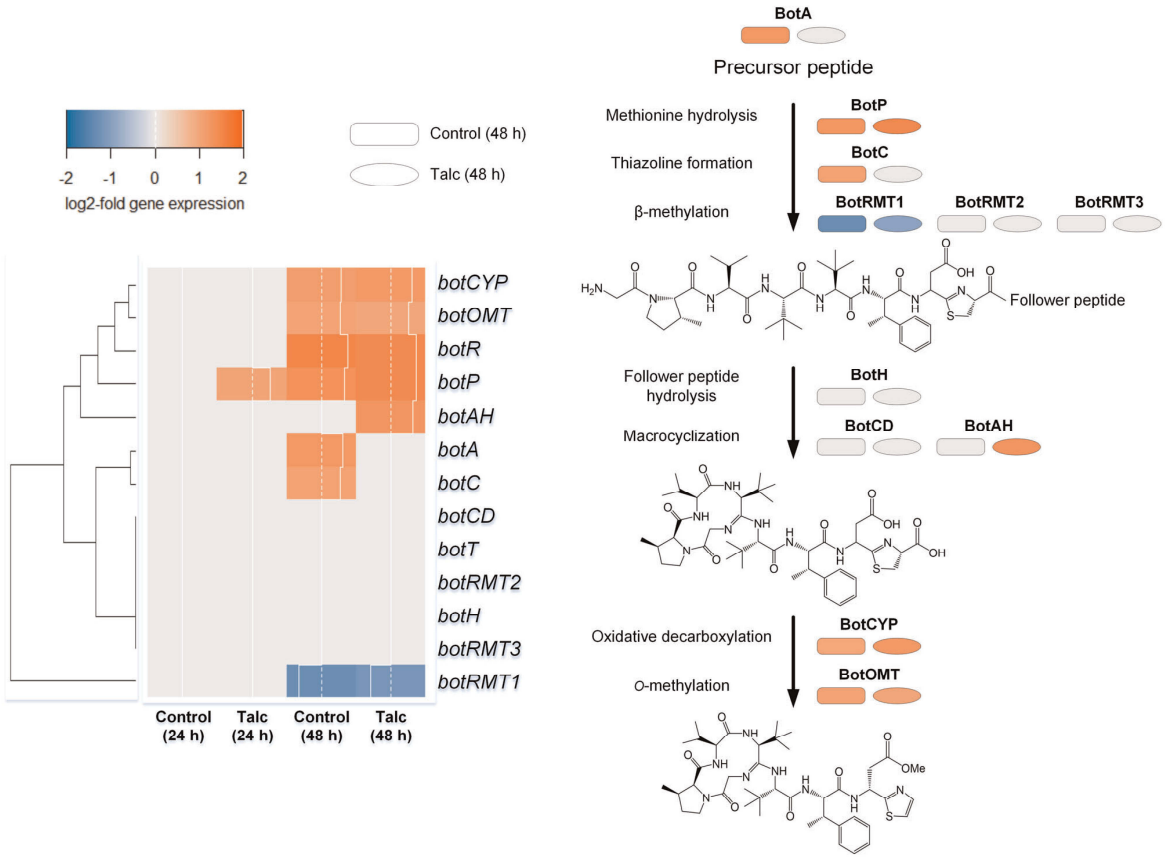

FIGURE 6 Hierarchical cluster analysis of expression dynamics of bottromycin biosynthetic pathway genes in *Streptomyces lividans* TK24 DG2-Km-P41hyg+. Samples were taken from a control and a talc supplied culture (10 g L^{-1}) during growth (12 h), production start (24 h), and major production phase (48 h). The expression level of the control during growth (12 h) was set as reference. The bottromycin cluster comprised the genes *botA*, encoding the precursor peptide; *botP*, leucyl-aminopeptidase; *botC*, YcaO domain protein; *botRMT1*, radical SAM; *botRMT2*, radical SAM; *botRMT3*, radical SAM; *botCD*, YcaO domain protein; *botAH*, aminohydrolase; *botH*, hydrolase; *botCYP*, CYP450 enzyme; *botOMT*, *O*-methyl transferase; *botT*, multidrug transporter; *botR*, transcriptional regulator (Huo et al., 2012). $n = 3$ [Color figure can be viewed at wileyonlinelibrary.com]

3.5 | The addition of talc to various *Streptomyces* cultures enhances the formation of natural products up to thirteen-fold

Given the stimulating effects of microparticles on bottromycin production in *S. lividans* (this study) and pamamycin production in *S. albus* (Kuhl et al., 2020), we now tested the concept on a broader scale. To facilitate the screening, we miniaturized production and established cultures at the microliter scale in a parallelized microtiter plate incubator. For appropriate mixing and oxygen transfer, the microtiter plates contained flower-shaped wells, optimized in geometry for the applied 3 mm shaking diameter of the instrument (Funke et al., 2009). To validate the microliter scale against conventional shake flasks, a first round of experiments was conducted for *S. lividans* TK24 DG2-Km-P41hyg + (Figure 2) and *S. albus* J1074/R2 (Kuhl et al., 2020), for which the stimulating microparticle effects had been already proven in shake flasks. Both strains were grown in microtiter plates over 5 days at different levels of talc (0–50 g L^{-1}) on their preferred medium (Table 1), followed by culture harvesting, natural product extraction and HPLC-ESI-MS analysis. As shown, the production of the bottromycins and undecylprodigiosin by *S. lividans* TK24 DG2-Km-P41hyg + , as well as the production of pamamycins by *S. albus* J1074/R2 was significantly enhanced by talc (Figure 7). Obviously, the miniaturized scale yielded the same picture as observed before for the 50 mL scale in shake flasks, although titers were somewhat lower, and it seemed appropriate to screen for the microparticle-based effects.

Subsequently, we investigated the production of different classes of natural products in a variety of *Streptomyces* species at the miniaturized scale including cinnamycins, another family of RiPPs (in addition to bottromycin), alpiniamides, another family of polyketides (in addition to pamamycins), the tetracycline derivative oxytetracycline, usabamycins of the anthramycin-type, the tetrahydroisochinoline-type perquinolines, and nybomycin, exhibiting a so far unique structure

TABLE 2 Gene expression profiling of recombinant *Streptomyces lividans* TK24 DG2-Km-P41hyg + during growth (12 h) and bottromycin production (24 h and 48 h) in the presence of talc (10 g L^{-1}) and without talc (control)

Gene	Annotation	Common gene name	Control (24 h)	Talc (24 h)	Control (48 h)	Talc (48 h)
SLIV_00805	Nucleotide-binding protein	*eshA*	0.0	0.0	4.9	4.8
SLIV_03010	Hypothetical protein	*chpB*	0.0	0.0	4.6	5.6
SLIV_04280	Regulatory protein	*absR2*	0.0	0.0	3.0	4.4
SLIV_04285	Regulatory protein	*absR1*	0.0	0.0	2.2	2.0
SLIV_09200	Response regulator	*redZ*	0.0	0.0	1.5	1.5
SLIV_09220	Transcriptional regulator RedD	*redD*	0.0	0.0	2.7	2.9
SLIV_09960	BldB	*bldB*	0.0	1.2	1.2	1.1
SLIV_12810	ABC transporter integral membrane protein BldKC	*bldKC*	0.0	−1.6	−1.6	−1.7
SLIV_12810	ABC transporter lipoprotein BldKB	*bldKB*	0.0	0.0	−1.3	−1.5
SLIV_12810	ABC transporter integral membrane protein BldKA	*bldKA*	0.0	0.0	−1.2	−1.5
SLIV_12835	Hypothetical protein	*act*II-ORF4	0.0	0.0	4.6	3.7
SLIV_14520	Two component regulator	*bldM*	0.0	1.6	4.9	5.1
SLIV_16305	Regulatory protein	*afsR*	0.0	1.1	1.1	1.5
SLIV_16310	Hypothetical protein	*afsS*	0.0	0.0	0.0	0.0
SLIV_17970	Hypothetical protein	*bldC*	0.0	0.0	1.5	1.5
SLIV_18635	SsgA	*ssgA*	0.0	1.7	4.2	4.1
SLIV_20395	WhiB-family transcriptional regulator	*wblA*	0.0	1.5	4.4	4.5
SLIV_21560	Two component system response regulator	*absA2*	0.0	0.0	−1.8	−2.0
SLIV_21565	Two component sensor kinase	*absA1*	0.0	0.0	0.0	0.0
SLIV_21605	Transcriptional regulator	*cdaR*	0.0	2.4	3.6	3.4
SLIV_23715	AraC family transcription regulator	*bldH*	0.0	0.0	1.6	1.8
SLIV_24075	Secreted protein	*rdlB*	0.0	0.0	5.1	5.2
SLIV_24080	Hypothetical protein	*rdlA*	0.0	3.9	10.0	10.6
SLIV_24085	Hypothetical protein	*chpD*	0.0	3.1	8.2	8.9
SLIV_24090	Hypothetical protein	*chpA*	0.0	0.0	6.0	7.1
SLIV_24145	Putative secreted protein	*chpF*	0.0	0.0	5.3	6.2
SLIV_24175	Hypothetical protein	*chpG*	0.0	0.0	7.5	7.4
SLIV_28720	Putative secreted protein	*chpE*	0.0	0.0	5.2	5.0
SLIV_29370	Putative secreted protein	*chpH*	0.0	0.0	4.2	3.3
SLIV_29375	Secreted protein	*chpC*	0.0	0.0	4.9	4.4
SLIV_29590	Hypothetical protein	*rarA*	0.0	0.0	4.9	5.0
SLIV_29595	Hypothetical protein	*rarB*	0.0	0.0	6.4	6.5
SLIV_29600	Hypothetical protein	*rarC*	2.0	2.0	8.1	7.7
SLIV_29605	ATP-GTP binding protein	*rarD*	1.8	1.7	7.7	7.5
SLIV_29610	Cytochrome P450	*rarE*	0.0	1.8	7.8	7.8
SLIV_30050	Regulator	*ssgB*	0.0	1.0	1.9	1.9

Note: The table lists the expression of genes involved in the regulation of morphology and secondary metabolism. The values correspond to $\log_2$-fold expression changes and refer to the control (12 h) as reference. $n = 3$.

TABLE 3 Transcriptional changes of selected sigma factors in *Streptomyces lividans* TK24 DG2-Km-P41hyg + during growth (12 h) and bottromycin production (24 h and 48 h) in the presence of talc (10 g L^{-1}) and without talc (control)

Gene	Annotation	Control (24 h)	Talc (24 h)	Control (48 h)	Talc (48 h)
SLIV_03325	Sigma factor	0.0	0.0	3.1	3.4
SLIV_03750	RNA polymerase sigma factor	0.0	0.0	3.9	4.4
SLIV_10445	RNA polymerase sigma factor WhiG	0.0	0.0	2.1	2.7
SLIV_12150	SigH protein	0.0	0.0	1.4	1.5
SLIV_14045	ECF sigma factor	0.0	0.0	−2.5	−2.1
SLIV_14515	RNA polymerase sigma factor SigD	0.0	0.0	2.8	2.9
SLIV_16170	RNA polymerase sigma factor	0.0	0.0	1.5	1.2
SLIV_16385	RNA polymerase sigma factor	0.0	1.2	2.4	2.9
SLIV_18240	RNA polymerase sigma factor SigN	0.0	1.3	2.0	1.9
SLIV_21180	ECF sigma factor BldN	0.0	1.7	6.4	6.4
SLIV_22925	RNA polymerase sigma factor SigU	0.0	0.0	3.9	5.0
SLIV_23960	sigma factor	0.0	0.0	2.5	2.2
SLIV_25360	RNA polymerase principal sigma factor HrdA	0.0	0.0	7.4	7.1
SLIV_29905	RNA polymerase sigma factor	0.0	6.4	6.7	7.2
SLIV_31410	RNA polymerase ECF sigma factor	0.0	0.0	2.3	0.0
SLIV_33600	ECF family RNA polymerase sigma factor	3.1	1.8	6.9	6.7
SLIV_33610	ECF family RNA polymerase sigma factor	0.0	0.0	2.8	2.5
SLIV_36925	Sigma factor LitS	0.0	0.0	1.7	2.4

Note: The values correspond to $\log_2$-fold expression changes and refer to the control (12 h) as reference. $n = 3$.

(Figure 7). Talc addition enhanced natural product formation in six out of nine cases (67%) resulting in increased titers for cinnamycins, bottromycins, undecylprodigiosin, pamamycins, oxytetracycline, and usabamycins. In each case, a production optimum could be identified. Interestingly, the optimal talc concentration strongly differed for each strain and compound. Among all products, the highest increase was observed for the alkaloid undecylprodigiosin (thirteen-fold, at 20 g L^{-1} talc). For certain products, the microparticles not only influenced the overall yield, but specifically altered the spectrum of the formed derivatives. This resulted in notable changes, including enhancing and diminishing effects on derivatives that were minor side products in the control without talc. As example, usabamycin C production was more than doubled by the addition of 10 g L^{-1} talc, whereas the deoxycinnamycin level was reduced three-fold, when 20 g L^{-1} talc was present.

3.6 | Microparticles boost natural product formation across actinobacterial genera and families

Finally, the applicability of the microparticle approach was tested for other actinobacteria, outside of the genus of *Streptomyces* (Figure 7). Therefore, we examined the production of two glycopeptides (vancomycin and teicoplanin) and one angucyclinone-type antibiotic (simocyclinone), which were formed by *Amycolatopsis japonicum* DSM 44213 (vancomycin), *Actinoplanes teichomyceticus* ATCC 31121 (teicoplanin), and *Kitasatospora sp.* (simocyclinone). Talc addition boosted formation of all products in all three strains. Interestingly, the positive effects were found for native as well as for heterologous producers. For teicoplanin, the addition of talc was even crucial since the compound was barely detectable in the control. As a result of talc addition, the enhancement was almost 100-fold. As observed for the *Streptomyces* strains, the optimum amount of talc was different for the different strains.

4 | DISCUSSION

4.1 | Microparticle-enhanced production provides bottromycins at a next level of performance and adds remarkable potential to drug development and further biosynthetic studies

As shown, talc microparticles significantly increased the production of the macrocyclic peptides bottromycin A2 and Met-bottromycin A2 in recombinant *S. lividans* TK24 DG2-Km-P41hyg + (Figure 2). Generally, bottromycins are difficult to obtain and their research has developed into a "nightmare" over the past 65 years

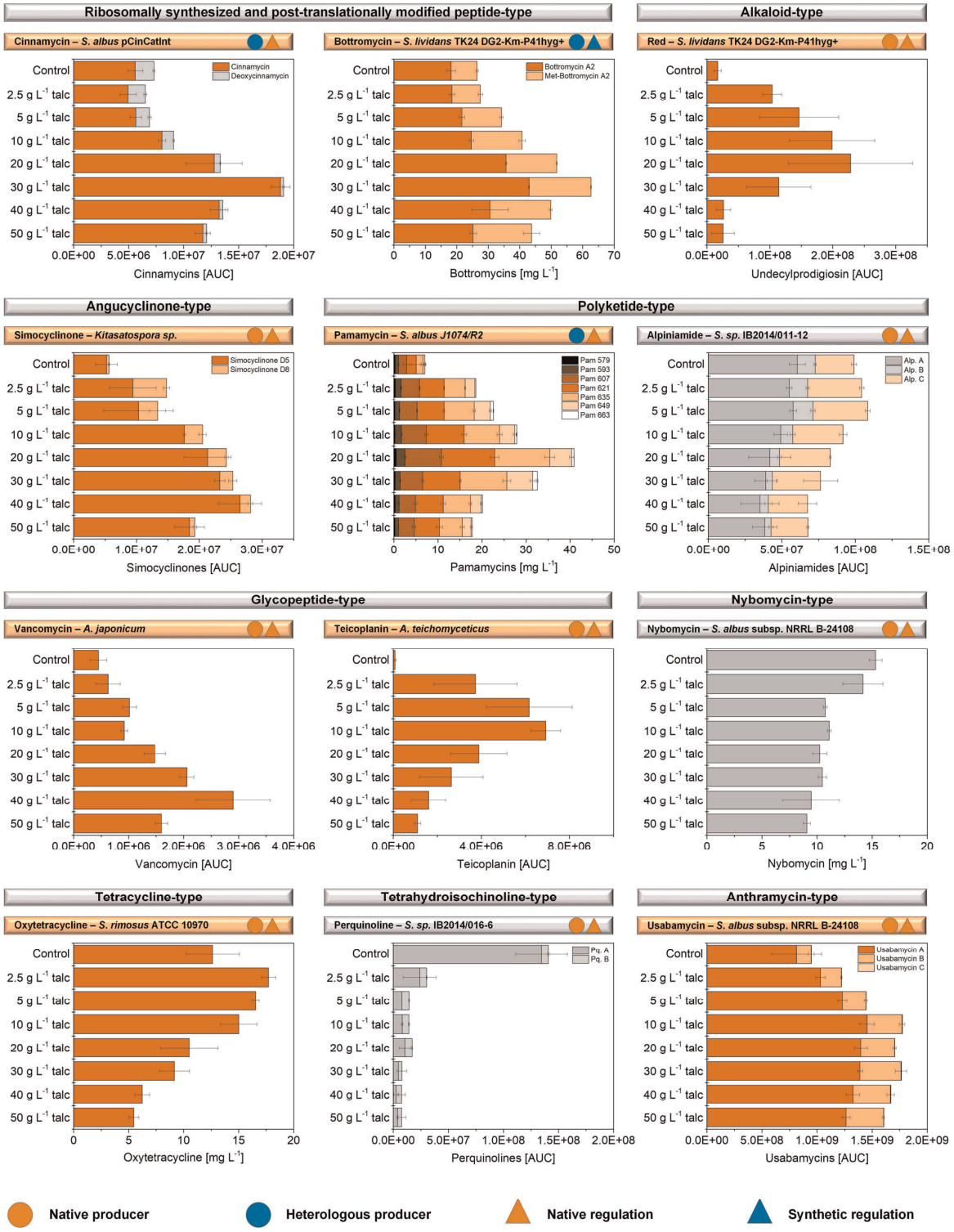

FIGURE 7 (See caption on next page)

(Kazmaier, 2020). Various homologous as well as heterologous producers provide bottromycins only in the low milligram range and even below 1 mg L^{-1} (Crone et al., 2016; Horbal et al., 2018; Huo et al., 2012). Due to this, improvement of titer and yield is regarded crucial (Vior et al., 2020), especially as the pathway seems inefficient in laboratory conditions (Crone et al., 2016; Eyles et al., 2018). In this study, the refactored synthetic strain *S. lividans* TK24 DG2-Km-P41hyg + , apparently among the top bottromycin producers available (Franz et al., 2021), reached 109 mg L^{-1} bottromycins of the A2 type in the presence of 15 g L^{-1} talc, exceeding all previously reported efforts. This achievement will greatly support drug development and further biosynthetic studies of bottromycins and derivatives therefrom (Vior et al., 2020). It also demonstrates that the particle approach can be successfully used to boost the performance of even top-level microbial cell factories.

4.2 | Microparticle-enhanced production of bottromycins in recombinant *S. lividans* is supported by re-balanced expression of individual bottromycin cluster genes driven by a complex promoter architecture

The obtained genomic, transcriptomic, and metabolomic data sets were now integrated to understand the involved molecular processes on a systems level (Kohlstedt et al., 2014). Resequencing of the bottromycin cluster verified the previously designed architecture with a synthetic bidirectional promotor cassette in between the left and the right part of the bottromycin cluster (Horbal et al., 2018). While precursor availability on the amino acid level could be ruled out as a limiting factor (Figure 4b,c), the talc-induced increase of prebottromycins together with the simultaneous decrease of noncyclized shunt products from the upper pathway, indicated a higher efficiency of the posttranslational modification process (Figure 4a). Notably, this was accompanied by a few significant changes in gene expression. Previous studies showed that the main limiting factor in bottromycin production, at least in the native host *S. scabies*, is the posttranslational maturation of the precursor peptide (Vior et al., 2020) and that the pathway inefficiently stalls at numerous biosynthetic steps (Crone et al., 2016). We conclude that the increased production efficiency in talc-supplied cultures largely resulted from the specifically increased expression of the aminohydrolase of the cluster (encoded by *botAH*, 2.4-fold, 48 h, Figure 6), responsible for the unique amidine-forming macrocyclodehydration of the molecule (Huo et al., 2012). Since this step follows after β-methylation of the valine, proline, and phenylalanine residues in the forming peptide, catalyzed by BotRMT1, BotRMT2, and BotRMT3 (Figure 6), this link nicely explains that the titer of both bottromycin derivatives was increased simultaneously (Crone et al., 2016; Horbal et al., 2018).

It appears likely that also the lower abundance of *botA*, encoding for precursor peptide (Figure 6) helped to balance biosynthesis, as previous attempts to increase precursor peptide levels were not found suitable to trigger bottromycin A2 synthesis, (Horbal et al., 2018; Vior et al., 2020). Taken together, fine-tuned rebalancing of the expression of individual cluster genes obviously mediated the improved biosynthesis. This picture differs largely from that obtained for talc-enhanced pamamycin production in *S. albus*, where the entire gene cluster was activated, up to 1000-fold (Kuhl et al., 2020). Likely, the difference originated from the different expression control strategies: the expression control of the bottromycin cluster in *S. lividans* was of synthetic nature (Horbal et al., 2018), whereas the pamamycin cluster was expressed under its native control (Kuhl et al., 2020). Hereby, it appeared surprising that the bottromycin cluster was affected at all, as the synthetic design was expected to uncouple expression from the host metabolism. A close inspection of the RNA sequencing data revealed that the expression control was much more complex than expected (Figure S5). It was only weakly driven by the synthetic promoters but largely relied on the highly active promoter of the hygromycin marker gene *hygR*, inserted in between of them, and transcribing the right cluster genes (Figure S5b). In addition, a so far unknown but apparently even stronger antisense promoter sequence (P_{AS}) downstream of *hygR*, transcribed the cluster in the opposite direction and expressed the left cluster genes, plus an additional antisense transcript of *hygR* (Figure S5c). These previously not considered promoters created a complex control architecture and could play a major role in mediating the talc-effect.

FIGURE 7 Impact of talc microparticles on nine major classes of natural products across different actinobacterial families. RiPP-type cinnamycins using *S. albus* pCinCatInt (Lopatniuk et al., 2017), RiPP-type bottromycins using *S. lividans* TK24 DG2-Km-P41hyg + (Horbal et al., 2018), alkaloid-type undecylprodigiosin using *S. lividans* TK24 DG2-Km-P41hyg + (Horbal et al., 2018), angucyclinone-type simocyclinones using *K. sp.* (Bilyk et al., 2016), polyketide-type pamamycins using *S. albus* J1074/R2 (Rebets et al., 2015), polyketide-type alpiniamides using *S. sp.* IB2014/011-12 (Paulus et al., 2018), glycopeptide-type vancomycin using *A. japonicum* DSM 44213 (Stegmann et al., 2014), glycopeptide-type teicoplanin using *A. teichomyceticus* ATCC 31121 (Horbal et al., 2012), nybomycin using *S. albus* subsp. *chlorinus* NRRL B-24108 (Rodriguez Estevez et al., 2018), tetracycline-type oxytetracycline using *S. rimosus* ATCC 10970 (Pethick et al., 2013), tetrahydroisochinoline-type perquinolines using *S. sp.* IB2014/016-6 (Rebets et al., 2019), and anthramycin-type usabamycins using *S. albus* subsp. *chlorinus* NRRL B-24108 (nybomycin) (Rodriguez Estevez et al., 2018). All strains were incubated over 5 days using miniaturized microtiter plate cultures (1 ml) at different talc levels between 0 and 50 g L^{-1}. The natural product levels were determined after solvent extraction using HPLC-ESI-MS and reflect final titers after 5 days. The colored circles given beside strain names indicate the type of producers studied: native (blue circle) and heterologous strains (orange circle). The colored squares denote the underlying control type for cluster expression: native (blue square) and synthetic regulation (orange square). $n = 3$ [Color figure can be viewed at wileyonlinelibrary.com]

4.3 | Microparticles affect submerged culture morphology and accelerate morphological development and aging of *S. lividans* and *S. albus*

The insights into the impact of talc microparticles on morphological development (Figure 4) and the associated cellular program of *S. lividans* (Figures 5, 6, S4, and S6) and the picture recently obtained for the talc effects on the related strain *S. albus* (Kuhl et al., 2020), now allowed to draw a few important conclusions related to morphology and its control in these type of bacteria.

As shown, talc reduced the pellet size of both strains (Figure 3a) (Kuhl et al., 2020), and this response can be expected also in other actinobacteria (Ren et al., 2015), although exceptions cannot be excluded. From the bioengineering viewpoint, smaller pellets appear favorable, as they reduce problems with mass and oxygen transfer limitation, slow growth, and culture heterogeneity (Mehmood et al., 2012; Tamura et al., 1997; van Dissel & van Wezel, 2018; van Dissel et al., 2014).

The strength of the talc-effect was quite different for the two strains. While 10 g L^{-1} of the talc material reduced the pellet size of *S. albus* more than six-fold (Kuhl et al., 2020), the same amount of talc did much less to *S. lividans*, as its pellets still maintained 60% of the size of the control culture. The stronger resistance of *S. lividans* might be related to its more dense and compact aggerates, offering less attack points for fragmentation and segregation than the more open and loose structures of *S. albus* (Zacchetti et al., 2018). In addition, differences in cell wall composition, mechanical strength, and hydrophobicity of spores, hyphae, and mycelia could explain the different accessibility of these bacteria to talc-mediated morphology engineering and might be interesting to study further (Driouch, Roth, Dersch, et al., 2010a, 2010b; Driouch et al., 2010; Driouch et al., 2012; Walisko et al., 2012).

Notably, the microparticles accelerated the morphological development of the studied *Streptomyces* in submerged culture. *S. lividans* revealed a premature activation of regulator genes, such as *sigN*, *bldN*, *ssgA*, *ssgB*, and *wblA* (Tables 2 and 3), important control elements of morphology development in *Streptomyces* (Kang et al., 2007; Rebets et al., 2018; Traag & van Wezel, 2008). The same picture of accelerated aging was recently observed for talc-treated *S. albus* (Kuhl et al., 2020), although the microparticles affected the expression of a much higher number of genes in this microbe (56% of all genes) (Kuhl et al., 2020). *S. lividans*, in contrast to *S. albus*, does not sporulate in liquid culture (Daza et al., 1989; Rebets et al., 2018). Differences in morphology control and development on the species level are likely the reason for the observed individual differences. However, the overall response to the microparticle addition apparently was the same for both strains: accelerated morphology development and aging and it appears likely that other actinobacteria will behave in a similar way.

4.4 | The use of microparticles displays a powerful approach to support natural product research in actinobacteria

As shown, microparticle-based cultures revealed a notably increased performance in producing natural products. First, the addition of talc beneficially increased the formation of 75% of the tested natural products, covering seven important classes with a highly diverse structure: polyketides, glycopeptides, RiPPs, alkaloids, tetracyclines, anthramycin-analogs, and angucyclinone-analogs with different structure (Figures 1 and 7). Stimulating production was observed for molecules of clinical relevance as antibiotics (vancomycin, oxytetracycline, and teicoplanin) (Elsayed et al., 2015; Fung et al., 2012; Liu et al., 2018) for several high-potential candidates presently under development into antibiotics (bottromycin, cinnamycin, pamamycin, and simocyclinone) (Buttner et al., 2017; Kobayashi et al., 2010; Lefèvre et al., 2004; Lopatniuk et al., 2017) and antitumor drugs (undecylprodigiosin and usabamycin) (Sato et al., 2011; Stankovic et al., 2014). Second, the microparticle-approach worked on actinobacteria from different families, including six strains of the most important *Streptomyces* group, plus representatives of the genera *Amycolatopsis*, *Actinoplanes*, and *Kitasatospora*. Third, optimized performance was observed for various strain backgrounds: natural producers, heterologous hosts, and strains expressing the gene cluster of interest under native and under synthetic control. Hereby, one example (teicoplanin) demonstrated that microparticles can even enable formation of a natural product, normally not observed (Figure 7). Fourth, the approach is simple. All what is needed is to add a little bit of talcum powder into the medium. Although the optimum talc level differed between strains and products, a concentration of 10 g L^{-1} always revealed a significant effect. Altogether, microparticle-enhanced cultivation provides a valuable concept for natural product research in actinobacteria, complementing efforts to streamline eukaryotic filamentous fungi (Böl et al., 2020; Veiter et al., 2018).

5 | CONCLUSIONS

As shown, talc-supplementation boosted production of seven classes of commercially relevant natural products across strains from different actinobacterial families, including natural as well as heterologous producers. The improvement was up to 100-fold. Obviously, the talc-effect generally accelerated morphological development and aging, inter alia leading to enhanced expression (Kuhl et al., 2020) and re-balanced expression (this study) of the bacterial gene clusters of interest. It is well known that antibiotic production in *Streptomyces* correlates to morphological development (Chater, 1984) and certain natural products are even part of programmed cell death (PCD) (Tenconi et al., 2018) so that the microparticles obviously trigger a sweet spot towards enhanced performance.

Without doubt, the microparticle concept appears useful to be systematically applied to the field of natural product research, where it offers several striking opportunities. Its successful application at the small scale shows potential for screening efforts to support research on major questions: discovery of novel molecules, activation of silent gene clusters, supply of sufficient amounts for structure elucidation, and exploration of biosynthetic control mechanisms, among others. The applicability to the microliter and microtiter plate scale provides a nice extension to recent developments on miniaturized physiological characterization of *Streptomyces* (Koepff et al., 2017). It appears promising to rescreen some of the libraries of isolates available worldwide, adding a bit of talc (Barka et al., 2016; Landwehr et al., 2016; Silva et al., 2020; Steele et al., 2019). Moreover, given the enormous interest to tailor cellular morphology in actinobacteria for improved performance (Koebsch et al., 2009; van Dissel et al., 2014; van Wezel et al., 2006; Wang et al., 2017; Xu et al., 2008), the microparticle addition seems useful to be tested on the many existing actinobacterial strains, genetically not accessible (Atanasov et al., 2021).

Regarding industrial manufacturing of natural products at large scale, talc could provide a straightforward drop-in solution. It is available in huge amounts, approximately 8 million tons per year according to recent market reviews. The material is cheap, in the range of 10 EUR cents per kg. As an example, supplementation of a 100 m^3 production process with 10 g L^{-1} talc (found effective) would add only costs in the range of 100 EUR. Moreover, co-harvested talc could upgrade fermentation biomass for post-process valorization, given its excellent performance as coating and baking agent in fertilizer formulations (Kaji et al., 2017) and its proven safety and efficacy as feed additive to all animal species (Mallet et al., 2005; Rychen et al., 2018).

Furthermore, it appears interesting to explore the interaction between microparticles and cells in more detail. On the particle side, talc prevented spore agglomeration during the initial culture phase of the fungus *Aspergillus niger*, whereas chemical (nutritional) effects by leached talc minerals played no significant role for the altered morphogenesis (Driouch et al., 2010). Moreover, particle size and shape were found critical. Even a small increase in particle diameter from 6 to 15 µm resulted in a severe loss of the morphology effects, and lamellar shaped talc particles were found more efficient to tailor morphology than round shaped materials (Driouch, 2009). Given the various sizes and shapes of talc, achievable from ball, rod, and autogenous mills, more systematic studies appear feasible. So far not explored but interesting seems the importance of the material softness, as talc is the softest known mineral. Hereby, several other micro materials such as aluminum oxide (Driouch et al., 2010) and titanium silicate oxide (Driouch et al., 2012) await to be tested. On the cellular side, an inspection of the impact of cell wall composition, mechanical strength, and hydrophobicity of spores, hyphae, and mycelia seems relevant, as stated above. Moreover, more research will be needed to clarify the talc-effects in stirred tanks and at large scale, exhibiting different hydrodynamics and mixing regimes (Bliatsiou et al., 2020; Kowalska et al., 2020).

ACKNOWLEDGMENTS

This study is dedicated to the memory Dr. Judith Becker (2.2. 1981 – 27.4. 2021), our close and cherished colleague at the Institute of Systems Biotechnology at Saarland University and our true friend. Christoph Wittmann acknowledges funding by the German Ministry of Education and Research through the grants MyBio (031B0344), MISSION (031B0611), and Explomare (031B0868), and by the German Research Foundation (INST 256/418-1). Andriy Luzhetskyy and Jörn Kalinowski acknowledge funding by the BMBF through the grant MyBio (031B0344). The funding bodies did not contribute to study design, data collection, analysis, and interpretation, or writing of the manuscript. Andriy Luzhetskyy has submitted a patent application to produce pamamycin in *S. albus*.

CONFLICT OF INTERESTS

The authors declare that there are no conflict of interests.

AUTHOR CONTRIBUTIONS

Christoph Wittmann designed and supervised the project. Martin Kuhl conducted the cultures and performed substrate and natural product analysis. Christian Rückert and Jörn Kalinowski performed genomics and transcriptomics of *S. lividans*. Martin Kuhl and Lars Gläser performed metabolomics of *S. lividans*. Martin Kuhl and Christoph Wittmann analyzed the data, drew the figures, and wrote the first draft of the manuscript. All authors commented, extended, and improved the manuscript. All authors read and approved the final version of the manuscript.

DATA AVAILABILITY STATEMENT

The data that supports the findings of this study are available in the supplementary material of this article.

ORCID

Christoph Wittmann http://orcid.org/0000-0002-7952-985X

REFERENCES

Ahmed, Y., Rebets, Y., Estevez, M. R., Zapp, J., Myronovskyi, M., & Luzhetskyy, A. (2020). Engineering of *Streptomyces lividans* for heterologous expression of secondary metabolite gene clusters. *Microbial Cell Factories*, *19*(1), 5. https://doi.org/10.1186/s12934-020-1277-8

Angert, E. R. (2005). Alternatives to binary fission in bacteria. *Nature Reviews Microbiology*, *3*(3), 214–224. https://doi.org/10.1038/nrmicro1096

Arcamone, F., Cassinelli, G., Fantini, G., Grein, A., Orezzi, P., Pol, C., & Spalla, C. (1969). Adriamycin, 14-hydroxydaimomycin, a new antitumor antibiotic from *S. Peucetius* var. *caesius*. *Biotechnology and Bioengineering*, *11*(6), 1101–1110. https://doi.org/10.1002/bit.260110607

Atanasov, A. G., Zotchev, S. B., Dirsch, V. M., & Supuran, C. T. (2021). Natural products in drug discovery: Advances and opportunities. *Nature Reviews Drug Discovery*, *20*, 1–17.

Barka, E. A., Vatsa, P., Sanchez, L., Gaveau-Vaillant, N., Jacquard, C., Klenk, H.-P., Clément, C., Ouhdouch, Y., & van Wezel, G. P. (2016). Taxonomy, physiology, and natural products of Actinobacteria. *Microbiology and Molecular Biology Reviews*, *80*(1), 1–43.

Bayer, vE., Gugel, K., Hägele, K., Hagenmaier, H., Jessipow, S., König, W., & Zähner, H. (1972). Stoffwechselprodukte von mikroorganismen. 98. Mitteilung. Phosphinothricin und phosphinothricyl-alanyl-alanin. *Helvetica Chimica Acta*, *55*(1), 224–239. https://doi.org/10.1002/hlca.19720550126

Bibb, M. J. (2013). Understanding and manipulating antibiotic production in Actinomycetes. *Biochemical Society Transactions*, *41*(6), 1355–1364. https://doi.org/10.1042/BST20130214

Bilyk, O., Brötz, E., Tokovenko, B., Bechthold, A., Paululat, T., & Luzhetskyy, A. (2016). New simocyclinones: Surprising evolutionary and biosynthetic insights. *ACS Chemical Biology*, *11*(1), 241–250.

Bliatsiou, C., Schrinner, K., Waldherr, P., Tesche, S., Böhm, L., Kraume, M., & Krull, R. (2020). Rheological characteristics of filamentous cultivation broths and suitable model fluids. *Biochemical Engineering Journal*, *163*, 107746.

Böl, M., Schrinner, K., Tesche, S., & Krull, R. (2020). Challenges of influencing cellular morphology by morphology engineering techniques and mechanical induced stress on filamentous pellet systems: A critical review. *Engineering in Life Sciences*, *21*, 51–67.

Butterworth, J. H., & Morgan, E. (1968). Isolation of a substance that suppresses feeding in locusts. *Chemical Communications (London)*, 1), 23–24.

Buttner, M. J., Schäfer, M., Lawson, D. M., & Maxwell, A. (2017). Structural insights into simocyclinone as an antibiotic, effector ligand and substrate. *FEMS Microbiology Reviews*, *42*(1):fux055. https://doi.org/10.1093/femsre/fux055

Campbell, W. C., Fisher, M. H., Stapley, E. O., Albers-Schönberg, G., & Jacob, T. A. (1983). Ivermectin: A potent new antiparasitic agent. *Science*, *221*(4613), 823–828. https://doi.org/10.1126/science.6308762

Chater, K. F. (1984). Morphological and physiological differentiation in *Streptomyces*. *Microbial Development*, *16*, 89–115. https://doi.org/10.1101/0.89-115

Chater, K. F., & Losick, R. (1997). Mycelial life style of *Streptomyces coelicolor* A3 (2) and itrs relatives. *Multicellular and interactive Behavior of Bacteria: In Nature, Industry and the Laboratory*, 149–182.

Cragg, G. M., & Newman, D. J. (2013). Natural products: A continuing source of novel drug leads. *Biochimica et Biophysica Acta (BBA)-General Subjects*, *1830*(6), 3670–3695.

Crone, W. J., Vior, N. M., Santos-Aberturas, J., Schmitz, L. G., Leeper, F. J., & Truman, A. W. (2016). Dissecting bottromycin biosynthesis using comparative untargeted metabolomics. *Angewandte Chemie*, *128*(33), 9791–9795.

Daza, A., Martin, J. F., Dominguez, A., & Gil, J. A. (1989). Sporulation of several species of *Streptomyces* in submerged cultures after nutritional downshift. *Microbiology*, *135*(9), 2483–2491.

Demain, A. L. (2006). From natural products discovery to commercialization: a success story. *Journal of Industrial Microbiology and Biotechnology*, *33*(7), 486–495.

Driouch, H. (2009). Morphology engineering of *Aspergillus niger* for improved β-fructofuranosidase roduction. *New Biotechnology*, *25*(25), S212.

Driouch, H., Sommer, B., & Wittmann, C. (2010). Morphology engineering of *Aspergillus niger* for improved enzyme production. *Biotechnology and Bioengineering*, *105*(6), 1058–1068. https://doi.org/10.1002/bit.22614

Driouch, H., Roth, A., Dersch, P., & Wittmann, C. (2010a). Filamentous fungi in good shape: Microparticles for tailor-made fungal morphology and enhanced enzyme production. *Bioengineered Bugs*, *2*(2), 100–104. https://doi.org/10.4161/bbug.2.2.13757

Driouch, H., Roth, A., Dersch, P., & Wittmann, C. (2010b). Optimized bioprocess for production of fructofuranosidase by recombinant *Aspergillus niger*. *Applied Microbiology and Biotechnology*, *87*(6), 2011–2024. https://doi.org/10.1007/s00253-010-2661-9

Driouch, H., Hänsch, R., Wucherpfennig, T., Krull, R., & Wittmann, C. (2012). Improved enzyme production by bio-pellets of *Aspergillus niger*: targeted morphology engineering using titanate microparticles. *Biotechnology and Bioengineering*, *109*(2), 462–471. https://doi.org/10.1002/bit.23313

Droste, J., Rückert, C., Kalinowski, J., Hamed, M. B., Anne, J., Simoens, K., Bernaerts, K., Economou, A., & Busche, T. (2021). Extensive reannotation of the genome of the model Streptomycete *Streptomyces lividans* TK24 based on transcriptome and proteome information. *Frontiers in Microbiology*, *12*, 744.

Elsayed, E. A., Omar, H. G., & El-Enshasy, H. A. (2015). Development of fed-batch cultivation strategy for efficient oxytetracycline production by *Streptomyces rimosus* at semi-industrial scale. *Brazilian Archives of Biology and Technology*, *58*(5), 676–685. https://doi.org/10.1590/s1516-89132015050184

Eyles, T. H., Vior, N. M., & Truman, A. W. (2018). Rapid and robust yeast-mediated pathway refactoring generates multiple new bottromycin-related metabolites. *ACS Synthetic Biology*, *7*(5), 1211–1218.

Fleming, A. (2001). On the antibacterial action of cultures of a penicillium, with special reference to their use in the isolation of *B. influenzae*. *Bulletin of the World Health Organization*, *79*, 780–790.

Franz, L., Kazmaier, U., Truman, A. W., & Koehnke, J. (2021). Bottromycins-biosynthesis, synthesis and activity. *Natural Product Reports*, https://doi.org/10.1039/D0NP00097C

Fung, F. H., Tang, J. C., Hopkins, J. P., Dutton, J. J., Bailey, L. M., & Davison, A. S. (2012). Measurement of teicoplanin by liquid chromatography-tandem mass spectrometry: Development of a novel method. *Annals of Clinical Biochemistry*, *49*(5), 475–481.

Funke, M., Diederichs, S., Kensy, F., Müller, C., & Büchs, J. (2009). The baffled microtiter plate: Increased oxygen transfer and improved online monitoring in small scale fermentations. *Biotechnology and Bioengineering*, *103*(6), 1118–1128.

Gläser, L., Kuhl, M., Jovanovic, S., Fritz, M., Vögeli, B., Erb, T., Becker, J., & Wittmann, C. (2020). A common approach for absolute quantification of short chain CoA thioesters in industrially relevant gram-positive and gram-negative prokaryotic and eukaryotic microbes. *Microbial Cell Factories*, *19*(1), 160.

Hanson, J. R. (2003). *Natural products: The secondary metabolites* (17). Royal Society of Chemistry

Harvey, A. (2000). Strategies for discovering drugs from previously unexplored natural products. *Drug Discovery Today*, *5*(7), 294–300.

Hilker, R., Stadermann, K. B., Schwengers, O., Anisiforov, E., Jaenicke, S., Weisshaar, B., Zimmermann, T., & Goesmann, A. (2016). ReadXplorer 2: Detailed read mapping analysis and visualization from one single source. *Bioinformatics*, *32*(24), 3702–3708.

Horbal, L., Zaburannyy, N., Ostash, B., Shulga, S., & Fedorenko, V. (2012). Manipulating the regulatory genes for teicoplanin production in *Actinoplanes teichomyceticus*. *World Journal of Microbiology and Biotechnology*, *28*(5), 2095–2100.

Horbal, L., Marques, F., Nadmid, S., Mendes, M. V., & Luzhetskyy, A. (2018). Secondary metabolites overproduction through transcriptional gene cluster refactoring. *Metabolic Engineering*, *49*, 299–315. https://doi.org/10.1016/j.ymben.2018.09.010

Horinouchi, S., & Beppu, T. (1984). Production in large quantities of actinorhodin and undecylprodigiosin induced by afsB in *Streptomyces lividans*. *Agricultural and Biological Chemistry*, *48*(8), 2131–2133.

Huo, L., Rachid, S., Stadler, M., Wenzel, S. C., & Müller, R. (2012). Synthetic biotechnology to study and engineer ribosomal bottromycin biosynthesis. *Chemistry & Biology*, *19*(10), 1278–1287.

Kaji, T., Igarashi, S., Fujibayashi, N., & Kobayashi, S. (2017). Solidity reduction effect of granular compound fertilizer (BB fertilizer) by high purity fine powder talc. *Journal of Japanese Soil Fertilizer Science*, *88*(6), 519–526.

Kang, S.-H., Huang, J., Lee, H.-N., Hur, Y.-A., Cohen, S. N., & Kim, E.-S. (2007). Interspecies DNA microarray analysis identifies WblA as a

pleiotropic down-regulator of antibiotic biosynthesis in *Streptomyces*. *Journal of Bacteriology*, *189*(11), 4315–4319.

Kazmaier, U. (2020). The long, long way to bottromycin. *Israel Journal of Chemistry*, https://doi.org/10.1002/ijch.202000068

Kobayashi, Y., Ichioka, M., Hirose, T., Nagai, K., Matsumoto, A., Matsui, H., Hanaki, H., Masuma, R., Takahashi, Y., & Ōmura, S. (2010). Bottromycin derivatives: Efficient chemical modifications of the ester moiety and evaluation of anti-MRSA and anti-VRE activities. *Bioorganic & Medicinal Chemistry Letters*, *20*(20), 6116–6120.

Koebsch, I., Overbeck, J., Piepmeyer, S., Meschke, H., & Schrempf, H. (2009). A molecular key for building hyphae aggregates: The role of the newly identified *Streptomyces* protein HyaS. *Microbial Biotechnology*, *2*(3), 343–360. https://doi.org/10.1111/j.1751-7915.2009.00093.x

Koepff, J., Keller, M., Tsolis, K. C., Busche, T., Rückert, C., Hamed, M. B., Anne, J., Kalinowski, J., Wiechert, W., Economou, A., & Oldiges, M. (2017). Fast and reliable strain characterization of *Streptomyces lividans* through micro-scale cultivation. *Biotechnology and Bioengineering*, *114*(9), 2011–2022.

Kohlstedt, M., Sappa, P. K., Meyer, H., Maass, S., Zaprasis, A., Hoffmann, T., Becker, J., Steil, L., Hecker, M., van Dijl, J. M., Lalk, M., Mader, U., Stulke, J., Bremer, E., Volker, U., & Wittmann, C. (2014). Adaptation of *Bacillus subtilis* carbon core metabolism to simultaneous nutrient limitation and osmotic challenge: A multi-omics perspective. *Environmental Microbiology*, *16*(6), 1898–1917. https://doi.org/10.1111/1462-2920.12438

Kowalska, A., Boruta, T., & Bizukojć, M. (2020). Performance of fungal microparticle-enhanced cultivations in stirred tank bioreactors depends on species and number of process stages. *Biochemical Engineering Journal*, *161*, 107696.

Kuhl, M., Gläser, L., Rebets, Y., Rückert, C., Sarkar, N., Hartsch, T., Kalinowski, J., Luzhetskyy, A., & Wittmann, C. (2020). Microparticles globally reprogram *Streptomyces albus* toward accelerated morphogenesis, streamlined carbon core metabolism, and enhanced production of the antituberculosis polyketide pamamycin. *Biotechnology and Bioengineering*, *117*(112), 3858–3875. https://doi.org/10.1002/bit.27537

Landwehr, W., Wolf, C., & Wink, J. (2016). Actinobacteria and myxobacteria: Two of the most important bacterial resources for novel antibiotics. *How to Overcome the Antibiotic Crisis*, *398*, 273–302.

Langmead, B., & Salzberg, S. L. (2012). Fast gapped-read alignment with Bowtie 2. *Nature Methods*, *9*(4), 357–359.

Lefèvre, P., Peirs, P., Braibant, M., Fauville-Dufaux, M., Vanhoof, R., Huygen, K., Wang, X.-M., Pogell, B. M., Wang, Y., Fischer, P., Metz, P., & Content, J. (2004). Antimycobacterial activity of synthetic pamamycins. *Journal of Antimicrobial Chemotherapy*, *54*(4), 824–827. https://doi.org/10.1093/jac/dkh402

Li, J. W.-H., & Vederas, J. C. (2009). Drug discovery and natural products: End of an era or an endless frontier? *Science*, *325*(5937), 161–165.

Liao, Y., Smyth, G. K., & Shi, W. (2014). featureCounts: An efficient general purpose program for assigning sequence reads to genomic features. *Bioinformatics*, *30*(7), 923–930.

Liu, M., Yang, Z.-H., & Li, G.-H. (2018). A novel method for the determination of vancomycin in serum by high-performance liquid chromatography-tandem mass spectrometry and its application in patients with diabetic foot infections. *Molecules*, *23*(11), 2939.

Lopatniuk, M., Myronovskyi, M., & Luzhetskyy, A. (2017). *Streptomyces albus*: A new cell factory for non-canonical amino acids incorporation into ribosomally synthesized natural products. *ACS Chemical Biology*, *12*(9), 2362–2370. https://doi.org/10.1021/acschembio.7b00359

Love, M. I., Huber, W., & Anders, S. (2014). Moderated estimation of fold change and dispersion for RNA-seq data with DESeq. 2. *Genome Biology*, *15*(12), 1–21.

Mallet, S., Delord, P., Juin, H., & Lessire, M. (2005). Effect of in feed talc supplementation on broiler performance. *Animal Research*, *54*(6), 485–492.

Mehmood, N., Olmos, E., Goergen, J.-L., Blanchard, F., Marchal, P., Klöckner, W., Büchs, J., & Delaunay, S. (2012). Decoupling of oxygen transfer and power dissipation for the study of the production of pristinamycins by *Streptomyces pristinaespiralis* in shaking flasks. *Biochemical Engineering Journal*, *68*, 25–33.

Myronovskyi, M., Rosenkränzer, B., Stierhof, M., Petzke, L., Seiser, T., & Luzhetskyy, A. (2020). Identification and heterologous expression of the albucidin gene cluster from the marine strain *Streptomyces Albus* subsp. *Chlorinus* NRRL B-24108. *Microorganisms*, *8*(2), 237.

Patridge, E. V., Gareiss, P. C., Kinch, M. S., & Hoyer, D. W. (2015). An analysis of original research contributions toward FDA-approved drugs. *Drug Discovery Today*, *20*(10), 1182–1187.

Paulus, C., Rebets, Y., Zapp, J., Rückert, C., Kalinowski, J., & Luzhetskyy, A. (2018). New alpiniamides from *Streptomyces sp.* IB2014/011-12 assembled by an unusual hybrid non-ribosomal peptide synthetase trans-AT polyketide synthase enzyme. *Frontiers in Microbiology*, *9*, 1959.

Pethick, F., MacFadyen, A., Tang, Z., Sangal, V., Liu, T.-T., Chu, J., Kosec, G., Petkovic, H., Guo, M., & Kirby, R. (2013). Draft genome sequence of the oxytetracycline-producing bacterium *Streptomyces rimosus* ATCC 10970. *Genome Announcements*, *1*(2), e0006313.

Rebets, Y., Brotz, E., Manderscheid, N., Tokovenko, B., Myronovskyi, M., Metz, P., Petzke, L., & Luzhetskyy, A. (2015). Insights into the pamamycin biosynthesis. *Angewandte Chemie*, *54*(7), 2280–2284. https://doi.org/10.1002/anie.201408901

Rebets, Y., Tsolis, K. C., Guðmundsdóttir, E. E., Koepff, J., Wawiernia, B., Busche, T., Bleidt, A., Horbal, L., Myronovskyi, M., & Ahmed, Y. (2018). Characterization of sigma factor genes in *Streptomyces lividans* TK24 using a genomic library-based approach for multiple gene deletions. *Frontiers in Microbiology*, *9*, 3033.

Rebets, Y., Nadmid, S., Paulus, C., Dahlem, C., Herrmann, J., Hübner, H., Rückert, C., Kiemer, A. K., Gmeiner, P., & Kalinowski, J. (2019). Perquinolines A–C: Unprecedented bacterial tetrahydroisoquinolines involving an intriguing biosynthesis. *Angewandte Chemie International Edition*, *58*(37), 12930–12934.

Ren, H., Wang, B., & Zhao, H. (2017). Breaking the silence: New strategies for discovering novel natural products. *Current Opinion in Biotechnology*, *48*, 21–27.

Ren, X.-D., Xu, Y.-J., Zeng, X., Chen, X.-S., Tang, L., & Mao, Z.-G. (2015). Microparticle-enhanced production of ε-poly-L-lysine in fed-batch fermentation. *RSC Advances*, *5*(100), 82138–82143. https://doi.org/10.1039/C5RA14319E

Rodriguez Estevez, M., Myronovskyi, M., Gummerlich, N., Nadmid, S., & Luzhetskyy, A. (2018). Heterologous expression of the nybomycin gene cluster from the marine strain *Streptomyces albus* subsp. *chlorinus* NRRL B-24108. *Marine Drugs*, *16*(11), https://doi.org/10.3390/md16110435

Rychen, G., Aquilina, G., Azimonti, G., Bampidis, V., Bastos, M.dL., Bories, G., Chesson, A., Cocconcelli, P. S., & Flachowsky, G. (2018). EFSA panel on additives. products or substances used in animal feed. Safety and efficacy of natural mixtures of talc (steatite) and chlorite (E 560) as a feed additive for all animal species. *EFSA Journal*, *16*(3), e05205.

Sato, S., Iwata, F., Yamada, S., Kawahara, H., & Katayama, M. (2011). Usabamycins A–C: New anthramycin-type analogues from a marine-derived actinomycete. *Bioorganic & Medicinal Chemistry Letters*, *21*(23), 7099–7101.

Schneider, C. A., Rasband, W. S., & Eliceiri, K. W. (2012). NIH Image to ImageJ: 25 years of image analysis. *Nature Methods*, *9*(7), 671–675. https://doi.org/10.1038/nmeth.2089

Schwechheimer, S. K., Becker, J., Peyriga, L., Portais, J.-C., Sauer, D., Müller, R., Hoff, B., Haefner, S., Schröder, H., & Zelder, O. (2018).

Improved riboflavin production with *Ashbya gossypii* from vegetable oil based on 13C metabolic network analysis with combined labeling analysis by GC/MS, LC/MS, 1D, and 2D NMR. *Metabolic Engineering*, *47*, 357–373.

Ser, H.-L., Law, J. W.-F., Chaiyakunapruk, N., Jacob, S. A., Palanisamy, U. D., Chan, K.-G., Goh, B.-H., & Lee, L.-H. (2016). Fermentation conditions that affect clavulanic acid production in *Streptomyces clavuligerus*: A systematic review. *Frontiers in Microbiology*, *7*, 522.

Sevillano, L., Vijgenboom, E., van Wezel, G. P., Díaz, M., & Santamaría, R. I. (2016). New approaches to achieve high level enzyme production in *Streptomyces lividans*. *Microbial Cell Factories*, *15*(1), 1–10.

Silva, L. J., Crevelin, E. J., Souza, D. T., Lacerda-Júnior, G. V., de Oliveira, V. M., Ruiz, A. L. T. G., Rosa, L. H., Moraes, L. A. B., & Melo, I. S. (2020). Actinobacteria from Antarctica as a source for anticancer discovery. *Scientific Reports*, *10*(1), 1–15.

Stankovic, N., Senerovic, L., Ilic-Tomic, T., Vasiljevic, B., & Nikodinovic-Runic, J. (2014). Properties and applications of undecylprodigiosin and other bacterial prodigiosins. *Applied Microbiology and Biotechnology*, *98*(9), 3841–3858.

Steele, A. D., Teijaro, C. N., Yang, D., & Shen, B. (2019). Leveraging a large microbial strain collection for natural product discovery. *Journal of Biological Chemistry*, *294*(45), 16567–16576.

Stegmann, E., Albersmeier, A., Spohn, M., Gert, H., Weber, T., Wohlleben, W., Kalinowski, J., & Rückert, C. (2014). Complete genome sequence of the actinobacterium *Amycolatopsis japonica* MG417-CF17T (= DSM 44213T) producing (S, S)-N, N′-ethylenediaminedisuccinic acid. *Journal of Biotechnology*, *189*, 46–47.

Takeuchi, S., Hirayama, K., Ueda, K., Sakai, H., & Yonehara, H. (1958). Blasticidin S, a new antibiotic. *The Journal of Antibiotics, Series A*, *11*(1), 1–5.

Tamura, S., Park, Y., Toriyama, M., & Okabe, M. (1997). Change of mycelial morphology in tylosin production by batch culture of Streptomyces fradiae under various shear conditions. *Journal of Fermentation and Bioengineering*, *83*(6), 523–528.

Tang, L., Zhang, Y.-X., & Hutchinson, C. R. (1994). Amino acid catabolism and antibiotic synthesis: Valine is a source of precursors for macrolide biosynthesis in *Streptomyces ambofaciens* and *Streptomyces fradiae*. *Journal of Bacteriology*, *176*(19), 6107–6119.

Tenconi, E., Traxler, M. F., Hoebreck, C., Van Wezel, G. P., & Rigali, S. (2018). Production of prodiginines is part of a programmed cell death process in *Streptomyces coelicolor*. *Frontiers in Microbiology*, *9*, 1742.

Thykaer, J., Nielsen, J., Wohlleben, W., Weber, T., Gutknecht, M., Lantz, A. E., & Stegmann, E. (2010). Increased glycopeptide production after overexpression of shikimate pathway genes being part of the balhimycin biosynthetic gene cluster. *Metabolic Engineering*, *12*(5), 455–461.

Traag, B. A., & van Wezel, G. P. (2008). The SsgA-like proteins in Actinomycetes: Small proteins up to a big task. *Antonie Van Leeuwenhoek*, *94*(1), 85–97. https://doi.org/10.1007/s10482-008-9225-3

van Dissel, D., & van Wezel, G. P. (2018). Morphology-driven downscaling of *Streptomyces lividans* to micro-cultivation. *Antonie Van Leeuwenhoek*, *111*(3), 457–469. https://doi.org/10.1007/s10482-017-0967-7

van Dissel, D., Claessen, D., & van Wezel, G. P. (2014). Morphogenesis of *Streptomyces* in submerged cultures. *Advances in Applied Microbiology*, *89*, 1–45.

van Wezel, G. P., White, J., Hoogvliet, G., & Bibb, M. J. (2000). Application of *redD*, the transcriptional activator gene of the undecylprodigiosin biosynthetic pathway, as a reporter for transcriptional activity in *Streptomyces coelicolor* A3 (2) and *Streptomyces lividans*. *Journal of Molecular Microbiology and Biotechnology*, *2*(4), 551–556.

van Wezel, G. P., Krabben, P., Traag, B. A., Keijser, B. J., Kerste, R., Vijgenboom, E., Heijnen, J. J., & Kraal, B. (2006). Unlocking *Streptomyces spp.* for use as sustainable industrial production platforms by morphological engineering. *Applied and Environmental Microbiology*, *72*(8), 5283–5288. https://doi.org/10.1128/AEM.00808-06

Veiter, L., Rajamanickam, V., & Herwig, C. (2018). The filamentous fungal pellet: Relationship between morphology and productivity. *Applied Microbiology and Biotechnology*, *102*(7), 2997–3006.

Vézina, C., Kudelski, A., & Sehgal, S. (1975). Rapamycin (AY-22, 989), a new antifungal antibiotic. I. Taxonomy of the producing Streptomycete and isolation of the active principle. *The Journal of Antibiotics*, *28*(10), 721–726. https://doi.org/10.7164/antibiotics.28.721

Vior, N. M., Cea-Torrescassana, E., Eyles, T. H., Chandra, G., & Truman, A. W. (2020). Regulation of bottromycin biosynthesis involves an internal transcriptional start site and a cluster-situated modulator. *Frontiers in Microbiology*, *11*, 495.

Waisvisz, J., Van Der Hoeven, M., Van Peppen, J., & Zwennis, W. (1957). Bottromycin. I. A new sulfur-containing antibiotic. *Journal of the American Chemical Society*, *79*(16), 4520–4521.

Walisko, R., Krull, R., Schrader, J., & Wittmann, C. (2012). Microparticle based morphology engineering of filamentous microorganisms for industrial bio-production. *Biotechnology Letters*, *34*(11), 1975–1982. https://doi.org/10.1007/s10529-012-0997-1

Wang, H., Zhao, G., & Ding, X. (2017). Morphology engineering of *Streptomyces coelicolor* M145 by sub-inhibitory concentrations of antibiotics. *Scientific Reports*, *7*(1), 13226. https://doi.org/10.1038/s41598-017-13493-y

Wickham, H., Chang, W., & Wickham, M. H. (2016). Package 'ggplot2'. *Create Elegant Data Visualisations Using the Grammar of Graphics. Version*, *2*(1), 1–189.

Wittmann, C., Hans, M., & Heinzle, E. (2002). In vivo analysis of intracellular amino acid labelings by GC/MS. *Analytical Biochemistry*, *307*(2), 379–382.

Xu, H., Chater, K. F., Deng, Z., & Tao, M. (2008). A cellulose synthase-like protein involved in hyphal tip growth and morphological differentiation in *Streptomyces*. *Journal of Bacteriology*, *190*(14), 4971–4978. https://doi.org/10.1128/JB.01849-07

Zacchetti, B., Smits, P., & Claessen, D. (2018). Dynamics of pellet fragmentation and aggregation in liquid-grown cultures of *Streptomyces lividans*. *Frontiers in Microbiology*, *9*, 943. https://doi.org/10.3389/fmicb.2018.00943

Zmijewski, M. J., Jr., Briggs, B. (1989). Biosynthesis of vancomycin: Identification of TDP-glucose: aglycosyl-vancomycin glucosyltransferase from *Amycolatopsis orientalis*. *FEMS Microbiology Letters*, *59*(1-2), 129–133.

SUPPORTING INFORMATION

Additional Supporting Information may be found online in the supporting information tab for this article.

How to cite this article: Kuhl, M., Rückert, C., Gläser, L., Beganovic, S., Luzhetskyy, A., Kalinowski, J., & Wittmann, C. (2021). Microparticles enhance the formation of seven major classes of natural products in native and metabolically engineered actinobacteria through accelerated morphological development. *Biotechnology and Bioengineering*, 1–18. https://doi.org/10.1002/bit.27818

3.3 A common approach for absolute quantification of short chain CoA thioesters in prokaryotic and eukaryotic microbes

Lars Gläser, Martin Kuhl, Sofija Jovanovic, Michel Fritz, Bastian Vögeli, Tobias J. Erb, Judith Becker, and Christoph Wittmann

Microbial Cell Factories. 2020; 19:160

https://doi.org/10.1186/s12934-020-01413-1

B. V. synthesized CoA thioesters. L. G., M. K., and M. F. developed the CoA thioester extraction and analytical protocol. L. G. produced the 13C labeled extracts and conducted cultivation of *S. albus*, *C. glutamicum*, and *P. putida*. S. J. performed cultivation of *Y. lipolytica*. L. G. conducted thioester analysis. C. W. conceived and structured the work. L. G., J. B. and C. W. wrote the first draft of the manuscript. All authors critically commented and improved the manuscript. All authors read and approved the final manuscript.

 The supplementary information to this article is available in the appendix.

Gläser *et al. Microb Cell Fact* (2020) 19:160
https://doi.org/10.1186/s12934-020-01413-1

Microbial Cell Factories

RESEARCH Open Access

A common approach for absolute quantification of short chain CoA thioesters in prokaryotic and eukaryotic microbes

Lars Gläser[1], Martin Kuhl[1], Sofija Jovanovic[1], Michel Fritz[1], Bastian Vögeli[2], Tobias J. Erb[2], Judith Becker[1] and Christoph Wittmann[1*]

Abstract

Background: Thioesters of coenzyme A participate in 5% of all enzymatic reactions. In microbial cell factories, they function as building blocks for products of recognized commercial value, including natural products such as polyketides, polyunsaturated fatty acids, biofuels, and biopolymers. A core spectrum of approximately 5–10 short chain thioesters is present in many microbes, as inferred from their genomic repertoire. The relevance of these metabolites explains the high interest to trace and quantify them in microbial cells.

Results: Here, we describe a common workflow for extraction and absolute quantification of short chain CoA thioesters in different gram-positive and gram-negative bacteria and eukaryotic yeast, i.e. *Corynebacterium glutamicum*, *Streptomyces albus*, *Pseudomonas putida*, and *Yarrowia lipolytica*. The approach assessed intracellular CoA thioesters down to the picomolar level and exhibited high precision and reproducibility for all microbes, as shown by principal component analysis. Furthermore, it provided interesting insights into microbial CoA metabolism. A succinyl-CoA synthase defective mutant of *C. glutamicum* exhibited an unaffected level of succinyl-CoA that indicated a complete compensation by the L-lysine pathway to bypass the disrupted TCA cycle. Methylmalonyl-CoA, an important building block of high-value polyketides, was identified as dominant CoA thioester in the actinomycete *S. albus*. The microbe revealed a more than 10,000-fold difference in the abundance of intracellular CoA thioesters. A recombinant strain of *S. albus*, which produced different derivatives of the antituberculosis polyketide pamamycin, revealed a significant depletion of CoA thioesters of the ethylmalonyl CoA pathway, influencing product level and spectrum.

Conclusions: The high relevance of short chain CoA thioesters to synthetize industrial products and the interesting insights gained from the examples shown in this work, suggest analyzing these metabolites in microbial cell factories more routinely than done so far. Due to its broad application range, the developed approach appears useful to be applied this purpose. Hereby, the possibility to use one single protocol promises to facilitate automatized efforts, which rely on standardized workflows.

Keywords: *Corynebacterium glutamicum*, *Streptomyces albus*, *Pseudomonas putida*, *Yarrowia lipolytica*, Lysine, Pamamycin, CoA thioester, LC–MS

Background

Microbial cell factories are a key to the bio-based industry [1]. Upgrading and streamlining their biocatalytic activity through systems metabolic engineering requires detailed understanding of the underlying metabolism [2–5]. Among other techniques, the assessment of intracellular metabolite

*Correspondence: christoph.wittmann@uni-saarland.de
[1] Institute of Systems Biotechnology, Saarland University, Saarbrücken, Germany
Full list of author information is available at the end of the article

levels and pathway fluxes has proven valuable to understand metabolic network function and its regulation and derive novel targets for strain engineering [1, 6].

A relevant group of metabolites are thioesters, esters between a carboxylic acid and a thiol. In microbial metabolism, the best-known and most relevant thioesters are short chain CoA thioesters, derivatives of coenzyme A (CoA) [7, 8]. Notably, CoA thioesters such as acetyl-CoA and succinyl-CoA participate in 5% of all enzymatic reactions and at least one-third of all cellular carbon is typically metabolized through a CoA thioester [7]. As example, they provide activated groups to drive the anabolic synthesis of cellular constituents such as peptides, fatty acids, sterols, and terpenes, display intermediates of catabolic pathways, and are essential to central energy metabolism [8]. Today, bioinformatics databases reveal more than two hundred naturally occurring CoA thioester derivatives [8], of which a core spectrum between approximately 5–10 compounds is potentially present in most microbes, based on their genomic repertoire [9, 10].

From a commercial perspective, CoA thioesters display building blocks of a wide range of industrially interesting products. Prominent examples are polyketides [11], polyunsaturated fatty acids (PUFAs) [12], polyhydroxyalkanoates (PHAs) [13], biofuels [14], amino acids [15], and dicarboxylic acids [16], among others [17]. This relevance might explain the increasing interest to trace CoA thioesters. Previous efforts have provided different experimental approaches, each specifically designed for a particular microbe, including indirect analysis of CoA thioesters via measurement of the respective organic acid, isotope dilution and enzymatic assays [17–20].

In this work, we have set up a sensitive, robust, and reproducible workflow to quantify short chain CoA thioesters in microbes. For this purpose, we adapted a previous protocol, used to assess a wide spectrum of CoA thioesters in the methylotrophic bacterium *Methylobacterium extorquens* [21]. After improvement and careful validation, we demonstrated the approach for industrially relevant microorganisms, which utilize CoA thioesters to form value-added products: the gram-positive bacteria *Corynebacterium glutamicum* [15], and *Streptomyces albus* [11], the gram-negative bacterium *Pseudomonas putida* [13], and the eukaryotic yeast *Yarrowia lipolytica* [12].

Results

Set up and validation of a single protocol for extraction and quantification of short chain CoA thioesters in gram-positive and gram-negative bacteria and eukaryotic yeast

A synthetic mixture of 11 CoA thioesters of interest was used to set up a chromatographic method. Using a porous organo-silica reversed phase column (100 × 2.1 mm, 1.5 µm), efficient separation of the analytes was achieved within 25 min, including the isobaric derivatives succinyl-CoA/methylmalonyl-CoA and methylsuccinyl-CoA/ethylmalonyl-CoA, respectively (Additional file 1: Fig. S1). As exception butyryl-CoA and isobutyryl-CoA coeluted in all cases tested (data not shown). They could not be distinguished in the MS due to their identical mass either and were therefore regarded as one pool. The linear range for quantification covered 5–8 orders of magnitude, down to the picomolar level (Additional file 1: Fig. S2).

Next, we aimed to develop one common workflow, which was suitable to analyze real samples from the different microbes. Initial tests with *C. glutamicum* revealed that combined quenching and extraction was straightforward to handle experimentally and provided extracts of reproducible quality (data not shown), so that we used it as a starting point for development. Several practical challenges resulted from the nature of the different microbes and the used culture conditions and had to be addressed.

First, the chosen small column geometry and particle size turned out incompatible with certain samples. Over rather few injections (10–20), the column pressure increased from initially 250 to 1000 bar, which required extensive cleaning with water to regenerate the separation column. However, despite such efforts, we faced a rapid loss of separation efficiency. This was especially true for samples of *S. albus* and *C. glutamicum*, grown in media with elevated ionic strength. The use of a larger column (100 × 4.6 mm) and a twofold increased particle size of the separation material (3 µm) solved this issue so that more than 500 samples could be analyzed on the same column without pressure increase and loss in separation performance, independent of the microbe investigated. Due to the larger geometry, the eluent flow was increased to 600 µL min^{-1}, which kept the analysis time at 25 min and provided a robust approach for the analytics. By far the best separation was achieved using a core–shell silica column instead of the porous silica column (Fig. 1). Due to superior properties of the core–shell material, the resulting peaks were narrower so that the gradient could be increased substantially. Altogether, this shortened the analysis time for all CoA esters to only 10 min (Fig. 1a). The analysis of cell extracts yielded clean chromatograms with high signal quality, even for low abundance thioesters (Fig. 1 b, c).

Second, small biomass amounts, typically chosen for sampling in metabolomics due to easier handling, were not suitable to precisely quantify all CoA thioesters present in vivo due to an extremely low abundance of some of them. As example, *S. albus* contained ultralow amounts of crotonyl-CoA, which yielded low quality

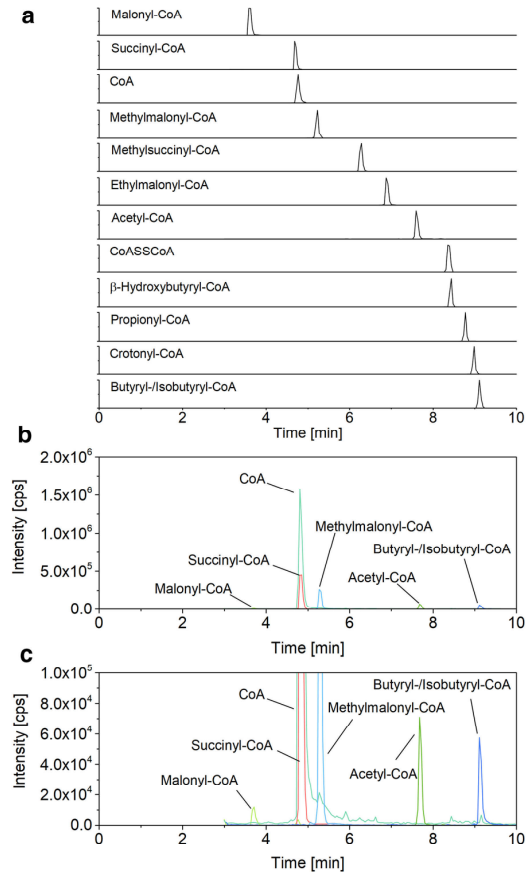

Fig. 1 LC–MS/MS chromatogram of a synthetic CoA thioester standard sorted by the retention time of each analyte (**a**). LC–MS/MS chromatogram of *C. glutamicum* LYS-9 (**b**, **c**). Co-eluting CoA thioesters were distinguished by their different specific mass-to-charge ratio (*m/z*), except for butyryl- and isobutyryl-CoA. Analysis was performed on a triple quadrupole MS (AB Sciex QTRAP 6500$^+$, AB Sciex Germany GmbH, Darmstadt, Germany) coupled to an HPLC system (Agilent Infinity 1290 System)

signals near the threshold, when extracted from 0.6 mg biomass. Similar observations were made for the other microbes studied. An increase of the sample amount to 8 mg, however, allowed clean detection and quantification of all CoA thioesters to be expected from the genomic repertoire for each of the tested strains and conditions.

Third, the higher biomass amounts caused difficulties in dissolving lyophilized extracts, after freeze-drying them together with extracted cell fragments. The obtained solutions were too viscous, especially when sampling the filamentous actinomycete, to appropriately filter them prior to analysis. Due to this, we introduced a centrifugation step between extraction and lyophilization, which allowed a better handling, especially for *S. albus*. Additional tests for all strains revealed that after two washing cycles the cell pellets did not contain any significant residuals of the analytes of interest, which ensured complete extraction. In the following, ^{13}C labeled cell extracts were prepared by growing each microbe on its corresponding [U-^{13}C] substrate and conducting the established sample processing. The concentration of the ^{13}C CoA thioesters was precisely quantified against synthetic standards so that the ^{13}C extracts could then be used to quantify absolute concentrations.

Fourth, free CoA underwent dimerization to a certain degree during the sample processing. When analyzing the synthetic standard, approximately 15% ± 3% of free coenzyme A was observed as CoA-disulfide (CoA-S–S-CoA), eluting 3.5 min after the free monomer (Fig. 1, Additional file 1: Table S1). This phenomenon was also observed for cell extract samples.

C. glutamicum reveals a small spectrum of CoA thioesters with methylmalonyl-CoA as the dominating metabolite

The L-lysine producing mutant *C. glutamicum* LYS-9 was analyzed during batch growth on glucose. It continuously accumulated L-lysine to a final titer of 10.5 mM at a yield of 190 mmol mol^{-1} (Fig. 2a). The specific growth rate remained constant over the whole cultivation ($\mu = 0.27$ h^{-1}). The cell interior of *C. glutamicum* LYS-9 contained five CoA thioesters: acetyl-CoA, malonyl-CoA, methylmalonyl-CoA, succinyl-CoA, and butyryl/isobutyryl-CoA. The esters differed almost 200-fold in abundance. Methylmalonyl-CoA exhibited the highest concentration (up to 750 nmol g^{-1}), followed by succinyl-CoA (110 nmol g^{-1}), malonyl-CoA (30 nmol g^{-1}), acetyl-CoA (5 nmol g^{-1}), and butyryl/isobutyryl-CoA (3 nmol g^{-1}). Additionally, free coenzyme A was observed in significant amount (820 nmol g^{-1}). The level of all CoA thioesters remained stable over time, except for malonyl-CoA, which decreased by approximately 50% in later cultivation stages (Fig. 2c, d). Incubated under the same conditions as its ancestor, *C. glutamicum* LYS-9 Δ*sucCD* (lacking succinyl-CoA synthetase) formed 12 mM L-lysine at an increased yield of 243 mmol mol^{-1}, while growing at a specific growth rate of $\mu = 0.25$ h^{-1} (Fig. 2b). The spectrum of intracellular CoA thioesters was almost unaffected in the TCA-cycle defective mutant, as compared to LYS-9. This was also true for succinyl-CoA, the substrate of the deleted enzyme. Its pool size was identical

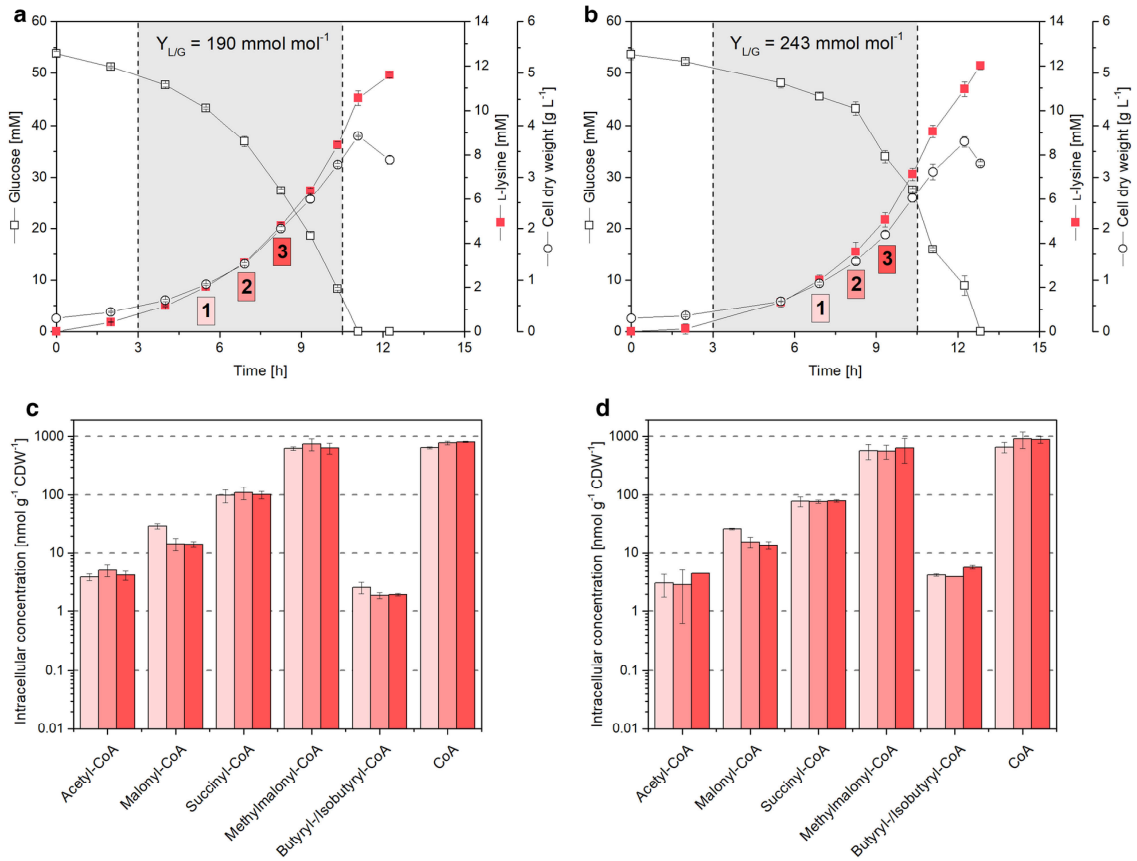

Fig. 2 Absolute quantification of intracellular CoA thioesters in L-lysine producing *Corynebacterium glutamicum* LYS-9 (left) and LYS-9 Δ*sucCD* (right) during growth on glucose. The data comprise the time profile of glucose, L-lysine, and cell concentration (**a**, **b**) and absolute levels of intracellular CoA thioesters (**c**, **d**). The yield for L-lysine reflects the major production phase, indicated by the gray area, and analyzed for free CoA and CoA thioesters at three time points. The data for these time points are shown in subfigures **c** and **d**. n = 3

in both strains. Only butyryl/isobutyryl-CoA slightly differed (Student's *t* test, $p = 0.01$).

The actinomycete *S. albus* exhibits a rich set of CoA thioesters varying more than 10,000-fold in intracellular availability

The wild type *S. albus* J1074 was grown on mannitol-based minimal medium (Fig. 3a). The substrate was consumed over a time of 25 h and cells reached a cell dry weight of 4.5 g L^{-1}. CoA thioesters were sampled at three time points during the mid-growth phase. The actinomycete revealed a rich spectrum of eleven CoA thioesters with side chains of two, three, four and five carbons (Fig. 3c). Acetyl-CoA was most abundant (up to 230 nmol g^{-1}), followed by succinyl-CoA, malonyl-CoA, and butyryl/isobutyryl-CoA. The other six thioesters partly exhibited much lower levels. Crotonyl-CoA and β-hydroxybutyryl-CoA were contained only in trace amounts down to 0.3 nmol g^{-1}. Furthermore, *S. albus* contained free coenzyme A up to 60 nmol g^{-1}. Along the cultivation, most pools (including those of high abundance) remained stable, but selected CoA thioesters changed to some extent. As example, the level of the carbon-five side-chain esters ethylmalonyl-CoA and methylsuccinyl-CoA increased over time.

The recombinant strain *S. albus* J1074/R2 produced 1.3 mg L^{-1} total pamamycin during growth on mannitol (Fig. 3b). The polyketide was produced from early on, accumulated in an exponential manner during the first hours and levelled off toward the end. The mutant revealed the same number of CoA thioesters as its ancestor *S. albus* J1074, but strongly differed in amount for some of them. As example, the level of crotonyl CoA was decreased up to more

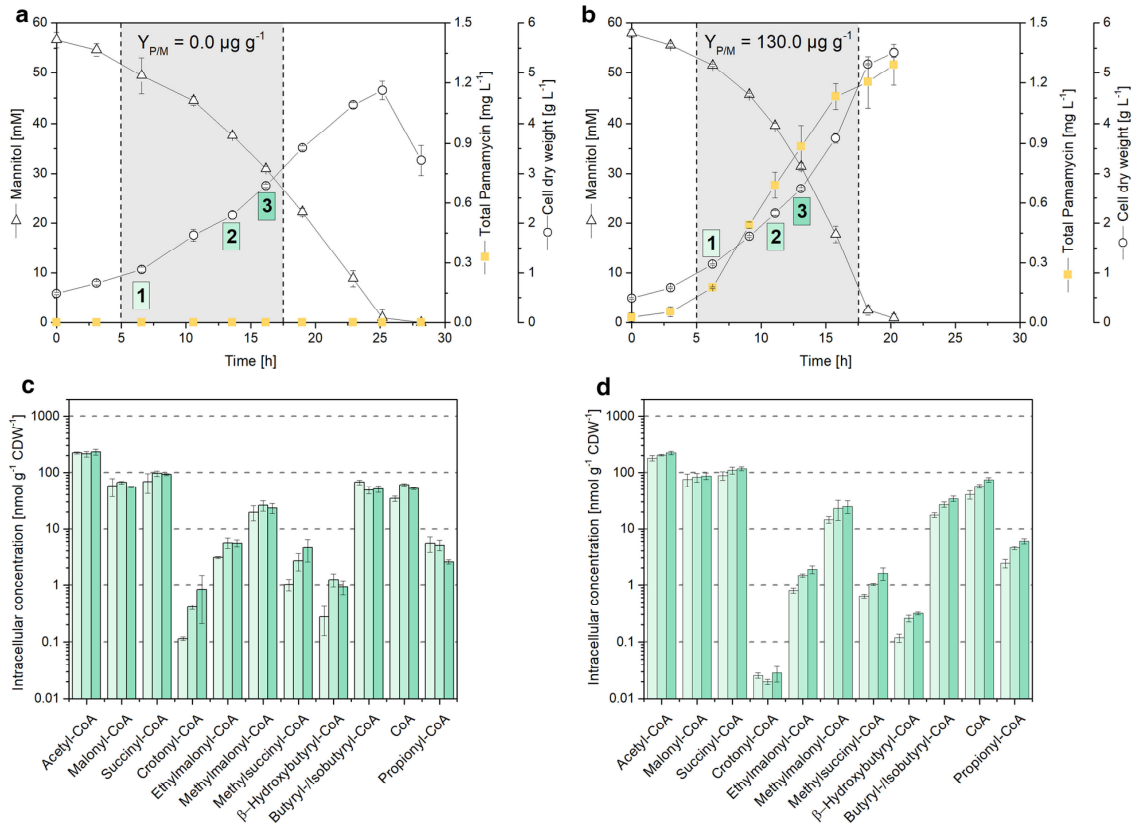

Fig. 3 Absolute quantification of intracellular CoA thioesters in *Streptomyces albus* J1074 (left) and its pamamycin producing mutant J1074/R2 (right) during growth on mannitol. The data comprise the time profile of mannitol, total pamamycin and cell concentration (**a**, **b**), and absolute levels of intracellular CoA thioesters and free CoA (**c**, **d**). The yield for pamamycin reflects the major production phase, indicated by the gray area, and analyzed for CoA thioesters at three time points. n = 3

than ten-fold to 0.02 nmol g^{-1}. In addition, the levels of β-hydroxybutyryl-CoA, ethylmalonyl-CoA, and methylsuccinyl-CoA were reduced up to five-fold (Fig. 3c, d). The other CoA thioesters, including pools of highest abundance (acetyl-CoA, malonyl-CoA, succinyl-CoA) appeared relatively unaffected by pamamycin production. Regarding the pamamycin spectrum, the strain synthetized various derivatives that differed in their mass, due to divergent side chains (Pam 579, Pam 593, Pam 607, Pam 621, Pam 635, Pam 649, Pam 663), which is known to be caused by the alternative incorporation of three-carbon malonyl-CoA, four-carbon methyl-malonyl-CoA, and five-carbon ethyl-malonyl-CoA during biosynthesis. At the end of the process, the distribution was Pam 579 (1.5%), Pam 593 (5.6%), Pam 607 (40.5%), Pam 622 (48.1%), Pam 635 (3.9%), Pam 649 (0.3%) and Pam 663 (0.0%).

Glucose-grown *P. putida* KT2440 shows a high abundance of free coenzyme A up to 1000-fold more than bound CoA thioesters

When grown on glucose, *P. putida* KT2440 contained six intracellular CoA thioesters with two, three and four carbon side chains, respectively: acetyl-CoA, malonyl-CoA, succinyl-CoA, β-hydroxybutyryl-CoA, butyryl/isobutyryl-CoA, and crotonyl-CoA. The level of the CoA thioesters ranged from 280 nmol g^{-1} (succinyl-CoA) to 1 nmol g^{-1} (crotonyl-CoA). *P. putida* KT2440 contained a huge amount of free coenzyme A (1,260 nmol g^{-1}),

(See figure on next page.)

Fig. 4 Impact of environmental and genetic perturbation on the spectrum of short-chain CoA thioesters and free coenzyme A in different microbes. The data show direct correlations in absolute CoA thioester levels between different strains of *Corynebacterium glutamicum* (**a**, **b**), *Streptomyces albus* (**c**, **d**), and *Pseudomonas putida* (**e**, **f**), and between glucose and glycerol grown *Yarrowia lipolytica* (**g**, **h**). The analysis comprised *C. glutamicum* LYS-9 and its succinyl-CoA synthetase deletion mutant LYS-9 Δ*sucCD*, which achieved a higher L-lysine yield, due to flux coupling of the L-lysine pathway with the disrupted TCA cycle (**a**, **b**) [15]. In comparison to the wild type *S. albus* J1074, the recombinant producer J1074/R2 formed the polyketide pamamycin from CoA thioester building blocks malonyl-CoA, methylmalonyl-CoA, ethylmalonyl-CoA, succinyl-CoA, and acetyl-CoA (**c**, **d**) [11]. In addition, the data comprise *Pseudomonas putida* KT2440 and its glucose dehydrogenase deficient mutant KT2440 Δ*gcd* (**e**, **f**) [13], and *Yarrowia lipolytica* Po1h::Af4 using glucose and glycerol as sole carbon source (**g**, **h**) [12]. The statistical significance for observed differences in CoA thioester levels (t-test $p < 0.05$) is marked by an asterisk. n = 3

exceeding the sum of all thioester pools more than two-fold and the level of individual thioesters up to more than 1000-fold (Fig. 4f). The glucose dehydrogenase (*gcd*) deletion mutant KT2440 Δ*gcd*, grown under the same conditions, showed a five-fold decreased level for succinyl-CoA (p = 0.01) and β-hydroxybutyryl-CoA (0.6-fold, p = 0.01). The most obvious consequence of the *gcd* deletion was a dramatically decreased abundance of free coenzyme A (172 nmol g^{-1}) (Fig. 4f).

Y. lipolytica adapts the level of carbon three thioesters, when grown on glucose and glycerol

Acetyl-CoA, malonyl-CoA, butyryl/isobutyryl-CoA, β-hydroxybutyryl-CoA, crotonyl-CoA, and succinyl CoA were present, when the yeast was grown on glucose or on glycerol (Fig. 4h). The carbon source specifically affected the intracellular level of carbon-three CoA thioesters. Whereas malonyl-CoA was significantly increased on glucose (19 nmol g^{-1}) as compared to glycerol (15 nmol g^{-1}) (Student's t-test, $p = 0.04$), propionyl-CoA was reduced more than threefold as compared glycerol-grown cells. The other CoA thioesters as well as free CoA showed similar concentrations on both substrates.

Discussion

The developed experimental workflow enables precise and reproducible quantification of CoA thioesters in gram-positive and gram-negative bacteria and eukaryotic yeast

Thioesters of coenzyme A play an important role in metabolism and participate in 5% of all enzymatic conversions [7]. However, only selected studies so far have managed to assess their presence in microbial cells using different protocols, specifically elaborated for the given question [8, 20, 22, 23]. In this work, we successfully adapted a workflow with integrated quenching and extraction using pre-cooled acetonitrile and formic acid, previously described for the methanol-utilizing bacterium *Methylobacterium extorquens* [21] to quantitatively extract intracellular CoA thioesters from *C. glutamicum, S. albus, P. putida,* and *Y. lipolytica*. The method precisely yielded absolute concentrations due to the use of internal ^{13}C-standards. The addition of the standard during the initial extraction step allowed to compensate for potential concentration changes during sample processing, whereby all thioesters were found rather stable under the given conditions. Notably, the workflow should also deliver robust estimates of free CoA levels. This compound, due its reactive free thiol group, exhibited a certain degree of dimerization into the disulfide (and heterodimers might have been potentially formed with other reduced thiols such as glutathione and mycothiol). All these effects should be compensated by the internal standard (assuming that isotope effects in dimerization were negligible), underling its importance. One should, however, be aware of such side reactions and eventually explore them in more detail, when needed.

Following specific improvement in sampling, sample processing and analytics, we could separate, detect, and quantify CoA thioesters in cell extracts of all studied microbes down to the attomole level within only 10 min (Fig. 1, 3, and 4). Each microbe revealed a unique CoA thioester spectrum, regarding thioester number, type, and level (Fig. 5a). The method allowed to assess also low abundance CoA thioesters, such as crotonyl-CoA in recombinant *S. albus* (Fig. 4c, d). The wide linear range of 10^5–10^8 achieved for quantification (Additional file 1: Fig. S2) appeared crucial to cover the full spectrum of CoA thioesters, which differed more than 10,000-fold in intracellular concentration (Fig. 3d). Statistical analysis of the data, using principal component analysis, revealed that biological triplicates clustered closely for each experiment, independent of the studied strain (Fig. 5b). The concentrations, determined for single CoA esters, were in the same range as values previously observed in these and similar microbes [17–20]. The achieved high reproducibility appears valuable to identify even small phenotypic differences, particularly when considering the general difficulties to obtain precise metabolite and metabolome data [24]. The microbes selected in this study differed significantly in properties that potentially affect the suitability of experimental approaches in metabolomics: cell size and morphology, composition of the cell wall, and presence of specific cellular barriers, such as outer layers or

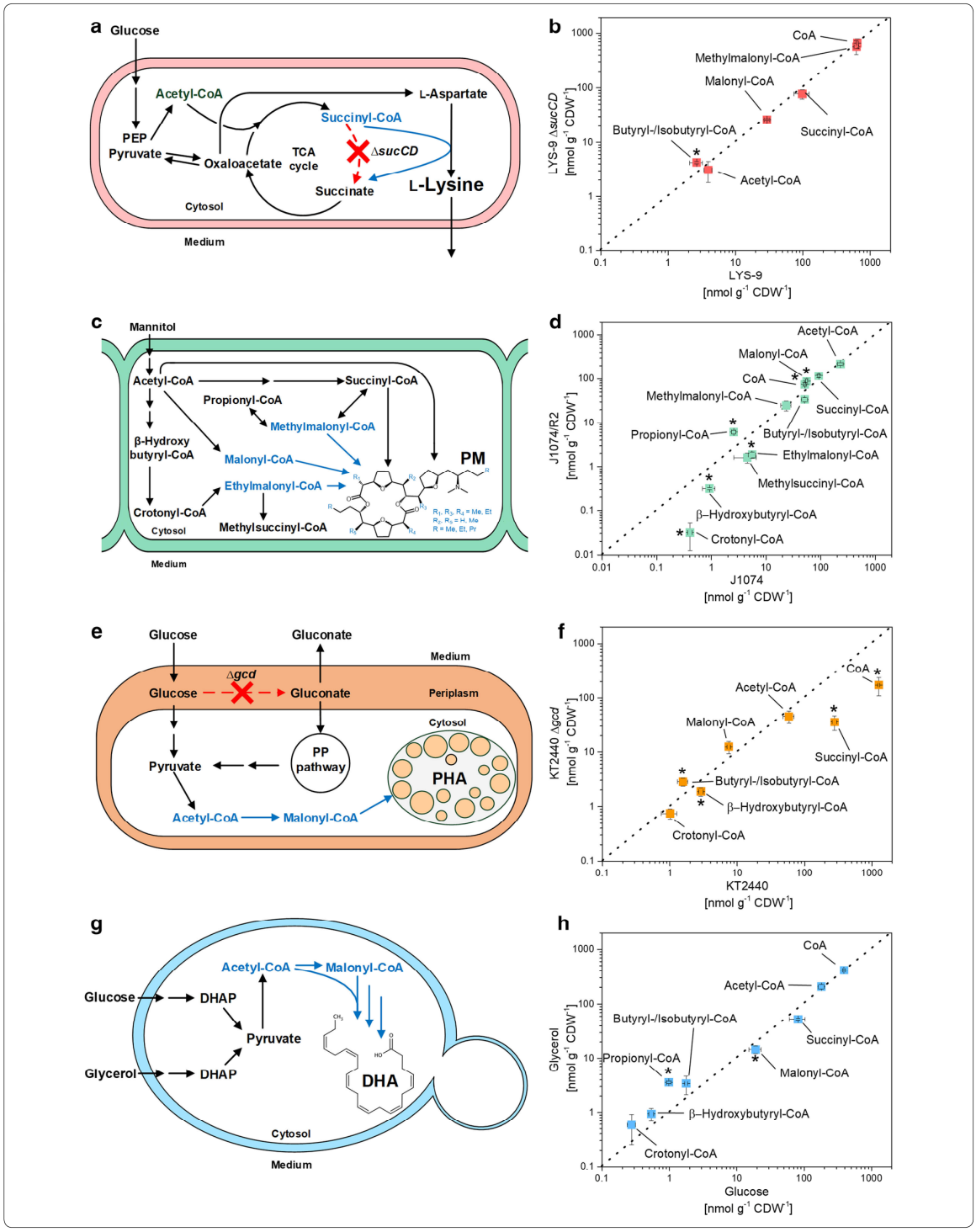
a
Glucose
Acetyl-CoA
L-Aspartate
Succinyl-CoA
PEP
Pyruvate
Oxaloacetate
TCA cycle
ΔsucCD
Succinate
L-Lysine
Cytosol
Medium
b
LYS-9 ΔsucCD [nmol g-1 CDW-1]
LYS-9 [nmol g-1 CDW-1]
CoA
Methylmalonyl-CoA
Malonyl-CoA
Succinyl-CoA
Butyryl-/Isobutyryl-CoA
Acetyl-CoA
c
Mannitol
Acetyl-CoA
Succinyl-CoA
Propionyl-CoA
Methylmalonyl-CoA
β-Hydroxy butyryl-CoA
Malonyl-CoA
PM
Ethylmalonyl-CoA
Crotonyl-CoA
Cytosol
Methylsuccinyl-CoA
Medium
d
J1074/R2 [nmol g-1 CDW-1]
J1074 [nmol g-1 CDW-1]
Acetyl-CoA
Malonyl-CoA
CoA
Methylmalonyl-CoA
Succinyl-CoA
Propionyl-CoA
Butyryl-/Isobutyryl-CoA
Ethylmalonyl-CoA
Methylsuccinyl-CoA
β–Hydroxybutyryl-CoA
Crotonyl-CoA
e
Glucose
Gluconate
Medium
Δgcd
Periplasm
Cytosol
PP pathway
PHA
Pyruvate
Acetyl-CoA
Malonyl-CoA
f
KT2440 Δgcd [nmol g-1 CDW-1]
KT2440 [nmol g-1 CDW-1]
CoA
Acetyl-CoA
Malonyl-CoA
Succinyl-CoA
Butyryl-/Isobutyryl-CoA
β–Hydroxybutyryl-CoA
Crotonyl-CoA
g
Acetyl-CoA
Malonyl-CoA
Glucose
DHAP
Pyruvate
Glycerol
DHAP
DHA
Cytosol
Medium
h
Glycerol [nmol g-1 CDW-1]
Glucose [nmol g-1 CDW-1]
CoA
Acetyl-CoA
Butyryl-/Isobutyryl-CoA
Succinyl-CoA
Propionyl-CoA
Malonyl-CoA
β–Hydroxybutyryl-CoA
Crotonyl-CoA

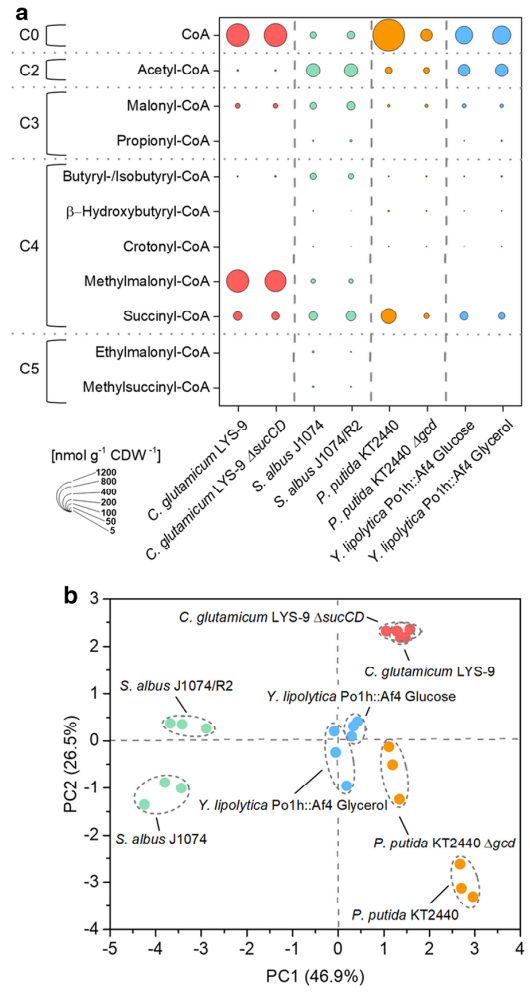

Fig. 5 Spectra of short-chain CoA thioesters and free coenzyme A in different strains of *Corynebacterium glutamicum*, *Streptomyces albus*, *Pseudomonas putida*, and *Yarrowia lipolytica*. Absolute fingerprints of free CoA and carbon two to carbon five CoA thioesters for eight studied scenarios (**a**). Principal component analysis of the intracellular spectrum of CoA thioesters and free CoA of all studied scenarios (**b**). Detailed information on the studied strains is given in the legend to Fig. 3. n = 3

compartmental membranes [25–27]. The fact that they all could be appropriately analyzed with the same workflow suggests a broad applicability of the method. The possibility to use of one common method for different microbes seems also interesting for automatized screening efforts, which more and more get into focus and benefit from standardized workflows [28].

In the following, the approach was applied to different industrial microbes to demonstrate its potential. As example, we could show that growth of *Y. lipolytica* on glycerol results in significantly enhanced levels of propionyl-CoA (Fig. 4h). This finding is interesting for the synthesis of odd-chain fatty acids in the yeast, which relies on propionyl-CoA availability and usually requires toxic propionate supplementation or massive strain engineering [29]. In contrast, glucose resulted in a higher amount of malonyl-CoA. In line, this substrate has proven more efficient than glycerol to derive PUFAs, built from this two CoA thioester, in *Y. lipolytica* [12].

P. putida KT2440 revealed a huge amount of free CoA, more than the other microbes (Fig. 5a), which might be involved in metabolic control, but requires more investigation. A disruption of the periplasmic oxidation route, the major pathway for glucose-breakdown [30] has been previously used to drive PHA synthesis in engineered *P. putida* [13]. As shown, the mutation did not significantly alter the availability of the PHA building blocks but affected the pools of free CoA and the TCA cycle intermediate succinyl-CoA, suggesting a broader impact on metabolism (Figs. 4e, f, and 5a). In addition, the CoA thioester analysis revealed interesting insights into the metabolism of *C. glutamicum* and *S. albus*, which are discussed below in more detail.

The succinylase branch of L-lysine biosynthesis efficiently bridges the disrupted TCA cycle in succinate dehydrogenase deficient *C. glutamicum*

The amino acid L-lysine is an important industrial feed additive, largely produced with *C. glutamicum* [5]. The TCA cycle competes for carbon with L-lysine biosynthesis but is essential for the aerobic microbe and therefore cannot be eliminated [31]. Increased production, however, can be achieved by flux coupling of the TCA cycle to L-lysine biosynthesis [15]. Succinate dehydrogenase deficient strains cannot convert succinyl-CoA into succinate through the TCA cycle but use the succinylase branch of the L-lysine pathway instead, which results in significantly increased yield (Figs. 2a, b and 4b). One unanswered question so far related to the fact, how the genetic modification affected the availability of succinyl-CoA for L-lysine biosynthesis [15]. Here, we could show that a block of the TCA cycle at the level of succinate dehydrogenase did not affect the succinyl-CoA pool (Figs. 2 and 4b), and also not that of acetyl-CoA at the entry into the TCA cycle. The TCA cycle mutant and its parent strain exhibited an identical CoA thioester spectrum (Fig. 4b). This demonstrates that the three enzymes of the succinylase branch, succinyl-transferase (DapD), aminotransferase (DapC), and desuccinylase (DapE) [32] fully compensated for the disrupted TCA cycle. An insufficient capacity of this pathway would have otherwise presumably caused an accumulation of succinyl-CoA in

the mutant. This finding displays a valuable insight into TCA cycle disrupted L-lysine hyper-producing strains. Future profiling of CoA thioesters seems also interesting for other *C. glutamicum* mutants, in which the L-lysine pathway [33], the TCA cycle [34] and pathways around the CoA thioester metabolism [35–37] have been engineered.

The high abundance of methylmalonyl-CoA in *C. glutamicum* is promising towards heterologous production of complex polyketides

As shown, methylmalonyl-CoA was the dominating CoA thioester in *C. glutamicum* (Fig. 4b). From our data, we conclude that methylmalonyl-CoA is formed from succinyl-CoA by methylmalonyl-CoA mutase, eventually as response to TCA cycle activity. Propionyl-CoA, the potentially alternative source for methylmalonyl-CoA via propionyl-CoA carboxylase was proven absent so that this route can be excluded, matching with the fact that propionyl-CoA typically occurs as catabolic intermediate during the degradation of odd-chain fatty acids [38, 39] and branched-chain amino acids [40], not present here.

Methylmalonyl-CoA is a common extender substrate for the biosynthesis of complex polyketides by modular polyketide synthases [41]. The lack of this metabolite has been identified as a barrier to heterologous production of complex polyketides and extensive efforts have been made to install pathways to supply methylmalonyl-CoA as a building block [42, 43]. The discovered high abundance of methylmalonyl-CoA is therefore promising for future production of complex polyketides in *C. glutamicum*, which has been recently demonstrated via functional polyketide synthase expression and 6-methylsalicate biosynthesis in the microbe [36]. For future efforts, the 50-fold excess of methylmalonyl CoA over malonyl-CoA might display an interesting feature, because the relative availability of the two metabolites often impacts the final product structure due to promiscuous enzymes in polyketide synthase assembly lines [41]. Without doubt, the protocol for CoA thioester profiling developed in this work, appears useful for a broad characterization of precursor availability in polyketide producing *C. glutamicum* mutants.

CoA thioester intermediates from the ethylmalonyl pathway are depleted in pamamycin-producing *S. albus* and indicate an impact of precursor availability on product formation

As shown, the CoA thioester spectrum significantly differed between the pamamycin-producing mutant of *S. albus* and the non-producing wildtype (Fig. 3). In particular, intermediates of the ethylmalonyl-CoA pathway [44] were decreased up to more than ten-fold in the producer: β-hydroxybutyryl-CoA, crotonyl-CoA, ethylmalonyl-CoA, and methylsuccinyl-CoA (Fig. 4d). The formation of pamamycin in the heterologous host obviously consumed more CoA thioester building blocks than were supplied from central metabolism. This could display a bottleneck towards higher titers and deserves further investigation in the future. It was interesting to note that introduction of the heterologous pamamycin pathway perturbed the ratio between malonyl-CoA, methylmalonyl-CoA, and ethylmalonyl-CoA. It was approximately 100:40:10 in the wild type and changed to 100:30:1 in the producer (Fig. 3c, d). The three building blocks compete for incorporation into pamamycin. Unusual polyketide synthases in the assembly line equally accept them as substrates, which leads to 16 pamamycin homologues that differ in their side chains at six positions [11, 45]. As shown from our data, the dramatically reduced availability of ethylmalonyl-CoA, together with the accumulation of malonyl-CoA, promoted the synthesis of smaller pamamycins. Indeed, 95.7% of all pamamycin derivatives observed (Pam 579, Pam 593, Pam 607, Pam 621) were light ones (had a lower mass), which could be formed without any contribution of ethylmalonyl-CoA. The pamamycins of higher mass (Pam 635, 649 and 663), which required one, two or even more ethylmalonyl-CoA units, became exceedingly rare, based on this effect. It would be interesting to further explore this link in other natural producers, which obviously differ in the spectrum of pamamycin homologues [46–48]. Metabolic engineering of CoA thioester supply appears promising to streamline pamamycin production towards selective derivatives, as proven valuable for other polyketides [18]. Likewise, a variation of bioprocess parameters appears promising to tailor the CoA ester spectrum [49].

Materials and methods

Microorganisms

Strains used in this study were obtained from previous work. This included *Streptomyces albus* J1074 and its pamamycin producing derivative J1074/R2 [11], the two L-lysine producing strains *Corynebacterium glutamicum* LYS-9 and LYS-9 *ΔsucCD* [15], *Pseudomonas putida* KT2440 and its mutant KT2440 *Δgcd* [13], and the docosahexaenoic acid (DHA) producing recombinant yeast *Yarrowia lipolytica* Po1h::Af4 [12]. All strains were maintained as glycerol stocks at − 80 °C.

Media

Streptomyces albus was kept on mannitol-soy flour (MS) agar containing per liter: 20 g mannitol, 20 g soy flour (Schoenenberger Hensel, Magstadt, Germany), and 20 g agar (Becton–Dickinson, Heidelberg, Germany) [49]. Liquid pre-cultures of *S. albus* were grown in LB broth

(20 g L^{-1}, Sigma-Aldrich, Darmstadt, Germany) and main cultures were grown in minimal medium, which contained per liter: 10 g mannitol, 200 mM potassium phosphate buffer (pH 7.8), 15 g $(NH_4)_2SO_4$, 1 g NaCl, 550 mg $MgCl_2$*$7H_2O$, 200 mg $CaCl_2$, 30 mg 3,4-dihydroxybenzoic acid, 20 mg $FeSO_4$, 2 mg $FeCl_3$*$6H_2O$, 2 mg $MnSO_4$*H_2O, 0.5 mg $ZnSO_4$*H_2O, 0.2 mg $CuCl_2$*$2H_2O$, 0.2 mg $Na_2B_4O_7$*$10H_2O$, 0.1 mg $(NH_4)_6Mo_7O_{24}$*$4H_2O$, 1 mg nicotinamide, 1 mg riboflavin, 0.5 mg thiamine hydrochloride, 0.5 mg pyridoxine hydrochloride, 0.2 mg biotin, and 0.1 mg p-aminobenzoic acid. In addition, liquid media were amended with 30 g L^{-1} glass beads (soda-lime glass, 5 mm, Sigma-Aldrich) to avoid cell agglomeration.

Corynebacterium glutamicum was kept on BHI agar (37 g L^{-1} BHI, 20 g L^{-1} agar, Becton–Dickinson). Precultures and main cultures of *C. glutamicum* were grown on complex BHI medium and minimal glucose medium, respectively, as described previously [3].

Pseudomonas putida was kept on BHI agar (37 g L^{-1} BHI, 20 g L^{-1} agar, Becton–Dickinson). The mineral M9 medium, used for all liquid cultures, contained per liter: 20 g glucose, 12.8 g Na_2HPO_4*$7H_2O$, 3 g KH_2O_4, 1 g NH_4Cl, 0.5 g NaCl, 0.25 g $MgSO_4$*$7H_2O$, 6 mg $FeSO_4$*$7H_2O$, 2.7 mg $CaCO_3$, 2.0 mg $ZnSO_4$*H_2O, 1.2 mg $MnSO_4$*H_2O, 0.4 mg $CoSO_4$*$7H_2O$, 0.3 mg $CuSO_4$*$5H_2O$, and 0.1 mg H_3BO_3 [13].

Yarrowia lipolytica was incubated on YNB-N5000 agar, which contained per liter: 10 g glucose, 5 g $(NH_4)_2SO_4$, 1.7 g YNB (yeast nitrogen base w/o amino acids and ammonium sulfate, Sigma-Aldrich), and 20 g agar. All liquid cultures of the yeast were conducted in minimal medium, containing per liter: 10 g glycerol or 10 g glucose, 200 mM 2-(*N*-morpholino)ethanesulfonic acid (MES, pH 6.8), 5 g $(NH_4)2SO_4$, and 1.7 g YNB.

Cultivation in shake flasks

Liquid cultures were incubated in baffled shake flasks (500 mL, 10% filling volume) on an orbital shaker (Multitron, Infors AG, Bottmingen, Switzerland, 5 cm shaking diameter, 230 rpm, 75% relative humidity), whereby the temperature was adjusted individually (30 °C for *P. putida* and *C. glutamicum*; 28 °C for *S. albus* and *Y. lipolytica*). For each strain, a specific protocol for inoculation and pre-culturing was used to obtain reproducibly growing main cultures. *S. albus* was incubated on MS agar at 28 °C for 3 days until sporulation occurred. Spores of a single colony were collected to inoculate the preculture, which was incubated overnight in LB medium. Afterwards, cells were collected (5000×*g*, 25 °C, 6 min), resuspended in main culture medium, and used to inoculate the main culture. *C. glutamicum* was grown overnight on BHI agar at 30 °C. A single colony was used to inoculate an overnight pre-culture, which was then collected (5,000 x*g*, 25 °C, 6 min), resuspended in main culture medium, and used to inoculate the main culture. *P. putida* was grown overnight on M9 agar (30 °C). A single colony served as inoculum for the pre-culture which was then grown overnight, harvested (5,000 x*g*, 25 °C, 6 min), resuspended in main culture medium, and used to inoculate the main culture. *Y. lipolytica* was grown overnight on YNB-N5000 agar at 28 °C. A single colony was used to inoculate the pre-culture, which was incubated overnight, harvested (5000×*g*, 25 °C, 6 min), resuspended in main culture medium and then served as inoculum for the main culture. All growth experiments were conducted as biological triplicate.

Determination of cell concentration

All investigated microbes were analyzed for their cell dry weight. Cells of *S. albus* were vacuum-filtered using a nitrocellulose filter (0.2 µM, Sartorius, Göttingen, Germany), washed twice with 15 mL deionized water, and gravimetrically analyzed using a moisture analyzer (HB43-S, Mettler-Toledo, Columbus, USA). The parallel measurement of the cell concentration as optical density at 600 nm (OD_{600}) resulted in a correlation factor of CDW (g L^{-1}) = 0.62 × OD_{600}. The cell dry weight of *C. glutamicum* was inferred from the optical density measurement at 660 nm as previously described [3]. The cell dry weight of *P. putida* and *Y. lipolytica* was measured as follows. Cells were collected (15,000×*g*, 4 °C, 10 min), washed twice with 15 mL deionized water, and freeze-dried. Afterwards, the dry biomass was gravimetrically determined.

Quantification of substrates

Mannitol and glucose were quantified by HPLC (1260 Infinity Series, Agilent, Darmstadt, Germany) using a Metacarb 87C column (300 × 7.8 mm, Agilent), a Metacarb 87C guard column (50 × 7.8 mm, Agilent), a desalting column (Microguard Deashing Cartridge, Bio-Rad, Munich, Germany), and demineralized water as mobile phase (85 °C, 0.6 mL min^{-1}). Refraction index measurement was used for detection, and external standards were used for quantification [2, 3].

Extraction and quantification of pamamycins

Prior to analysis, pamamycins were extracted from *S. albus* culture broth. For this purpose, 200 µL broth was mixed with 200 µL acetone and incubated for 15 min (1,000 rpm, room temperature, Thermomixer F1.5, Eppendorf, Wesseling, Germany). Afterwards, 200 µL ethyl acetate was added, and the mixture was incubated for further 15 min. The organic phase was collected by centrifugation (20,000×*g*, 5 min, room temperature).

Subsequently, the solvent mixture was evaporated under nitrogen. The obtained extract was dissolved in methanol and clarified from debris (20,000 x*g*, 5 min, 4 °C). Afterwards, the different pamamycin derivatives were analyzed using LC–ESI–MS/MS (QTRAP 6500$^+$, AB Sciex, Darmstadt, Germany) coupled to an HPLC system (Agilent Infinity 1290 System). In short, the analytes were separated on a C18 column (Vision HT C18 HighLoad, 100 mm × 2 mm, 1.5 µm, Dr. Maisch, Ammerbuch-Entringen, Germany) at 45 °C and a flow rate of 300 µL min^{-1} (8 mM ammonium formate in 92% acetonitrile). Detection was carried out in positive selected ion monitoring (SIM) mode, using the $[M+H]^+$ ion for each pamamycin derivative.

Quantification of L-lysine

The amino acid L-lysine was quantified using HPLC with pre-column derivatization and fluorescence detection as described before [50]. For quantification, α-aminobutyric acid was used as internal standard [2].

Extraction of intracellular CoA thioesters

A broth sample (approximately 8 mg CDW) was collected and immediately transferred into a pre-cooled extraction and quenching buffer (95% acetonitrile, 25 mM formic acid, -20 °C) [21]. The volume ratio was 1:4. The obtained solution was thoroughly mixed while cooled on ice for 10 min, and then clarified from debris (15,000×*g*, 4 °C, 10 min). The obtained supernatant was mixed with 10 mL super cooled deionized water (− 2 °C). The cell pellet was twice washed with 8 mL super cooled deionized water. Afterwards, all supernatants were combined, frozen with liquid nitrogen, freeze-dried, and then re-dissolved in 500 µL pre-cooled resuspension buffer (25 mM ammonium formate, pH 3.0, 2% MeOH, 4 °C) [51]. The buffered extract was filtered (Ultrafree-MC 0.22 µm, Merck, Millipore, Germany) prior to analysis.

Quantification of CoA thioesters using LC–ESI–MS/MS

The analysis of CoA thioesters was performed on a triple quadrupole MS (QTRAP 6500$^+$, AB Sciex, Darmstadt, Germany) coupled to an HPLC system (Agilent Infinity 1290 System). Generally, the injection volume was 10 µL. Separation of the analytes of interest was conducted on a porous reversed phase column (Gemini C18, 100 mm × 4.6 mm, 3 µm, 110 Å, Phenomenex, Aschaffenburg, Germany) at 40 °C using a gradient of formic acid (50 mM, adjusted to pH 8.1 with ammonium hydroxide 25% in H_2O, eluent A) and methanol (eluent B) at a flow rate of 600 µL min^{-1}. The fraction of eluent B was as follows: 0–12 min, 0–15% B; 12–16 min, 15–100% B; 16–18 min, 100% B; 18–20 min, 100–0% B; 20–25 min, 0% B. Initial tests were further done, using a smaller column geometry and pore size (Gemini C18, 100 mm × 2.1 mm, 1.5 µm, 110 Å, Phenomenex), using the same gradient, but a reduced flow rate of 300 µL min^{-1}. In addition (and finally used in the optimized workflow), a core–shell reversed phase column (Kinetex XB-C18, 100 × 2.1 mm, 2.6 µm, 100 Å, Phenomenex) was applied at 40 °C, using a gradient of formic acid (50 mM, adjusted to pH 8.1 with ammonium hydroxide 25% in H_2O, eluent A) and methanol (eluent B) at a flow rate of 300 µL min^{-1}. The fraction of eluent B was as follows: 0–7 min, 0–10% B; 7–10 min, 10–100% B; 10–11 min, 100% B; 11–12 min, 100–0% B; 12–15 min, 0% B. During the first 3 min of the analysis, the outflow from the chromatographic column was discharged to minimize the entry of salts from samples into the mass spectrometer. The individual CoA thioesters were detected using multiple reaction monitoring (MRM), involving the corresponding parent ion and its respective daughter ion (Additional file 1: Table S1). Further instrument settings were as follows: curtain gas, 35 psi; collision gas flowrate, medium; ion spray voltage, 4.5 kV; temperature, 400 °C; ion source gas, 60 psi; and entrance potential, 10 V. The declustering potential, the collision energy and the collision cell exit potential were optimized individually for each CoA thioester using synthetic standards. Acetyl-CoA, propionyl-CoA, succinyl-CoA, methylmalonyl-CoA, and free CoA were purchased (Sigma-Aldrich), whereas malonyl-CoA, β-hydroxybutyryl-CoA, butyryl-CoA, isobutyryl-CoA, crotonyl-CoA, methylsuccinyl-CoA and ethylmalonyl-CoA were chemo-enzymatically synthesized as previously described [7].

Absolute quantification of CoA thioesters using ^{13}C-labeled extracts

Absolute quantification of CoA thioesters was conducted using the MIRACLE approach [52]. For this purpose, ^{13}C-labeled cell extracts were used as internal standard, whereby an individual standard was produced for each microbe. For this purpose, the different organisms were grown on ^{13}C-enriched substrates, i.e. the naturally labeled carbon source was replaced by an equimolar amount of the [U-^{13}C] enriched isomer: 99% [$^{13}C_6$] D-mannitol (*S. albus*), 99% [$^{13}C_6$] D-glucose (*P. putida* and *C. glutamicum*), and 99% [$^{13}C_3$] D-glycerol (*Y. lipolytica*). The ^{13}C tracer substrates were obtained from Cambridge Isotope Laboratories (Tewksbury, MA, USA). For each microbe, the second pre-culture and the main culture was conducted in the ^{13}C-enriched minimal medium. In each case, the inoculum size was below 1% of the later harvested cell concentration to finally provide fully ^{13}C enriched cell extracts as standard and exclude potential interference [27]. The culture broth from the main ^{13}C culture was

extracted during the late exponential growth phase, using the extraction protocol described above. After freeze-drying and re-suspension, the ^{13}C extract was stored as aliquots at − 80 °C. The level of the individual CoA thioesters in each ^{13}C extract was precisely quantified using the synthetic standards and corresponding instrument settings (Additional file 1: Tables S1 and S2). During later analysis, an appropriate volume of ^{13}C extract (of the respective microbe) was thawn on ice, and then simultaneously added with the sample into the quenching solution. This protocol allowed to to infer absolute metabolite levels and to take any eventual changes during sample processing into account.

Principal component analysis

Principle component analysis (PCA) was performed using the ClustVis web tool [53].

Supplementary information

Supplementary information accompanies this paper at https://doi.org/10.1186/s12934-020-01413-1.

Additional file 1: Figure S1. LC-MS chromatogram of a synthetic CoA thioester standard using a porous organo-silica reversed phase column (100 × 2.1 mm, 1.5 µm) for the chromatographic separation. Co-eluting analytes were distinguished by a different specific mass-to-charge ratio (*m/z*). **Figure S2.** Calibration curves for different CoA thioesters using LC-MS/MS analysis. **Table S1.** Instrumental settings for LC-MS/MS analysis of CoA thioesters. The declustering potential (DP), the collision energy (CE) and the cell exit potential (CXP) were individually tuned for each CoA thioester. The parent ion reflects the positive proton adduct $[M+H]^+$, except for the CoA homodimer (CoA-S-S-CoA), where the parent ion was $[M+2H]^{2+}$. In each case, the daughter ion reflects the positive proton adduct after neutral loss of 507 (*m/z*). **Table S2.** Instrumental settings for LC-MS/MS analysis of fully ^{13}C-labeled CoA thioesters used as internal standard for absolute CoA thioesters quantification. The respective mass of the fully labeled parent ion was determined by adding the number of carbon atoms to the monoisotopic mass of the non-labelled parent ion (Table S1). The mass of each daughter ion was then calculated by subtraction of *m/z* 517 form this value, considering the neutral loss of a fragment with ten ^{13}C atoms.

Authors' contributions

BV synthesized CoA thioesters. LG, MK and MF developed the CoA thioester extraction and analytical protocol. LG produced the ^{13}C labeled extracts and conducted cultivation of *S. albus*, *C. glutamicum*, and *P. putida*. SJ performed cultivation of *Y. lipolytica*. LG conducted thioester analysis. CW conceived and structured the work. LG, JB and CW wrote the first draft of the manuscript. All authors critically commented and improved the manuscript. All authors read and approved the final manuscript.

Funding

Open access funding providedby Projekt DEAL. This work was supported by the German Ministry of Education and Research (BMBF) through the Grants MyBio (FKZ 031B034A) and MYXO4PUFA (FKZ 031B0346B) and by the German Research Foundation (FKZ INST 256/418-1). Further support was provided by the Max Planck Society and the LOEWE program (Landes-Offensive zur Entwicklung wissenschaftlich-ökonomischer Exzellenz) of the state of Hessen within the framework of the MegaSyn Research Cluster. The funding bodies did not contribute to study design, data collection, analysis, and interpretation, or writing of the manuscript.

Availability of data and materials

The dataset(s) supporting the conclusions of this article are all included within the article.

Ethics approval and consent to participate

Not applicable. The manuscript does not contain data collected from humans or animals.

Consent for publication

Not applicable.

Competing interests

The authors declare that they have no competing interests.

Author details

[1] Institute of Systems Biotechnology, Saarland University, Saarbrücken, Germany. [2] Max Planck Institute for Terrestrial Microbiology, Marburg, Germany.

Received: 4 May 2020 Accepted: 20 July 2020
Published online: 10 August 2020

References

1. Becker J, Wittmann C. From systems biology to metabolically engineered cells-an omics perspective on the development of industrial microbes. Curr Opin Microbiol. 2018;45:180–8.
2. Hoffmann SL, Jungmann L, Schiefelbein S, Peyriga L, Cahoreau E, Portais JC, Becker J, Wittmann C. Lysine production from the sugar alcohol mannitol: design of the cell factory *Corynebacterium glutamicum* SEA-3 through integrated analysis and engineering of metabolic pathway fluxes. Metab Eng. 2018;47:475–87.
3. Rohles CM, Giesselmann G, Kohlstedt M, Wittmann C, Becker J. Systems metabolic engineering of *Corynebacterium glutamicum* for the production of the carbon-5 platform chemicals 5-aminovalerate and glutarate. Microb Cell Fact. 2016;15:154.
4. Rohles CM, Gläser L, Kohlstedt M, Giesselmann G, Pearson S, del Campo A, Becker J, Wittmann C. A bio-based route to the carbon-5 chemical glutaric acid and to bionylon-6,5 using metabolically engineered *Corynebacterium glutamicum*. R Soc Chem Green Chem. 2018;20:4662–74.
5. Becker J, Rohles CM, Wittmann C. Metabolically engineered *Corynebacterium glutamicum* for bio-based production of chemicals, fuels, materials, and healthcare products. Metab Eng. 2018;50:122–41.
6. Veras HCT, Campos CG, Nascimento IF, Abdelnur PV, Almeida JRM, Parachin NS. Metabolic flux analysis for metabolome data validation of naturally xylose-fermenting yeasts. BMC Biotechnol. 2019;19:58.
7. Peter DM, Vogeli B, Cortina NS, Erb TJ. A chemo-enzymatic road map to the synthesis of CoA esters. Molecules. 2016;21:517.
8. Zimmermann M, Thormann V, Sauer U, Zamboni N. Nontargeted profiling of coenzyme A thioesters in biological samples by tandem mass spectrometry. Anal Chem. 2013;85:8284–90.
9. Kanehisa M, Goto S. KEGG: kyoto encyclopedia of genes and genomes. Nucleic Acids Res. 2000;28:27–30.
10. Kanehisa M, Sato Y, Furumichi M, Morishima K, Tanabe M. New approach for understanding genome variations in KEGG. Nucleic Acids Res. 2019;47:D590–5.
11. Rebets Y, Brotz E, Manderscheid N, Tokovenko B, Myronovskyi M, Metz P, Petzke L, Luzhetskyy A. Insights into the pamamycin biosynthesis. Angew Chem. 2015;54:2280–4.
12. Gemperlein K, Dietrich D, Kohlstedt M, Zipf G, Bernauer HS, Wittmann C, Wenzel SC, Müller R. Polyunsaturated fatty acid production by *Yarrowia lipolytica* employing designed myxobacterial PUFA synthases. Nat Commun. 2019;10:4055.
13. Poblete-Castro I, Binger D, Rodrigues A, Becker J, Martins Dos Santos VA, Wittmann C. In-silico-driven metabolic engineering of *Pseudomonas putida* for enhanced production of poly-hydroxyalkanoates. Metab Eng. 2013;15:113–23.
14. Kang A, Lee TS. Converting sugars to biofuels: ethanol and beyond. Bioengineering. 2015;2:184–203.
15. Kind S, Becker J, Wittmann C. Increased lysine production by flux coupling of the tricarboxylic acid cycle and the lysine biosynthetic

pathway–metabolic engineering of the availability of succinyl-CoA in *Corynebacterium glutamicum*. Metab Eng. 2013;15:184–95.
16. Schada von Borzyskowski L, Sonntag F, Poschel L, Vorholt JA, Schrader J, Erb TJ, Buchhaupt M. Replacing the ethylmalonyl-CoA pathway with the glyoxylate shunt provides metabolic flexibility in the central carbon metabolism of *Methylobacterium extorquens* AM1. ACS Synth Biol. 2018;7:86–97.
17. Huang YY, Jian XX, Lv YB, Nian KQ, Gao Q, Chen J, Wei LJ, Hua Q. Enhanced squalene biosynthesis in *Yarrowia lipolytica* based on metabolically engineered acetyl-CoA metabolism. J Biotechnol. 2018;281:106–14.
18. Lu C, Zhang X, Jiang M, Bai L. Enhanced salinomycin production by adjusting the supply of polyketide extender units in Streptomyces albus. Metab Eng. 2016;35:129–37.
19. Martinez-Garcia E, Nikel PI, Aparicio T, de Lorenzo V. Pseudomonas 2.0: genetic upgrading of *P. putida* KT2440 as an enhanced host for heterologous gene expression. Microbial cell factories. 2014;13:159.
20. Botella L, Lindley ND, Eggeling L. Formation and metabolism of methylmalonyl coenzyme A in *Corynebacterium glutamicum*. J Bacteriol. 2009;191:2899–901.
21. Peyraud R, Kiefer P, Christen P, Massou S, Portais JC, Vorholt JA. Demonstration of the ethylmalonyl CoA pathway by using ^{13}C metabolomics. Proc Natl Acad Sci USA. 2009;106:4846–51.
22. Seifar RM, Ras C, Deshmukh AT, Bekers KM, Suarez-Mendez CA, da Cruz AL, van Gulik WM, Heijnen JJ. Quantitative analysis of intracellular coenzymes in *Saccharomyces cerevisiae* using ion pair reversed phase ultra high performance liquid chromatography tandem mass spectrometry. J Chromatogr A. 2013;1311:115–20.
23. Park JW, Jung WS, Park SR, Park BC, Yoon YJ. Analysis of intracellular short organic acid-coenzyme A esters from actinomycetes using liquid chromatography-electrospray ionization-mass spectrometry. Journal of mass spectrometry: JMS. 2007;42:1136–47.
24. Rost LM, Brekke Thorfinnsdottir L, Kumar K, Fuchino K, Eide Langorgen I, Bartosova Z, Kristiansen KA, Bruheim P. Absolute quantification of the central carbon metabolome in eight commonly applied prokaryotic and eukaryotic model systems. Metabolites. 2020;10:74.
25. Bolten CJ, Kiefer P, Letisse F, Portais JC, Wittmann C. Sampling for metabolome analysis of microorganisms. Anal Chem. 2007;79:3843–9.
26. Wittmann C, Krömer JO, Kiefer P, Binz T, Heinzle E. Impact of the cold shock phenomenon on quantification of intracellular metabolites in bacteria. Anal Biochem. 2004;327:135–9.
27. Wittmann C. Fluxome analysis using GC-MS. Microb Cell Fact. 2007;6:6.
28. Weber RJM, Lawson TN, Salek RM, Ebbels TMD, Glen RC, Goodacre R, Griffin JL, Haug K, Koulman A, Moreno P, et al. Computational tools and workflows in metabolomics: an international survey highlights the opportunity for harmonisation through Galaxy. Metabolomics. 2017;13:12.
29. Park YK, Ledesma-Amaro R, Nicaud JM. De novo biosynthesis of odd-chain fatty acids in *Yarrowia lipolytica* enabled by modular pathway engineering. Front Bioeng Biotechnol. 2019;7:484.
30. Kohlstedt M, Wittmann C. GC-MS-based (13)C metabolic flux analysis resolves the parallel and cyclic glucose metabolism of *Pseudomonas putida* KT2440 and *Pseudomonas aeruginosa* PAO1. Metab Eng. 2019;54:35–53.
31. Becker J, Klopprogge C, Schroder H, Wittmann C. Metabolic engineering of the tricarboxylic acid cycle for improved lysine production by *Corynebacterium glutamicum*. Appl Environ Microbiol. 2009;75:7866–9.
32. Sonntag K, Eggeling L, De Graaf AA, Sahm H. Flux partitioning in the split pathway of lysine synthesis in *Corynebacterium glutamicum*. Quantification by 13C- and 1H-NMR spectroscopy. Eur J Biochem. 1993;213:1325–31.
33. Becker J, Zelder O, Haefner S, Schröder H, Wittmann C. From zero to hero–design-based systems metabolic engineering of *Corynebacterium glutamicum* for l-lysine production. Metab Eng. 2011;13:159–68.
34. Zhang Y, Shang X, Wang B, Hu Q, Liu S, Wen T. Reconstruction of tricarboxylic acid cycle in *Corynebacterium glutamicum* with a genome-scale metabolic network model for trans-4-hydroxyproline production. Biotechnol Bioeng. 2019;116:99–109.
35. Milke L, Kallscheuer N, Kappelmann J, Marienhagen J. Tailoring *Corynebacterium glutamicum* towards increased malonyl-CoA availability for efficient synthesis of the plant pentaketide noreugenin. Microb Cell Fact. 2019;18:71.
36. Kallscheuer N, Kage H, Milke L, Nett M, Marienhagen J. Microbial synthesis of the type I polyketide 6-methylsalicylate with *Corynebacterium glutamicum*. Appl Microbiol Biotechnol. 2019;103:9619–31.
37. Chang Z, Dai W, Mao Y, Cui Z, Wang Z, Chen T. Engineering *Corynebacterium glutamicum* for the efficient production of 3-hydroxypropionic acid from a mixture of glucose and acetate via the malonyl-CoA pathway. Catalysts. 2020;10:203.
38. Zhang YQ, Brock M, Keller NP. Connection of propionyl-CoA metabolism to polyketide biosynthesis in *Aspergillus nidulans*. Genetics. 2004;168:785–94.
39. Dolan SK, Wijaya A, Geddis SM, Spring DR, Silva-Rocha R, Welch M. Loving the poison: the methylcitrate cycle and bacterial pathogenesis. Microbiology. 2018;164:251–9.
40. Xu Z, Liu Y, Ye BC. PccD regulates branched-chain amino acid degradation and exerts a negative effect on erythromycin production in *Saccharopolyspora erythraea*. Appl Environ Microbiol. 2018;84:e00049-18.
41. Helfrich EJ, Piel J. Biosynthesis of polyketides by trans-AT polyketide synthases. Nat Prod Rep. 2016;33:231–316.
42. Dayem LC, Carney JR, Santi DV, Pfeifer BA, Khosla C, Kealey JT. Metabolic engineering of a methylmalonyl-CoA mutase-epimerase pathway for complex polyketide biosynthesis in *Escherichia coli*. Biochemistry. 2002;41:5193–201.
43. Gross F, Ring MW, Perlova O, Fu J, Schneider S, Gerth K, Kuhlmann S, Stewart AF, Zhang Y, Müller R. Metabolic engineering of *Pseudomonas putida* for methylmalonyl-CoA biosynthesis to enable complex heterologous secondary metabolite formation. Chem Biol. 2006;13:1253–64.
44. Wang J, Wang C, Song K, Wen J. Metabolic network model guided engineering ethylmalonyl-CoA pathway to improve ascomycin production in *Streptomyces hygroscopicus* var. *ascomyceticus*. Microb Cell Fact. 2017;16:169.
45. Kuhl M, Gläser L, Rebets Y, Rückert C, Sarkar N, Hartsch T, Kalinowksi J, Luzhetskyy A, Wittmann C: Microparticles globally reprogram the metabolism of *Streptomyces albus* towards accelerated morphogenesis, streamlined carbon core metabolism and enhanced production of the antituberculosis polyketide pamamycin. Biotechnol Bioeng 2020, submitted.
46. Natsume M, Tazawa J, Yagi K, Abe H, Kondo S, Marumo S. Structure-activity relationship of pamamycins: effects of alkyl substituents. J Antibiotics. 1995;48:1159–64.
47. Kozone I, Chikamoto N, Abe H, Natsume M. De-*N*-methylpamamycin-593A and B, new pamamycin derivatives isolated from *Streptomyces alboniger*. J Antibiotics. 1999;52:329–31.
48. Natsume M, Yasui K, Kondo S, Marumo S. The structure of four new pamamycin homologues isolated from *Streptomyces alboniger*. Tetrahedron Lett. 1991;32:3087–90.
49. Kieser T, Bibb M, Buttner M, Chater K, Hopwood D. Practical streptomyces genetics *John Innes Foundation*. United Kingdom: Norwich; 2000.
50. Krömer JO, Fritz M, Heinzle E, Wittmann C. In vivo quantification of intracellular amino acids and intermediates of the methionine pathway in *Corynebacterium glutamicum*. Anal Biochem. 2005;340:171–3.
51. Schneider K, Peyraud R, Kiefer P, Christen P, Delmotte N, Massou S, Portais JC, Vorholt JA. The ethylmalonyl-CoA pathway is used in place of the glyoxylate cycle by Methylobacterium extorquens AM1 during growth on acetate. J Biol Chem. 2012;287:757–66.
52. Mashego MR, Wu L, Van Dam JC, Ras C, Vinke JL, Van Winden WA, Van Gulik WM, Heijnen JJ. MIRACLE: mass isotopomer ratio analysis of U-^{13}C-labeled extracts. A new method for accurate quantification of changes in concentrations of intracellular metabolites. Biotechnol Bioeng. 2004;85:620–8.
53. Metsalu T, Vilo J. ClustVis: a web tool for visualizing clustering of multivariate data using Principal Component Analysis and heatmap. Nucleic Acids Res. 2015;43:W566–70.

Publisher's Note

4 Discussion

4.1 The importance of the genus *Streptomyces* to overcome the threat of antimicrobial resistance

Actinobacteria, especially the genus *Streptomyces,* produce a plethora of biological active natural products with many of them functioning as antibiotics, antifungals, and anthelmintics, amongst others (Barka et al., 2016). Thereby, natural products and their derivatives greatly helped to increase human life expectation over the last decades (Demain, 2006) and display more than 50% of today's approved drugs (Cragg & Newman, 2013). Cases of infections with antimicrobial resistant pathogens strongly increased, due to the ubiquitous and often non-advantageous use of antibiotics (Van Boeckel et al., 2017; Pouwels et al., 2018; Roope et al., 2019). In the past, the use of *Streptomyces*-derived antibiotics, such as the in this work examined oxytetracycline from *S. rimosus*, as well as streptomycin from *S. griseus,* cephalosporins from *S. clavuligerus,* chloramphenicol from *S. venezuelae,* tetracycline from *S. aureofaciens,* nystatin from *S. noursei,* kanamycin from *S. kanamyceticus,* and fosfomycin from *S. fradiae,* helped to guarantee the safety of medical procedures and treatments (Procópio et al., 2012; Pethick et al., 2013). Therefore, it does not seem unlikely that *Streptomyces* microbes have the capability to produce additional compounds that guarantee our safety in the future with new modes of action of which we currently not know (Lasch et al., 2020; Rodríguez Estévez et al., 2020; Shuai et al., 2020). But also other secondary metabolite producers of the phylum actinobacteria, such as the in this work used *Amycolatopsis, Actinoplanes,* and *Kitasatospora* (Kuhl et al., 2021) are promising for the research of new drugs. To identify such compounds for the treatment of infections caused by multi-resistant pathogens, new methods to enhance natural product formation and to activate silent biosynthetic clusters are needed. Prominent examples of such clinically relevant strains are methicillin-resistant *Staphylococcus aureus* (MRSA) and vancomycin-resistant *Enterococci* (VRE) (Cetinkaya et al., 2000; Gurusamy et al., 2013). It has been demonstrated that bottromycin derivatives exhibit potent biological activity against these dangerous strains (Kobayashi et al., 2010). However, bottromycins are difficult to obtain and their research has developed into a challenge for scientists over the last 65 years (Kazmaier, 2020). Thus, the particle-based cultivation strategy, resulting in high titers for bottromycin A2 and its methylated derivative (109 mg L^{-1} combined), appear very promising towards future drug development (Kuhl et al., 2021). It might also drive the RiPP cinnamycin, investigated here, and RiPP antibiotics in general, which could create

extra impact, as the biosynthetic flexibility of this class of compounds sets them apart from other natural products (Arnison et al., 2013; Kuhl et al., 2021). This unique feature provides RiPPs with remarkable engineering potential and gives belief to generate novel compounds to address the rise of antibiotic resistance and to overcome their problems of low solubility and bioavailability in the future (Weissman, 2016; Winn et al., 2016; Hudson & Mitchell, 2018). The abovementioned problems of antimicrobial resistance clearly justify the number of different approaches in today's research in natural product drug discovery (Atanasov et al., 2021).

4.2 Systems-biology analyses provide fascinating insights into pamamycin and bottromycin production

Classical strain engineering, relying on random mutagenesis and selection, inherently causes growth deficiencies, weak stress tolerance, and undesired by-product formation in the obtained mutants or even leads to dead-end mutants, which are completely resistant to subsequent rounds of optimization. These strains may carry up to several thousand mutations, which makes it difficult to unravel the mechanisms of their biosynthetic pathways (Becker et al., 2011). Thus, intense research efforts, using systems metabolic engineering, have been invested in the past to enable the construction of tailor-made production strains based on highly vital wild types (Olano et al., 2008; Tyo et al., 2010; Becker et al., 2011). Systems metabolic engineering relies on a profound understanding of the biological networks of a cellular system (Wittmann & Lee, 2012). Today, these information are gathered using state-of-the-art omics technologies, such as transcriptomics and metabolomics, which interlock to decipher the key interactions for maximizing titers, yields, or growth rates (Becker et al., 2011; García-Granados et al., 2019).

In this work, we could demonstrate the power of such holistic approaches for cellular optimization. First, we developed a method for the absolute quantification of short chain CoA-thioesters in prokaryotic and eukaryotic microbes, which exhibits high precision and reproducibility for various microbes studied (Gläser et al., 2020). Then, we applied this metabolomics tool, together with RNA sequencing, to unravel molecular details mechanisms of how talc microparticles boosted pamamycin production and shifted the product spectrum in *S. albus* J1074/R2 (Kuhl et al., 2020) and how the microparticles boosted bottromycin A2 production in *S. lividans* TK24 DG2-Km-P41hyg+ (Kuhl et al., 2021).

Based on the obtained systems-view on pamamycin production and supporting pathways, we discovered that talc supply strongly upregulated the pamamycin biosynthetic gene cluster (up to 1,024-fold), explaining the tripled titer (Kuhl et al., 2020). Moreover, the microparticles upregulated most genes encoding for enzymes of the CoA-ester metabolism, which resulted in a modulation of intracellular CoA-ester availability. This finding, together with the discovery of a modified ratio between malonyl-CoA, methylmalonyl-CoA, and ethylmalonyl-CoA, nicely explained the altered production spectrum, since the three building blocks compete for incorporation into pamamycin and thereby determine the final product spectrum (Rebets et al., 2015). As consequence of a higher availability of the larger building block methylmalonyl-CoA, together with a reduced availability of the smaller building block malonyl-CoA, heavier pamamycin derivatives (Pam 621, Pam 635, Pam 649, and Pam 663) were enhanced, whereas more than twofold less small pamamycins (Pam 579 and Pam 593) were present, when talc was supplied (Kuhl et al., 2020). Albeit the regulatory mechanisms of CoA-metabolism are highly complex and CoA-ester converting enzymes show a certain degree of promiscuity, these findings highlight how promising metabolic engineering of CoA-ester supply appears to streamline pamamycin production towards selective derivatives and support future exploration of pamamycins for the development of new potent drugs (Kuhl et al., 2020; Gummerlich et al., 2021).

In contrast to pamamycin and other natural products (Lu et al., 2016; Kallifidas et al., 2018), precursor availability could be ruled out for increased bottromycin production in *S. lividans* TK24 DG2-Km-P41hyg+ (Kuhl et al., 2021). Instead, the analysis of pathway intermediates and inefficient shunt products, as well as of the transcriptomic data, indicated a higher production efficiency with microparticle supply, orchestrated by a rebalancing of biosynthetic cluster genes. We discovered that specifically the increased expression (2.4-fold) of aminohydrolase, encoded by *botAH,* during main production phase was responsible for the increased production efficiency of (Met-)bottromycin A2. The enzyme catalyzes the unique amidine-forming macrocyclodehydration, which follows β-methylation in the post-translational modification of bottromycins (Huo et al., 2012; Crone et al., 2016). This was a surprising finding, as the cluster was designed to uncouple expression from the metabolism of the host using synthetic promoters (Horbal et al., 2018). However, the RNA sequencing data revealed that the expression was only weakly driven by the synthetic promoters, but largely relied on the highly active promoter of the hygromycin marker gene hygR and a so far unknown, but apparently even stronger antisense promoter sequence downstream of hygR, which transcribed the cluster in the opposite direction and expressed the left cluster genes and an additional anti-

sense transcript of hygR (Kuhl et al., 2021). These conclusions are different of the findings for pamamycin production in *S. albus* J1074/R2, where the microparticles induced an entire activation of the biosynthetic cluster. Most likely, this derives from a distinct regulation of the clusters, as the pamamycin cluster was under the control of native promoters (Kuhl et al., 2020), different to the synthetic control of the bottromycin cluster. Still, this demonstrated again that talc microparticle supply results in specific transcriptional changes of biosynthetic cluster genes.

4.3 Microparticle-enhanced cultivation of actinobacteria is a strong addition to the OSMAC principle and could enable natural product drug discovery in the future

With the discovery that microbes with large genomes have the capacity to produce about ten times more secondary metabolites than previously recognized and that the most gifted strains among Actinomycetes can produce up to 30-50 secondary metabolites, a new era in natural product discovery has begun (Katz & Baltz, 2016). Still, problems in natural product drug discovery relate to the inaccessibility of strains in laboratory cultures and the fact that the microbes often produce certain substances only in their natural environment. Thus, it remains difficult to elucidate the molecular structure of a substance and to examine its bioactivity, its molecular targets, and potential side-effects (Atanasov et al., 2021). Finding new methods for strain culturing, in situ analysis, natural product synthesis, extraction and pre-fractionation of extracts, and molecular mode of action elucidation therefore plays a crucial role for natural product drug discovery (Atanasov et al., 2021). In this regard, the developed microparticle enhanced cultivation of actinobacteria in shake-flasks and especially in miniaturized microtiter plates appears a highly useful approach to facilitate natural product research. In this regard, it nicely complements recent breakthroughs in co-cultivation of producer strains. As example, the co-cultivation of microorganisms with helper strains, in particular fungi simulates the natural habitat of the producers and thereby supports the production and identification of new natural products (Abdel-Razek et al., 2018; Moussa et al., 2019).

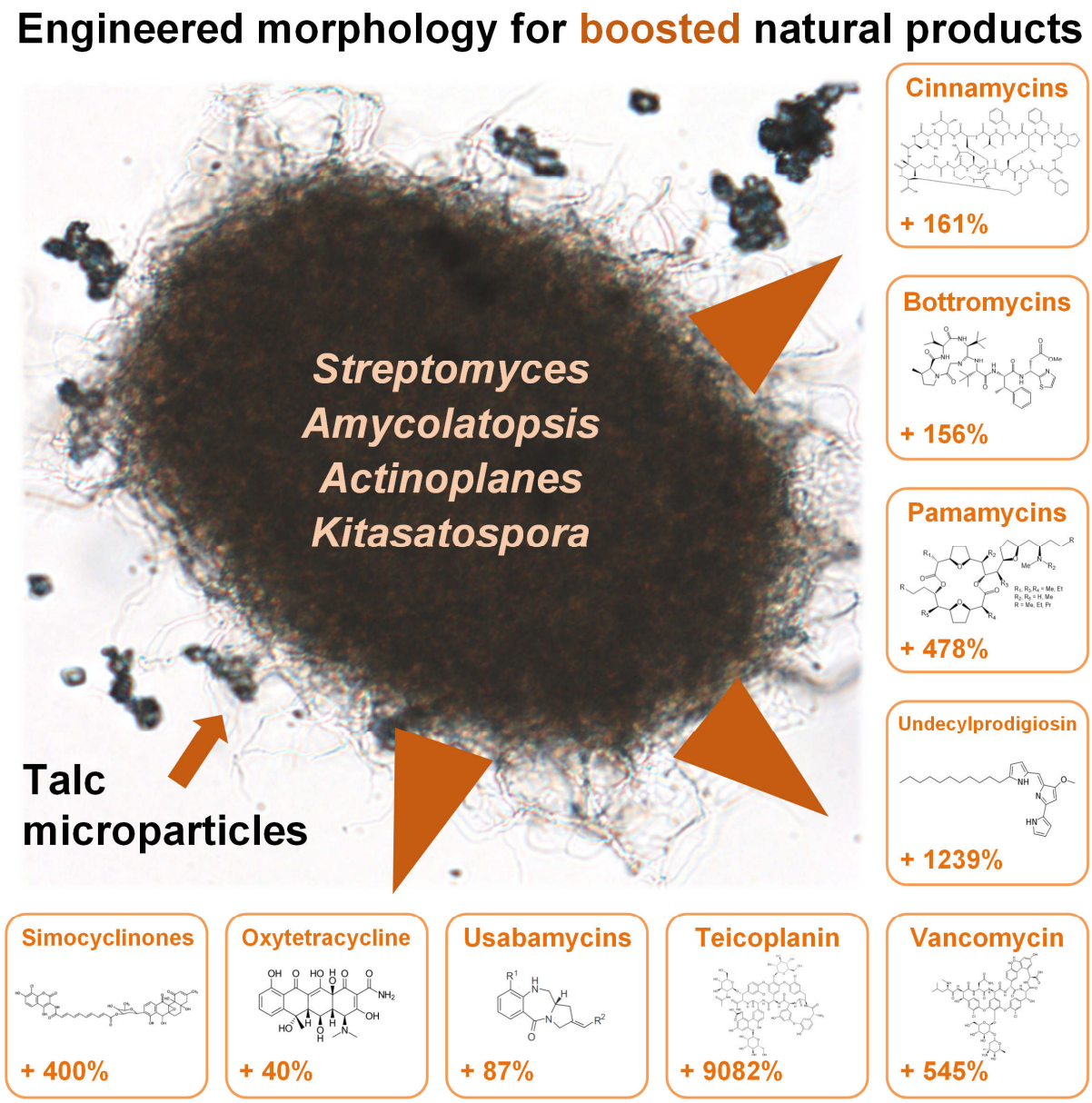

Figure 8: Overview of talc-enhanced natural product formation in actinobacteria. MPEC of actinobacteria resulted in 75% of the investigated cases in enhanced formation of the natural product. The approach did not only work for actinobacteria from different genera, i.e. *Streptomyces, Amycolatopsis, Actinoplanes* and *Kitasatospora*, but it also enhanced production performance in natural producers and heterologous hosts as well as in strains expressing the biosynthetic gene cluster of interest under native and synthetic control (Kuhl and Wittmann, 2021, graphical abstract to Kuhl et al., 2021).

As shown, by supplying talc microparticles to shake-flask cultures, we could strongly increase pamamycin production in *S. albus* J1074/R2 (50 mg L^{-1}, 300%) and bottromycin A2 (109 mg L^{-1}, 141%) as well as undecylprodigiosin (164%) production *S. lividans* TK24 DG2-Km-P41hyg+ (Kuhl et al., 2020; Kuhl et al., 2021). Moreover, the addition of microparticles to micro-scale cultures of numerous actinobacteria resulted in a strong increase of natural product formation in 75% of the investigated cases, covering polyketides,

glycopeptides, RiPPs, an alkaloid, a tetracycline, an anthramycin-analogue and an angucyclinone-analogue with highly different structures, and was even crucial for teicoplanin production in *Actinoplanes teichomyceticus* (Figure 8) (Kuhl et al., 2021). It seems therefore fair to state that the here described findings demonstrate that MPEC of actinobacteria serves as a valuable addition to the OSMAC principle (one strain many compounds), which summarizes the use of cultivation-based approaches to trigger or enhance secondary metabolite production (Romano et al., 2018). Not only did the approach work for actinobacteria from different genera, i.e. *Streptomyces, Amycolatopsis, Actinoplanes* and *Kitasatospora*, it also enhanced production in natural producers and heterologous hosts as well as in strains expressing the biosynthetic gene cluster of interest under native and synthetic control (Kuhl et al., 2021). The immense stimulation of teicoplanin production indicates that supplying talc microparticles could lead to the activation of silent clusters. As consequence, the discovery of new derivatives of previously known natural products or completely new substances seems possible. Thus, MPEC appears as a powerful tool to support natural product research in actinobacteria and could be commonly applied when newly isolated strains are cultivated for the first time, also to investigate a potential link between complex morphology and production of a certain compound. Although the approach was in the past mainly used to enhance the formation of enzymes, alcohols, polyketides, and drugs in various fungi (Walisko et al., 2012; Coban et al., 2015; Etschmann et al., 2015; Antecka et al., 2016b; Gonciarz et al., 2016; Yatmaz et al., 2016), it does not seem too surprising that it also seems beneficial for actinobacteria, as fungi and many actinobacteria possess a similar mycelial lifestyle. Finally, as demonstrated in this work, its effectiveness, its applicability in different scales, its simplicity, its low cost, and its possibility to specifically tailor the morphology of the microorganisms underlines the capabilities of MPEC of actinobacteria and is what makes this approach so interesting for future applications.

4.4 Microparticles reduce the average size of cell pellets and accelerate morphology development in submerged cultures of *S. albus* and *S. lividans*

Streptomycetes possess, unlike unicellular bacteria, a complex, multicellular life-cycle, which is strictly regulated by a morphological development program (Barka et al., 2016). In competitive soil habitants, the timing of development is crucial, as Streptomycetes degrade their own substrate mycelium under nutrient depletion in a way similar to programmed cell death

(PCD) mechanisms, which allows the cells to gather precursors for the next round of biomass formation (Méndez et al., 1985; Miguélez et al., 1999; Manteca et al., 2006; Rigali et al., 2006). During this work, we observed a strong size reduction of cell pellets in microparticle presence and gathered detailed information on how the talc microparticles modified and accelerated morphogenesis in submerged cultures of *S. albus* and *S. lividans* (Kuhl et al., 2020; Kuhl et al., 2021). It appears clear that smaller pellet diameters are favored from a bioprocess engineering point of view, as there are less problems with mass transfer rates, slow growth, and culture heterogeneity in liquid cultures (Tamura et al., 1997; Mehmood et al., 2012; van Dissel et al., 2014; van Dissel & van Wezel, 2018; Kuhl et al., 2021). In the cases presented here, talc addition resulted in a 40% size reduction of submerged *S. lividans* pellets during growth and even a more than sixfold size reduction for pellets of pamamycin producing *S. albus* (Kuhl et al., 2020; Kuhl et al., 2021). The distinct pellet characteristics, as pellets of *S. albus* possess a much more open morphology than the dense pellets of *S. lividans*, are the most likely explanation for this different impact, as open morphologies offer more attack points to the talc microparticles for fragmentation and to stop aggregation (Zacchetti et al., 2018). But also differences in cell wall composition, mechanical strength, and hydrophobicity of spores, hyphae, and mycelia could explain the different accessibility of these bacteria to talc-mediated morphology engineering and might be interesting to study further (Driouch et al., 2010a; Driouch et al., 2010c; Driouch et al., 2010b; Driouch et al., 2012; Walisko et al., 2012; Kuhl et al., 2021). Even though exceptions cannot be excluded, it can be expected that talc microparticles also reduce the average pellet size of other mycelium forming actinobacteria.

Moreover, talc did not only affect the phenotypes of producer strains on the cellular level, but also on the molecular level, as the transcriptomic data revealed strong changes in the morphogenesis program between control and microparticle supplied cultures. In *S. albus,* the regulatory program was massively upregulated in talc presence, which was observed for practically all genes as part of the morphology control cascade: activation was already visible during the initial growth phase and was even higher during production phase, including famous representatives of morphogenesis in Streptomycetes, such as *relA* (*XNRR2_1071*), *eshA* (*XNRR2_1554*), *ssgA* (*XNRR2_5315*), *facC* (*XNRR2_2306*), the hydrophobic chaplin and rodlin coat proteins of spores, and σ^{BldN} (*XNRR2_3527*), amongst many others (Kuhl et al., 2020). Although it was not possible to identify the specific link between morphology development and pamamycin production, it appears likely that the enhanced formation was a consequence of the talc-induced accelerated morphogenesis, as it is long known that

morphology and pamamycins are somehow connected (McCann & Pogell, 1979; Kuhl et al., 2020).

In contrast to *S. albus, S. lividans* does not sporulate in liquid cultures, which, besides other variations in morphology control, could explain the differences in the regulatory responses with talc supply: talc amended cultures of *S. lividans* did not show an upregulation of morphology development genes, but only demonstrated a faster morphogenesis (Daza et al., 1989; Rebets et al., 2018). Throughout the cultivation, the dynamics of the morphology program varied between control and microparticle enhanced cultures, although cultures possessed an almost identical cellular program in later stages (Kuhl et al., 2021). This accelerated program was especially highlighted by premature activation of the morphological development regulators *sigN* (*SLIV_18240*) and *bldN* (*SLIV_21180*), but also of other morphology regulators, such as *ssgA* (*SLIV_18635*), *ssgB* (*SLIV_30050*), and *wblA* (*SLIV_20395*) (Kuhl et al., 2021). All in all, the overall response to talc supply was somehow similar between *S. albus* and *S. lividans,* resulting in an accelerated morphology development and aging. Again, albeit exceptions cannot be excluded, it seems likely that other mycelium forming actinobacteria would response in a similar way.

5 Conclusions and outlook

In this work, we showed the impact and effectiveness of microparticle-enhanced cultivation of actinobacteria. First, we developed an approach for the absolute quantification of short chain CoA-thioesters in prokaryotic and eukaryotic microbes, which exhibited high precision and reproducibility for all microbes, (Gläser et al., 2020). By combining this technique with RNA sequencing, we could unravel the mechanisms that led to an enhanced and shifted pamamycin production in *S. albus* J1074/R2. We could show that talc microparticles globally reprogrammed the metabolism, forced an accelerated morphological development, and triggered expression of the pamamycin cluster and supporting pathways of pamamycin production (Kuhl et al., 2020). In a next step, we transferred MPEC to bottromycin producing *S. lividans* TK24 DG2-Km-P41hyg+, resulting in the so far highest reported titer for bottromycin A2. Moreover, we identified the aminohydrolase BotAH as key enzyme for the enhanced efficiency of the bottromycin production pathway and observed an accelerated aging of the producer (Kuhl et al., 2021). In a final step, we miniaturized the approach and investigated the formation of twelve different natural products in presence of up to 50 g L^{-1} talc, resulting in 75% of the investigated cases in an enhanced formation. For teicoplanin production, talc presence was even crucial, as it was almost non-detectable in the control culture (Kuhl et al., 2021). The fact that the approach not only worked for actinobacteria from different genera, i.e. *Streptomyces, Amycolatopsis, Actinoplanes* and *Kitasatospora*, but also in natural producers and heterologous hosts as well as for native and synthetic controlled biosynthetic clusters show its potential for future applications in natural product drug discovery.

In the past, it has remained largely unclear how microparticle supply leads to the observed effects on the molecular level (Antecka et al., 2016a). Using transcriptomics throughout various time points of the cultivation, we demonstrated that cultures in presence of talc possessed an accelerated morphogenesis and that, in this context, our findings could be valuable for future strain optimizations by suggesting targets for metabolic engineering. The correlation between morphological development and antibiotic production in *Streptomyces* is well known for a very long time (Chater, 1984). In this regard, it looks like the microparticles trigger a sweet spot towards enhanced antibiotic formation in most cases (Kuhl et al., 2021). Cultivating new strains isolates and re-screening of strain libraries could potentially lead to the discovery of new (derivatives of) secondary metabolites by activating (silent) biosynthetic gene clusters. Moreover, it appears interesting to investigate the addition of microparticles to actinobacterial strains, which are, at least for now, genetically not accessible (Atanasov et al., 2021). In this

regard, the approach is also an excellent addition to recently developed approaches for the micro-scale characterization of *Streptomyces* (Koepff et al., 2017; van Dissel & van Wezel, 2018).

Given effectiveness, applicability to different scales, simplicity, low cost, proven safety, and the possibility to specifically tailor the morphology of mycelium forming strains, it seems fair to state that morphology engineering of actinobacteria using talc microparticles has a high potential and could help in the fight against emerging multi-resistant pathogens in the future.

6 References

Abdel-Razek, A. S., Hamed, A., Frese, M., Sewald, N., & Shaaban, M. (2018). Penicisteroid C: New polyoxygenated steroid produced by co-culturing of Streptomyces piomogenus with Aspergillus niger. *Steroids, 138*, 21-25.

Ahmed, Y. (2019). Engineering of Streptomyces albus J1074 and Streptomyces lividans TK24 for natural products production.

Ahmed, Y., Rebets, Y., Estevez, M. R., Zapp, J., Myronovskyi, M., & Luzhetskyy, A. (2020). Engineering of *Streptomyces lividans* for heterologous expression of secondary metabolite gene clusters. *Microbial Cell Factories, 19*(1), 5. doi:10.1186/s12934-020-1277-8

Angert, E. R. (2005). Alternatives to binary fission in bacteria. *Nature reviews. Microbiology, 3*(3), 214-224. doi:10.1038/nrmicro1096

Anné, J., & Van Mellaert, L. (1993). Streptomyces lividans as host for heterologous protein production. *FEMS microbiology letters, 114*(2), 121-128.

Antecka, A., Bizukojc, M., & Ledakowicz, S. (2016a). Modern morphological engineering techniques for improving productivity of filamentous fungi in submerged cultures. *World journal of microbiology & biotechnology, 32*(12), 193. doi:10.1007/s11274-016-2148-7

Antecka, A., Blatkiewicz, M., Bizukojc, M., & Ledakowicz, S. (2016b). Morphology engineering of basidiomycetes for improved laccase biosynthesis. *Biotechnology Letters, 38*(4), 667-672. doi:10.1007/s10529-015-2019-6

Arcamone, F., Cassinelli, G., Fantini, G., Grein, A., Orezzi, P., Pol, C., & Spalla, C. (1969). Adriamycin, 14-hydroxydaimomycin, a new antitumor antibiotic from *S. Peucetius* var. *caesius*. *Biotechnology and Bioengineering, 11*(6), 1101-1110. doi:10.1002/bit.260110607

Arnison, P. G., Bibb, M. J., Bierbaum, G., Bowers, A. A., Bugni, T. S., Bulaj, G., Camarero, J. A., Campopiano, D. J., Challis, G. L., & Clardy, J. (2013). Ribosomally synthesized and post-translationally modified peptide natural products: overview and recommendations for a universal nomenclature. *Natural Product Reports, 30*(1), 108-160.

Atanasov, A. G., Zotchev, S. B., Dirsch, V. M., & Supuran, C. T. (2021). Natural products in drug discovery: advances and opportunities. *Nature Reviews Drug Discovery*, 1-17.

Baltz, R. H. (2007). Antimicrobials from Actinomycetas: back to the future. *Mecrobe, 2*, 125-133.

Baltz, R. H. (2010). Streptomyces and Saccharopolyspora hosts for heterologous expression of secondary metabolite gene clusters. *Journal of Industrial Microbiology and Biotechnology, 37*(8), 759-772.

Barka, E. A., Vatsa, P., Sanchez, L., Gaveau-Vaillant, N., Jacquard, C., Klenk, H.-P., Clément, C., Ouhdouch, Y., & van Wezel, G. P. (2016). Taxonomy, physiology, and natural products of Actinobacteria. *Microbiology and Molecular Biology Reviews, 80*(1), 1-43.

Bayer, v. E., Gugel, K., Hägele, K., Hagenmaier, H., Jessipow, S., König, W., & Zähner, H. (1972). Stoffwechselprodukte von Mikroorganismen. 98. Mitteilung. Phosphinothricin und Phosphinothricyl-Alanyl-Alanin. *Helvetica Chimica Acta, 55*(1), 224-239. doi:10.1002/hlca.19720550126

Becker, J., Zelder, O., Häfner, S., Schröder, H., & Wittmann, C. (2011). From zero to hero-Design-based systems metabolic engineering of Corynebacterium glutamicum for l-lysine production. *Metabolic Engineering, 13*(2), 159-168.

doi:10.1016/j.ymben.2011.01.003

Berdy, J. (2005). Bioactive microbial metabolites. *The Journal of antibiotics, 58*(1), 1-26.

Bibb, M. J. (2005). Regulation of secondary metabolism in streptomycetes. *Current Opinion in Microbiology, 8*(2), 208-215.

Bibb, M. J., Domonkos, Á., Chandra, G., & Buttner, M. J. (2012). Expression of the chaplin and rodlin hydrophobic sheath proteins in *Streptomyces venezuelae* is controlled by σ^{BldN} and a cognate anti-sigma factor, RsbN. *Molecular microbiology, 84*(6), 1033-1049. doi:10.1111/j.1365-2958.2012.08070.x

Bibb, M. J. (2013). Understanding and manipulating antibiotic production in Actinomycetes. *Biochemical Society Transactions, 41*(6), 1355-1364. doi:10.1042/BST20130214

Brown, E. D., & Wright, G. D. (2016). Antibacterial drug discovery in the resistance era. *Nature, 529*(7586), 336-343.

Butterworth, J. H., & Morgan, E. (1968). Isolation of a substance that suppresses feeding in locusts. *Chemical Communications (London)*(1), 23-24.

Campbell, W. C., Fisher, M. H., Stapley, E. O., Albers-Schönberg, G., & Jacob, T. A. (1983). Ivermectin: a potent new antiparasitic agent. *Science, 221*(4613), 823-828. doi: 10.1126/science.6308762

Cetinkaya, Y., Falk, P., & Mayhall, C. G. (2000). Vancomycin-resistant enterococci. *Clinical microbiology reviews, 13*(4), 686-707.

Challis, G. L., & Hopwood, D. A. (2003). Synergy and contingency as driving forces for the evolution of multiple secondary metabolite production by Streptomyces species. *Proceedings of the National Academy of Sciences, 100*(suppl 2), 14555-14561.

Chater, K. (1972). A morphological and genetic mapping study of white colony mutants of Streptomyces coelicolor. *Microbiology, 72*(1), 9-28.

Chater, K. F. (1984). Morphological and physiological differentiation in *Streptomyces*. *Microbial development, 16*, 89-115. doi:10.1101/0.89-115

Chater, K. F., Biró, S., Lee, K. J., Palmer, T., & Schrempf, H. (2010). The complex extracellular biology of Streptomyces. *FEMS microbiology reviews, 34*(2), 171-198.

Claessen, D., Wösten, H. A., Keulen, G. v., Faber, O. G., Alves, A. M., Meijer, W. G., & Dijkhuizen, L. (2002). Two novel homologous proteins of Streptomyces coelicolor and Streptomyces lividans are involved in the formation of the rodlet layer and mediate attachment to a hydrophobic surface. *Molecular microbiology, 44*(6), 1483-1492.

Claessen, D., Rink, R., de Jong, W., Siebring, J., de Vreugd, P., Boersma, F. H., Dijkhuizen, L., & Wösten, H. A. (2003). A novel class of secreted hydrophobic proteins is involved in aerial hyphae formation in Streptomyces coelicolor by forming amyloid-like fibrils. *Genes & development, 17*(14), 1714-1726.

Claessen, D., Stokroos, I., Deelstra, H. J., Penninga, N. A., Bormann, C., Salas, J. A., Dijkhuizen, L., & Wösten, H. A. (2004). The formation of the rodlet layer of *Streptomycetes* is the result of the interplay between rodlins and chaplins. *Molecular microbiology, 53*(2), 433-443. doi:10.1111/j.1365-2958.2004.04143.x

Coban, H. B., Demirci, A., & Turhan, I. (2015). Microparticle-enhanced Aspergillus ficuum phytase production and evaluation of fungal morphology in submerged fermentation. *Bioprocess and biosystems engineering, 38*(6), 1075-1080. doi:10.1007/s00449-014-1349-4

Cragg, G. M., & Newman, D. J. (2013). Natural products: a continuing source of novel drug leads. *Biochimica et Biophysica Acta (BBA)-General Subjects, 1830*(6), 3670-3695.

Crone, W. J., Vior, N. M., Santos-Aberturas, J., Schmitz, L. G., Leeper, F. J., & Truman, A. W. (2016). Dissecting bottromycin biosynthesis using comparative untargeted metabolomics. *Angewandte Chemie, 128*(33), 9791-9795.

Daza, A., Martin, J. F., Dominguez, A., & Gil, J. A. (1989). Sporulation of several species of *Streptomyces* in submerged cultures after nutritional downshift. *Microbiology, 135*(9), 2483-2491.

Demain, A. L. (2006). From natural products discovery to commercialization: a success story. *Journal of Industrial Microbiology and Biotechnology, 33*(7), 486-495.

Den Hengst, C. D., Tran, N. T., Bibb, M. J., Chandra, G., Leskiw, B. K., & Buttner, M. J. (2010). Genes essential for morphological development and antibiotic production in Streptomyces coelicolor are targets of BldD during vegetative growth. *Molecular microbiology, 78*(2), 361-379. doi:10.1111/j.1365-2958.2010.07338.x

Di Berardo, C., Capstick, D. S., Bibb, M. J., Findlay, K. C., Buttner, M. J., & Elliot, M. A. (2008). Function and redundancy of the chaplin cell surface proteins in aerial hypha formation, rodlet assembly, and viability in Streptomyces coelicolor. *Journal of Bacteriology, 190*(17), 5879-5889.

Driouch, H., Roth, A., Dersch, P., & Wittmann, C. (2010a). Filamentous fungi in good shape: Microparticles for tailor-made fungal morphology and enhanced enzyme production. *Bioengineered Bugs, 2*(2), 100-104. doi:10.4161/bbug.2.2.13757

Driouch, H., Sommer, B., & Wittmann, C. (2010b). Morphology engineering of *Aspergillus niger* for improved enzyme production. *Biotechnology and Bioengineering, 105*(6), 1058-1068. doi:10.1002/bit.22614

Driouch, H., Roth, A., Dersch, P., & Wittmann, C. (2010c). Optimized bioprocess for production of fructofuranosidase by recombinant *Aspergillus niger*. *Applied Microbiology and Biotechnology, 87*(6), 2011-2024. doi:10.1007/s00253-010-2661-9

Driouch, H., Hänsch, R., Wucherpfennig, T., Krull, R., & Wittmann, C. (2012). Improved enzyme production by bio-pellets of *Aspergillus niger*: targeted morphology

engineering using titanate microparticles. *Biotechnology and Bioengineering, 109*(2), 462-471. doi:10.1002/bit.23313

Edwards, C. (1993). Isolation properties and potential applications of thermophilic actinomycetes. *Applied Biochemistry and Biotechnology, 42*(2), 161-179.

Etschmann, M. M., Huth, I., Walisko, R., Schuster, J., Krull, R., Holtmann, D., Wittmann, C., & Schrader, J. (2015). Improving 2-phenylethanol and 6-pentyl-α-pyrone production with fungi by microparticle-enhanced cultivation (MPEC). *Yeast, 32*(1), 145-157. doi:10.1002/yea.3022

Feitelson, J. S., Malpartida, F., & Hopwood, D. A. (1985). Genetic and biochemical characterization of the red gene cluster of Streptomyces coelicolor A3 (2). *Microbiology, 131*(9), 2431-2441.

Feng, Z., Wang, L., Rajski, S. R., Xu, Z., Coeffet-LeGal, M. F., & Shen, B. (2009). Engineered production of iso-migrastatin in heterologous Streptomyces hosts. *Bioorganic & medicinal chemistry, 17*(6), 2147-2153.

Flärdh, K. (2003). Growth polarity and cell division in Streptomyces. *Current Opinion in Microbiology, 6*(6), 564-571.

Flärdh, K., & Buttner, M. J. (2009). Streptomyces morphogenetics: dissecting differentiation in a filamentous bacterium. *Nature Reviews Microbiology, 7*(1), 36-49.

Fleming, A. (2001). On the antibacterial action of cultures of a penicillium, with special reference to their use in the isolation of *B. influenzae*. *Bulletin of the World Health Organization, 79*, 780-790.

García-Granados, R., Lerma-Escalera, J. A., & Morones-Ramírez, J. R. (2019). Metabolic engineering and synthetic biology: synergies, future, and challenges. *Frontiers in bioengineering and biotechnology, 7*, 36.

Gläser, L., Kuhl, M., Jovanovic, S., Fritz, M., Vögeli, B., Erb, T., Becker, J., & Wittmann, C. (2020). A common approach for absolute quantification of short chain CoA thioesters in industrially relevant gram-positive and gram-negative prokaryotic and eukaryotic microbes. *Microbial Cell Factories, 19*(1), 160.

Gonciarz, J., Kowalska, A., & Bizukojc, M. (2016). Application of microparticle-enhanced cultivation to increase the access of oxygen to Aspergillus terreus ATCC 20542 mycelium and intensify lovastatin biosynthesis in batch and continuous fed-batch stirred tank bioreactors. *Biochemical engineering journal, 109*, 178-188.

Gross, H. (2009). Genomic mining--a concept for the discovery of new bioactive natural products. *Current opinion in drug discovery & development, 12*(2), 207-219.

Gullón, S., Olano, C., Abdelfattah, M. S., Braña, A. F., Rohr, J., Méndez, C., & Salas, J. A. (2006). Isolation, characterization, and heterologous expression of the biosynthesis gene cluster for the antitumor anthracycline steffimycin. *Applied and Environmental Microbiology, 72*(6), 4172-4183.

Gummerlich, N., Manderscheid, N., Rebets, Y., Myronovskyi, M., Gläser, L., Kuhl, M., Wittmann, C., & Luzhetskyy, A. (2021). Engineering the precursor pool to modulate

the production of pamamycins in the heterologous host *S. albus* J1074. *Metabolic Engineering.,67,* 11-18.

Gurusamy, K. S., Koti, R., Toon, C. D., Wilson, P., & Davidson, B. R. (2013). Antibiotic therapy for the treatment of methicillin-resistant Staphylococcus aureus (MRSA) infections in surgical wounds. *Cochrane Database of Systematic Reviews*(8).

Harvey, A. (2000). Strategies for discovering drugs from previously unexplored natural products. *Drug discovery today, 5*(7), 294-300.

Hashimoto, M., Komatsu, H., Kozone, I., Kawaide, H., Abe, H., & Natsume, M. (2005). Biosynthetic origin of the carbon skeleton and nitrogen atom of pamamycin-607, a nitrogen-containing polyketide. *Bioscience, biotechnology, and biochemistry, 69*(2), 315-320. doi:10.1271/bbb.69.315

Holtmann, D., Vernen, F., Müller, J., Kaden, D., Risse, J. M., Friehs, K., Dähne, L., Stratmann, A., & Schrader, J. (2017). Effects of particle addition to *Streptomyces* cultivations to optimize the production of actinorhodin and streptavidin. *Sustainable Chemistry and Pharmacy, 5*, 67-71. doi:10.1016/j.scp.2016.09.001

Hong, J. (2011). Role of natural product diversity in chemical biology. *Current Opinion in Chemical Biology, 15*(3), 350-354.

Hopwood, D., Chater, K., & Bibb, M. (1995). Genetics of antibiotic production in Streptomyces coelicolor A3 (2), a model streptomycete. *Genetics and biochemistry of antibiotic production*, 65-102.

Hopwood, D. A., Wildermuth, H., & Palmer, H. M. (1970). Mutants of Streptomyces coelicolor defective in sporulation. *Microbiology, 61*(3), 397-408.

Hopwood, D. A., & Wright, H. M. (1983). CDA is a new chromosomally-determined antibiotic from Streptomyces coelicolor A3 (2). *Microbiology, 129*(12), 3575-3579.

Horbal, L., Marques, F., Nadmid, S., Mendes, M. V., & Luzhetskyy, A. (2018). Secondary metabolites overproduction through transcriptional gene cluster refactoring. *Metabolic Engineering, 49*, 299-315. doi:10.1016/j.ymben.2018.09.010

Hu, P., Chase, T., & Eveleigh, D. (1993). Cloning of a Microbispora bispora cellobiohydrolase gene in Streptomyces lividans. *Applied Microbiology and Biotechnology, 38*(5), 631-637.

Hudson, G. A., & Mitchell, D. A. (2018). RiPP antibiotics: biosynthesis and engineering potential. *Current Opinion in Microbiology, 45*, 61-69.

Huo, L., Rachid, S., Stadler, M., Wenzel, S. C., & Müller, R. (2012). Synthetic biotechnology to study and engineer ribosomal bottromycin biosynthesis. *Chemistry & biology, 19*(10), 1278-1287.

Ilic, S., Konstantinovic, S., Todorovic, Z., Lazic, M., Veljkovic, V., Jokovic, N., & Radovanovic, B. (2007). Characterization and antimicrobial activity of the bioactive metabolites in streptomycete isolates. *Microbiology, 76*(4), 421-428.

Jakimowicz, D., & van Wezel, G. P. (2012). Cell division and DNA segregation in Streptomyces: how to build a septum in the middle of nowhere? *Molecular microbiology, 85*(3), 393-404.

Kallifidas, D., Jiang, G., Ding, Y., & Luesch, H. (2018). Rational engineering of *Streptomyces albus* J1074 for the overexpression of secondary metabolite gene clusters. *Microbial Cell Factories, 17*(1), 25. doi:10.1186/s12934-018-0874-2

Katz, L., & Baltz, R. H. (2016). Natural product discovery: past, present, and future. *Journal of Industrial Microbiology and Biotechnology, 43*(2-3), 155-176.

Kaup, B. A., Ehrich, K., Pescheck, M., & Schrader, J. (2008). Microparticle-enhanced cultivation of filamentous microorganisms: increased chloroperoxidase formation by *Caldariomyces fumago* as an example. *Biotechnology and Bioengineering, 99*(3), 491-498. doi:10.1002/bit.21713

Kazmaier, U. (2020). The Long, Long Way to Bottromycin. *Israel Journal of Chemistry*.

Keijser, B. J., Noens, E. E., Kraal, B., Koerten, H. K., & van Wezel, G. P. (2003). The Streptomyces coelicolor ssgB gene is required for early stages of sporulation. *FEMS microbiology letters, 225*(1), 59-67.

Kendrick, K. E., & Ensign, J. C. (1983). Sporulation of Streptomyces griseus in submerged culture. *Journal of Bacteriology, 155*(1), 357-366.

Kieser, T., & Hopwood, D. A. (1991). Genetic manipulation of Streptomyces: Integrating vectors and gene replacement. *Methods in enzymology, 204*, 430-458.

Kim, I.-S., Kang, S.-G., & Lee, K.-J. (1995). Physiological importance of trypsin-like protease during morphological differentiation of streptomycetes. *Journal of Microbiology, 33*(4), 315-321.

Kim, S.-Y., Zhao, P., Igarashi, M., Sawa, R., Tomita, T., Nishiyama, M., & Kuzuyama, T. (2009). Cloning and heterologous expression of the cyclooctatin biosynthetic gene cluster afford a diterpene cyclase and two p450 hydroxylases. *Chemistry & biology, 16*(7), 736-743.

Kobayashi, Y., Ichioka, M., Hirose, T., Nagai, K., Matsumoto, A., Matsui, H., Hanaki, H., Masuma, R., Takahashi, Y., & Ōmura, S. (2010). Bottromycin derivatives: efficient chemical modifications of the ester moiety and evaluation of anti-MRSA and anti-VRE activities. *Bioorganic & medicinal chemistry letters, 20*(20), 6116-6120.

Koepff, J., Keller, M., Tsolis, K. C., Busche, T., Rückert, C., Hamed, M. B., Anne, J., Kalinowski, J., Wiechert, W., & Economou, A. (2017). Fast and reliable strain characterization of Streptomyces lividans through micro-scale cultivation. *Biotechnology and Bioengineering, 114*(9), 2011-2022.

Kormanec, J., Ševčíková, B., Sprušanský, O., Benada, O., Kofroňová, O., Novakova, R., Řežuchová, B., Potúčková, L., & Homerova, D. (1998). TheStreptomyces aureofaciens homologue of thewhiB gene is essential for sporulation; Its expression correlates with the developmental stage. *Folia microbiologica, 43*(6), 605-612.

Kuhl, M., Gläser, L., Rebets, Y., Rückert, C., Sarkar, N., Hartsch, T., Kalinowski, J., Luzhetskyy, A., & Wittmann, C. (2020). Microparticles globally reprogram

Streptomyces albus toward accelerated morphogenesis, streamlined carbon core metabolism, and enhanced production of the antituberculosis polyketide pamamycin. *Biotechnology and Bioengineering, 117*(112), 3858-3875. doi:10.1002/bit.27537

Kuhl, M., Rückert, C., Gläser, L., Beganovic, S., Luzhetskyy, A., Kalinowski, J., & Wittmann, C. (2021). Microparticles enhance the formation of seven major classes of natural products in native and metabolically engineered actinobacteria through accelerated morphological development. *Biotechnology and Bioengineering*.

Lasch, C., Stierhof, M., Estévez, M. R., Myronovskyi, M., Zapp, J., & Luzhetskyy, A. (2020). Dudomycins: New Secondary Metabolites Produced after Heterologous Expression of an Nrps Cluster from Streptomyces albus ssp. Chlorinus Nrrl B-24108. *Microorganisms, 8*(11), 1800.

Lechevalier, H., & Lechevalier, M. (1965). Classification of aerobic actinomycetes based on their morphology and their chemical composition. *Ann. Inst. Pasteur, Paris, 108*(5), 662-673.

Lefèvre, P., Peirs, P., Braibant, M., Fauville-Dufaux, M., Vanhoof, R., Huygen, K., Wang, X.-M., Pogell, B., Wang, Y., & Fischer, P. (2004). Antimycobacterial activity of synthetic pamamycins. *Journal of antimicrobial chemotherapy, 54*(4), 824-827.

Liu, X., Tang, J., Wang, L., & Liu, R. (2019). Mechanism of CuO nano-particles on stimulating production of actinorhodin in *Streptomyces coelicolor* by transcriptional analysis. *Scientific reports, 9*(1), 1-10. doi:10.1038/s41598-019-46833-1

Lombó, F., Velasco, A., Castro, A., De la Calle, F., Braña, A. F., Sánchez-Puelles, J. M., Méndez, C., & Salas, J. A. (2006). Deciphering the biosynthesis pathway of the antitumor thiocoraline from a marine actinomycete and its expression in two Streptomyces species. *ChemBioChem, 7*(2), 366-376.

Lu, C., Zhang, X., Jiang, M., & Bai, L. (2016). Enhanced salinomycin production by adjusting the supply of polyketide extender units in Streptomyces albus. *Metabolic Engineering, 35*, 129-137.

Ma, H., & Kendall, K. (1994). Cloning and analysis of a gene cluster from Streptomyces coelicolor that causes accelerated aerial mycelium formation in Streptomyces lividans. *Journal of Bacteriology, 176*(12), 3800-3811.

Makitrynskyy, R., Rebets, Y., Ostash, B., Zaburannyi, N., Rabyk, M., Walker, S., & Fedorenko, V. (2010). Genetic factors that influence moenomycin production in streptomycetes. *Journal of Industrial Microbiology and Biotechnology, 37*(6), 559-566.

Manteca, A., Mäder, U., Connolly, B. A., & Sanchez, J. (2006). A proteomic analysis of Streptomyces coelicolor programmed cell death. *Proteomics, 6*(22), 6008-6022.

Mayfield, C., Williams, S., Ruddick, S., & Hatfield, H. (1972). Studies on the ecology of actinomycetes in soil IV. Observations on the form and growth of streptomycetes in soil. *Soil Biology and Biochemistry, 4*(1), 79-91.

McCann, P. A., & Pogell, B. M. (1979). Pamamycin: a new antibiotic and stimulator of aerial mycelia formation. *The Journal of antibiotics, 32*(7), 673-678.

Medema, M. H., Breitling, R., Bovenberg, R., & Takano, E. (2011). Exploiting plug-and-play synthetic biology for drug discovery and production in microorganisms. *Nature Reviews Microbiology, 9*(2), 131-137.

Mehmood, N., Olmos, E., Goergen, J.-L., Blanchard, F., Marchal, P., Klöckner, W., Büchs, J., & Delaunay, S. (2012). Decoupling of oxygen transfer and power dissipation for the study of the production of pristinamycins by *Streptomyces pristinaespiralis* in shaking flasks. *Biochemical engineering journal, 68*, 25-33.

Mendez, C., & Chater, K. F. (1987). Cloning of whiG, a gene critical for sporulation of Streptomyces coelicolor A3 (2). *Journal of Bacteriology, 169*(12), 5715-5720.

Méndez, C., Brana, A. F., Manzanal, M. B., & Hardisson, C. (1985). Role of substrate mycelium in colony development in Streptomyces. *Canadian Journal of Microbiology, 31*(5), 446-450.

Merrick, M. (1976). A morphological and genetic mapping study of bald colony mutants of Streptomyces coelicolor. *Microbiology, 96*(2), 299-315.

Metz, P. (2005). Synthetic studies on the pamamycin macrodiolides. In *Natural Products Synthesis II* (pp. 215-249): Springer.

Miguélez, E. M., Hardisson, C., & Manzanal, M. B. (1999). Hyphal death during colony development in Streptomyces antibioticus: morphological evidence for the existence of a process of cell deletion in a multicellular prokaryote. *The Journal of cell biology, 145*(3), 515-525.

Moussa, M., Ebrahim, W., Bonus, M., Gohlke, H., Mándi, A., Kurtán, T., Hartmann, R., Kalscheuer, R., Lin, W., & Liu, Z. (2019). Co-culture of the fungus Fusarium tricinctum with Streptomyces lividans induces production of cryptic naphthoquinone dimers. *Rsc Advances, 9*(3), 1491-1500.

Myronovskyi, M., Rosenkranzer, B., Nadmid, S., Pujic, P., Normand, P., & Luzhetskyy, A. (2018). Generation of a cluster-free *Streptomyces albus* chassis strains for improved heterologous expression of secondary metabolite clusters. *Metabolic Engineering, 49*, 316-324. doi:10.1016/j.ymben.2018.09.004

Nair, S., & Abraham, J. (2020). Natural Products from Actinobacteria for Drug Discovery. In *Advances in Pharmaceutical Biotechnology* (pp. 333-363): Springer.

Natsume, M. (2016). Studies on bioactive natural products involved in the growth and morphological differentiation of microorganisms. *Journal of Pesticide Science, 41*(3), 96-101. doi:10.1584/jpestics.J16-03

Noens, E. E., Mersinias, V., Traag, B. A., Smith, C. P., Koerten, H. K., & van Wezel, G. P. (2005). SsgA-like proteins determine the fate of peptidoglycan during sporulation of Streptomyces coelicolor. *Molecular microbiology, 58*(4), 929-944.

Olano, C., Lombó, F., Méndez, C., & Salas, J. A. (2008). Improving production of bioactive secondary metabolites in actinomycetes by metabolic engineering. *Metabolic Engineering, 10*(5), 281-292.

Otaka, T., & Kaji, A. (1976). Mode of action of bottromycin A2. Release of aminoacyl-or peptidyl-tRNA from ribosomes. *Journal of Biological Chemistry, 251*(8), 2299-2306.

Otaka, T., & Kaji, A. (1981). Mode of action of bottromycin A2: effect on peptide bond formation. *FEBS letters, 123*(2), 173-176.

Patridge, E. V., Gareiss, P. C., Kinch, M. S., & Hoyer, D. W. (2015). An analysis of original research contributions toward FDA-approved drugs. *Drug discovery today, 20*(10), 1182-1187.

Paul, G. C., & Thomas, C. R. (1998). Characterisation of mycelial morphology using image analysis. *Relation Between Morphology and Process Performances*, 1-59.

Peng, Q., Gao, G., Lü, J., Long, Q., Chen, X., Zhang, F., Xu, M., Liu, K., Wang, Y., & Deng, Z. (2018). Engineered Streptomyces lividans strains for optimal identification and expression of cryptic biosynthetic gene clusters. *Frontiers in Microbiology, 9*, 3042.

Persson, J., Chater, K. F., & Flärdh, K. (2013). Molecular and cytological analysis of the expression of Streptomyces sporulation regulatory gene whiH. *FEMS microbiology letters, 341*(2), 96-105.

Pethick, F., MacFadyen, A., Tang, Z., Sangal, V., Liu, T.-T., Chu, J., Kosec, G., Petkovic, H., Guo, M., & Kirby, R. (2013). Draft genome sequence of the oxytetracycline-producing bacterium Streptomyces Rimosus ATCC 10970. *Genome announcements, 1*(2), e0006313.

Plackett, B. (2020). Why big pharma has abandoned antibiotics. *Nature, 586*(7830), S50-S52.

Pouwels, K. B., Dolk, F. C. K., Smith, D. R., Robotham, J. V., & Smieszek, T. (2018). Actual versus 'ideal'antibiotic prescribing for common conditions in English primary care. *Journal of antimicrobial chemotherapy, 73*(suppl_2), 19-26.

Procópio, R. E. d. L., Silva, I. R. d., Martins, M. K., Azevedo, J. L. d., & Araújo, J. M. d. (2012). Antibiotics produced by Streptomyces. *Brazilian Journal of Infectious Diseases, 16*(5), 466-471.

Rebets, Y., Brotz, E., Manderscheid, N., Tokovenko, B., Myronovskyi, M., Metz, P., Petzke, L., & Luzhetskyy, A. (2015). Insights into the pamamycin biosynthesis. *Angewandte Chemie, 54*(7), 2280-2284. doi:10.1002/anie.201408901

Rebets, Y., Tsolis, K. C., Guðmundsdóttir, E. E., Koepff, J., Wawiernia, B., Busche, T., Bleidt, A., Horbal, L., Myronovskyi, M., & Ahmed, Y. (2018). Characterization of sigma factor genes in *Streptomyces lividans* TK24 using a genomic library-based approach for multiple gene deletions. *Frontiers in Microbiology, 9*, 3033.

Ren, H., Wang, B., & Zhao, H. (2017). Breaking the silence: new strategies for discovering novel natural products. *Current Opinion in Biotechnology, 48*, 21-27.

Ren, X.-D., Xu, Y.-J., Zeng, X., Chen, X.-S., Tang, L., & Mao, Z.-G. (2015). Microparticle-enhanced production of ε-poly-L-lysine in fed-batch fermentation. *Rsc Advances, 5*(100), 82138-82143. doi:10.1039/C5RA14319E

Ridley, C., & Khosla, C. (2009). Polyketides.

Ridley, C. P., Lee, H. Y., & Khosla, C. (2008). Evolution of polyketide synthases in bacteria. *Proceedings of the National Academy of Sciences, 105*(12), 4595-4600.

Rigali, S., Nothaft, H., Noens, E. E., Schlicht, M., Colson, S., Muller, M., Joris, B., Koerten, H. K., Hopwood, D. A., Titgemeyer, F., & van Wezel, G. P. (2006). The sugar phosphotransferase system of Streptomyces coelicolor is regulated by the GntR-family regulator DasR and links N-acetylglucosamine metabolism to the control of development. *Molecular microbiology, 61*(5), 1237-1251. doi:10.1111/j.1365-2958.2006.05319.x

Rodríguez Estévez, M., Myronovskyi, M., Rosenkränzer, B., Paululat, T., Petzke, L., Ristau, J., & Luzhetskyy, A. (2020). Novel fredericamycin variant overproduced by a streptomycin-resistant Streptomyces albus subsp. chlorinus Strain. *Marine drugs, 18*(6), 284.

Romano, S., Jackson, S. A., Patry, S., & Dobson, A. D. (2018). Extending the "one strain many compounds"(OSMAC) principle to marine microorganisms. *Marine drugs, 16*(7), 244.

Roope, L. S., Smith, R. D., Pouwels, K. B., Buchanan, J., Abel, L., Eibich, P., Butler, C. C., San Tan, P., Walker, A. S., & Robotham, J. V. (2019). The challenge of antimicrobial resistance: what economics can contribute. *Science, 364*(6435).

Rückert, C., Albersmeier, A., Busche, T., Jaenicke, S., Winkler, A., Friðjónsson, Ó. H., Hreggviðsson, G. Ó., Lambert, C., Badcock, D., & Bernaerts, K. (2015). Complete genome sequence of Streptomyces lividans TK24. *Journal of Biotechnology, 199*, 21-22.

Rudd, B. A., & Hopwood, D. A. (1979). Genetics of actinorhodin biosynthesis by Streptomyces coelicolor A3 (2). *Microbiology, 114*(1), 35-43.

Schatz, A., & Waksman, S. A. (1944). Effect of Streptomycin and Other Antibiotic Substances upon Mycobacterium tuberculosis and Related Organisms. *Proceedings of the society for Experimental Biology and Medicine, 57*(2), 244-248.

Shuai, H., Myronovskyi, M., Nadmid, S., & Luzhetskyy, A. (2020). Identification of a Biosynthetic Gene Cluster Responsible for the Production of a New Pyrrolopyrimidine Natural Product—Huimycin. *Biomolecules, 10*(7), 1074.

Sinden, R. R. (1994). *DNA structure and function*: Gulf Professional Publishing.

Takeuchi, S., Hirayama, K., Ueda, K., Sakai, H., & Yonehara, H. (1958). Blasticidin S, a new antibiotic. *The Journal of Antibiotics, Series A, 11*(1), 1-5.

Tamura, S., Park, Y., Toriyama, M., & Okabe, M. (1997). Change of mycelial morphology in tylosin production by batch culture of *Streptomyces fradiae* under various shear conditions. *Journal of Fermentation and Bioengineering, 83*(6), 523-528.

Tenconi, E., Traxler, M. F., Hoebreck, C., Van Wezel, G. P., & Rigali, S. (2018). Production of prodiginines is part of a programmed cell death process in *Streptomyces coelicolor*. *Frontiers in Microbiology, 9*, 1742.

Traag, B. A., & van Wezel, G. P. (2008). The SsgA-like proteins in Actinomycetes: small proteins up to a big task. *Antonie Van Leeuwenhoek, 94*(1), 85-97. doi:10.1007/s10482-008-9225-3

Tyo, K. E., Kocharin, K., & Nielsen, J. (2010). Toward design-based engineering of industrial microbes. *Current Opinion in Microbiology, 13*(3), 255-262.

Van Boeckel, T. P., Glennon, E. E., Chen, D., Gilbert, M., Robinson, T. P., Grenfell, B. T., Levin, S. A., Bonhoeffer, S., & Laxminarayan, R. (2017). Reducing antimicrobial use in food animals. *Science, 357*(6358), 1350-1352.

van Dissel, D., Claessen, D., & van Wezel, G. P. (2014). Morphogenesis of *Streptomyces* in submerged cultures. In *Advances in applied microbiology* (Vol. 89, pp. 1-45): Elsevier.

van Dissel, D., & van Wezel, G. P. (2018). Morphology-driven downscaling of *Streptomyces lividans* to micro-cultivation. *Antonie Van Leeuwenhoek, 111*(3), 457-469. doi:10.1007/s10482-017-0967-7

van Wezel, G. P., van der Meulen, J., Kawamoto, S., Luiten, R. G., Koerten, H. K., & Kraal, B. (2000). ssgA Is Essential for Sporulation ofStreptomyces coelicolor A3 (2) and Affects Hyphal Development by Stimulating Septum Formation. *Journal of Bacteriology, 182*(20), 5653-5662.

Van Wezel, G. P., Krabben, P., Traag, B. A., Keijser, B. J., Kerste, R., Vijgenboom, E., Heijnen, J. J., & Kraal, B. (2006). Unlocking *Streptomyces spp*. for use as sustainable industrial production platforms by morphological engineering. *Applied and Environmental Microbiology, 72*(8), 5283-5288. doi:10.1128/AEM.00808-06

van Wezel, G. P., & McDowall, K. J. (2011). The regulation of the secondary metabolism of *Streptomyces*: new links and experimental advances. *Natural Product Reports, 28*(7), 1311-1333. doi:10.1039/c1np00003a

Vézina, C., Kudelski, A., & Sehgal, S. (1975). Rapamycin (AY-22, 989), a new antifungal antibiotic. I. Taxonomy of the producing Streptomycete and isolation of the active principle. *The Journal of antibiotics, 28*(10), 721-726. doi:10.7164/antibiotics.28.721

Vior, N. M., Cea-Torrescassana, E., Eyles, T. H., Chandra, G., & Truman, A. W. (2020). Regulation of bottromycin biosynthesis involves an internal transcriptional start site and a cluster-situated modulator. *Frontiers in Microbiology, 11*, 495.

Waisvisz, J., Van Der Hoeven, M., Van Peppen, J., & Zwennis, W. (1957). Bottromycin. I. A new sulfur-containing antibiotic. *Journal of the American Chemical Society, 79*(16), 4520-4521.

Waksman, S. A., & Woodruff, H. B. (1940). Bacteriostatic and bactericidal substances produced by a soil Actinomyces. *Proceedings of the society for Experimental Biology and Medicine, 45*(2), 609-614.

Waksman, S. A., & Woodruff, H. B. (1942). Selective antibiotic action of various substances of microbial origin. *Journal of Bacteriology, 44*(3), 373.

Walisko, J., Vernen, F., Pommerehne, K., Richter, G., Terfehr, J., Kaden, D., Dähne, L., Holtmann, D., & Krull, R. (2017). Particle-based production of antibiotic rebeccamycin with *Lechevalieria aerocolonigenes*. *Process Biochemistry, 53*, 1-9. doi:10.1016/j.procbio.2016.11.017

Walisko, R., Krull, R., Schrader, J., & Wittmann, C. (2012). Microparticle based morphology engineering of filamentous microorganisms for industrial bio-production. *Biotechnology Letters, 34*(11), 1975-1982. doi:10.1007/s10529-012-0997-1

Wang, G.-Y.-S., Graziani, E., Waters, B., Pan, W., Li, X., McDermott, J., Meurer, G., Saxena, G., Andersen, R. J., & Davies, J. (2000). Novel natural products from soil DNA libraries in a streptomycete host. *Organic letters, 2*(16), 2401-2404.

Weissman, K. J. (2016). Genetic engineering of modular PKSs: from combinatorial biosynthesis to synthetic biology. *Natural Product Reports, 33*(2), 203-230. doi:10.1039/C5NP00109A

Wendt-Pienkowski, E., Huang, Y., Zhang, J., Li, B., Jiang, H., Kwon, H., Hutchinson, C. R., & Shen, B. (2005). Cloning, Sequencing, Analysis, and Heterologous Expression of the Fredericamycin Biosynthetic Gene Cluster from Streptomyces g riseus. *Journal of the American Chemical Society, 127*(47), 16442-16452.

WHO. (2020). Antimicrobial resistance. *Antimicrobial resistance Fact sheet N°194"*.

Wildermuth, H., Wehrli, E., & Horne, R. W. (1971). The surface structure of spores and aerial mycelium in Streptomyces coelicolor. *Journal of ultrastructure research, 35*(1-2), 168-180.

Willemse, J., Borst, J. W., de Waal, E., Bisseling, T., & van Wezel, G. P. (2011). Positive control of cell division: FtsZ is recruited by SsgB during sporulation of Streptomyces. *Genes & development, 25*(1), 89-99. doi:10.1101/gad.600211

Williams, S., & Vickers, J. (1988). Detection of actinomycetes in the natural environment: problems and perspectives. *Biology of actinomycetes, 88*, 265-270.

Winn, M., Fyans, J., Zhuo, Y., & Micklefield, J. (2016). Recent advances in engineering nonribosomal peptide assembly lines. *Natural Product Reports, 33*(2), 317-347.

Winter, J. M., Moffitt, M. C., Zazopoulos, E., McAlpine, J. B., Dorrestein, P. C., & Moore, B. S. (2007). Molecular basis for chloronium-mediated meroterpene cyclization: cloning, sequencing, and heterologous expression of the napyradiomycin biosynthetic gene cluster. *Journal of Biological Chemistry, 282*(22), 16362-16368.

Wittmann, C., & Lee, S. Y. (2012). *Systems metabolic engineering*: Springer Science & Business Media.

Wu, Q., Zhang, G., Wang, B., Li, X., Yue, S., Chen, J., Zhang, H., & Wang, H. (2018). Production and identification of Inthomycin B produced by a Deep-Sea sediment-derived Streptomyces sp. YB104 based on cultivation-dependent approach. *Current Microbiology, 75*(7), 942-951.

Yatmaz, E., Karahalil, E., Germec, M., Ilgin, M., & Turhan, I. (2016). Controlling filamentous fungi morphology with microparticles to enhanced beta-mannanase production. *Bioprocess and biosystems engineering, 39*(9), 1391-1399. doi:10.1007/s00449-016-1615-8

Zaburannyi, N., Rabyk, M., Ostash, B., Fedorenko, V., & Luzhetskyy, A. (2014). Insights into naturally minimised Streptomyces albus J1074 genome. *BMC genomics, 15*(1), 97.

Zacchetti, B., Smits, P., & Claessen, D. (2018). Dynamics of Pellet Fragmentation and Aggregation in Liquid-Grown Cultures of *Streptomyces lividans*. *Frontiers in Microbiology, 9*, 943. doi:10.3389/fmicb.2018.00943

Zerikly, M., & Challis, G. L. (2009). Strategies for the discovery of new natural products by genome mining. *ChemBioChem, 10*(4), 625-633.

Zhou, Z., Gu, J., Du, Y.-L., Li, Y.-Q., & Wang, Y. (2011). The-omics era-toward a systems-level understanding of Streptomyces. *Current genomics, 12*(6), 404-416.

Zimmermann, W. (1990). Degradation of lignin by bacteria. *Journal of Biotechnology, 13*(2-3), 119-130.

7 Supporting Information

7.1 Supplementary information: Microparticles globally reprogram *Streptomyces albus* toward accelerated morphogenesis, streamlined carbon core metabolism, and enhanced production of the antituberculosis polyketide pamamycin

Martin Kuhl, Lars Gläser, Yuriy Rebets, Christian Rückert, Namrata Sarkar, Thomas Hartsch, Jörn Kalinowski, Andriy Luzhetskyy, and Christoph Wittmann

Biotechnology and Bioengineering. 2020; 117: 3858-3875.

Supplementary information to

Microparticles globally reprogram *Streptomyces albus* towards accelerated morphogenesis, streamlined carbon core metabolism and enhanced production of the antituberculosis polyketide pamamycin

Biotechnology and Bioengineering

Martin Kuhl[1], Lars Gläser[1], Yuriy Rebets[2], Christian Rückert[3], Namrata Sarkar[4] , Thomas Hartsch[4], Jörn Kalinowski[3], Andriy Luzhetskyy[2], and Christoph Wittmann[1*]

[1] Institute of Systems Biotechnology, Saarland University, Saarbrücken, Germany

[2] Pharmaceutical Biotechnology, Saarland University, Saarbrücken, Germany

[3] Center for Biotechnology, Bielefeld University, Bielefeld, Germany

[4] Genedata AG, Basel, Switzerland

* Phone: 0049-681-302-71971, FAX: -71972, Email: christoph.wittmann@uni-saarland.de

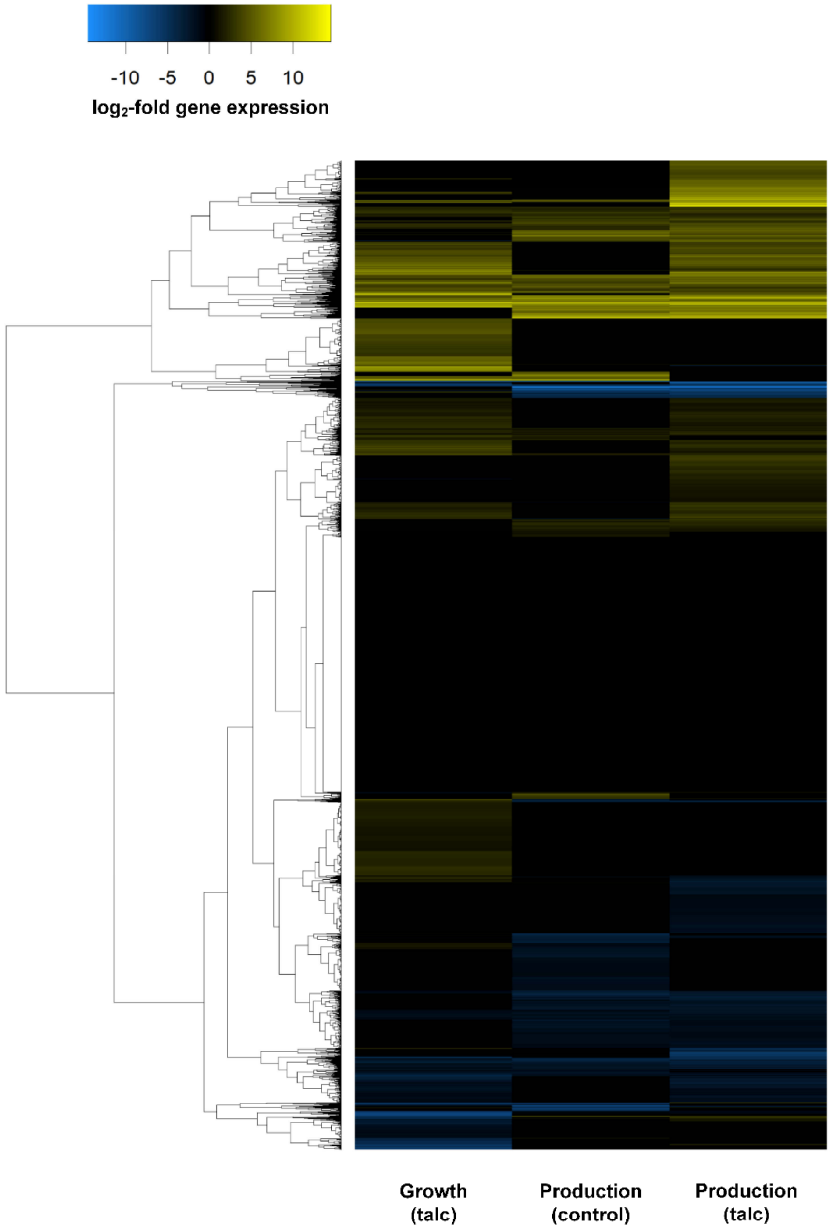

Figure S1: Hierarchical cluster analysis of global gene expression of *S. albus* J1074/R2 in liquid SGG medium. Samples were taken from a control and a talc supplied culture (10 g L^{-1}) during exponential growth and production phase. The sample out of the control culture during growth was set as reference.

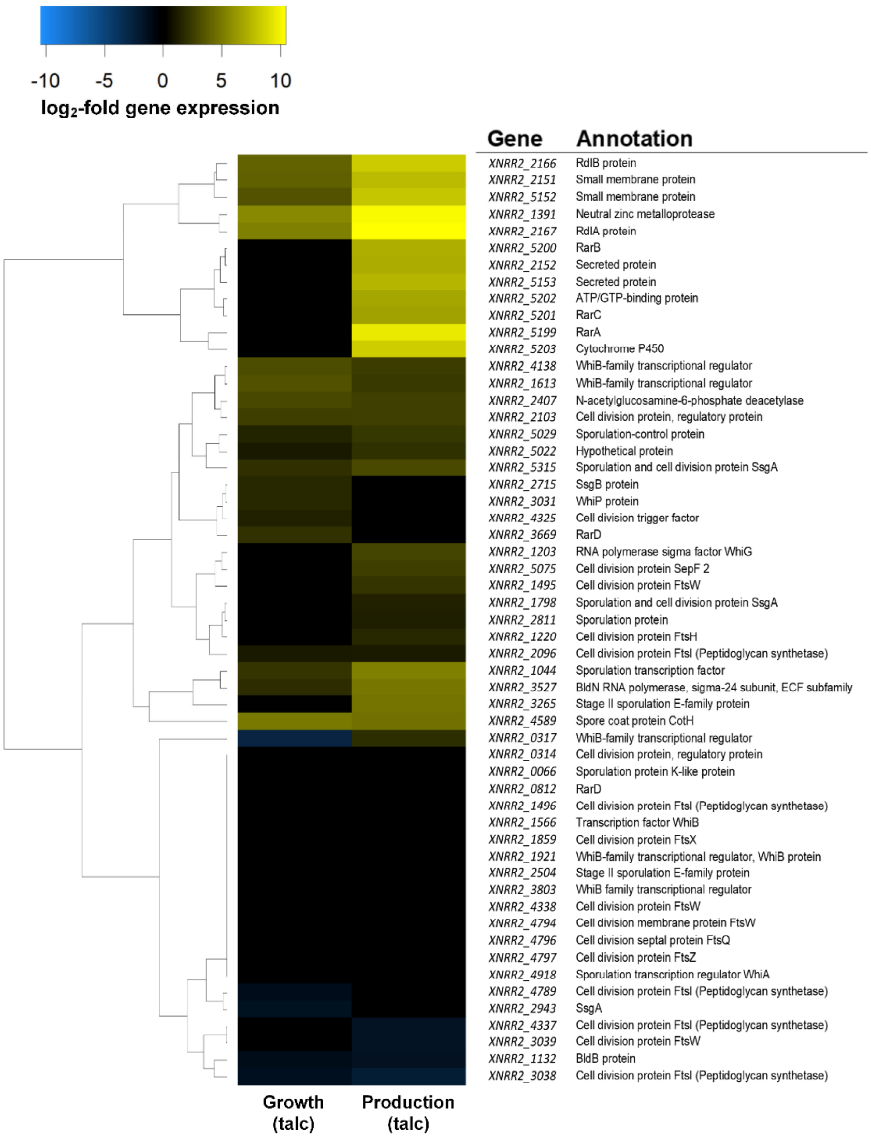

Figure S2: Hierarchical cluster analysis of gene expression for genes linked to the control of morphology and secondary metabolism in pamamycin producing *Streptomyces albus* J1074/R2. Samples were taken from a control and a talc supplied culture (10 g L^{-1}) in SGG medium during exponential growth (5 h) and production phase (21 h). For comparison, the expression levels of the control culture during growth were set as reference. Shown are the relative changes of the talc supplied culture during growth and production.

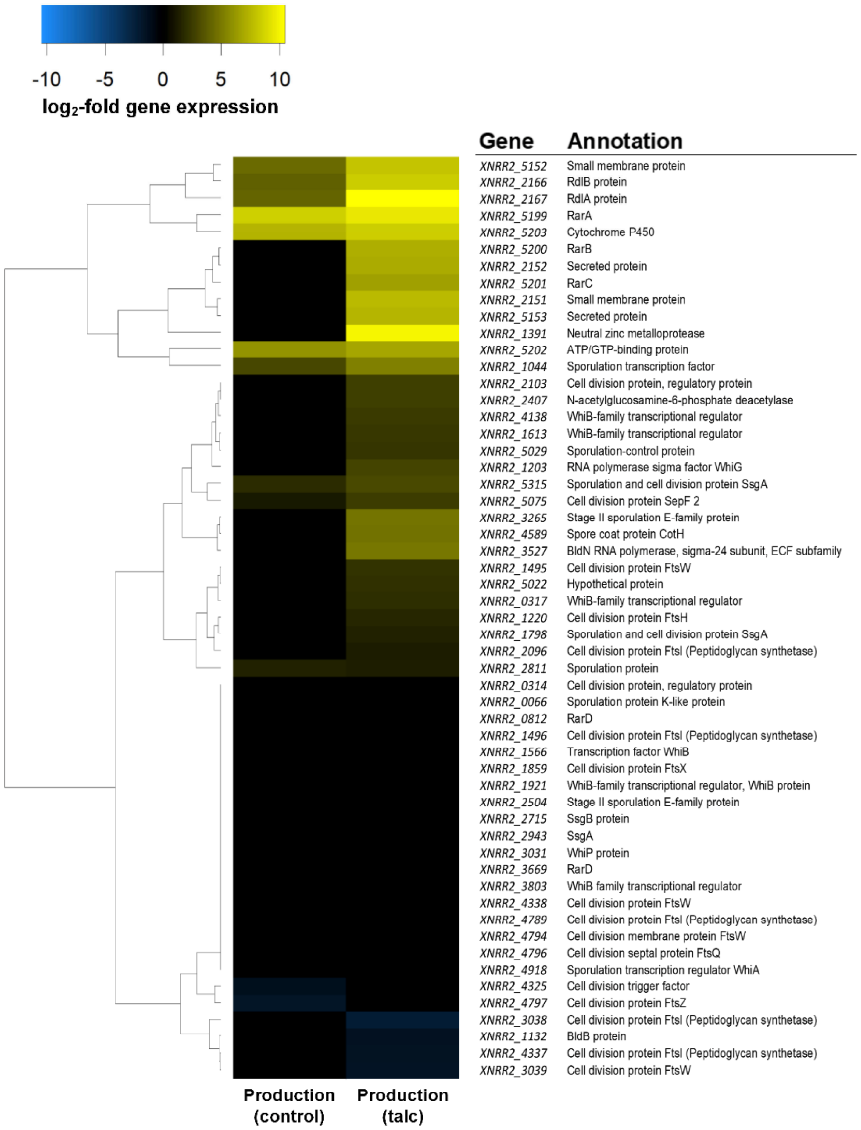

Figure S3: Hierarchical cluster analysis of gene expression for genes linked to the control of morphology and secondary metabolism in pamamycin producing *Streptomyces albus* J1074/R2. Samples were taken from a control and a talc supplied culture (10 g L^{-1}) in SGG medium during exponential growth (5 h) and production phase (21 h). For comparison, the expression levels of the control culture during growth were set as reference. Shown are the relative changes of the control culture and the talc supplied culture during production.

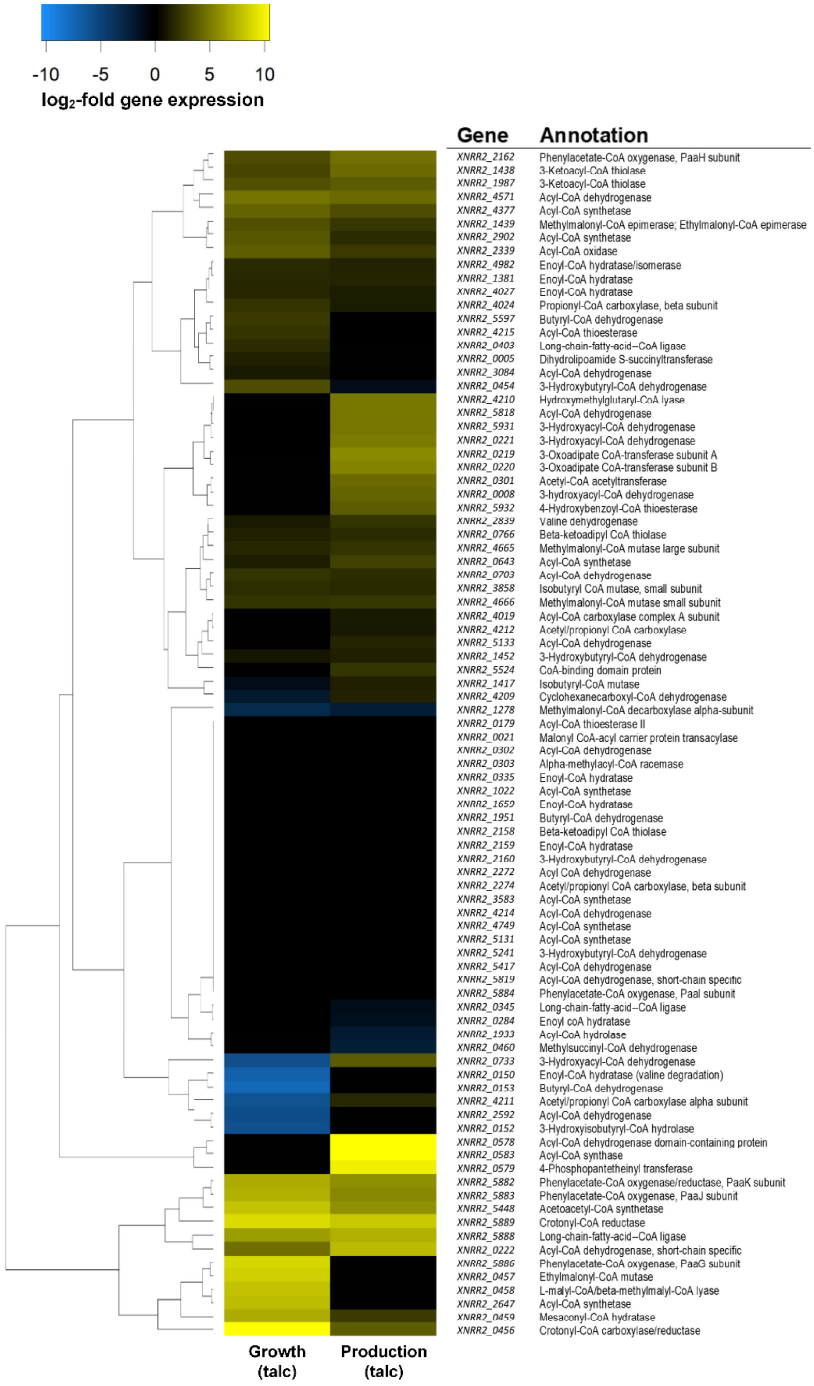

Figure S4: Hierarchical cluster analysis of gene expression for genes linked to CoA-ester metabolism in pamamycin producing *Streptomyces albus* J1074/R2. Samples were taken from a control and a talc supplied culture (10 g L^{-1}) in SGG medium during exponential growth (5 h)

and production phase (21 h). For comparison, the expression levels of the control culture during growth were set as reference. Shown are the relative changes of the talc supplied culture during growth and production.

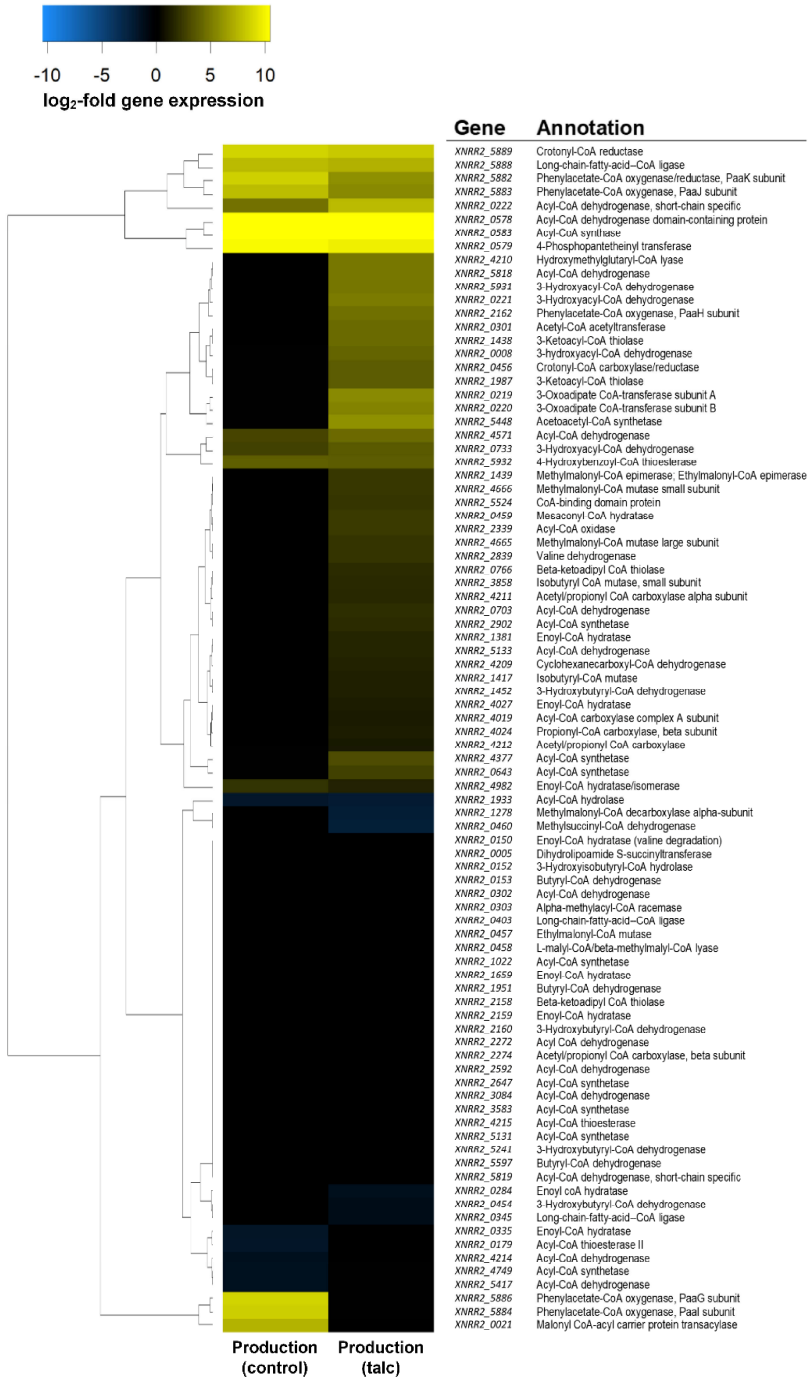

Figure S5: Hierarchical cluster analysis of gene expression for genes linked to CoA-ester metabolism in pamamycin producing *Streptomyces albus* J1074/R2. Samples were taken from a control and a talc supplied culture (10 g L^{-1}) in SGG medium during exponential growth (5 h)

and production phase (21 h). For comparison, the expression levels of the control culture during growth were set as reference. Shown are the relative changes of the control culture and the talc supplied culture during production.

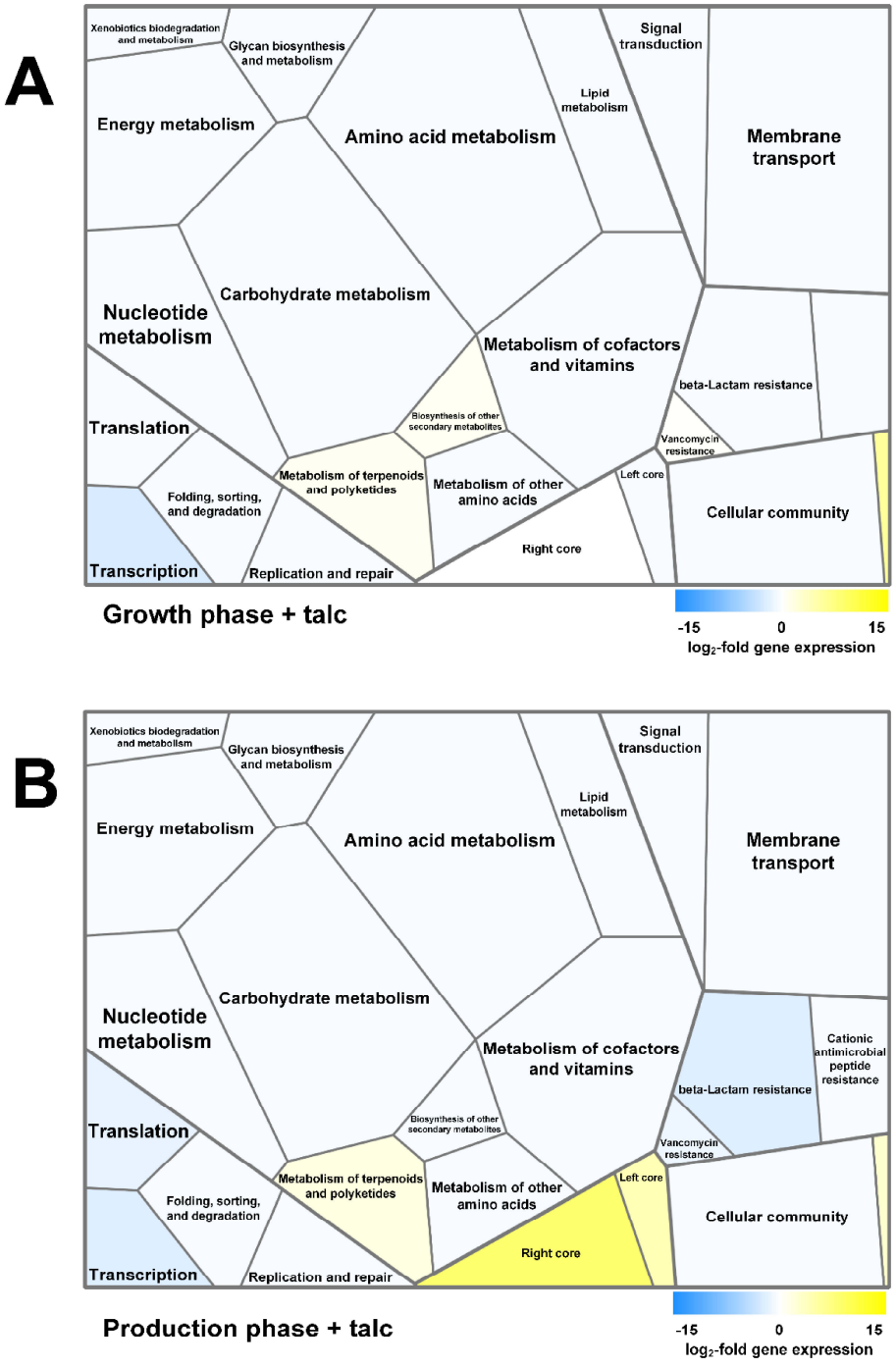

Figure S6: KEGG-orthology tree maps of talc supplied *Streptomyces albus* J1074/R2. Average gene expressions of growing (A) and producing (B) *S. albus* J1074/R2 in complex SGG medium

with addition of 10 g L^{-1} talc compared to a control culture in growth phase. Each cell represents a functional class of the orthology: Carbohydrate metabolism, amino acid metabolism, lipid metabolism, nucleotide metabolism, energy metabolism, glycan biosynthesis and metabolism, xenobiotics biodegradation and metabolism, metabolism of cofactors and vitamins, metabolism of terpenoids and polyketides, biosynthesis of other secondary metabolites, metabolism of other amino acids, signal transduction, membrane transport, replication and repair, transcription, translation, folding, sorting and degradation, cellular community, cell motility, and the right and left core of the pamamycin gene cluster.

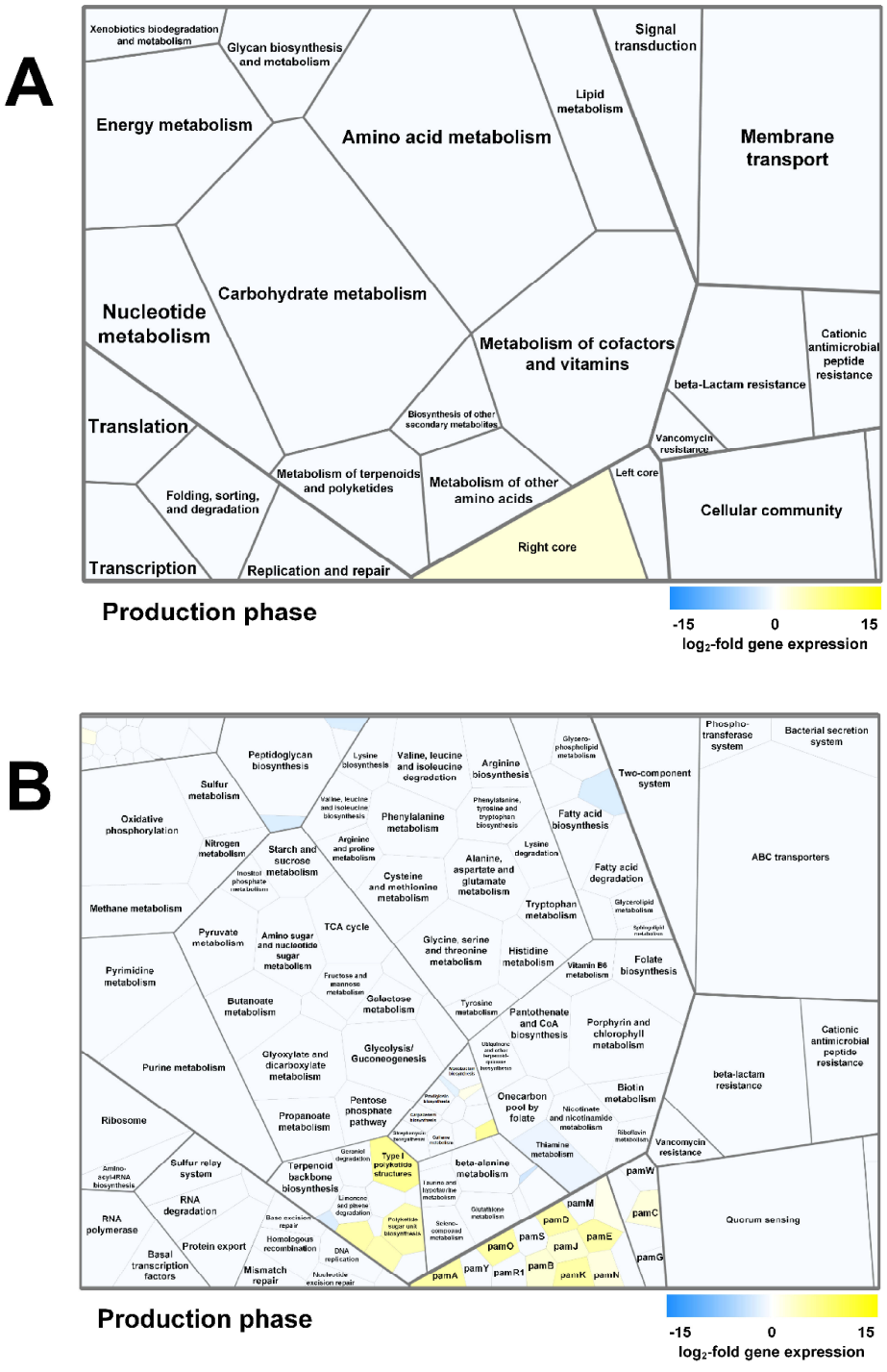

Figure S7: KEGG-orthology tree maps of *S. albus* J1074/R2 during production phase. Average gene expressions of *S. albus* J1074/R2 in complex SGG medium without talc addition

during production compared to growth phase of the control. **A:** Each cell represents a functional class of the orthology: Carbohydrate metabolism, amino acid metabolism, lipid metabolism, nucleotide metabolism, energy metabolism, glycan biosynthesis and metabolism, xenobiotics biodegradation and metabolism, metabolism of cofactors and vitamins, metabolism of terpenoids and polyketides, biosynthesis of other secondary metabolites, metabolism of other amino acids, signal transduction, membrane transport, replication and repair, transcription, translation, folding, sorting and degradation, cellular community, cell motility, and the right and left core of the pamamycin gene cluster. Additionally, the subclasses of these classes are included in B.

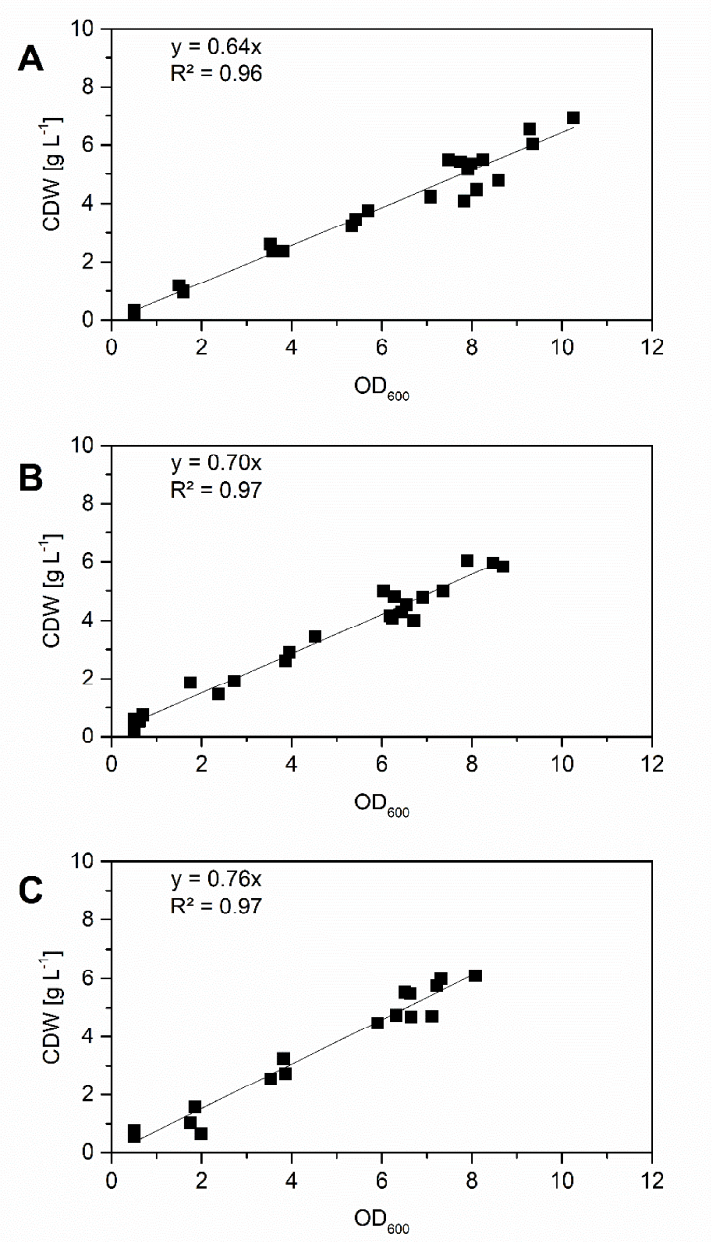

Figure S8: Correlation of cell dry weight (CDW) to optical density (OD_{600}) for different cultivation conditions. *Streptomyces albus* J1074/R2 was cultivated without talc supply (A) and in presence of 2.5 (B) and 10 g L^{-1} talc (C) over 24 hours. At different time points, optical density and cell dry weight of each culture were determined simultaneously.

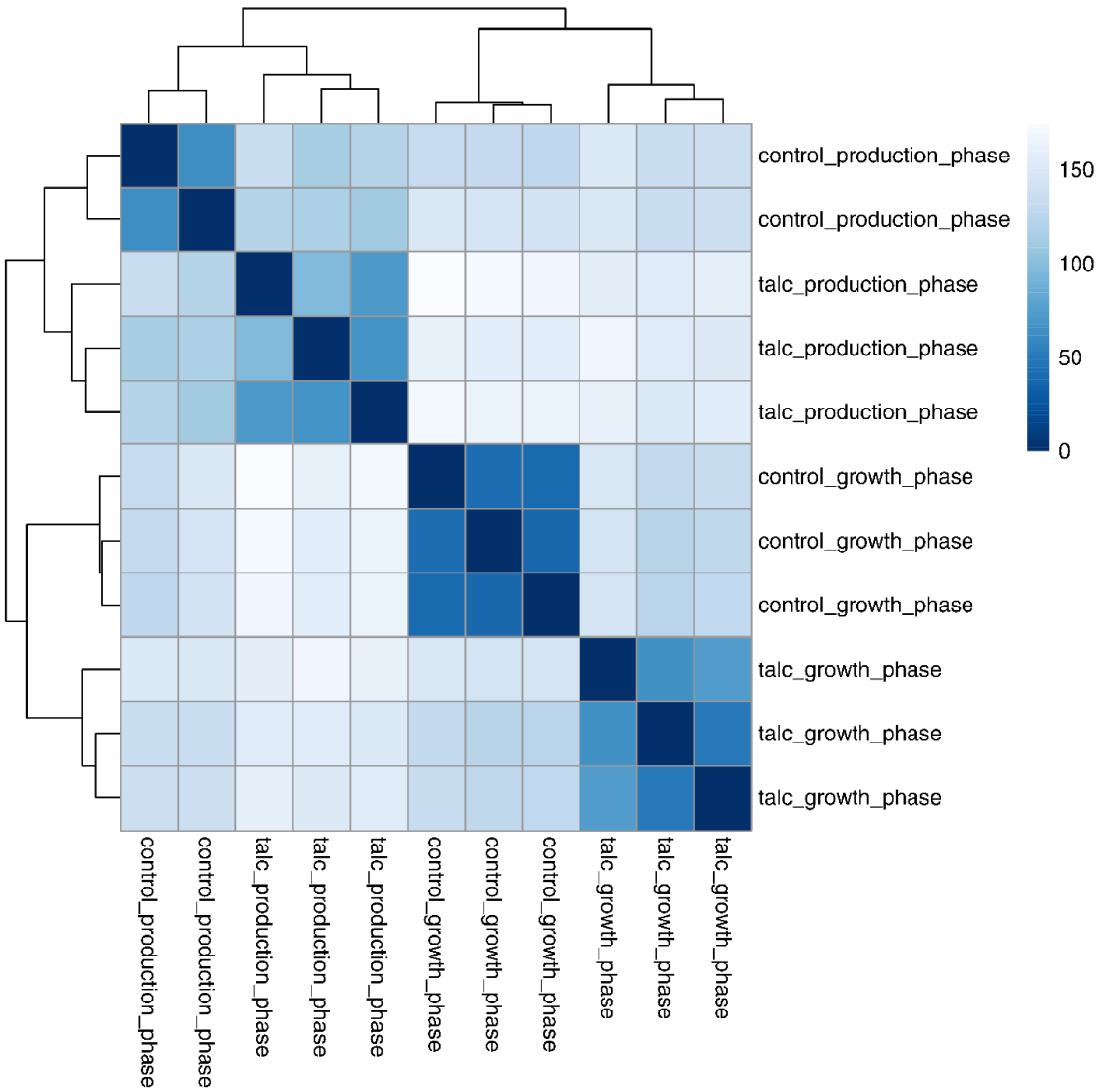

Figure S9: Heatmap of the sample-to-sample distances from the RNA seq data. The background corrected read count data were fed to DESeq2 (Love et al., 2014) to calculate normalized read counts. After regularized log transformation with blind dispersion estimation enabled, the sample to sample distances were calculated and used for hierarchical clustering, which in turn was visualized using pheatmap (Kolde, 2019).

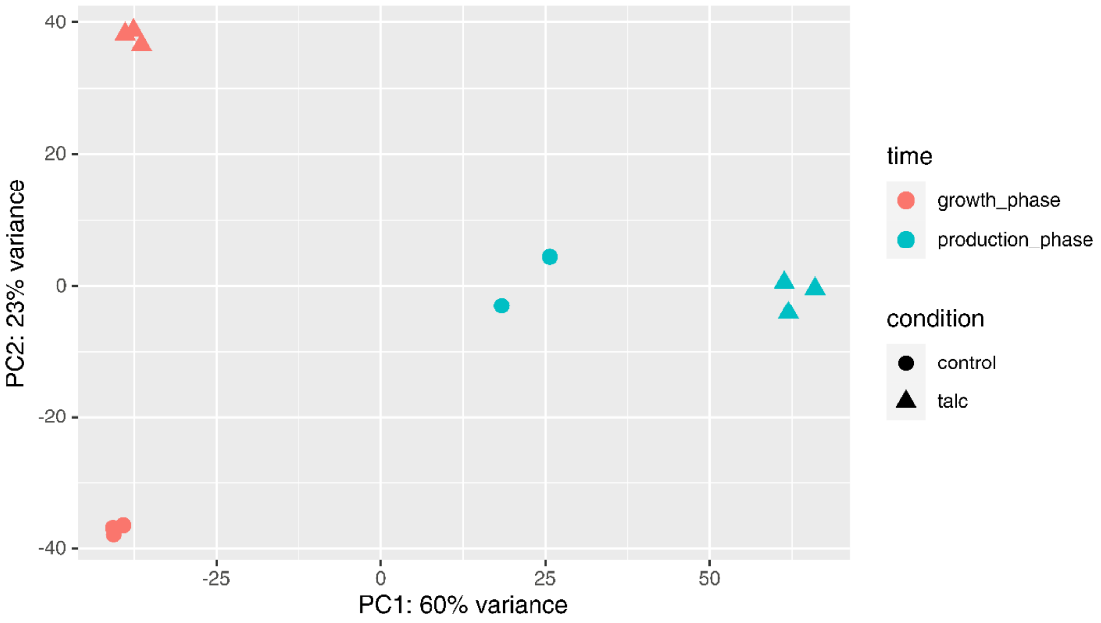

Figure S10: PCA of the RNA seq data. The background corrected read count data were fed to DESeq2 to calculate normalized read counts. After regularized log transformation with blind dispersion estimation enabled, a PCA was performed and visualized using ggplot2 (Wickham, 2016)

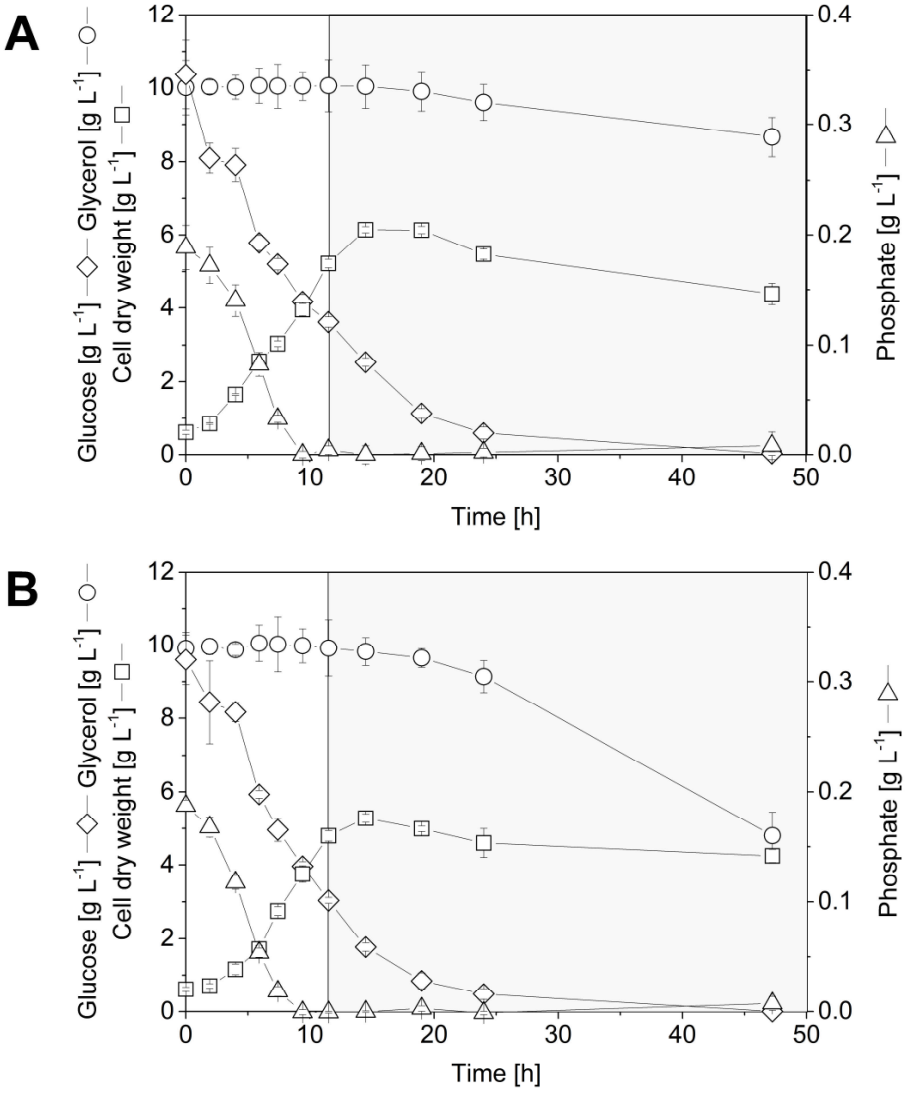

Figure S11: Impact of talc microparticles on growth and substrate consumption in *Streptomyces albus* J1074/R2 using complex SGG medium with starch and glycerol as main carbon source. Besides the cell density, the time dependent concentrations of glucose, glycerol, and phosphate are displayed. Control culture without microparticles (A). Microparticle-enhanced culture with 2.5 g L^{-1} talc (B).

Table S1: Gene expression of selected transcriptional regulators, primary σ-factors, and σ-factors of the ECF subfamily in pamamycin producing *Streptomyces albus* J1074/R2. Samples were taken from a control and a talc supplied culture (10 g L^{-1}) in SGG medium during exponential growth (5 h) and production phase (21 h). For comparison, the expression levels of the control culture during growth were set as reference.

Gene	Annotation	Growth (talc) log2-fold change	Production (talc) log2-fold change	Production (control) log2-fold change
XNRR2_1574	HTH-type transcriptional repressor DasR	0.0	0.0	0.0
XNRR2_5362	Pleiotropic negative regulator BldD	1.5	0.0	0.0
XNRR2_1043	RNA polymerase, sigma 70 subunit, RpoD	0.0	0.0	0.0
XNRR2_2142	RNA polymerase principal sigma factor hrdD	0.0	0.0	0.0
XNRR2_4476	RNA polymerase, sigma 70 subunit, RpoD	0.0	4.8	6.7
XNRR2_0615	RNA polymerase sigma factor ECF subfamily	0.0	0.0	0.0
XNRR2_0683	RNA polymerase sigma factor, ECF subfamily	0.0	-1.8	0.0
XNRR2_0749	RNA polymerase sigma factor, ECF subfamily	-1.9	-2.3	0.0
XNRR2_1515	RNA polymerase ECF-subfamily sigma factor	0.0	0.0	0.0
XNRR2_1584	RNA polymerase sigma factor RpoE, ECF subfamily	0.0	0.0	0.0
XNRR2_1656	RNA polymerase sigma factor SigE, ECF subfamily	0.0	2.3	0.0
XNRR2_2250	RNA polymerase ECF-subfamily sigma factor	-1.0	-1.3	0.0
XNRR2_2757	RNA polymerase ECF-subfamily sigma factor	1.1	0.0	0.0
XNRR2_2903	RNA polymerase ECF-subfamily sigma factor	3.5	2.5	0.0
XNRR2_2992	RNA polymerase sigma factor SigM, ECF subfamily	0.0	0.0	0.0
XNRR2_3275	RNA polymerase ECF sigma factor	0.0	0.0	-1.3
XNRR2_3298	ECF subfamily RNA polymerase sigma-70 factor	4.3	0.0	0.0
XNRR2_3489	RNA polymerase sigma factor, ECF subfamily	0.0	-2.9	-2.2
XNRR2_3527	BldN RNA polymerase, sigma-24 subunit, ECF subfamily	1.8	4.9	0.0
XNRR2_3805	RpoH RNA polymerase, sigma 32 subunit, ECF subfamily	-1.4	0.0	0.0
XNRR2_3945	ECF sigma factor	0.0	-2.3	-2.0
XNRR2_3984	RNA polymerase, sigma subunit, ECF family	1.7	2.9	0.0
XNRR2_3998	RNA polymerase ECF-subfamily sigma factor	-5.3	-4.0	-3.4
XNRR2_4039	RNA polymerase ECF-subfamily sigma factor	1.0	1.0	2.5
XNRR2_5208	RNA polymerase sigma factor SigK, ECF subfamily	1.7	-1.8	1.0
XNRR2_5283	RNA polymerase ECF-subfamily sigma factor	2.4	2.6	2.0
XNRR2_5529	RNA polymerase ECF-subfamily sigma factor	0.0	0.0	0.0
XNRR2_5625	RNA polymerase, sigma-24 subunit, ECF subfamily	1.0	1.5	1.0
XNRR2_5652	RNA polymerase sigma factor SigL, ECF subfamily	7.7	6.0	6.2
XNRR2_5893	ECF subfamily RNA polymerase sigma factor	8.0	4.6	7.8

Table S2: Gene expression of homologues in pamamycin producing *Streptomyces albus* J1074/R2 to genes, previously shown to be involved in *Streptomyces* programmed cell death. Samples were taken from a control and a talc supplied culture (10 g L^{-1}) in SGG medium during exponential growth (5 h) and production phase (21 h). For comparison, the expression levels of the control culture during growth were set as reference.

Gene	Annotation	Homologue & identity [%]	Growth (talc)	Production (talc)	Production (control)
XNRR2_2393	Heat shock protein 60 family chaperone GroEL	*SCO4296, S. coelicolor, 92.4*	2.0	0.0	0.0
XNRR2_3800	Heat shock protein 60 family chaperone GroEL	*SCO4296, S. coelicolor, 74.0*	0.0	0.0	2.3
XNRR2_3753	50S ribosomal protein L36	*SCO4726, S. coelicolor, 98.2*	0.0	-1.2	-1.2
XNRR2_4513	Transcriptional regulator, CdaR	*SCO2386, S. coelicolor, 82.9*	0.0	0.0	0.0
XNRR2_2416	Tellurium resistance protein TerD	*SCO4277, S. coelicolor, 92.5*	3.2	2.9	0.0
XNRR2_4120	AhpC	*SCO5032, S. coelicolor, 94.4*	0.0	1.1	0.0
XNRR2_1430	Transcriptional regulator, MarR family	*SCO5405, S. coelicolor, 75.9*	2.2	0.0	0.0
XNRR2_0641	Glyoxylate carboligase	*SCO6201, S. coelicolor, 84.4*	0.0	0.0	0.0
XNRR2_0992	RNA methyltransferase, TrmA family	*SCO5901, S. coelicolor, 82.4*	-1.3	-2.2	0.0
XNRR2_0640	Catalase	*SCO6204, S. coelicolor, 83.1*	0.0	0.0	0.0
XNRR2_1593	Catalase	*SCO6204, S. coelicolor, 72.5*	1.7	6.7	0.0
XNRR2_1945	Catalase	*SCO6204, S. coelicolor, 52.5*	4.7	5.5	0.0
XNRR2_4128	Catalase	*SCO6204, S. coelicolor, 57.4*	0.0	0.0	0.0
XNRR2_4489	Catalase	*SCO6204, S. coelicolor, 53.8*	0.0	0.0	0.0
XNRR2_1130	Polyribonucleotide nucleotidyltransferase	*SCO5737, S. coelicolor, 91.2*	-1.7	-1.9	0.0

Table S3: Gene expression of genes involved in the production of other secondary metabolites besides pamamycins. Samples were taken from a control and a talc supplied culture (10 g L^{-1}) in SGG medium during exponential growth (5 h) and production phase (21 h). For comparison, the expression levels of the control culture during growth were set as reference.

Gene	Annotation	Function	Growth (talc) log2-fold change	Production (talc) log2-fold change	Production (control) log2-fold change
XNRR2_5853	FscMIII	Candicidin bios.	5.4	2.6	1.0
XNRR2_5854	FscD	Candicidin bios.	11.4	9.3	11.4
XNRR2_5855	FscE	Candicidin bios.	5.7	5.1	6.4
XNRR2_5856	FscF	Candicidin bios.	8.4	9.1	11.0
XNRR2_5857	FscB	Candicidin bios.	7.0	4.6	6.5
XNRR2_5858	FscC	Candicidin bios.	6.6	5.7	7.5
XNRR2_5859	ABC-transporter	Candicidin bios.	9.4	6.7	7.3
XNRR2_5860	FscTI	Candicidin bios.	4.4	1.6	4.0
XNRR2_5861	FscA	Candicidin bios.	5.6	3.5	5.3
XNRR2_5862	Para-aminobenzoate synthase, amidotransferase component	Candicidin bios.	6.6	5.7	6.9
XNRR2_5863	FscTE	Candicidin bios.	6.6	5.0	1.0
XNRR2_5864	FscFE	Candicidin bios.	4.0	3.0	4.6
XNRR2_5865	Cytochrome P450	Candicidin bios.	6.1	4.9	1.0
XNRR2_5866	Aminotransferase	Candicidin bios.	5.9	3.8	5.5
XNRR2_5867	FscMI	Candicidin bios.	5.6	2.7	1.0
XNRR2_5868	LuxR family transcriptional regulator FscRIV	Candicidin bios.	5.4	3.3	5.0
XNRR2_5869	LuxR family transcriptional regulator FscRIII	Candicidin bios.	1.8	1.0	1.0
XNRR2_5870	LuxR family transcriptional regulator FscRII	Candicidin bios.	1.0	1.0	1.0
XNRR2_5871	LuxR family transcriptional regulator FscRI	Candicidin bios.	2.5	1.3	1.0
XNRR2_5872	PabC	Candicidin bios.	1.5	1.0	1.0
XNRR2_5873	FscO	Candicidin bios.	1.0	1.0	1.0
XNRR2_0573	dTDP-4-keto-6-deoxyhexose 3, 5-epimerase	PK sugar unit bios.	1.0	3.4	5.9
XNRR2_0574	dTDP-6-deoxy-L-hexose 3-O-methyltransferase	PK sugar unit bios.	1.3	4.4	6.2
XNRR2_0575	dTDP-4-keto-6-deoxy-L-hexose 2, 3-reductase	PK sugar unit bios.	1.0	2.4	5.0
XNRR2_0593	Glucose-1-phosphate thymidylyltransferase	PK sugar unit bios.	2.0	2.5	3.4
XNRR2_0594	dTDP-glucose 4, 6-dehydratase	PK sugar unit bios.	1.4	1.5	1.0
XNRR2_0596	2, 3-dihydro-2, 3-dihydroxybenzoate dehydrogenase	Siderophore bios.	4.3	4.5	1.0
XNRR2_1297	Germacradienol/geosmin synthase	Sesquiterp., tripernoid. bios.	1.5	1.7	1.1
XNRR2_1552	Polyprenyl diphosphate synthase	Terpenoid backbone bios.	6.7	7.8	5.4
XNRR2_0597	Phenazine biosynthesis protein PhzD	Phenazine bios.	4.3	5.3	6.8
XNRR2_0598	Phenazine biosynthesis protein PhzE	Phenazine bios.	1.9	3.2	1.0

References

Kolde, R. (2019). Pheatmap: Pretty Heatmaps. R Package Version 1.0.12. *https://CRANR-project.org/package=pheatmap*.

Love, M. I., Huber, W., & Anders, S. (2014). Moderated estimation of fold change and dispersion for RNA-seq data with DESeq2. *Genome biology, 15*(12), 550. doi:10.1186/s13059-014-0550-8

Wickham, H. (2016). *ggplot2: elegant graphics for data analysis*: springer.

7.2 Supplementary information: Microparticles enhance the formation of seven major classes of natural products in native and metabolically engineered actinobacteria through accelerated morphological development

Martin Kuhl, Christian Rückert, Lars Gläser, Selma Beganovic, Andriy Luzhetskyy, Jörn Kalinowski, and Christoph Wittmann

Biotechnology and Bioengineering. 2021; in press.

Supplementary Material: Microparticles enhance the formation of seven major classes of natural products in native and metabolically engineered actinobacteria through accelerated morphological development

Martin Kuhl[1], Christian Rückert[3], Lars Gläser[1], Selma Beganovic[1], Andriy Luzhetskyy[2], Jörn Kalinowski[3], and Christoph Wittmann[1*]

[1] Institute of Systems Biotechnology, Saarland University, Saarbrücken, Germany

[2] Pharmaceutical Biotechnology, Saarland University, Saarbrücken, Germany

[3] Center for Biotechnology, Bielefeld University, Bielefeld, Germany

* Phone: 0049-681-302-71971, FAX: -71972, Email: christoph.wittmann@uni-saarland.de

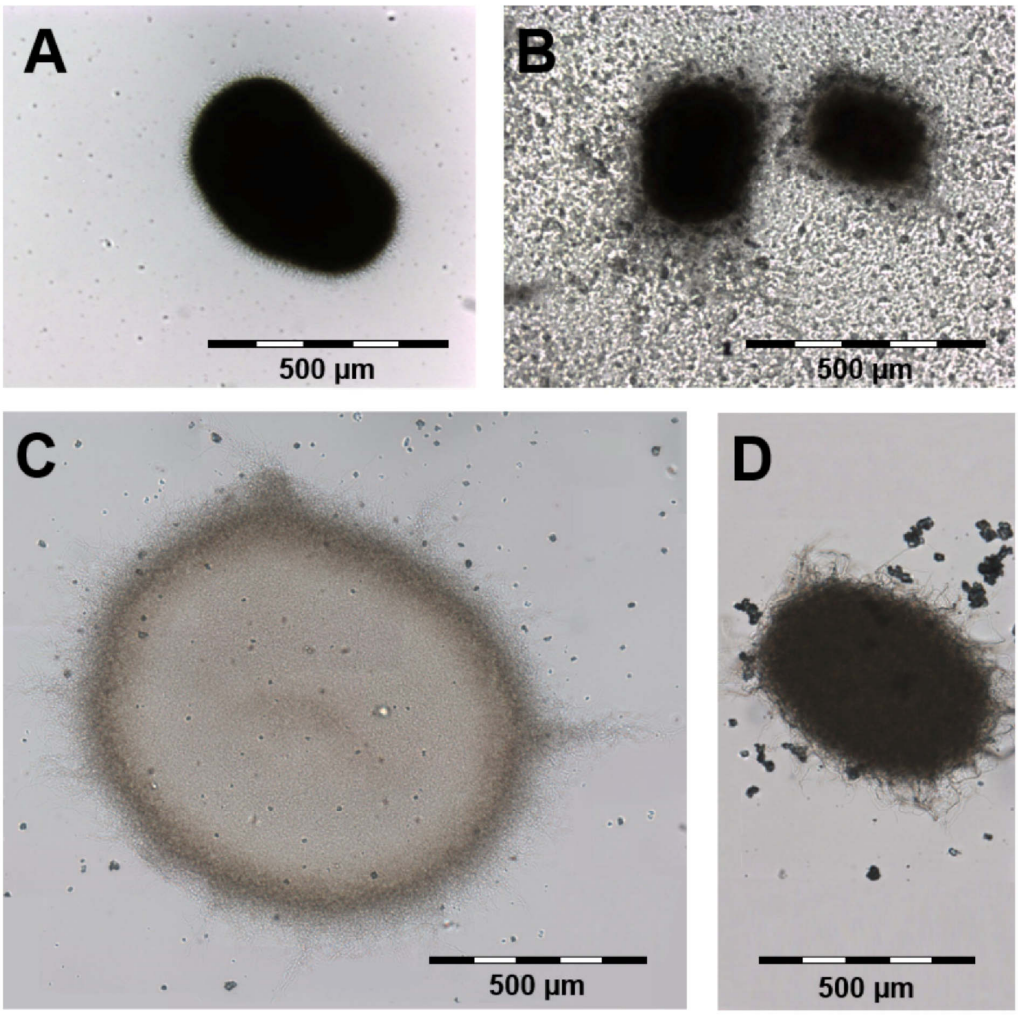

Figure S1: Impact of talc microparticles on pellet morphology of *Streptomyces lividans* TK24 DG2-Km-P41hyg+. Control culture without microparticles during production start (24 h, A) and main production phase (48 h, C). Microparticle-enhanced culture with 10 g L^{-1} talc during production start (24 h, B) and main production phase (48 h, D).

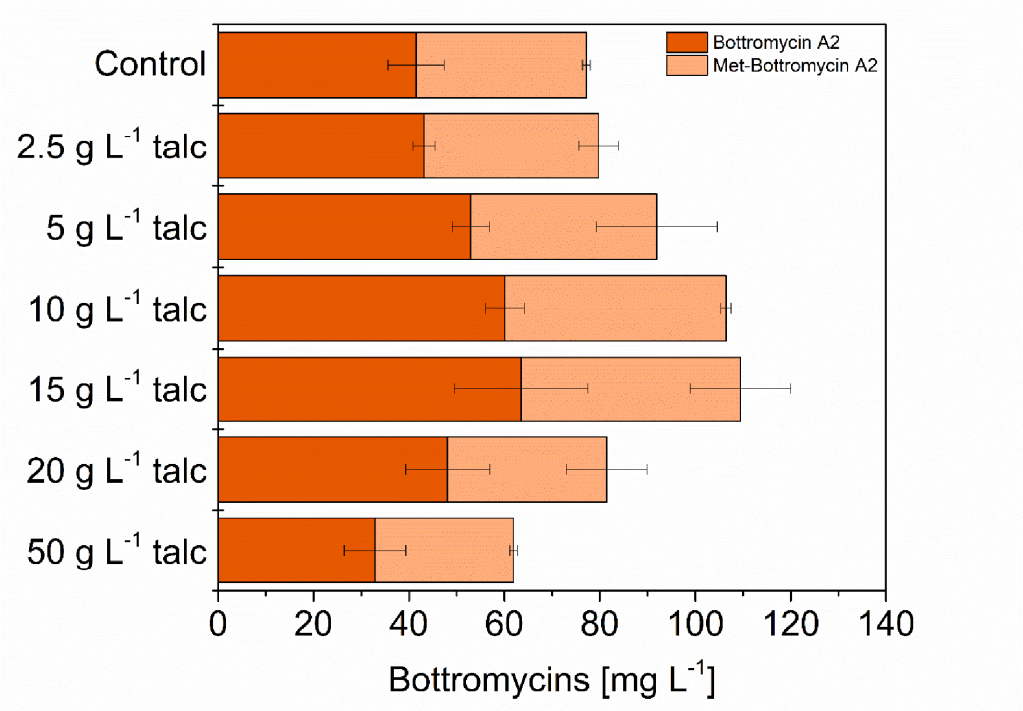

Figure S2: Impact of talc microparticles on bottromycin production by *Streptomyces lividans* TK24 DG2-Km-P41hyg+. The data reflect final titers after 120 hours from shake flasks cultures. n=3.

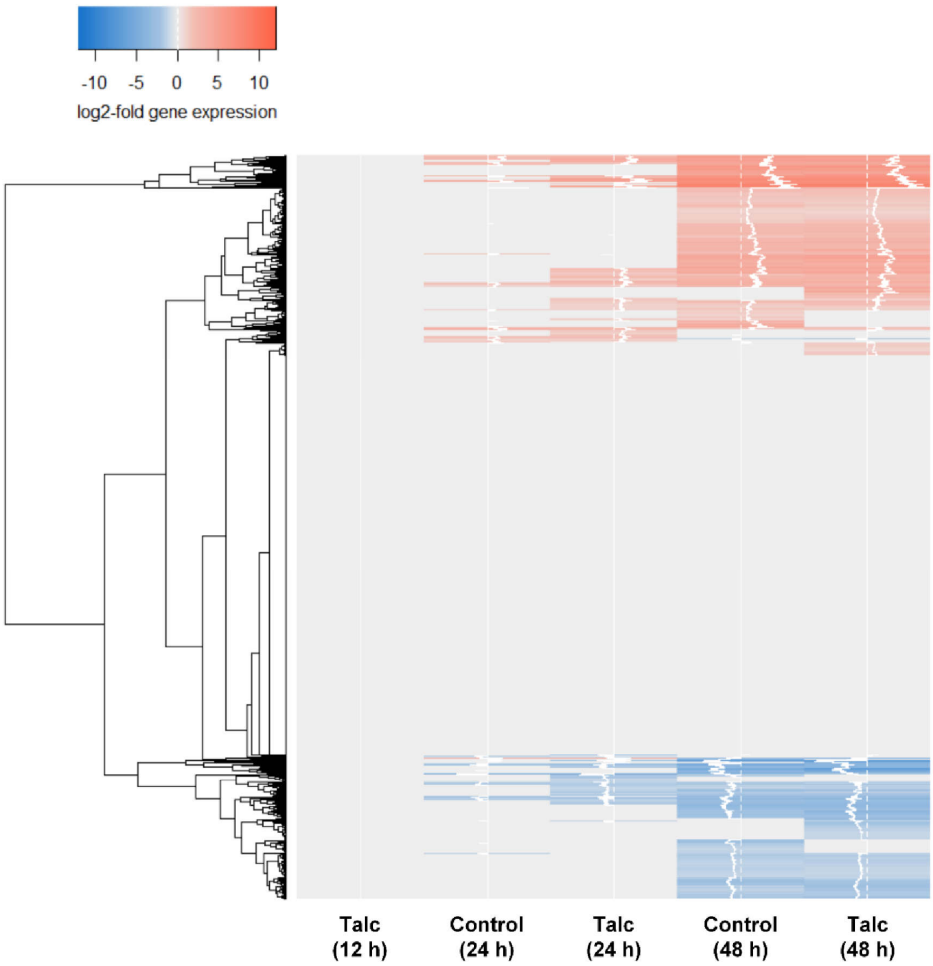

Figure S3: Hierarchical cluster analysis of global gene expression of *S. lividans* TK24 DG2-Km-P41hyg+ in liquid SG medium. Samples were taken from a control and a talc supplied culture (10 g L^{-1}) during exponential growth (12 h), the start of the production phase (24 h) and the major production phase (48 h). The sample out of the control culture during growth was set as reference. n=3.

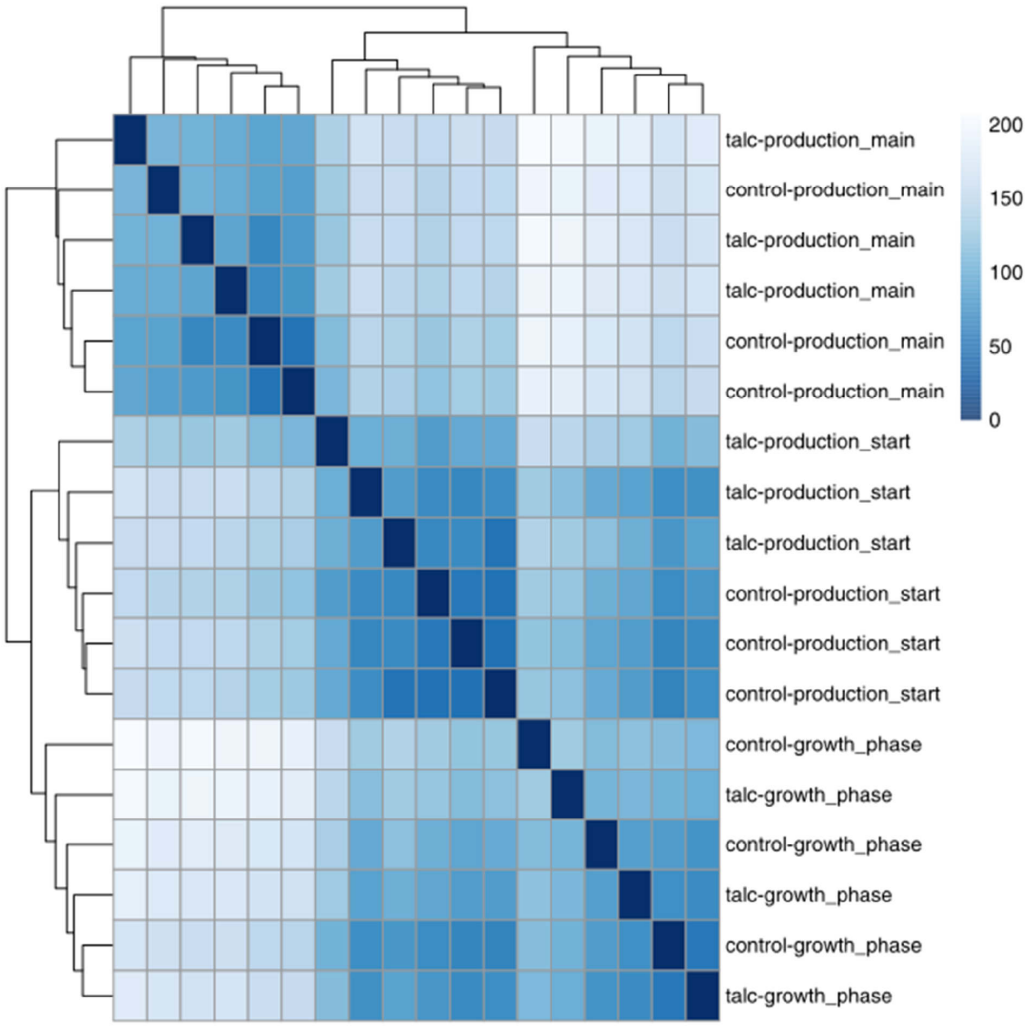

Figure S4: Heatmap of the sample-to-sample distances. The read count data were fed to DESeq2 (Love et al., 2014) to calculate normalized read counts. After regularized log transformation with blind dispersion estimation enabled, the sample to sample distances were calculated and used for hierarchical clustering, which in turn was visualized using pheatmap (Kolde, 2019).

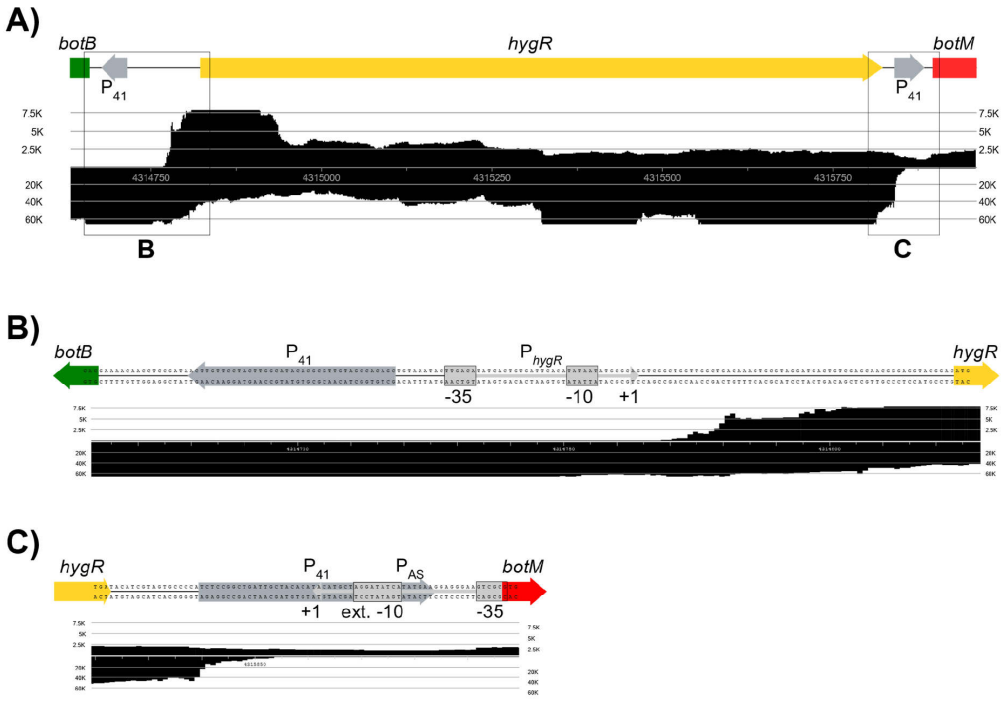

Figure S5: Transcriptional organization of the *botB-hygR-botM* region, inserted via the DG2 cosmid. a: Overview of the region and combined coverage from the RNAseq data (A). The genes *botB* (3'-end only), *hygR*, and *botM* (5'-end only) are shown in green, orange, and red color, respectively. The two synthetic promoters from previous work (Horbal et al., 2018) are shown in grey. The combined coverage from all transcriptome samples is shown in black, whereby the forward and the reverse strand coverage are given at different scale to support visualization. b: Detailed view of the intergenic region between *botB* and *hygR*. The P_{hygR} promoter, inferred from the RNAseq data, is shown in light grey. c: Detailed view of the intergenic region between *hygR* and *botM*. The so far unknown P_{AS} promoter, inferred from the RNAseq data and transcribing into the 5' direction, is marked in light grey.

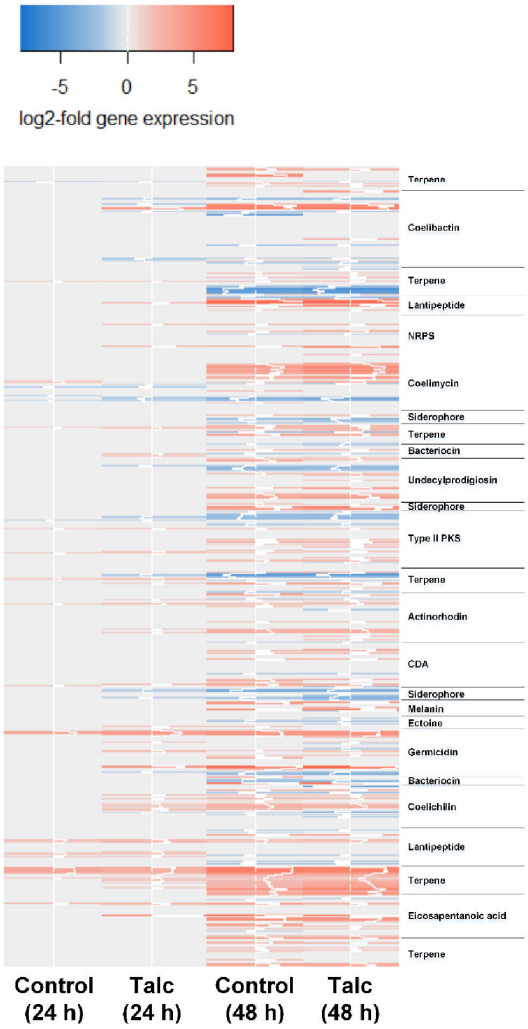

Figure S6: Differential gene expression analysis of endogenous cluster genes in *S. lividans* TK24 DG2-Km-P41hyg+ in liquid SG medium. Samples were taken from a control and a talc supplied culture (10 g L^{-1}) during exponential growth (growth), the start of the production phase (24 h) and the major production phase (48 h). The sample out of the control culture during growth was set as reference. n=3.

Table S1: Chromatographic and mass spectrometric settings for investigated compounds in this study.

Natural product	Eluents	HPLC settings	m/z values	Reference
Pamamycins	8 mM ammonium formate in 92% ACN	45 °C, 300 µL min^{-1} isocratic	580.4 $[M+H]^+$, 594.3 $[M+H]^+$, 608.4 $[M+H]^+$, 622.4 $[M+H]^+$, 636.4 $[M+H]^+$, 650.4 $[M+H]^+$, 664.4 $[M+H]^+$	(Kuhl et al., 2020)
Bottromycins	A: H_2O + 0.1% formic acid B: ACN + 0.1% formic acid	45 °C, 550 µL min^{-1} 0 - 1 min, 5% B, 1 - 8 min, 5 - 95% B, 8 - 10 min, 95% B, 10 - 11 min 95 - 5% B, 11 - 12 min, 5% B	A2: 823.4 $[M+H]^+$ Met-A2: 837.4 $[M+H]^+$	(Horbal et al., 2018)
Undecylprodigiosin	A: H_2O + 0.1% formic acid B: ACN + 0.1% formic acid	45 °C, 550 µL min^{-1} 0 - 1 min, 5% B, 1 - 8 min, 5 - 95% B, 8 - 10 min, 95% B, 10 - 11 min 95 - 5% B, 11 - 12 min, 5% B	394.4 $[M+H]^+$	(Meschke et al., 2012)
Cinnamycins	A: H_2O + 0.1% formic acid B: ACN + 0.1% formic acid	45 °C, 550 µL min^{-1} 0 - 1 min, 5% B, 1 - 8 min, 5 - 95% B, 8 - 10 min, 95% B, 10 - 11 min 95 - 5% B, 11 - 12 min, 5% B	Cinnamycin: 1021.2 $[M+2H]^{2+}$ Deoxycin.: 1013.1 $[M+2H]^{2+}$	(Lopatniuk et al., 2017)
Nybomycin	A: H_2O + 0.1% formic acid B: ACN + 0.1% formic acid	45 °C, 550 µL min^{-1} 0 - 1 min, 5% B, 1 - 8 min, 5 - 95% B, 8 - 10 min, 95% B, 10 - 11 min 95 - 5% B, 11 - 12 min, 5% B	299.1 $[M+H]^+$	(Rodriguez Estevez et al., 2018)
Usabamycins	A: H_2O + 0.1% formic acid B: ACN + 0.1% formic acid	45 °C, 550 µL min^{-1} 0 - 1 min, 5% B, 1 - 8 min, 5 - 95% B, 8 - 10 min, 95% B, 10 - 11 min 95 - 5% B, 11 - 12 min, 5% B	Usabamycin A: 273.2 $[M+H]^+$ Usabamycin B: 259.3 $[M+H]^+$ Usabamycin C: 243.2 $[M+H]^+$	(Ahmed et al., 2020)
Alpiniamides	A: H_2O + 0.1% formic acid B: ACN + 0.1% formic acid	45 °C, 550 µL min^{-1} 0 - 1 min, 5% B, 1 - 8 min, 5 - 95% B, 8 - 10 min, 95% B, 10 - 11 min 95 - 5% B, 11 - 12 min, 5% B	Alpiniamide A: 344.2 $[M+H]^+$ Alpiniamide C: 326.2 $[M+H]^+$ Alpiniamide D: 286.2 $[M+H]^+$	(Paulus et al., 2018)
Perquinolines	A: H_2O + 0.1% formic acid B: ACN + 0.1% formic acid	45 °C, 550 µL min^{-1} 0 - 1 min, 5% B, 1 - 8 min, 5 - 95% B, 8 - 10 min, 95% B, 10 - 11 min 95 - 5% B, 11 - 12 min, 5% B	Perquinoline A: 452.2 $[M+H]^+$ Perquinoline B: 438.2 $[M+H]^+$	(Rebets et al., 2019)
Vancomycin	A: H_2O + 0.1% formic acid B: ACN + 0.1% formic acid	45 °C, 550 µL min^{-1} 0 - 1 min, 5% B, 1 - 8 min, 5 - 95% B, 8 - 10 min, 95% B, 10 - 11 min 95 - 5% B, 11 - 12 min, 5% B	725.8 $[M+2H]^{2+}$ → 144.2	(Liu et al., 2018)
Teicoplanin	A: H_2O + 0.1% formic acid B: ACN + 0.1% formic acid	45 °C, 550 µL min^{-1} 0 - 1 min, 5% B, 1 - 8 min, 5 - 95% B, 8 - 10 min, 95% B, 10 - 11 min 95 - 5% B, 11 - 12 min, 5% B	$A_{2\text{-}2}$ & $A_{2\text{-}3}$: 940.5 $[M+2H]^{2+}$ → 316.5	(Fung et al., 2012)

References

Ahmed, Y., Rebets, Y., Estevez, M. R., Zapp, J., Myronovskyi, M., & Luzhetskyy, A. (2020). Engineering of Streptomyces lividans for heterologous expression of secondary metabolite gene clusters. *Microbial Cell Factories, 19*(1), 5. doi:10.1186/s12934-020-1277-8

Bilyk, O., Brötz, E., Tokovenko, B., Bechthold, A., Paululat, T., & Luzhetskyy, A. (2016). New simocyclinones: surprising evolutionary and biosynthetic insights. *ACS chemical biology, 11*(1), 241-250.

Fung, F. H., Tang, J. C., Hopkins, J. P., Dutton, J. J., Bailey, L. M., & Davison, A. S. (2012). Measurement of teicoplanin by liquid chromatography-tandem mass spectrometry: development of a novel method. *Annals of clinical biochemistry, 49*(5), 475-481.

Horbal, L., Marques, F., Nadmid, S., Mendes, M. V., & Luzhetskyy, A. (2018). Secondary metabolites overproduction through transcriptional gene cluster refactoring. *Metabolic Engineering, 49*, 299-315.

Kolde, R. (2019). Pheatmap: Pretty Heatmaps. R Package Version 1.0.12. *https://CRANR-project.org/package=pheatmap*.

Kuhl, M., Gläser, L., Rebets, Y., Rückert, C., Sarkar, N., Hartsch, T., Kalinowski, J., Luzhetskyy, A., & Wittmann, C. (2020). Microparticles globally reprogram Streptomyces albus toward accelerated morphogenesis, streamlined carbon core metabolism, and enhanced production of the antituberculosis polyketide pamamycin. *Biotechnology and Bioengineering*. doi:10.1002/bit.27537

Liu, M., Yang, Z.-H., & Li, G.-H. (2018). A novel method for the determination of vancomycin in serum by high-performance liquid chromatography-tandem mass spectrometry and its application in patients with diabetic foot infections. *Molecules, 23*(11), 2939.

Lopatniuk, M., Myronovskyi, M., & Luzhetskyy, A. (2017). Streptomyces albus: A New Cell Factory for Non-Canonical Amino Acids Incorporation into Ribosomally Synthesized Natural Products. *ACS chemical biology, 12*(9), 2362-2370. doi:10.1021/acschembio.7b00359

Love, M. I., Huber, W., & Anders, S. (2014). Moderated estimation of fold change and dispersion for RNA-seq data with DESeq2. *Genome biology, 15*(12), 550. doi:10.1186/s13059-014-0550-8

Meschke, H., Walter, S., & Schrempf, H. (2012). Characterization and localization of prodiginines from Streptomyces lividans suppressing Verticillium dahliae in the absence or presence of Arabidopsis thaliana. *Environmental Microbiology, 14*(4), 940-952.

Paulus, C., Rebets, Y., Zapp, J., Rückert, C., Kalinowski, J., & Luzhetskyy, A. (2018). New Alpiniamides From Streptomyces sp. IB2014/011-12 Assembled by an Unusual Hybrid Non-ribosomal Peptide Synthetase Trans-AT Polyketide Synthase Enzyme. *Frontiers in Microbiology, 9*, 1959.

Rebets, Y., Nadmid, S., Paulus, C., Dahlem, C., Herrmann, J., Hübner, H., Rückert, C., Kiemer, A. K., Gmeiner, P., & Kalinowski, J. (2019). Perquinolines A–C: Unprecedented Bacterial Tetrahydroisoquinolines Involving an Intriguing Biosynthesis. *Angewandte Chemie International Edition, 58*(37), 12930-12934.

Rodriguez Estevez, M., Myronovskyi, M., Gummerlich, N., Nadmid, S., & Luzhetskyy, A. (2018). Heterologous Expression of the Nybomycin Gene Cluster from the Marine Strain Streptomyces albus subsp. chlorinus NRRL B-24108. *Marine drugs, 16*(11). doi:10.3390/md16110435

7.3 Supplementary information: A common approach for absolute quantification of short chain CoA thioesters in prokaryotic and eukaryotic microbes.

Lars Gläser, Martin Kuhl, Sofija Jovanovic, Michel Fritz, Bastian Vögeli, Tobias J. Erb, Judith Becker, and Christoph Wittmann

Microbial Cell Factories. 2020; 19:160

Additional file 1 for

A common approach for absolute quantification of short chain CoA thioesters in prokaryotic and eukaryotic microbes

Lars Gläser[1], Martin Kuhl[1], Sofija Jovanovic[1], Michel Fritz[1], Bastian Vögeli[2], Tobias J. Erb[2], Judith Becker[1] and Christoph Wittmann[1#]

[1]Institute of Systems Biotechnology, Saarland University, Saarbrücken, Germany

[2]Max Planck Institute for Terrestrial Microbiology, Marburg, Germany

[#] Phone/FAX: +49 681 302 71970/71972, e-mail: christoph.wittmann@uni-saarland.de

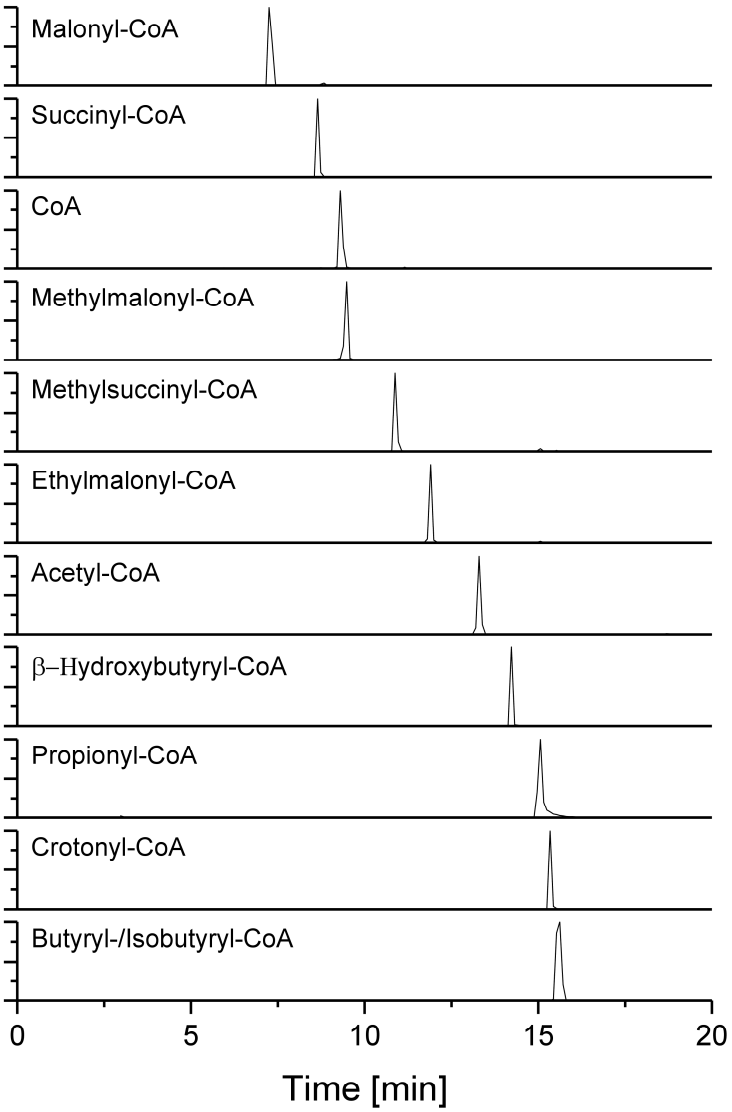

Figure S1: LC-MS chromatogram of a synthetic CoA thioester standard using a porous organo-silica reversed phase column (100 × 2.1 mm, 1.5 µm) for the chromatographic separation. Co-eluting analytes were distinguished by a different specific mass-to-charge ratio (*m/z*).

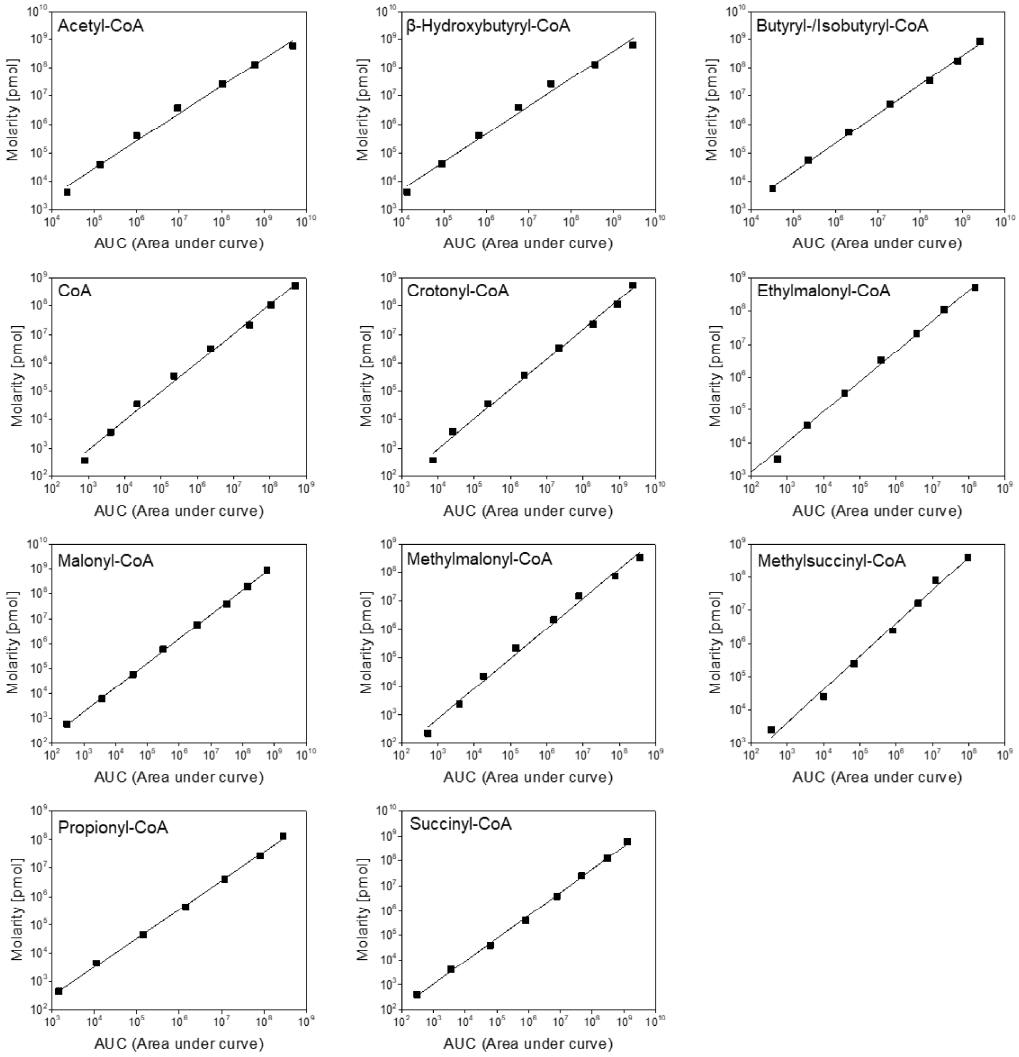

Figure S2: Calibration curves for different CoA thioesters using LC-MS/MS analysis.

Table S1: Instrumental settings for LC-MS/MS analysis of CoA thioesters. The declustering potential (DP), the collision energy (CE) and the cell exit potential (CXP) were individually tuned for each CoA thioester. The parent ion reflects the positive proton adduct $[M+H]^+$, except for the CoA homodimer (CoA-S-S-CoA), where the parent ion was $[M+2H]^{2+}$ In each case, the daughter ion reflects the positive proton adduct after neutral loss of 507 (*m/z*).

Analyte	Parent ion (*m/z*)	Daughter ion (*m/z*)	DP [V]	CE [V]	CXP [V]
CoA-S-S-CoA	767.4	136.0	80.00	47.00	11.00
CoA	768.5	261.0	80.00	47.00	11.00
Acetyl-CoA	810.2	303.0	154.57	38.87	17.01
Malonyl-CoA	854.0	346.6	46.50	43.84	21.75
Propionyl-CoA	824.6	317.1	80.00	47.00	11.00
Butyryl-/Isobutyryl-CoA	838.1	331.1	128.22	45.50	22.16
β-Hydroxybutyryl-CoA	854.1	347.1	142.36	39.95	10.73
Crotonyl-CoA	836.1	329.1	143.00	44.00	20.37
Methylmalonyl-CoA	868.0	361.1	90.06	42.50	11.87
Succinyl-CoA	868.1	361.1	15.96	46.78	21.68
Ethylmalonyl-CoA	882.1	375.1	177.58	37.80	25.30
Methylsuccinyl-CoA	882.0	375.1	131.79	50.40	23.73

Table S2: Instrumental settings for LC-MS/MS analysis of fully ^{13}C-labeled CoA thioesters used as internal standard for absolute CoA thioesters quantification. The respective mass of the fully labeled parent ion was determined by adding the number of carbon atoms to the monoisotopic mass of the non-labelled parent ion (Table S1). The mass of each daughter ion was then calculated by subtraction of *m/z* 517 form this value, considering the neutral loss of a fragment with ten ^{13}C atoms.

Analyte	Parent ion (*m/z*)	Daughter ion (*m/z*)	DP [V]	CE [V]	CXP [V]
CoA-S-S-CoA	788.1	141.1	80.00	47.00	11.00
CoA	789.5	272.5	80.00	47.00	11.00
Acetyl-CoA	833.2	316.2	154.57	38.87	17.01
Malonyl-CoA	878.0	361.0	46.50	43.84	21.75
Propionyl-CoA	848.6	331.6	80.00	47.00	11.00
Butyryl-/Isobutyryl-CoA	863.1	346.1	128.22	45.50	22.16
β-Hydroxybutyryl-CoA	879.1	362.1	142.36	39.95	10.73
Crotonyl-CoA	861.1	344.1	143.00	44.00	20.37
Methylmalonyl-CoA	893.0	376.0	90.06	42.50	11.87
Succinyl-CoA	893.1	376.1	15.96	46.78	21.68
Ethylmalonyl-CoA	908.1	391.1	177.58	37.80	25.30
Methylsuccinyl-CoA	908.0	391.0	131.79	50.40	23.73